TRW/DSSG REPORT NO. 36358.001

A STUDY ON VARIOUS METHODS OF SUPPLYING PROPELLANT TO AN ORBIT INSERTION ROCKET ENGINE

FINAL TECHNICAL REPORT
9 MAY 1980

PREPARED FOR

JET PROPULSION LABORATORY
CALIFORNIA INSTITUTE OF TECHNOLOGY
4800 OAK GROVE DRIVE
PASADENA, CALIFORNIA, 91103

UNDER
JPL CONTRACT NO. 955656
SUBCONTRACT NASA CONTRACT NAS7–100; TASK ORDER RD–156

TRW

ABSTRACT

Various types of pumps and pump drives were evaluated to determine the lightestweight system for supplying propellants to a planetary orbit insertion rocket engine. From these analyses four candidate propellant feed systems were identifies. Systems Nos. 1 and 2 were both battery-powered (lithium-thionyl-chloride or silver-zinc) motor driven pumps. System 3 was a monopropellant (N_2H_4) gas generator powered turbopump. System 4 was a bipropellant (MMH/N_2O_4) gas generator powered turbopump. System tradeoffs were conducted over a range of levels (1000 to 4000 lbf), thrust chamber pressures (150 to 500 psia), at a constant specific impulse of 310 seconds, and for a total impulse of 3.6×10^6 lbf-sec. Parameters considered were pump breake horsepower, weight, reliability, transient response and system stability. Figures of merit were established and the ranking of the candidate systems was determined. Conceptual designs were prepared for typical motor-driven pumps and turbopump configurations for a 1000 lbf thrust rocket engine.

ACKNOWLEDGEMENTS

This report, entitled "Study on Various Methods of Supplying Propellant to an Orbit Insertion Rocket Engine" was carried out for the California Institute of Technology, Jet Propulsion Laboratory, Pasadena, California, 91103. It is submitted in fulfillment of the Work Statement under JPL Contract 955656, which is a subcontract under NASA Contract NAS7-100; Task Order RD-156.

The Principal Investigator and Study Manager for this program was John E. Boretz. He was assisted by Dr. Sam Huniu (combustion thermodynamics), Matt Thompson (transient analyses), Mike Pagani (computer programming), Bob Paulsen (reliability analyses), Joe Lewis (mass properties), and Don Paul (preliminary design).

Technical direction and guidance were provided by Thomas W. Auslander and Paul N. Estey of the JPL Advanced Technology and Applications Branch, Pasadena, California, and is gratefully acknowledged.

This work was performed for the Jet Propulsion Laboratory, California Institute of Technology sponsored by the National Aeronautics and Space Administration under Contract NAS7-100.

CONTENTS

CONTENTS (Continued)

ILLUSTRATIONS

ILLUSTRATIONS (Continued)

ILLUSTRATIONS (Continued)

ILLUSTRATIONS (Continued)

TABLES

TABLES (Continued)

TABLES (Continued)

1. SUMMARY

1.1 SUMMARY

The purpose of this study was to identify and evaluate various pump-driven rocket engine bipropellant feed systems (PFS). The primary objective was to parametrically analyze these PFS concepts over a range of thrust levels (1000 to 4000 lbf) and thrust chamber pressures (150 to 500 psia) to identify the lowest mass system. Rocket engine total impulse was 3.6×10^6 lbf-sec and specific impulse was 310 sec. Other parameters that were to be evaluated included system complexity, development risk, reliability, and growth potential. Finally, combustion stability and start/stop transient characteristics were to be analyzed and evaluated.

Four candidate conceptual designs were identified and evaluated. These are shown in Table 1-1.

Because total system mass and total system dry weight would have to be traded off with the other important PFS parameter, weighting factors were established. These, together with the system rankings resulting from various analyses were used in arriving at a figure-of-merit for the candidate PFS. The details of these analyses are provided in Sections 4 and 5, Table 5-9, and are summarized in Table 1-2.

System No. 1 ranked first with a figure-of-merit of 2.8 out of a possible 4.0. Low ratings for development risk (due to LiTCl battery performance uncertainties) and growth potential (due to the increasing impact of battery weight for higher total impulse rocket engines) restrained the system from achieving a higher figure-of-merit. System No. 3, which was not constrained to any great extent in both these categories but was somewhat heavier, was a very close second choice.

All systems are convertible to the ultimate use of liquid fluorine (LF_2) and hydrazine (N_2H_4) propellants. However, the motor driven pumps (Systems No. 1 and 2) presented the least development problems for this conversion. A typical conceptual design of a motor driven pump unit is shown in Figure 1-1 (for $F = 1000$ lbf and $P_c = 150$ psia conditions). A similar conceptual design of a turbopump unit is shown in Figure 1-2 for the same conditions.

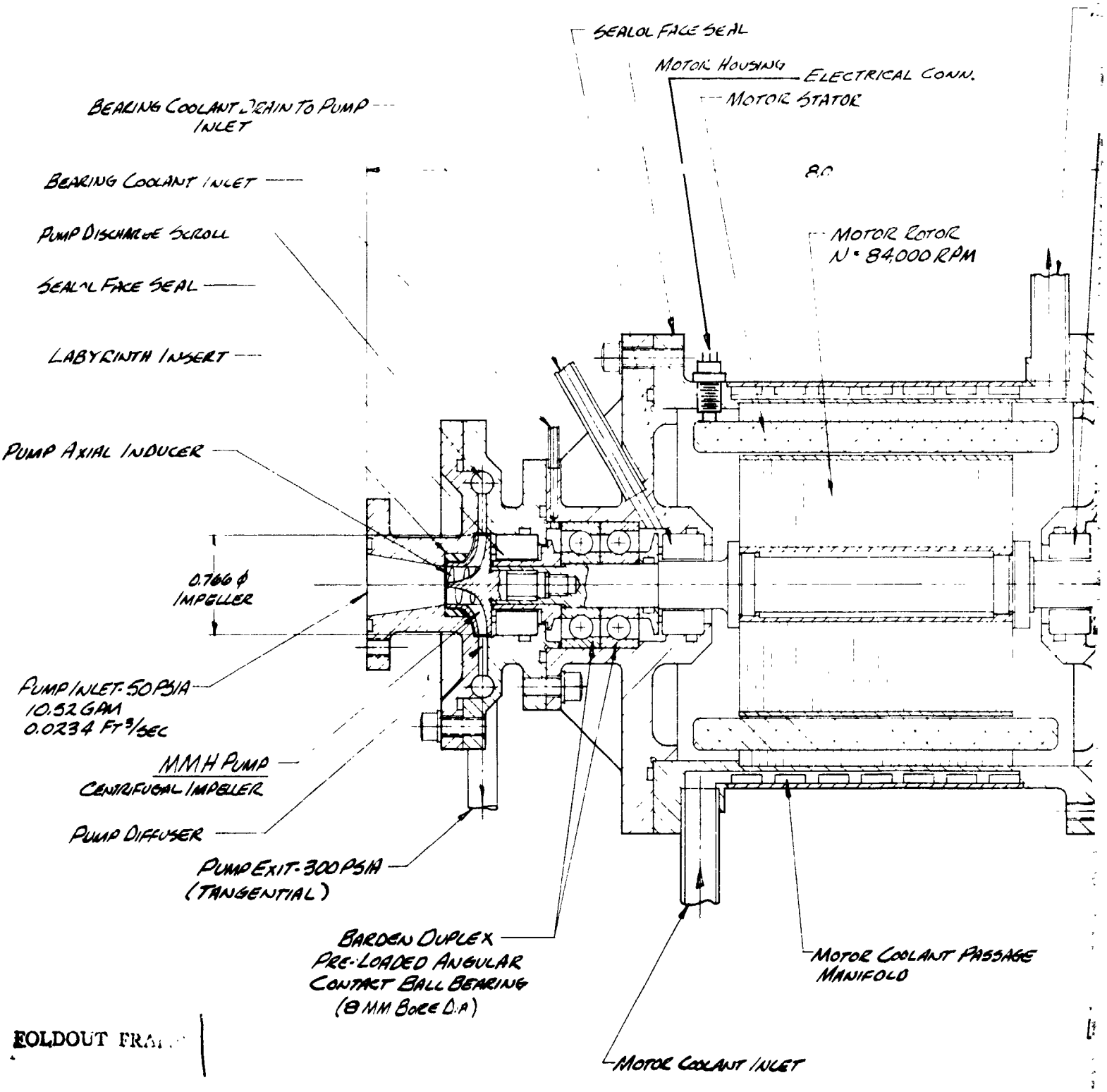

FOLDOUT FRAME

ORIGINAL PAGE IS
OF POOR QUALITY

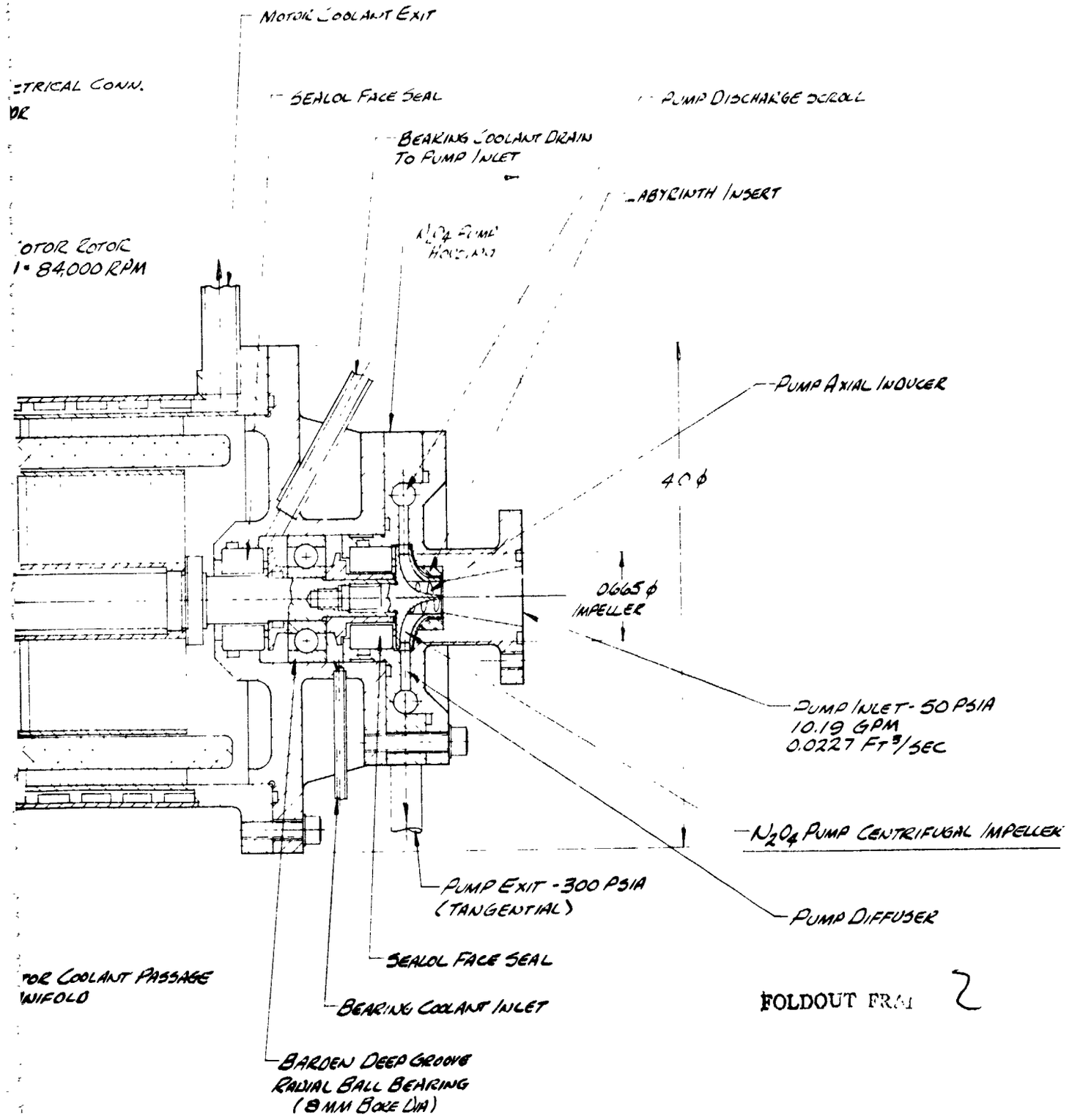

Figure 1-1. Motor Driven Pumps for 1000 lb Thrust Bipropellant Rocket Engine

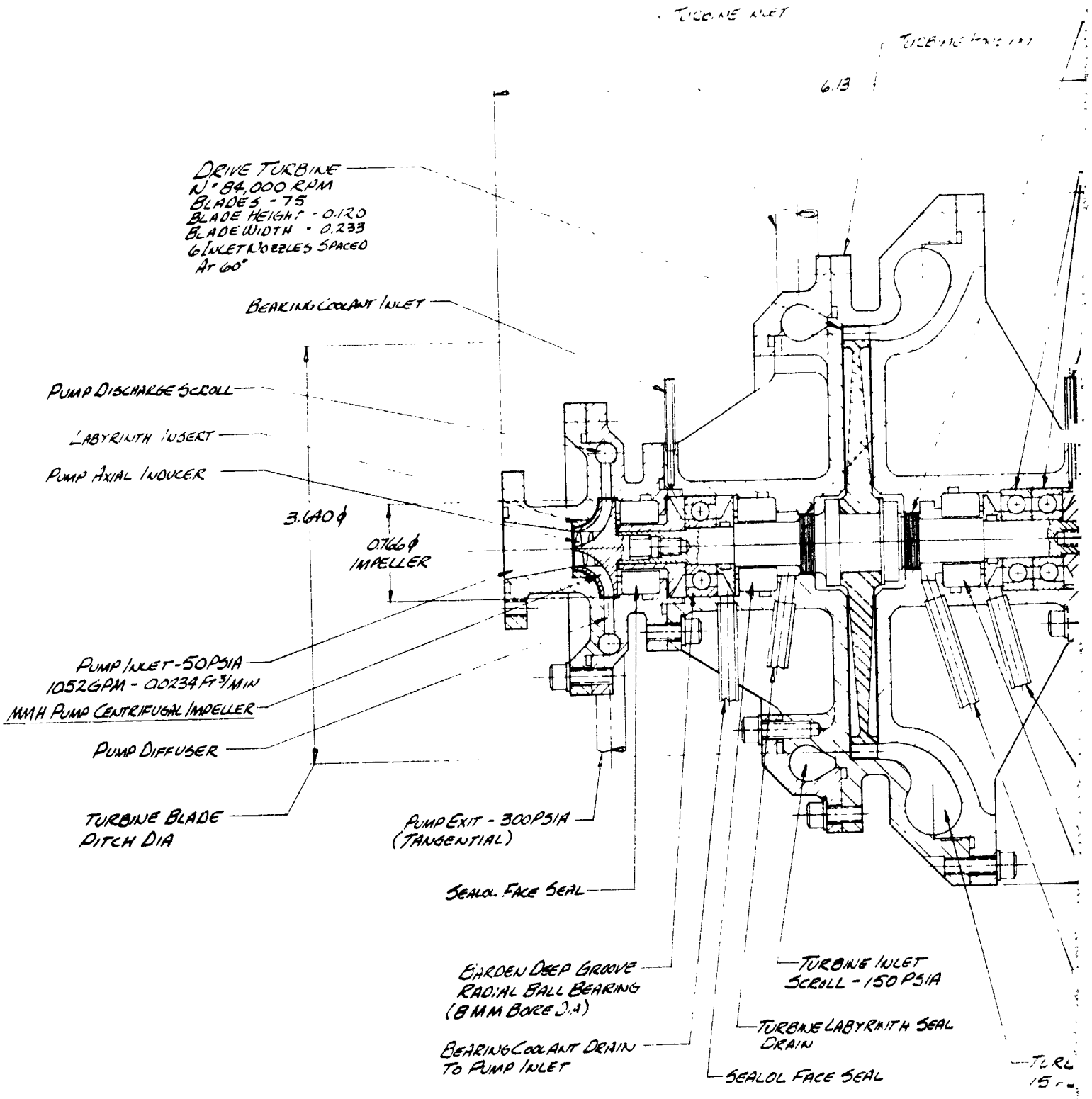
DRIVE TURBINE
N = 84,000 RPM
BLADES - 75
BLADE HEIGHT - 0.120
BLADE WIDTH - 0.233
6 INLET NOZZLES SPACED AT 60°
BEARING COOLANT INLET
PUMP DISCHARGE SCROLL
LABYRINTH INSERT
PUMP AXIAL INDUCER
3.640 ϕ
0.766 ϕ IMPELLER
PUMP INLET - 50 PSIA
1052 GPM - 0.0234 FT³/MIN
MMH PUMP CENTRIFUGAL IMPELLER
PUMP DIFFUSER
TURBINE BLADE PITCH DIA
PUMP EXIT - 300 PSIA (TANGENTIAL)
SEALOL FACE SEAL
BARDEN DEEP GROOVE RADIAL BALL BEARING (8 MM BORE)
BEARING COOLANT DRAIN TO PUMP INLET
TURBINE INLET SCROLL - 150 PSIA
TURBINE LABYRINTH SEAL DRAIN
SEALOL FACE SEAL

FOLDOUT

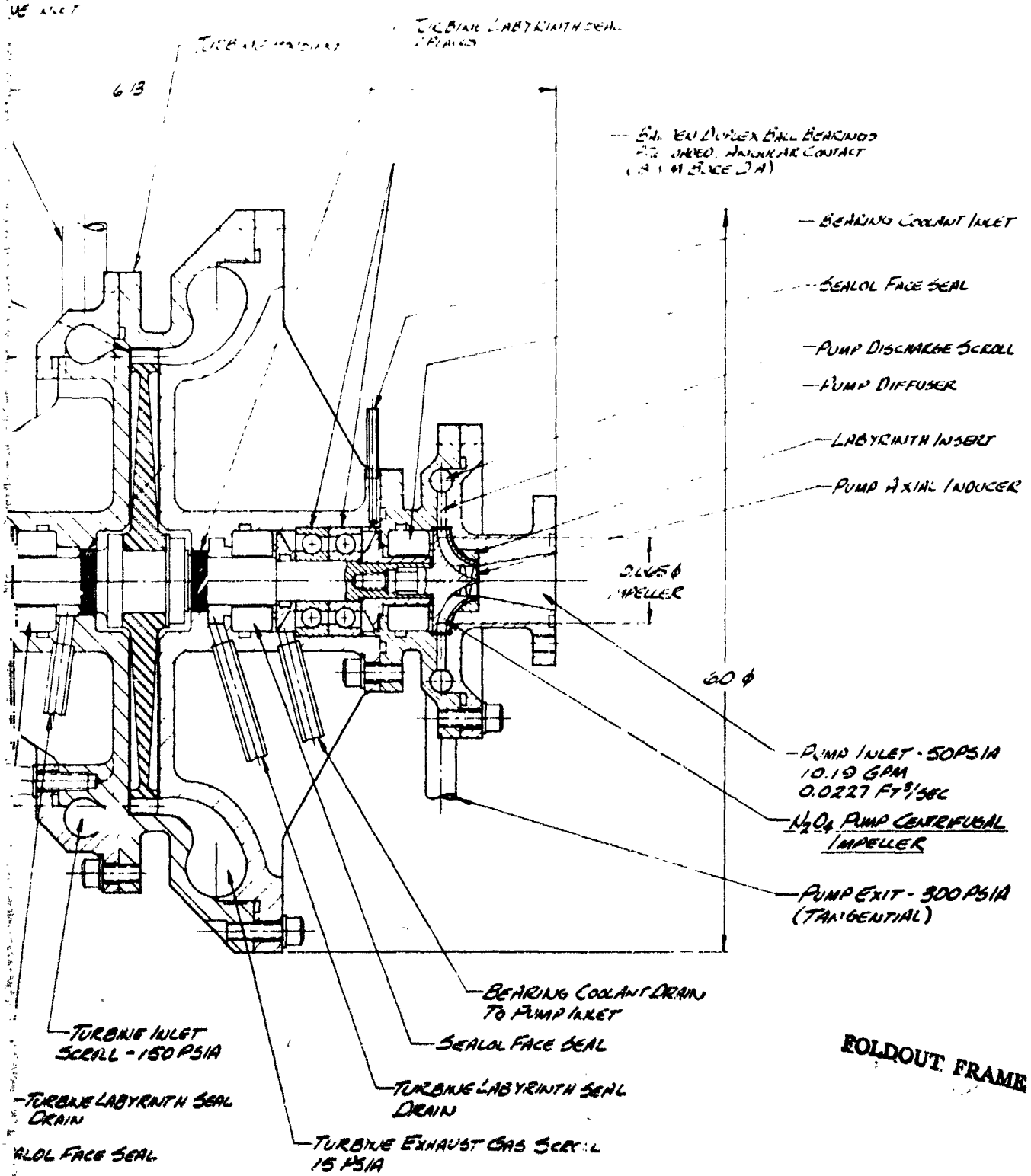

Figure 1-2 Turbine Driven Pumps for 1000 lb Thrust Bipropellant Rocket Engine

Table 1-1. Candidate Pump Drives for Bipropellant Feed Systems

System No.	System Description
1	Battery Powered, Electric Motor Driven Pumps (using lithium-thionyl-chloride batteries; at 100 watt-hr/lb energy density)
2	Battery Powered, Electric Motor Driven Pumps (using silver-zinc batteries; at 50 watt-hr/lb energy density)
3	Monopropellant (N_2H_4), Gas Generator Powered Turbopumps
4	Bipropellant (MMH/N_2O_4) Gas Generator Powered Turbopumps (using accumulators for restart)

Table 1-2. Candidate PFS Figure-of-Merit Summary

System No.	Figure-of-Merit (4.0 = maximum value)	System Ranking
1	2.80	1
3	2.65	2
2	2.20	3
4	2.05	4

1.2 CONCLUSIONS

Based upon the results of this study, the following conclusions were reached.

- **The figure-of-merit evaluation, rather than total systems mass alone, is a better criteria for ranking the candidate pump feed systems.**
- **The most significant factor for reducing bipropellant pump feed system total mass would be to convert a rocket engine from the MMH/N_2O_4 propellants with an I_{sp} of 310 seconds to LF_2/N_2H_4 with a potential of 385 seconds.**

- The battery-powered, electric motor driven pump propellant feed system (Nos. 1 and 2) can be developed for use with an "orbit insertion" rocket engine with either MMH/N_2O_4 or LF_2/N_2H_4 propellants.

- The decision as to whether lithium-thionyl-chloride batteries or silver zinc batteries should be used to power the motor-driven pumps, will depend upon the development status and reliability levels demonstrated by each type of battery at the time of program initiation.

- Because of the considerable propellant weight savings (approximately 20%) achievable with LF_2/N_2H_4, early conversion to these propellants should be considered.

- For larger total impulse rocket engine requirements, the monopropellant gas-generator powered turbopumps system (No. 3), using the LF_2/N_2H_4 propellants, would be the lightest weight candidate. Propellant for the gas generator could be stored in the main N_2H_4 tank and pressure fed to the gas generator from the main engine fuel pump. This eliminates the need for a separate N_2H_4 tank and pressure regulator, but does require the use of an accumulator (similar to system No. 4) for multiple starts.

2. INTRODUCTION

2.1 GENERAL

This study was conducted to analyze and evaluate various pump drive concepts for use with a propellant feed system for an orbit insertion, bi-propellant rocket engine. Positive displacement and centrifugal pumps were considered. In addition, battery-powered electric motors and gas-generator driven turbines were evaluated. The main emphasis was on establishing the lowest mass propellant feed system. Other factors considered were reliability, relative complexity, failure modes, transients and combustion stability characteristics and overall development risks.

2.2 GUIDELINES AND CONSTRAINTS

The pump feed system evaluations were carried out parametrically over a prescribed range of system requirements. These parameters and requirements are summarized in Table 2-1 for a baseline system and two alternate configurations.

Table 2-1. Pump Propellant Feed System Requirements

Parameter/Characteristic	Baseline System	Alternate Systems
Engine Thrust Level	1000 lbf ±30 lb	2500; 4000
Propellants		
• Oxidizer	N_2O_4	N_2O_4
• Fuel	MMH	MMH
Mixture Ratio	1.60 ±0.05	1.60 ± 0.05
Specific Impulse	310 sec	310 sec
Propellant Tank Pressure	50 psia (max)	50 psia (max)
Pump Dischange Pressure	300 psia	450; 650
Propellant Temperature Range	30° - 120°F	30° - 120°F
Total Impulse	3.6M lbf-sec	3.6M lbf-sec
Maximum Single Impulse	1.2M lbf-sec	1.2M lbf-sec
Number of Starts	20	20
Power Available During Off Times	300 watts	300 watts
Thrust Chamber Pressure, Nominal	150 psia	300, 500

A minimum of three pump-fed propulsion systems were to be evaluated. After review with the JPL Technical Monitor, the three systems selected were:

- Battery-powered, electric motor driven pumps
- Monopropellant, gas-generator powered turbopumps
- Bipropellant, gas-generator powered turbopumps

For this study, it was assumed that the pumps were not close-coupled to the rocket engine. This would permit flexibility in installing the pump feed system in the spacecraft.

2.3 STUDY OBJECTIVES

The main objective of this study was to provide parametric weight data at the subsystem and component levels for the various candidate pump-fed propulsion systems considered. In addition, system engineering analyses encompassing failure mode and effects, reliability, and development risk analyses were to be conducted. Also, dynamic systems analyses were to be carried out which would assess fluid dynamics, start and stop transients, and combustion system stability. Finally, a candidate pump-fed propulsion system was to be selected for a baseline 1000 lbf thrust engine.

3. SYSTEMS ANALYSIS

3.1 PROPELLANT CHARACTERISTICS

The most significant propellant characteristics affecting pump performance are density and vapor pressure. Other physical properties such as viscosity, thermal conductivity, and heat capacity usually have little impact on achievable performance. For the overall pump feed system, the impact of operational environmental factors must also be considered. These characteristics are outlined below for the various propellants considered in this study.

3.1.1 Nitrogen Tetroxide

The bipropellant thrust chamber oxidizer was nitrogen tetroxide (N_2O_4). The physical properties are given in Table 3-1.

Curves of density and vapor pressure versus temperature for the study range of 30° to 120°F are shown in Figures 3-1 and 3-2. Because the vapor pressure at 120°F is 50 psia and the propellant tank pressure is limited to 50 psia (maximum), the resultant net positive suction head (NPSH) available to the oxidizer pump is zero. Since this will cause cavitation to occur, the maximum temperature assumed for the N_2O_4 in this study was 100°F. This provides a NPSH of 20 psi which should be adequate. Similarly, the density was taken at 100°F in determining oxidizer pump volumetric flow and developed head.

3.1.2 Monomethyl Hydrazine

The bipropellant thrust chamber fuel utilized was monomethyl hydrazine (N_2H_3-CH_3). The physical properties are given in Table 3-2.

Curves of density and vapor pressure versus temperature for the study range of 30° to 120°F are shown in Figures 3-3 and 3-4.

3.1.3 Hydrazine

The gas generator for the monopropellant powered turbopumps uses hydrazine (N_2H_4). The physical properties are given in Table 3-3.

Curves of density and vapor pressure versus temperature are shown in Figures 3-5 and 3-6.

Table 3-1. Physical Properties of Nitrogen Tetroxide

Molecular Weight	92.016
Freezing Point	11.8°F
Boiling Point (at 14.7 psia)	70°F
Critical Temperature	316°F
Critical Pressure	1470 psia
Heat of Vaporization	1782 Btu/lb

	Temperature, °F		
	30	100	120
Vapor Pressure, psia	5	30	50
Specific Gravity	1.5	1.4	1.375
Heat Capacity, Btu/lb-°F	0.355	0.380	0.383
Viscosity, lb/ft-sec x 10^5	34	22	20
Thermal Conductivity, Btu/ft-hr-°F	0.083	0.071	0.069

3.2 ROCKET ENGINE CHARACTERISTICS

This study was related primarily to an evaluation of various bipropellant feed systems. It was conducted parametrically over a range of thrust levels and thrust chamber pressures for the system requirements specified in Table 1-1. However, various assumptions had to be made regarding the rocket engine characteristics. For the baseline system (1000 lbf thrust), these were based upon the Marquardt Model R-40B bipropellant rocket engine. For the higher thrust level alternate systems (2500, 4000 lbf thrust), the same characteristics were assumed. These are briefly discussed below.

3.2.1 Thrust Levels

The Model R-40B rocket engine has a nominal thrust level of 900 lbf at a feed pressure of 238 psia and a mixture ratio of 1.65. However, it has the capability of being operated over a thrust range from 600 to 1300 lbf with feed pressures from 150 to 400 psia and mixture ratios of 1.0 to 2.7. Hence, it is compatible with the requirements of the baseline propellant feed system. Similar engines could be developed for the higher thrust levels considered in the study.

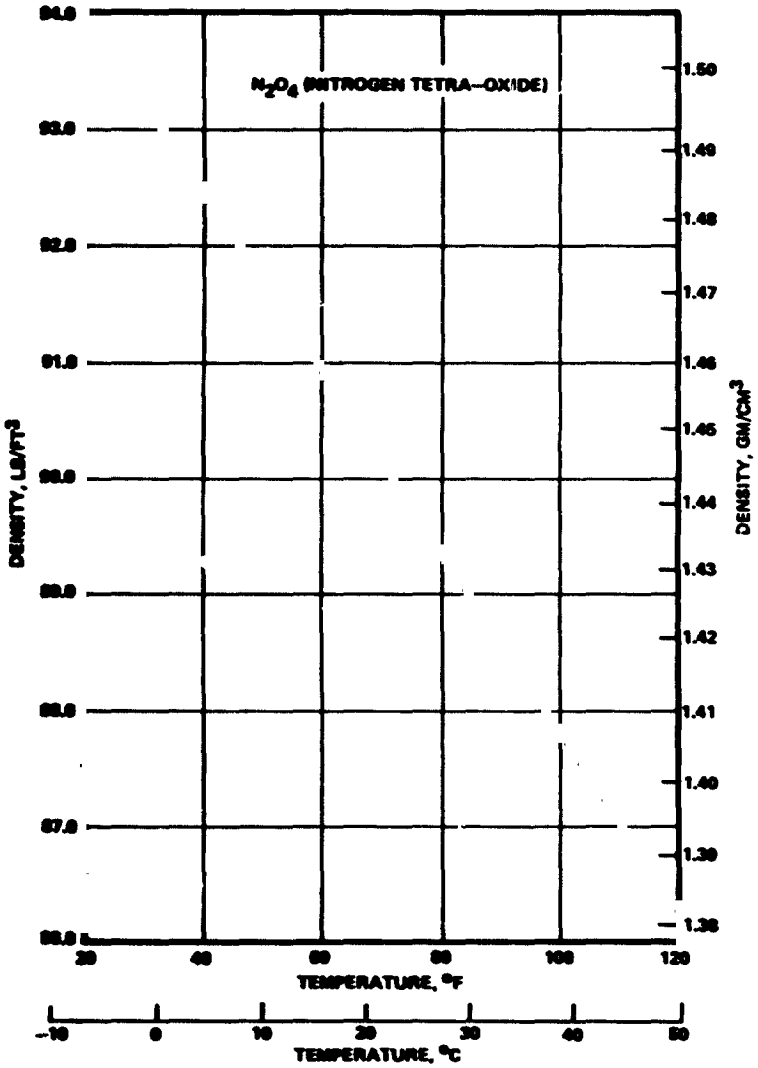

Figure 3-1. N_2O_4 Variation of Density with Temperature

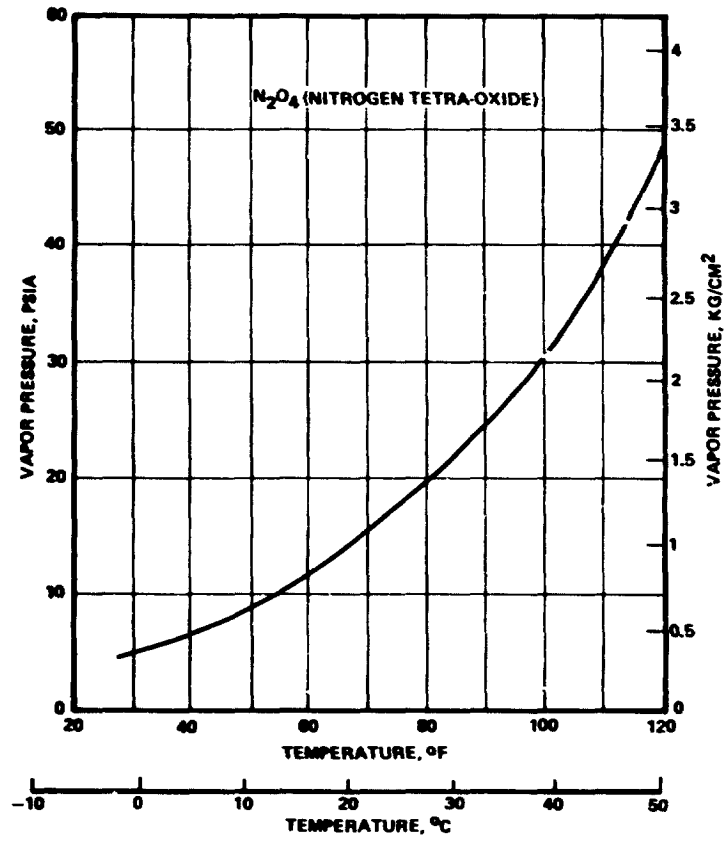

Figure 3-2. N_2O_4 Variation of Vapor Pressure with Temperature

Table 3-2. Physical Properties of Monomethyl Hydrazine

Molecular Weight	46.075
Freezing Point	-63°F
Boiling Point (at 14.7 psia)	189°F
Critical Temperature	609°F
Critical Pressure	1195 psia
Heat of Vaporization	377 Btu/lb

	Temperature, °F		
	30	100	120
Vapor Pressure, psia	0.20	2.0	5.0
Specific Gravity	0.90	0.86	0.84
Heat Capacity, Btu/lb-°F	0.69	0.70	0.71
Viscosity, lb/ft-sec x 10^5	90	45	36
Thermal Conductivity, Btu/ft-hr-°F	0.146	0.142	0.140

3.2.2 Specific Impulse

The Model R-40B rocket engine utilizing the standard configuration with a RAO type nozzle has a steady-state specific impulse, at an area ratio (ϵ) of 100, of 298 seconds (see Figure 3-7). This can be uprated to 310 seconds by using a 4-inch combustion chamber, an optimized RAO nozzle, and increasing the area ratio to 230. Minor injector modifications will yield a 310 I_{sp} at reduced area ratio. While the increased area ratio will create some weight and volume penalties over the standard configuration, this is more than compensated for by the 12-second improvement in specific impulse. Hence, for this study a specific impulse of 310 seconds was assumed for all thrust levels.

3.2.3 Propellant Flow Rates

The propellant flow rates for the thrust levels considered vary from 10 to 42 gpm. Since the total impulse for all systems remains constant (3.6M lbf-sec), the total mass of the propellants and the volume of the propellant tanks remains the same. However, since pump brake horsepower is a direct function of flow rate, the output power required from the pump drive (turbine; electric motor) is 4.2 times greater at the 4000 lbf thrust level than at the 1000 lbf thrust level. This results in a dry weight penalty of the pump drives for the higher thrust levels.

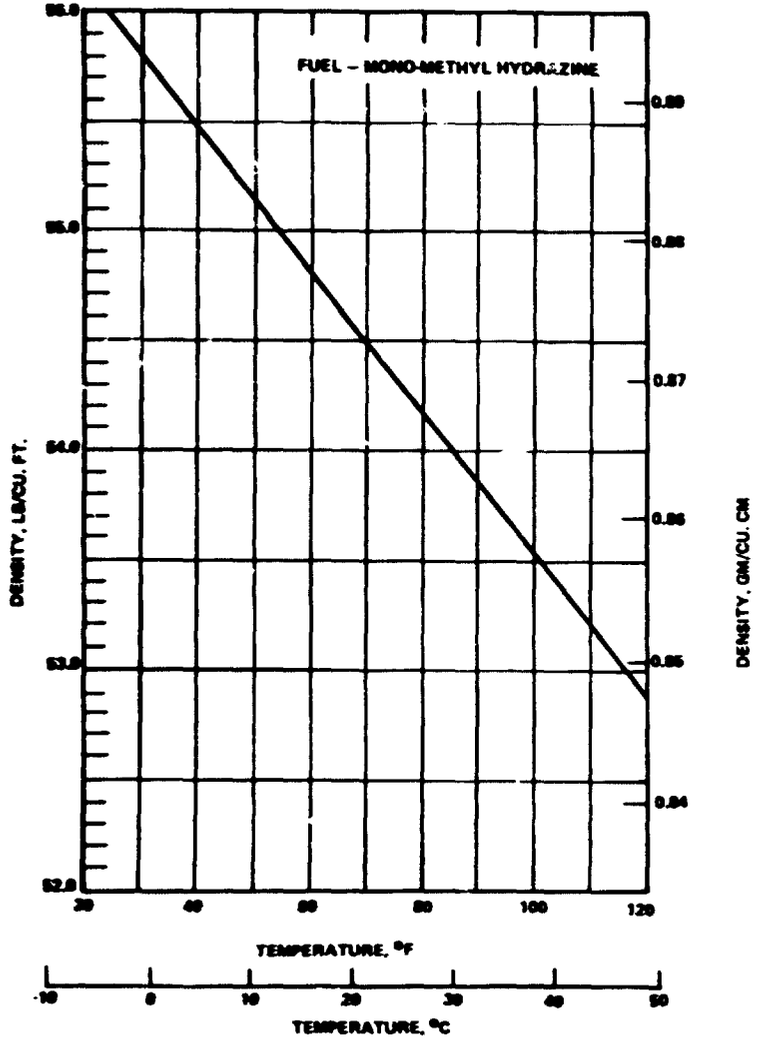

Figure 3-3. MMH Variation in Density with Temperature

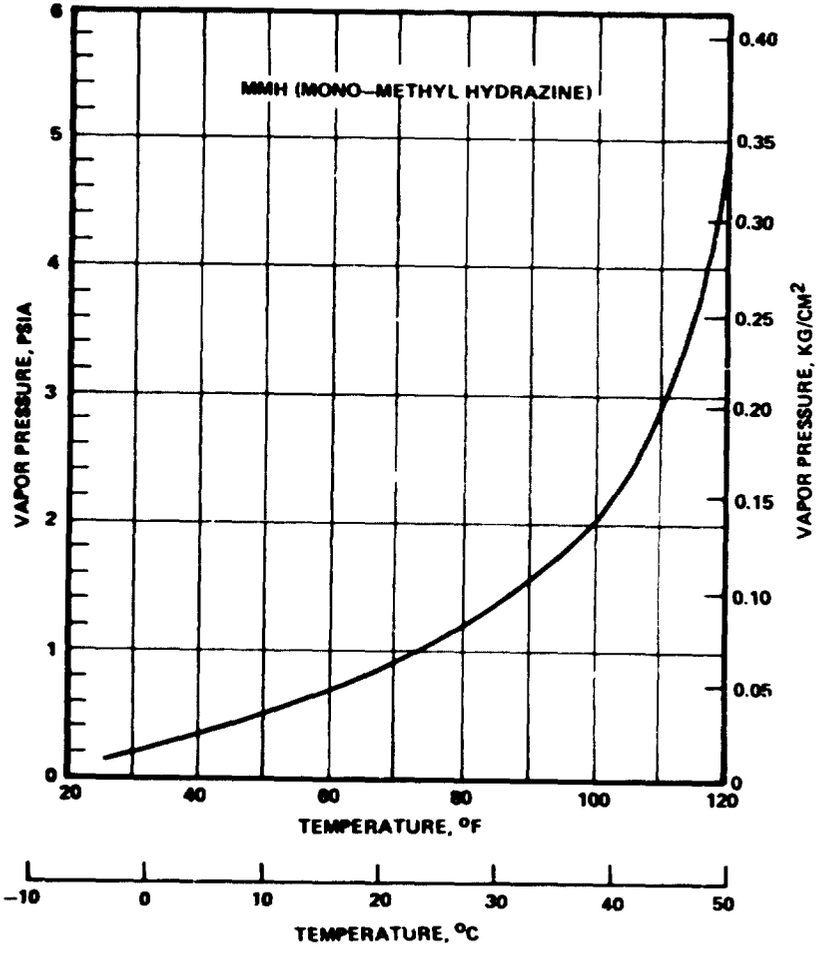

Figure 3-4. MMH Variation in Vapor Pressure with Temperature

Table 3-3. Physical Properties of Hydrazine

Molecular Weight	32.048
Freezing Point	35.1°F
Boiling Point (at 14.7 psia)	236.3°F
Critical Temperature	716°F
Critical Pressure	2131 psia
Heat of Vaporization	540 Btu/lb

	Temperature, °F		
	30	100	120
Vapor Pressure, psia	(.06	0.60	1.0
Specific Gravity	1.02	0.99	0.98
Heat Capacity, Btu/lb-°F	0.730	0.745	0.750
Viscosity, lb/ft-sec x 10^5	85	50	44
Thermal Conductivity, Btu/ft-hr-°F	0.212	0.202	0.200

3.2.4 Thrust Chamber Pressure

The rocket engine thrust chamber pressures used in this parametric study were 150, 300, and 500 psia. For a selected nozzle area ratio (ϵ = 230), the higher pressures result in a smaller size nozzle. However, this is offset to a degree by the increased wall thicknesses required to maintain acceptable stress levels. In addition, the higher chamber pressures also affect the required pump discharge pressures and pump drive brake horsepower requirements. It is beyond the scope of this study to consider weight tradeoffs for the thrust chamber assembly. However, if nozzle area ratios of 230 are required to achieve a specific impulse of 310 seconds, it is obvious the nozzle weight can become a fairly significant factor in the dry weight of an overall propellant feed system-thrust chamber assembly configuration. Allowable stowage volume introduces another important factor in this determination.

3.2.5 Injector Pressure Drop

The required TCA injector pressure drop is an important parameter since it is directly related to maintaining combustion stability. In general, the higher the pressure drop, the greater the certainty that combustion

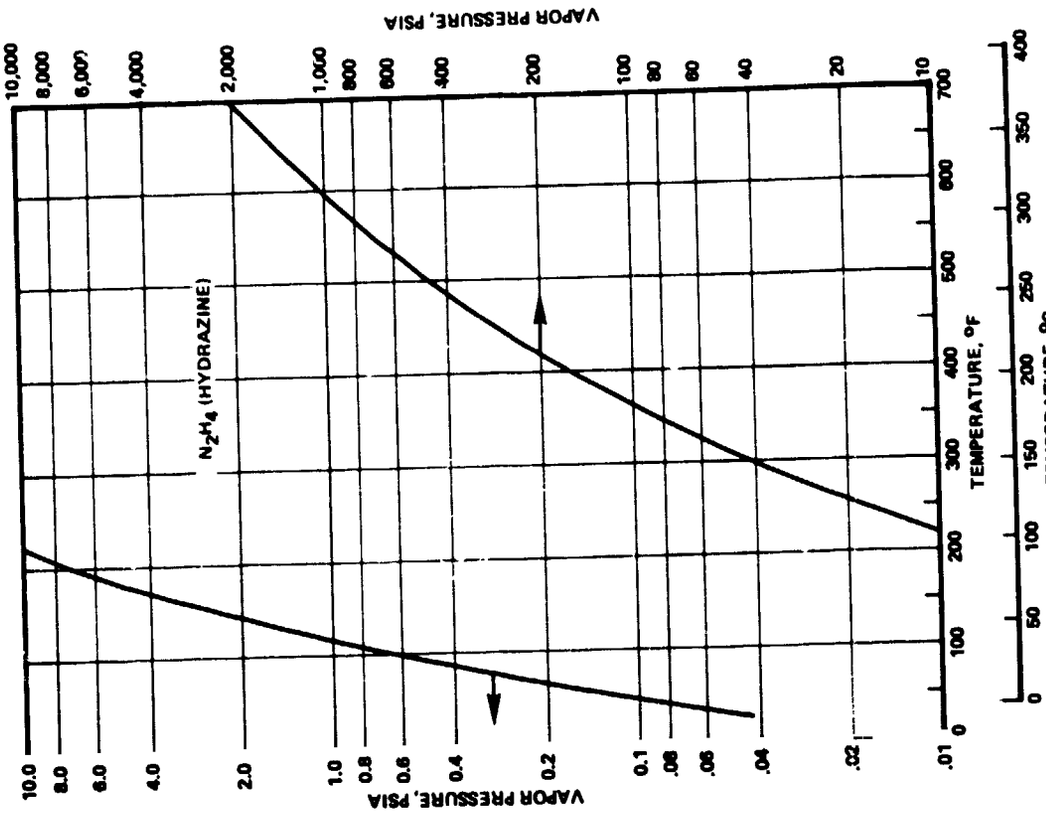

Figure 3-6. Hydrazine Variation in Vapor Pressure with Temperature

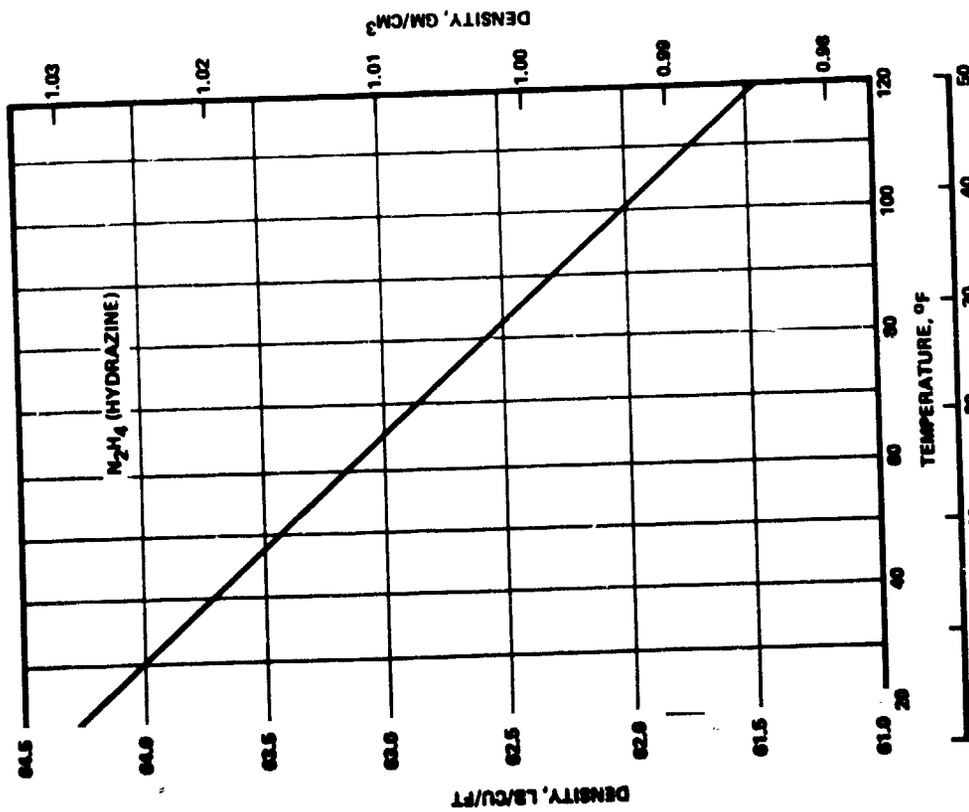

Figure 3-5. Hydrazine Variation in Density with Temperature

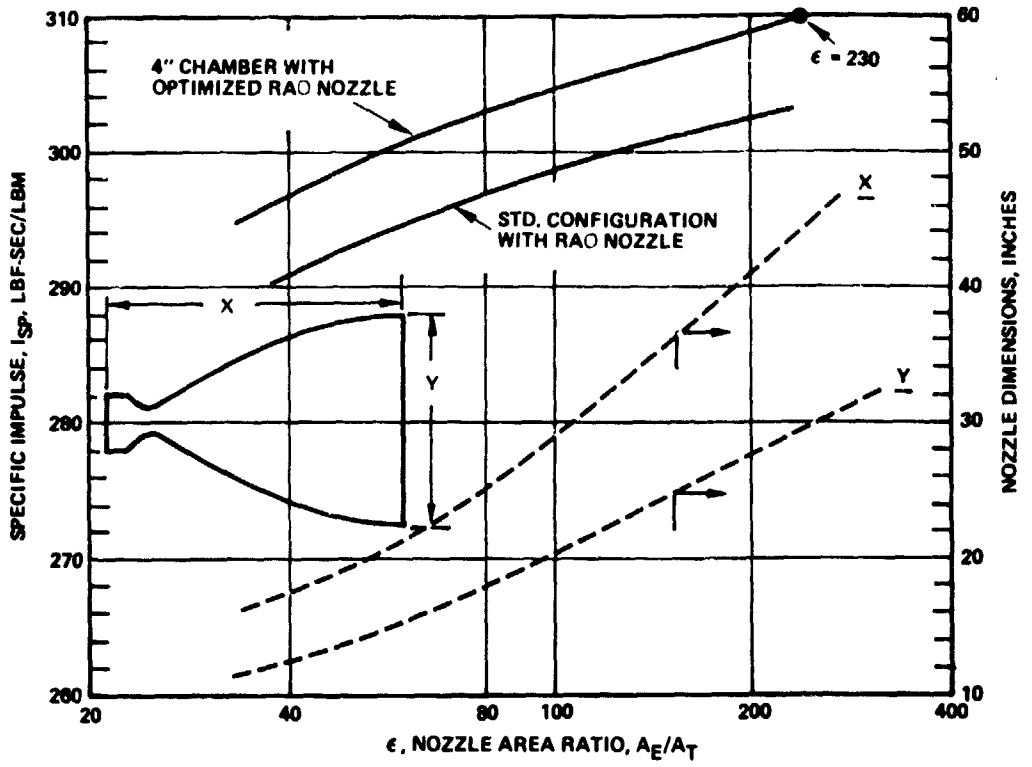

Figure 3-7. Marquardt Model R-40B Bipropellant Rocket Engine (Nominal 900 lbf Thrust)

stability will be maintained. However, similar to the thrust chamber level, the higher the injector ΔP, the greater the required pump discharge pressures and pump drive brake horsepower requirements. For this study, a moderately conservative approach was taken by assuming a 150 psid injector pressure drop for all systems (including feed line losses).

3.2.6 Pump Discharge Pressures

The pump discharge pressures ranged from 300 to 650 psia. With the pump inlet pressures remaining constant at 50 psia, the pump pressure rises varied from 250 to 600 psi. Since the pump brake horsepower requirements are directly proportional to pump pressure rise, this results in a pump BHP increase of 2.4 times over the range considered. Hence, the lower pump discharge pressures would tend to have a favorable effect on achieving low propellant system dry weights.

3.3 PUMP REQUIREMENTS

The pump flow rates are a function of the TCA specific impulse, the mixture ratio, and the thrust level. These are summarized in Table 3-4. Since the vapor pressure of N_2O_4 at 120°F is 50 psia (Table 3-1), which results in a zero net positive suction head (NPSH), the density of the oxidizer was taken at 100°F to determine pump volumetric flow rates. This results in a positive 20 psi NPSH which should be adequate to prevent pump cavitation. For consistency, the volumetric flow rates for the fuel pump were also taken at 100°F even though the available NPSH at 120°F was more than adequate.

Using the data in Table 3-4 and earlier TCA pressure drop assumptions, the pump design characteristics were established for the three thrust levels (Tables 3-5, 3-6, and 3-7). The pump efficiencies have been assumed to increase somewhat with the higher engine thrust levels (Figure 3-8). This is consistent with the increase in volumetric efficiencies and specific speeds resulting from the higher engine thrust level flow rates.

3.4 PUMP PERFORMANCE CHARACTERISTICS

There are two basic types of pumps that can be considered for the propellant feed system. These are positive displacement types and centrifugal types. Within these two categories there are also various configurations which can be considered. These are discussed below.

3.4.1 Positive Displacement Types

There are various types of positive displacement pumps. These are:

- Piston Pumps
- Vane Pumps
- Gear Pumps
- Rotary Pumps (IMO or Roots Type)

For positive displacement pumps, the flow rate is essentially constant for a given rotative speed. Leakage losses tend to increase with higher discharge pressures causing a small reduction in the flow rate, as is shown by the sloping dashed lines of Figure 3-9.

Table 3-4. Pump Flow Rate Requirements

Parameter	Thrust Level, lbf		
	1000	2500	4000
Specific Impulse, I_{sp}, sec	310	310	310
Engine Flow Rate, $\dot{m}$, lb/sec	3.23	8.06	12.9
Mixture Ratio, $r = \dot{W}_o/W_f$	1.60	1.60	1.60
Propellants			
• Oxidizer	N_2O_4	N_2O_4	N_2O_4
• Fuel	MMH	MMH	MMH
Density, ρ_o (at 100°F), lb/ft^3	87.8	87.8	87.8
ρ_f (at 120°F), lb/ft^3	52.9	52.9	52.9
ρ_i (at 100°F), lb/ft^3	53.6	53.6	53.6
Vapor Pressure, VP_o (at 100°F), psia	30.0	30.0	30.0
VP_f (at 120°F) psia	5.0	5.0	5.0
Pump Flow Rates, $\dot{W}_f$, lb/sec	1.24	3.10	4.96
$\dot{W}_o$, lb/sec	1.99	4.96	7.96

Piston Type

This pump essentially uses one or more reciprocating pistons to provide the flow rates required. When used in conjunction with a turbine or electric motor drive, a nutating wobble plate is employed to convert the rotary motion into reciprocating motion. This is usually a high-friction device and, because of limitations in piston velocities, operates at comparatively low pump drive rotative speeds. However, for very low specific speed conditions (i.e., low flow rate and high discharge pressures), it can sometimes result in achieving the highest efficiencies (Figure 3-9a).

Table 3-5. Pump Design Characteristics
(F = 1000 lbf)

Parameter	Thrust Level, lbf		
	1000	1000	1000
Chamber Pressure, P_c, psia	150	300	500
System ΔP, psi	150	150	150
Pump Discharge Pressure, psia	300	450	650
Pump Inlet Pressure, psia	50	50	50
Pump Pressure Rise, psi	250	400	600
ΔP_f, ft	643	1029	1543
ΔP_o, ft	405	650	975
Pump Flow Rate, V_f, gpm	10.52	10.52	10.52
, cfs	0.0234	0.0234	0.0234
Pump Flow Rate, V_o, gpm	10.19	10.19	10.19
, cfs	0.0227	0.0227	0.0227
Pump Efficiency	0.65	0.65	0.65
Pump Brake Horsepower			
BHP_f	2.36	3.79	5.66
BHP_o	2.29	3.66	5.48
Pump Speed, N, rpm	84,000	84,000	84,000
Specific Speed, N_{s_f} (cfs Basis)	100.7	81.2	52.3
N_{s_o} (cfs Basis)	140.0	98.3	72.5
Suction Specific Speed			
S_f (120°F, gpm Basis)	7,517	7,517	7,517
S_o (100°F, gpm Basis)	19,749	19,749	19,749

Table 3-6. Pump Design Characteristics
(F = 2500 lbf)

Parameter	Thrust Level, lbf		
	2500	2500	2500
Chamber Pressure, P_c, psia	150	300	500
System ΔP, psi	150	150	150
Pump Discharge Pressure, psia	300	450	650
Pump Inlet Pressure, psia	50	50	50
Pump Pressure Rise, ΔP, psi	250	400	600
ΔP_f, ft	643	1029	1543
ΔP_o, ft	405	650	975
Pump Flow Rate, V_f, gpm	26.35	26.35	26.35
cfs	0.0585	0.0585	0.0585
V_o, gpm	25.47	25.47	25.47
cfs	0.0568	0.0568	0.0568
Pump Efficiency	0.70	0.70	0.70
Pump Brake Horsepower			
BHP_f	5.46	8.76	13.1
BHP_o	5.30	8.48	12.73
Pump Speed, N, rpm	84,000	84,000	84,000
Specific Speed, N_{s_f} (cfs Basis)	159.2	111.9	82.5
N_{s_o} (cfs Basis)	220.7	154.7	114.2
Suction Specific Speed			
S_f (120°F, gpm Basis)	11,883	11,883	11,883
S_o (100°F, gpm Basis)	31,176	31,176	31,176

Table 3-7. Pump Design Characteristics
(F = 4000 lbf)

Parameter	Thrust Level, lbf		
	4000	4000	4000
Chamber Pressure, P_c, psia	150	300	500
System ΔP, psi	150	150	150
Pump Discharge Pressure, psia	300	450	650
Pump Inlet Pressure, psia	50	50	50
Pump Pressure Rise, ΔP, psi	250	400	600
ΔP_f, ft	643	1029	1543
ΔP_o, ft	405	650	975
Pump Flow Rate, V_f, gpm	42.08	42.08	42.08
cfs	0.0936	0.0936	0.0936
V_o, gpm	40.75	40.75	40.75
cfs	0.908	0.908	0.908
Pump Efficiency	0.75	0.75	0.75
Pump Brake Horsepower			
BHP_f	8.70	13.97	20.85
BHP_o	8.0	12.79	19.18
Pump Speed, N, rpm	84,000	84,000	84,000
Specific Speed, N_{s_f} (cfs Basis)	203.5	143.0	105.6
N_{s_o} (cfs Basis)	281.7	197.5	145.8
Suction Specific Speed			
S_f (120°F, gpm Basis)	15,504	15,504	15,504
S_o (100°F, gpm Basis)	39,670	39,670	39,670

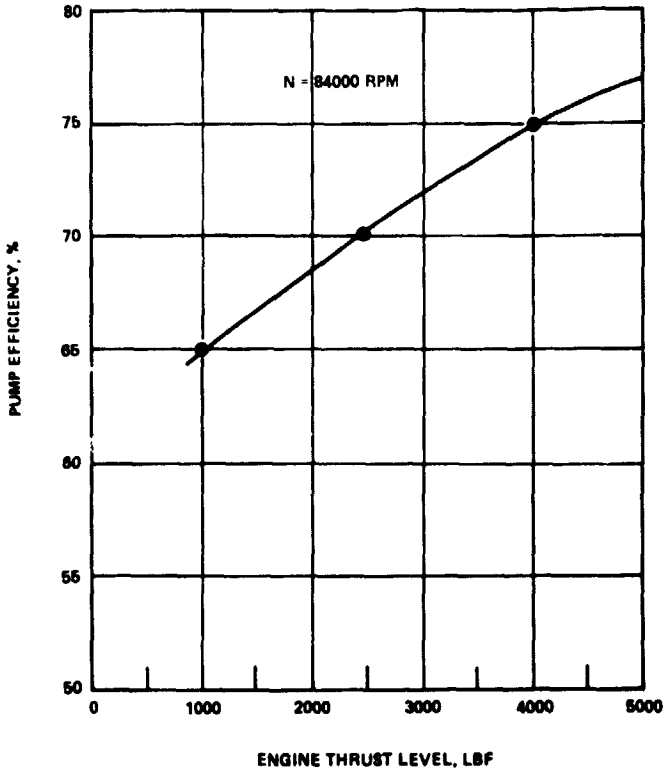

Figure 3-8. Pump Efficiency Variation with Engine Thrust Level

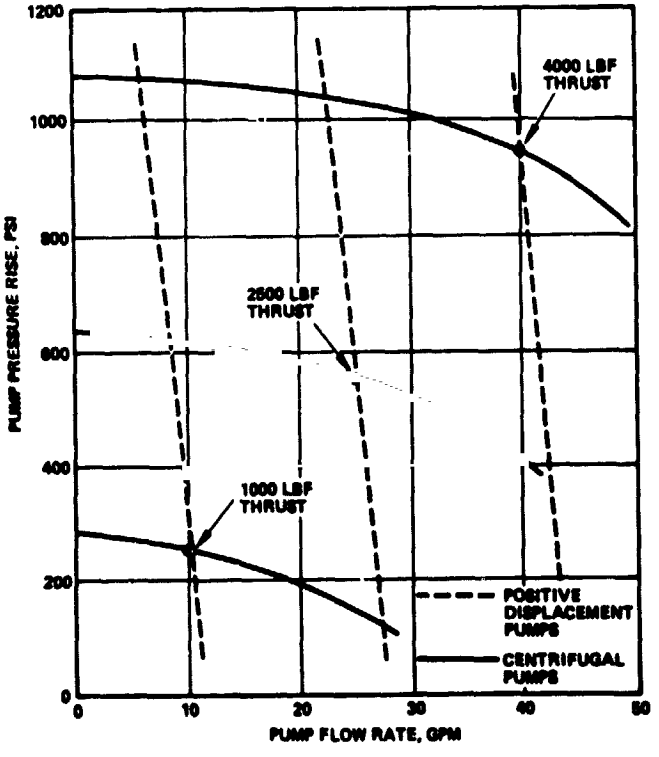

Figure 3-9. Typical Head Capacity Curves

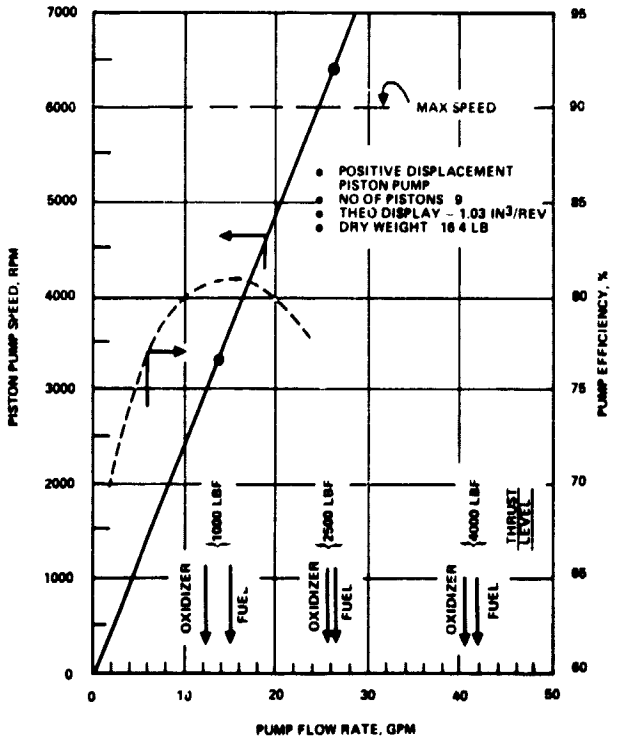

Figure 3-9a. Piston Type Pump Performance Range

Vane Type

Vane type pumps have one or more spring-loaded vanes operating in an eccentric circular housing. This eliminates the need for a wobble plate but essentially has the same performance characteristics of the piston pump. High discharge pressures tend to put a heavy load on the bearings, thus lowering the mechanical efficiency of the unit. However, because the vanes operate with essentially zero clearance with respect to the housing, high volumetric efficiencies can be achieved.

Gear Type

This pump uses the clearance spaces between a set of meshing spur gears and the housing to provide the required volumetric flow. It is capable of operating at higher rotative speeds than the piston or vane type pumps since a finite clearance is employed between the gears and the housing. In this case mechanical efficiencies can be quite high, but volumetric efficiencies are usually somewhat lower.

Rotary (IMO or Roots) Type

This pump is similar to the gear pump except that pumping and flow can occur in a longitudinal direction in the volume available in two meshing helical lobed rotors (IMO pump). Axial pressure balancing can be employed to minimize loads on the thrust bearing. Slide valve porting also gives this pump the capability of varying the flow rate over a fairly wide range while still operating at constant speed. Despite achievable high mechanical efficiencies, required lobe clearances result in low volumetric efficiencies.

3.4.2 Centrifugal Pumps

For high rotative speeds at moderate flow rates and pressure rises, the centrifugal pump can usually provide the highest efficiencies at the lowest mass. This makes them compatible with high speed turbine and motor drives. A centrifugal pump consists of an impeller, diffuser, and discharge scroll. To achieve high suction specific speeds, an axial inducer is utilized. Typical head-capacity curves are shown in Figure 3-9.

Radial Flow Type

The radial flow centrifugal pump is normally employed in the high specific speed range (40-600). For maximum efficiency, the radial impeller employs backward swept vanes which are shrouded to minimize recirculatory flow losses. Front and rear labyrinth or face seals are used to reduce leakage losses. The impeller outer diameter can be determined from the specific diameter value D_s, at the best efficiency point from the following relationship:

$$D_o = \frac{D_s \sqrt{Q}}{(\Delta P)^{0.25}}$$

where

D_s = specific diameter (at best efficiency point)

ΔP = pump pressure (ft)

Q = pump flow rate (gpm)

The value of D_s is obtained from experimental data. Since the impeller outer diameter directly affects the size of the pump, the higher the rotative speed, the smaller and lighter the pump becomes.

Axial Flow Type

The axial flow centrifugal pump is normally employed in the high specific speed range (600 to 10,000). These high values result from either high flow rates or low pressure rises and a combination of both. Axial pump impellers employ helical vanes, with the fluid entering and leaving the pump in an axial direction. Similar to radial flow pumps, shrouds, seals, and diffusers are also utilized to maximize the pump efficiency.

Axial Inducers

The axial inducer is similar to the axial flow pump. It is used at the inlet to a radial flow pump to increase its suction specific speed. Its function is to provide a small pressure rise at the inlet to the radial impeller to prevent the occurrence of cavitation when operating at high rotative speeds.

Diffusers

The function of a pump diffuser is to convert a portion of the kinetic energy in the fluid leaving the radial impeller into static pressure. By so doing, the overall efficiency of the pump is increased. Both vaneless and vaned diffusers can be utilized.

3.4.3 Candidate Propellant Feed Systems Pumps

The rationale for selection of the candidate propellant feed systems pumps is to choose the type that will provide the highest efficiency at the lowest weight. Tables 3-5 to 3-7 identified the desired pump performance characteristics. From these data it was determined that the pump specific speeds fell into the ranges shown in Table 3-8.

The actual values as a function of thrust level and pump pressure rise, are summarized in Figures 3-10 to 3-12. The estimated performance and design characteristics of the various type pumps considered in this study are depicted in Figure 3-13. It can clearly be seen that in the specific speed range from 50 to 270 (which encompasses all the values in Table 3-8), the highest efficiencies can be obtained with centrifugal pumps.

Figure 3-14 also reflects this as well as indicating that centrifugal pumps require smaller specific diameters and hence, result in lighter weight configurations.

Table 3-8. Pump Specific Speed Range

Thrust Level (lbf)	Specific Speed, N_s (on cfs basis)	
	Oxidizer Pump	Fuel Pump
1000	70-140	50-100
2500	110-220	80-160
4000	140-270	100-190

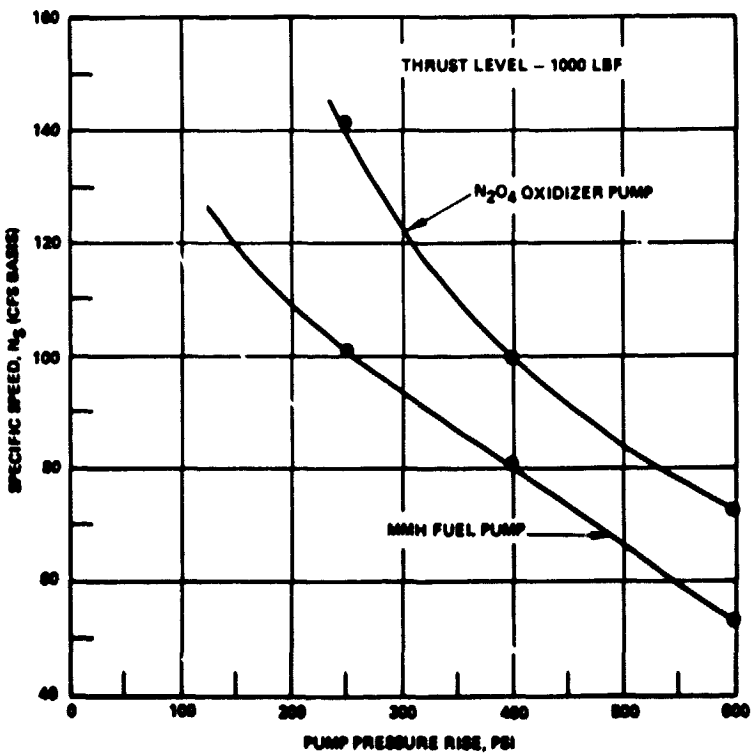

Figure 3-10. Specific Speed Versus Pump Pressure Rise (F = 1000 lbf)

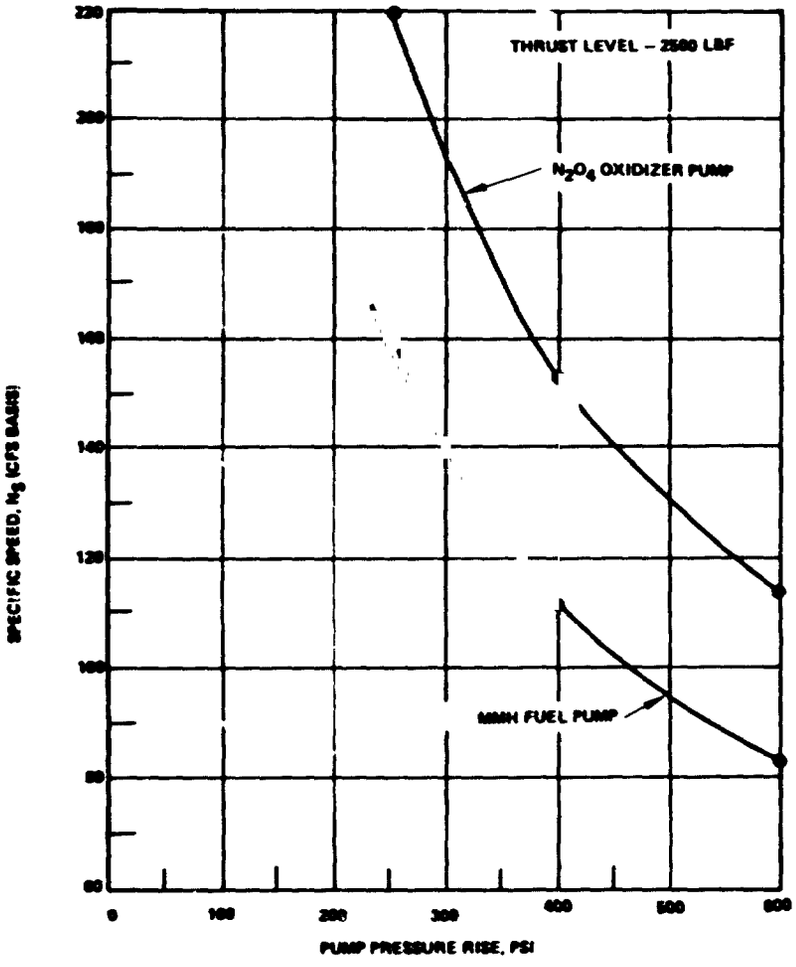

Figure 3-11. Specific Speed Versus Pump Pressure Rise (F = 2500 lbf)

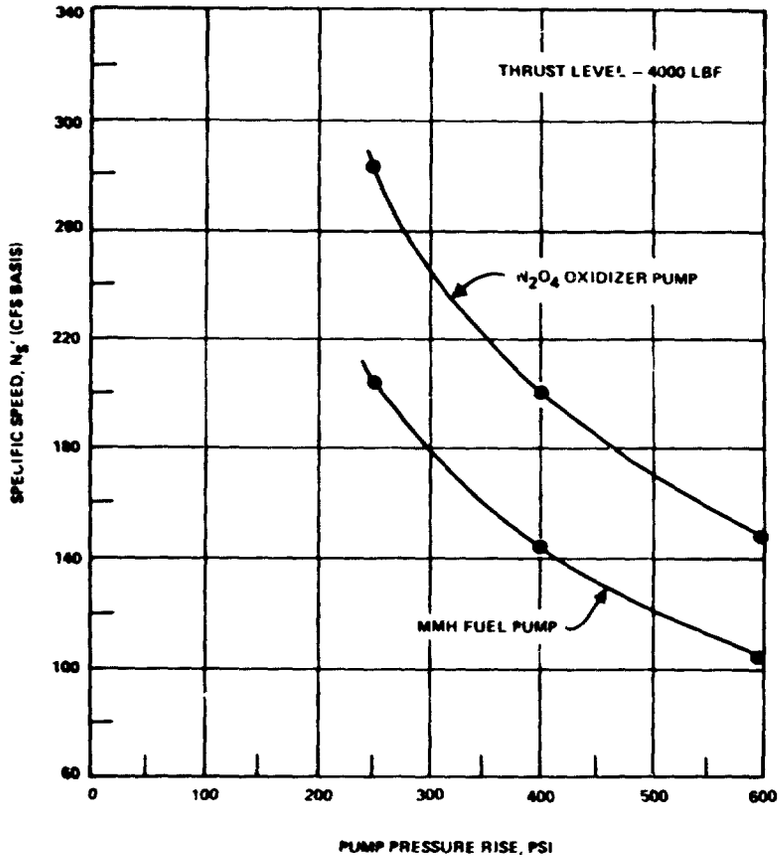

Figure 3-12. Specific Speed Versus Pump Pressure Rise (F = 4000 lbf)

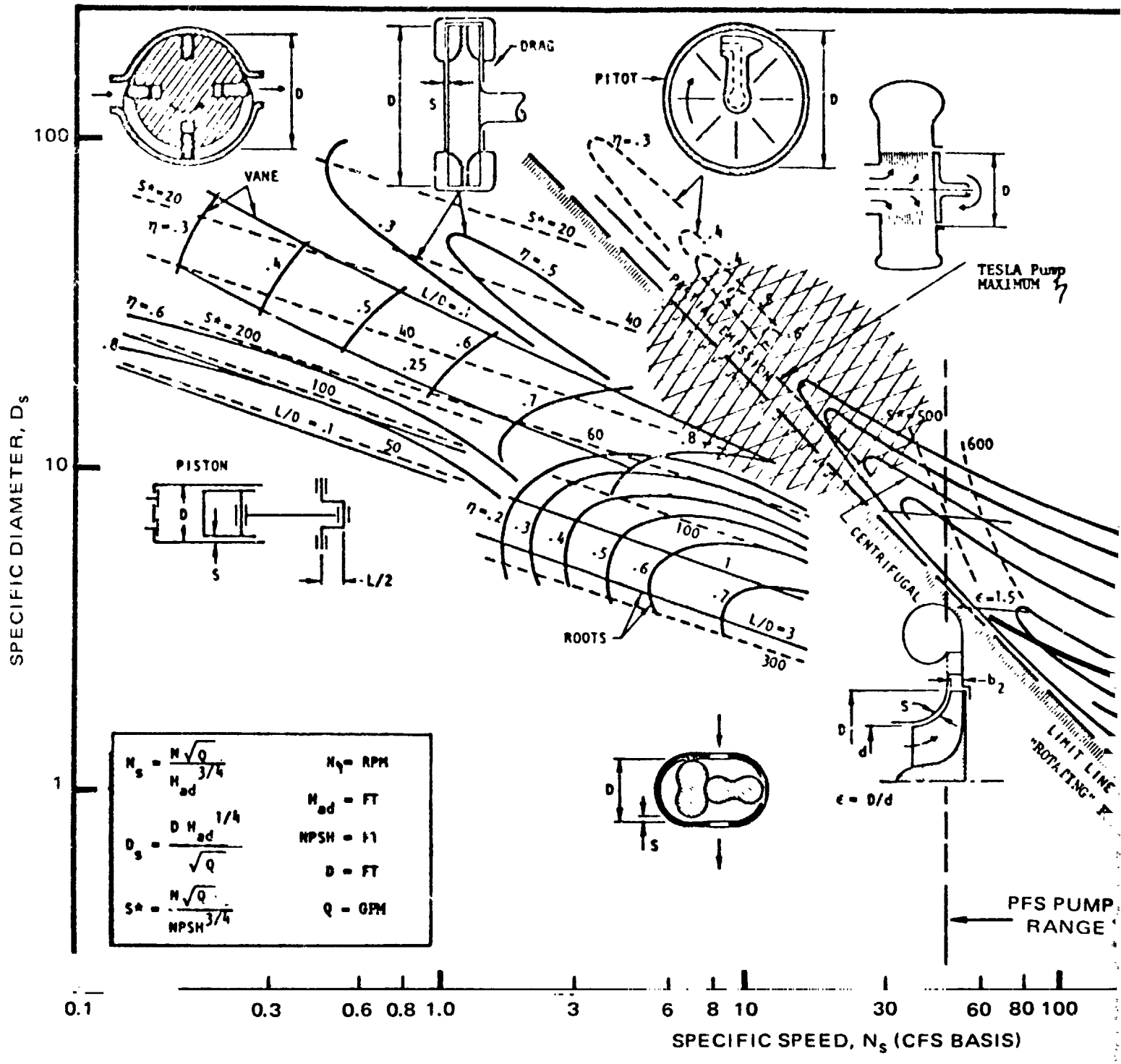

FOLDOUT FRAME

ORIGINAL PAGE IS
OF POOR QUALITY

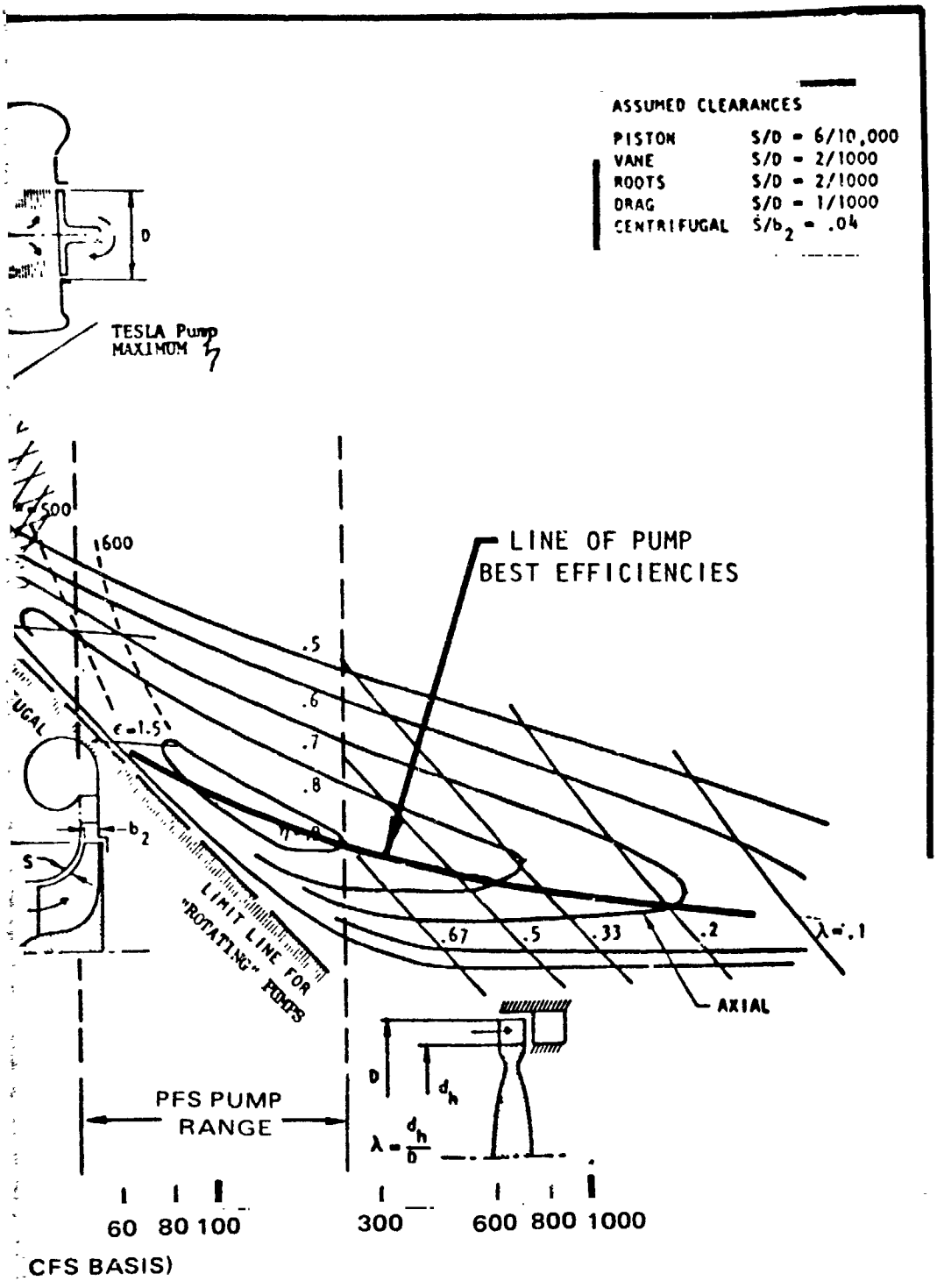

Figure 3-13. N_s-D_s Diagram for Pumps

FOLDOUT FRAME 2

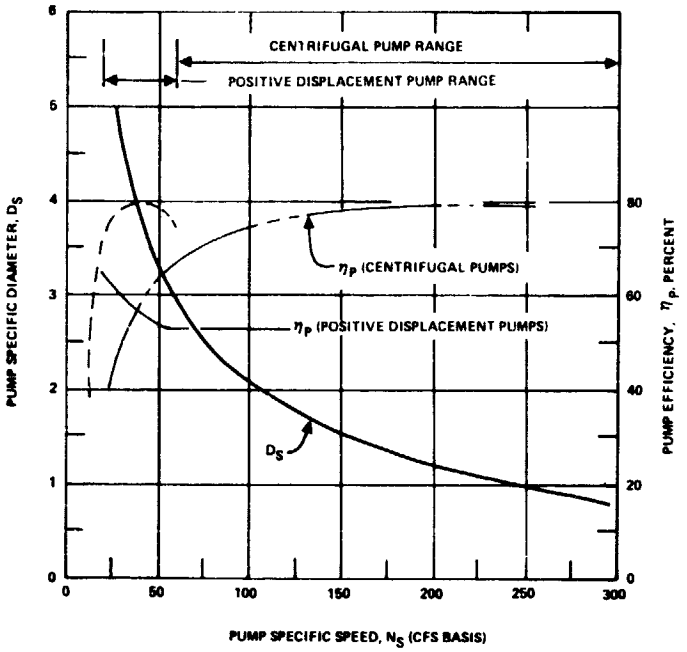

Figure 3-14. Pump Specific Diameters and Efficiencies as a Function of Specific Speed

Another factor in selecting a candidate pump is the required suction specific speed as indicated in Figure 3-15. The MMH fuel pump range is from 7700 to 15,200, and the N_2O_4 oxidizer pump requirements are much higher at 20,000 to 40,000. In order to achieve these values, the preferred pump configuration is to use an axial inducer in conjunction with a centrifugal impeller. Positive displacement pumps are usually limited to a suction specific speed range of 5,000 to 10,000. This would limit the speed of these type pumps to approximately 10,000 rpm, which would result in a much heavier configuration than centrifugal pumps rotating at 84,000 rpm.

Because of the foregoing, the candidate pump selected for the propellant feed system was the centrifugal pump with an axial inducer. The impeller diameters and weight estimates for the oxidizer and fuel pumps are shown in Tables 3-9 to 3-11 for the various engine thrust levels. Total pump weights vary from 0.7 to 2.2 pounds. The pump impeller outside diameters are plotted parametrically in Figures 3-16 and 3-17.

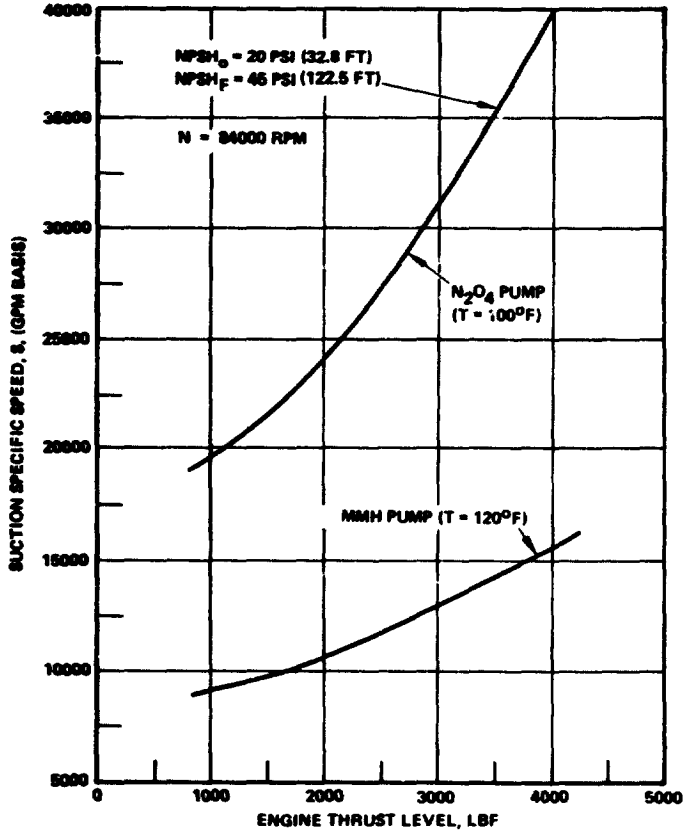

Figure 3-15. Pump Suction Specific Speed Versus Engine Thrust Level

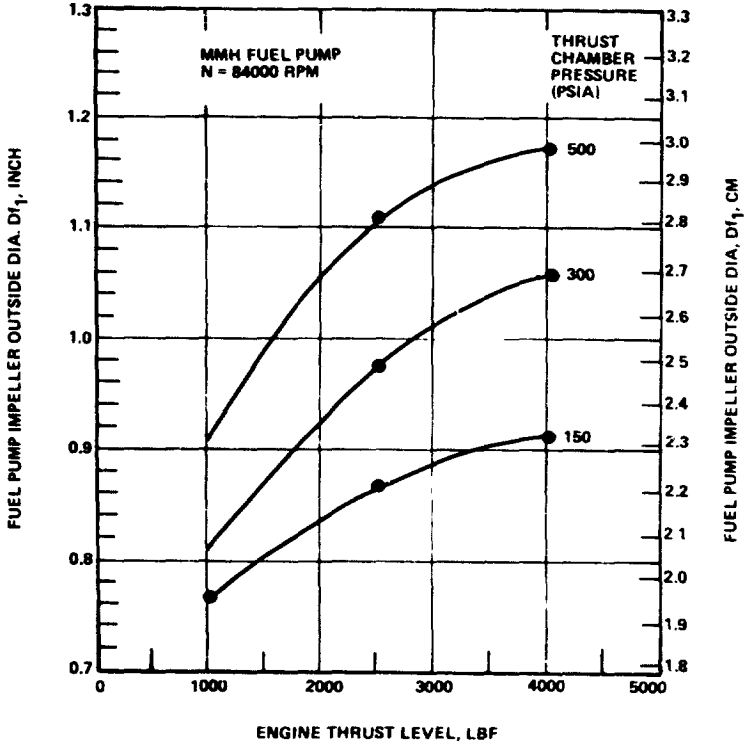

Figure 3-16. Fuel Pump Impeller Outside Diameter Variation with Engine Thrust Level and Thrust Chamber Pressure

Table 3-9. Centrifugal Pump – Impeller Diameter and Weight Estimate (F = 1000 lbf)

Parameter	Thrust Level, lbf		
	1000	1000	1000
Specific Speed, N_{s_f}	100.7	81.2	52.3
N_{s_o}	140.0	98.3	72.5
Specific Diameter, D_{s_f}	2.1	2.5	3.1
D_{s_o}	1.65	2.15	2.6
Pump Pressure Rise, ΔP_f (ft)	643	1029	1543
ΔP_o (ft)	405	650	975
Pump Flow Rate, V_f (cfs)	0.0234	0.0234	0.0234
V_o (cfs)	0.0227	0.0227	0.0227
$D_{l_f} = \frac{D_{s_f}\sqrt{V_f}}{(\Delta P_f)^{0.25}} \times 12$; inch	0.766	0.810	0.908
$D_{l_o} = \frac{D_{s_o}\sqrt{V_o}}{(\Delta P_o)^{0.25}} \times 12$; inch	0.665	0.770	0.841
Impeller Weight, lb			
$W_{Imp\ (f)}$	0.0115	0.0129	0.0162
$W_{Imp\ (o)}$	0.0087	0.0097	0.0122
Pump Weight, lb, $W_{p(f)}$	0.115	0.129	0.162
(Including Housings), $W_{p(o)}$	0.087	0.097	0.122
Pump Shaft, Bearings, Seals, Weight	0.5	0.75	1.0
Total Pump Weight, W_p	0.702	0.976	1.28

Table 3-10. Centrifugal Pump – Impeller Diameter, and Weight Estimate (F = 2500 lbf)

Parameter	Thrust Level, lbf		
	2500	2500	2500
Specific Speed, N_{s_f}	159.2	111.9	82.5
N_{s_o}	220.7	154.7	114.2
Specific Diameter, D_{s_f}	1.5	1.9	2.42
D_{s_o}	1.1	1.5	1.9
Pump Pressure Rise, ΔP_f (ft)	643	1029	1543
ΔP_o (ft)	405	650	975
Pump Flow Rate, V_f (cfs)	0.0585	0.0585	0.0585
V_o (cfs)	0.0568	0.0568	0.0568
$D_{1_f} = \frac{D_{s_f}\sqrt{V_f}}{(\Delta P_f)^{0.25}} \times 12$, inch	0.865	0.974	1.12
$D_{1_o} = \frac{D_{s_o}\sqrt{V_o}}{(\Delta P_o)^{0.25}} \times 12$, inch	0.701	0.850	0.972
Impeller Weight, lb, $W_{i(f)}$	0.0176	0.0224	0.0296
$W_{i(o)}$	0.0116	0.0170	0.0223
Pump Weight, lb, $W_{p(f)}$	0.176	0.224	0.296
(Including Housings), $W_{p(o)}$	0.116	0.170	0.223
Pump Shaft, Bearing, Seals, Weight	0.75	1.0	1.25
Total Pump Weight, W_p	1.04	1.40	1.77

Table 3-11. Centrifugal Pump – Impeller Diameter and Weight Estimate (F = 4000 lbf)

Parameter	Thrust Level, lbf		
	4000	4000	4000
Specific Speed, N_{s_f}	203.5	143.0	105.6
N_{s_o}	281.7	197.5	145.8
Specific Diameter, D_{s_f}	1.25	1.63	2.0
D_{s_o}	0.9	1.25	1.65
Pump Pressure Rise, ΔP_f (ft)	643	1029	1543
ΔP_o (ft)	405	650	975
Pump Flow Rate, V_f (cfs)	0.0936	0.0936	0.0936
V_o (cfs)	0.0908	0.0908	0.0908
$D_{l_f} = \frac{D_{s_f}\sqrt{V_f}}{(\Delta P_f)^{0.25}} \times 12$, inch	0.912	1.04	1.172
$D_{l_o} = \frac{D_{s_o}\sqrt{V_o}}{(\Delta P_o)^{0.25}} \times 12$, inch	0.725	0.895	1.068
Impeller Weight, lb, $W_{i(f)}$	0.0229	0.0297	0.0378
$W_{i(o)}$	0.0145	0.0220	0.0314
Pump Weight, lb, $W_{p(f)}$	0.229	0.297	0.378
(Including Housings), $W_{p(o)}$	0.145	0.220	0.314
Pump Shaft, Bearing, Seals, Weight	1.0	1.25	1.50
Total Pump Weight, W_p, lb	1.38	1.77	2.20

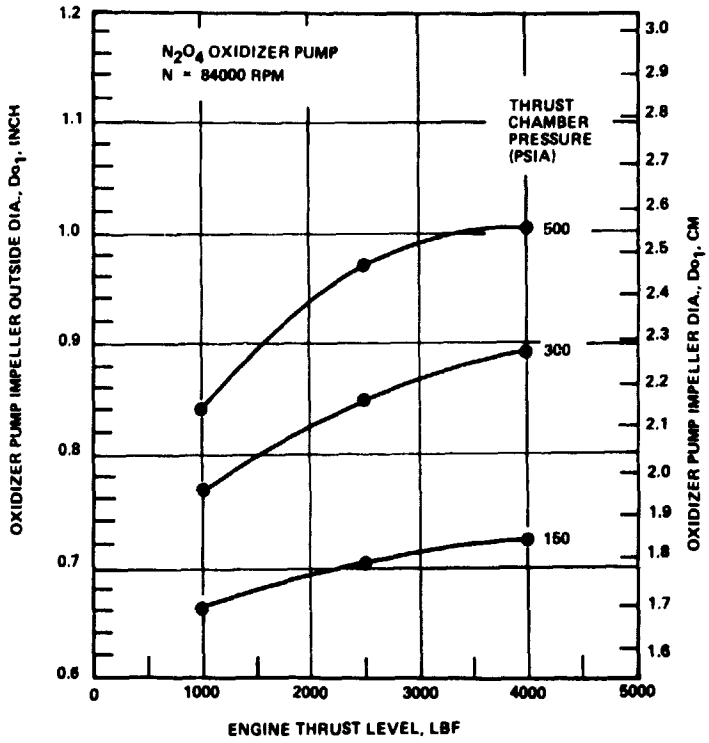

Figure 3-17. Oxidizer Pump Impeller Outside Diameter Variation with Engine Thrust Level and Thrust Chamber Pressure

3.5 PUMP DRIVE SYSTEMS

There are three basic design configurations that were considered for the propellant feed system. These were:

- Battery Powered Motor
- Monopropellant, Gas-Generator Powered Turbine
- Bipropellant, Gas-Generator Powered Turbine

An important factor in considering these three design options is the pump brake horsepower requirement. These are summarized on Figures 3-18 and 3-19. The fuel pump BHP range is from 2 to 20.5 HP; and the oxidizer pump BPH range is from 2 to 19.5 HP. The total output HP required from the pump drive is shown on Figure 3-20 and ranges from 4 to 40 HP. The applicability of the various pump drives to this power range is discussed below.

3.5.1 Battery Powered Motor

High speed (64,000 to 84,000 rpm) permanent magnet (samarium cobalt), brushless motors are available in the 5 to 40 HP (3.73 to 29.8 KW_E)

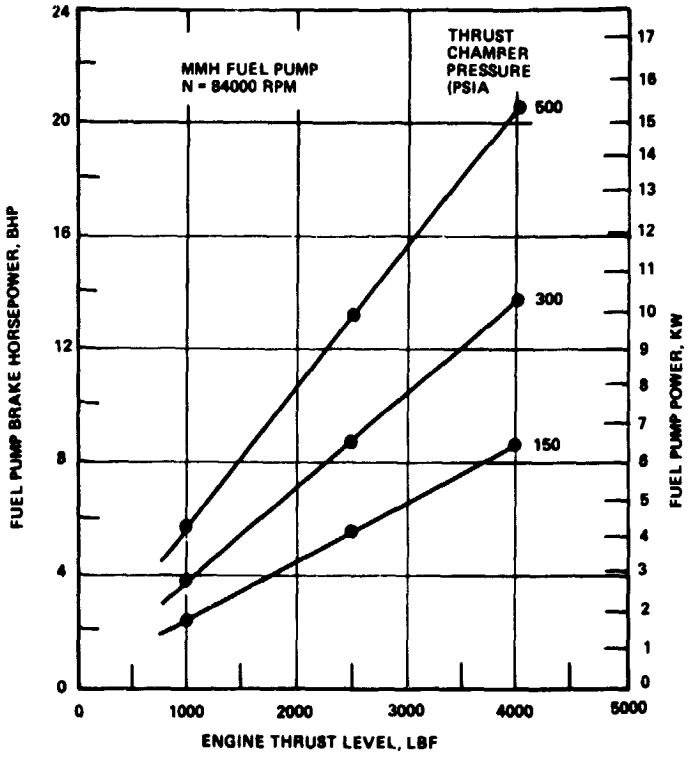

Figure 3-18. Fuel Pump Brake Horsepower vs. Engine Thrust Level

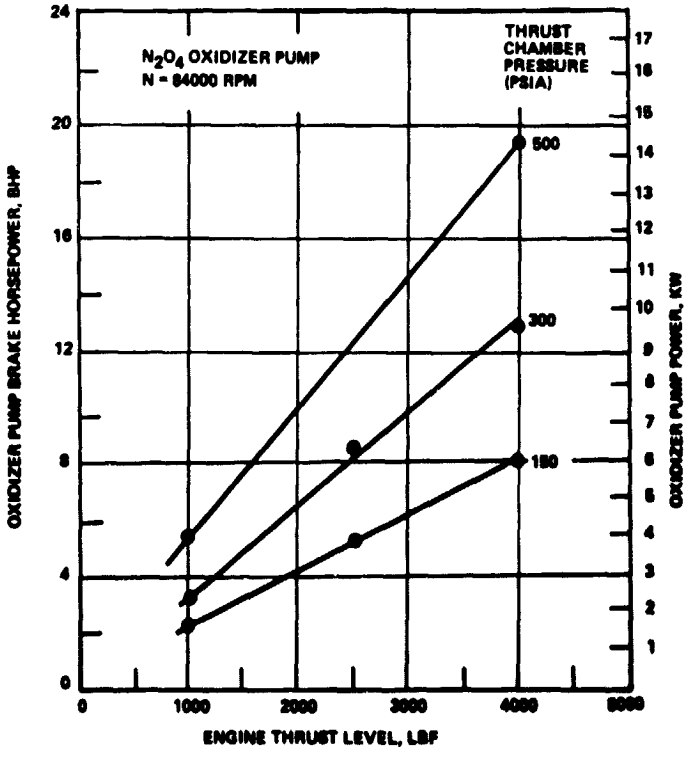

Figure 3-19. Oxidizer Pump Brake Horsepower vs. Engine Thrust Level

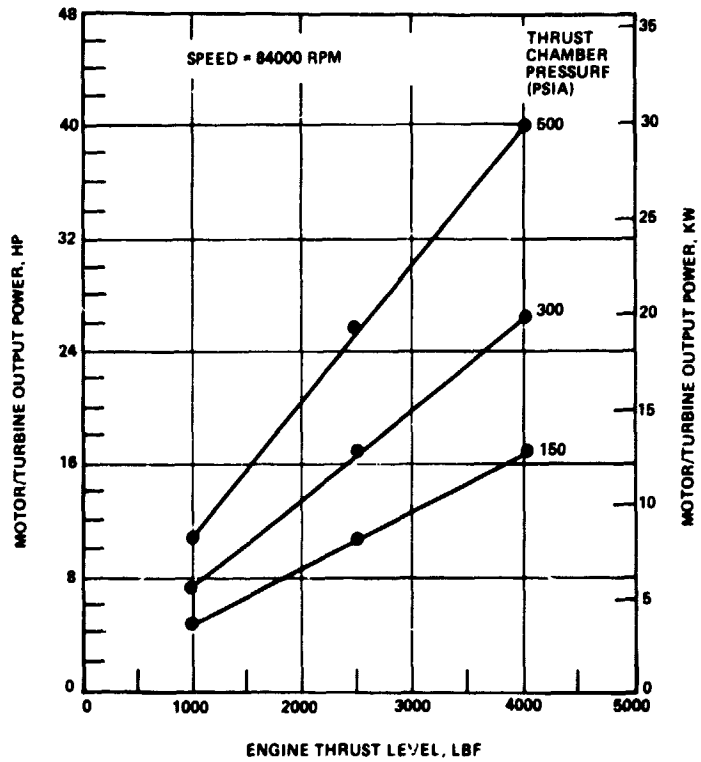

Figure 3-20. Motor/Turbine Output Power vs. Engine Thrust Level

range. At these speeds they are lightweight and comparatively small in volume (Figures 3-20a and 3-20b). In addition, an overall motor efficiency of 0.85 is readily achievable. The motor stator housing would include cooling passages so that heat can be rejected to the MMH fuel. Hence, these types of motors are very attractive candidates for the pump-fed propellant feed systems.

The major weight penalty associated with the motor drive option was that resulting from the batteries. There were two candidate batteries considered during this study. These are shown in Table 3-12.

These are primary (nonrechargeable) type batteries. While the LiTCl battery would potentially provide the lightest weight unit, the high current drain rate resulting from a 1-hour total thrusting time would require that this type battery be severely downrated. However, for this study, the assumption was made that the performance of this battery would be improved with additional development effort and that a nominal 100 watt-hour/lb specific energy would be achievable. The battery weights,

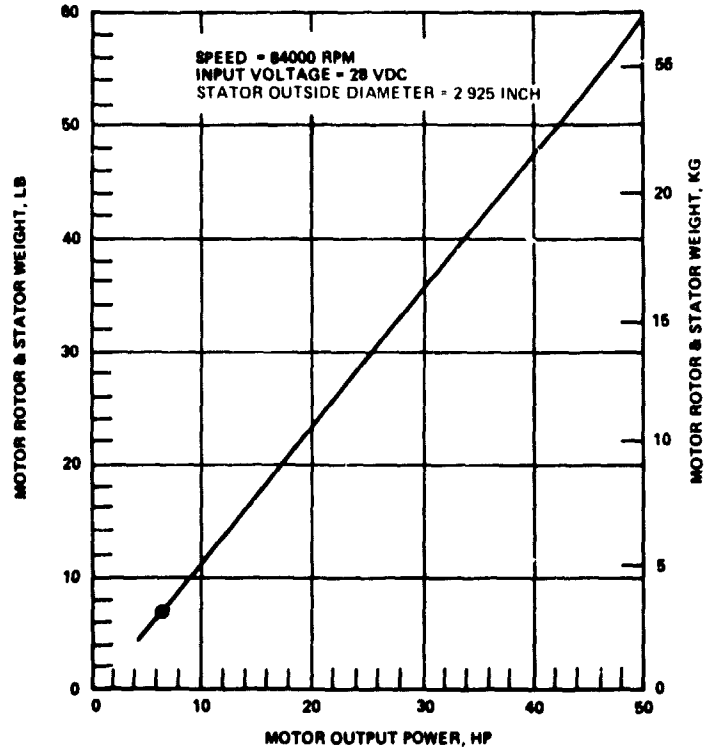

Figure 3-20a. Motor Rotor and Stator Weight vs. Motor Output Power

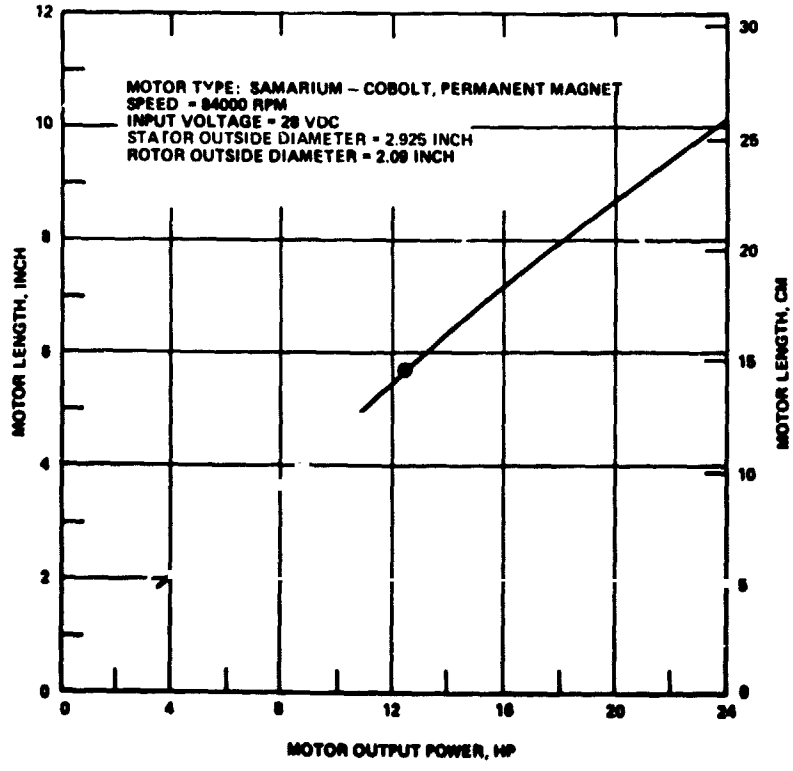

Figure 3-20b. Motor Length vs. Motor Output Power

as a function of total energy output, are shown in Figure 3-21. For the propellant feed systems considered in this study, the AgZn battery weights range from 80 to 200 pounds and the LiTCl from 40 to 100 pounds. A summary of the battery weight analyses for the various engine thrust levels and thrust chamber pressures is provided in Tables 3-13, 3-14, and 3-15. If low thrust chamber pressures (i.e., P_c = 150 psia) are utilized, the battery weights appear to make this an attractive option. For high thrust

Table 3-12. Candidate Batteries

Battery	Type	Specific Energy (watt-hr/lb)	Specific Volume (watt-hr/cu in)
Silver Zinc (AgZn)	Primary	50	2.25
Lithium-Thionyl Chloride (LiTCl)	Primary	114(1)	6.0

(1) Specific Energy achievable only with low current drain rate (i.e., 10-24 hours)

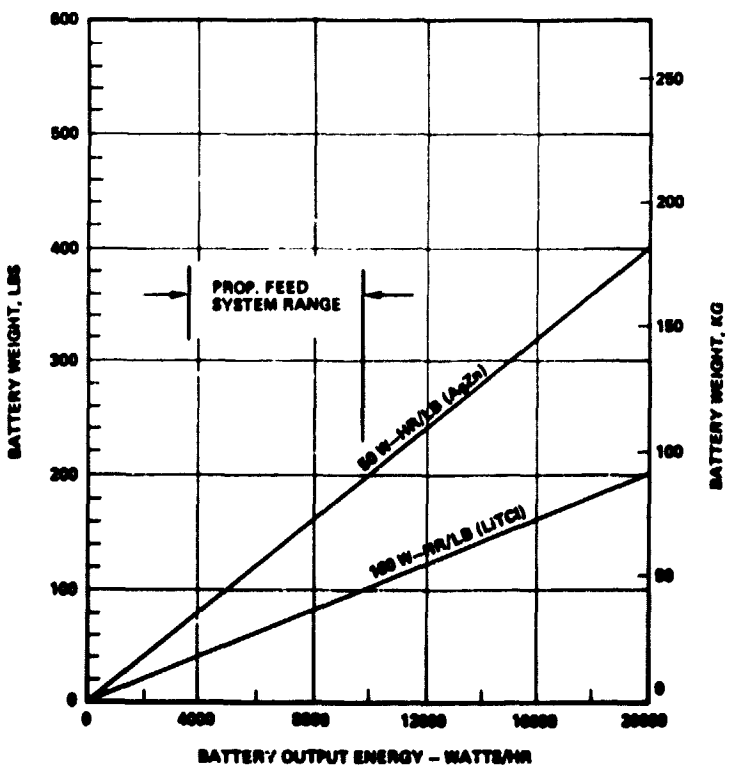

Figure 3-21. Battery Weight Versus Total Output Energy

Table 3-13. Battery Weight Analysis (F = 1000 lbf)

Parameter	Thrust Level, lbf		
	1000	1000	1000
Thrust Chamber Pressure, P_c, psia	150	300	500
Total Pump Brake Horsepower, BHP_T	4.65	7.45	11.14
Electric Motor Efficiency, η_m	0.85	0.85	0.85
Total Thrusting Time, hr	1.0	1.0	1.0
Total Energy Input, watt-hr	4081	6539	9777
Battery Specific Energy, w-hr/lb	50 100	50 100	50 100
Battery Weight, lb (50 w-hr/lb)	81.6	130.7	195.5
(100 w-hr/lb)	40.8	65.4	97.7
Battery Energy Density, w-hr/in^3			
(AgZn)	2.25	2.25	2.25
(LiTCl)	6.0	6.0	6.0
Battery Volume, ft^3			
(AgZn)	1.05	1.68	2.52
(LiTCl)	0.394	0.63	0.944

Table 3-14. Battery Weight Analysis (F = 2500 lbf)

Parameter	Thrust Level, lbf		
	2500	2500	2500
Thrust Chamber Pressure, P_c, psia	150	300	500
Total Pump Brake Horsepower, BHP_T	10.76	17.24	25.83
Electric Motor Efficiency, η_m	0.85	0.85	0.85
Total Thrusting Time, hr	0.4	0.4	0.4
Total Energy Input, watt-hr	3777	6052	9068
Battery Specific Energy, w-hr/lb	50 100	50 100	50 100
Battery Weight, lb (50 w-hr/lb)	75.6	121.0	181.4
(100 w-hr/lb)	37.8	60.5	90.7
Battery Energy Density, w-hr/cu in			
(AgZn)	2.25	2.25	2.25
(LiTCl)	6.0	6.0	6.0
Battery Volume, ft^3			
(AgZn)	0.972	1.5575	2.334
(LiTCl)	0.364	0.583	0.874

Table 3-15. Battery Weight Analysis (F = 4000 lbf)

Parameter	Thrust Level, lbf		
	4000	4000	4000
Thrust Chamber Pressure, P_c, psia	150	300	500
Total Pump Brake Horsepower, BHP_T	16.7	26.76	40.03
Electric Motor Efficiency, η_m	0.85	0.85	0.85
Total Thrusting Time, hr	0.25	0.25	0.25
Total Energy Input, watt-hr	3664	5871	8783
Battery Specific Energy, w-hr/lb	50 100	50 100	50 100
Battery Weight, lb (50 w-hr/lb)	73.2	117.4	165.6
(100 w-hr/lb)	36.6	58.7	87.8
Battery Energy Density, w-hr/cu in			
(AgZn)	2.25	2.25	2.25
(LiTCl)	6.0	6.0	6.0
Battery Volume, ft^3			
(AgZn)	0.942	1.51	2.26
(LiTCl)	0.353	0.566	0.850

chamber pressures (i.e., P_c = 500 psia), the required battery weights tend to become excessive, particularly if the AgZn batteries are the only fully developed option available.

3.5.2 Monopropellant, Gas Generator Powered Turbine

A high speed turbine powered by a monopropellant (N_2H_4) gas generator will also result in a lightweight pump drive. The thermodynamic characteristics of the decomposition products of hydrazine are shown in Figure 3-22. For an 80% ammonia dissociation rate, the adiabatic flame temperature is 1392°F. Allowing for a small temperature drop (approximately 17°) from the gas generator exit provides a turbine inlet temperature of 1375°F. The turbine design criteria utilized in this study are given in Table 3-16. The results of the turbine analyses for the various engine thrust levels and thrust chamber pressures are summarized in Tables 3-17, 3-18, and 3-19. Turbine efficiency estimates are given in Figures 3-22a and 3-23. The estimated efficiencies of Figure 3-23 were higher than those in Figure 3-22a. However, to be conservative, the lower values were used in conducting the turbine analyses. The turbine weights varied from 15.6 lb (F = 1000 lbf, P_c = 150 psia) to 43.8 lb (F = 4000 lbf, P_c = 500 psia). The variations in turbine pitch diameter are shown in Figure 3-23a.

The design criteria for the monopropellant gas generator were given in Table 3-16 and are supplemented with the additional values in Table 3-20. The results of these analyses are summarized in Tables 3-21, 3-22, and 3-23. As may be noted, the weight of the gas generator combustion chambers for all thrust levels and chamber pressures is less than 1 pound. Hence, this component is not a major factor in the overall dry weight of this type of pump drive. In addition, they are small in envelope dimensions (Figure 3-23b).

3.5.3 Bipropellant Gas Generator Powered Turbine

An alternate approach to the N_2H_4 monopropellant gas generator driven turbine is to employ the rocket engine propellant N_2O_4 and MMH in a bipropellant gas generator. This approach has the virtue of eliminating the need for a separate gas generator propellant tank and its pressurizing controls. The propellants are stored along with the main rocket

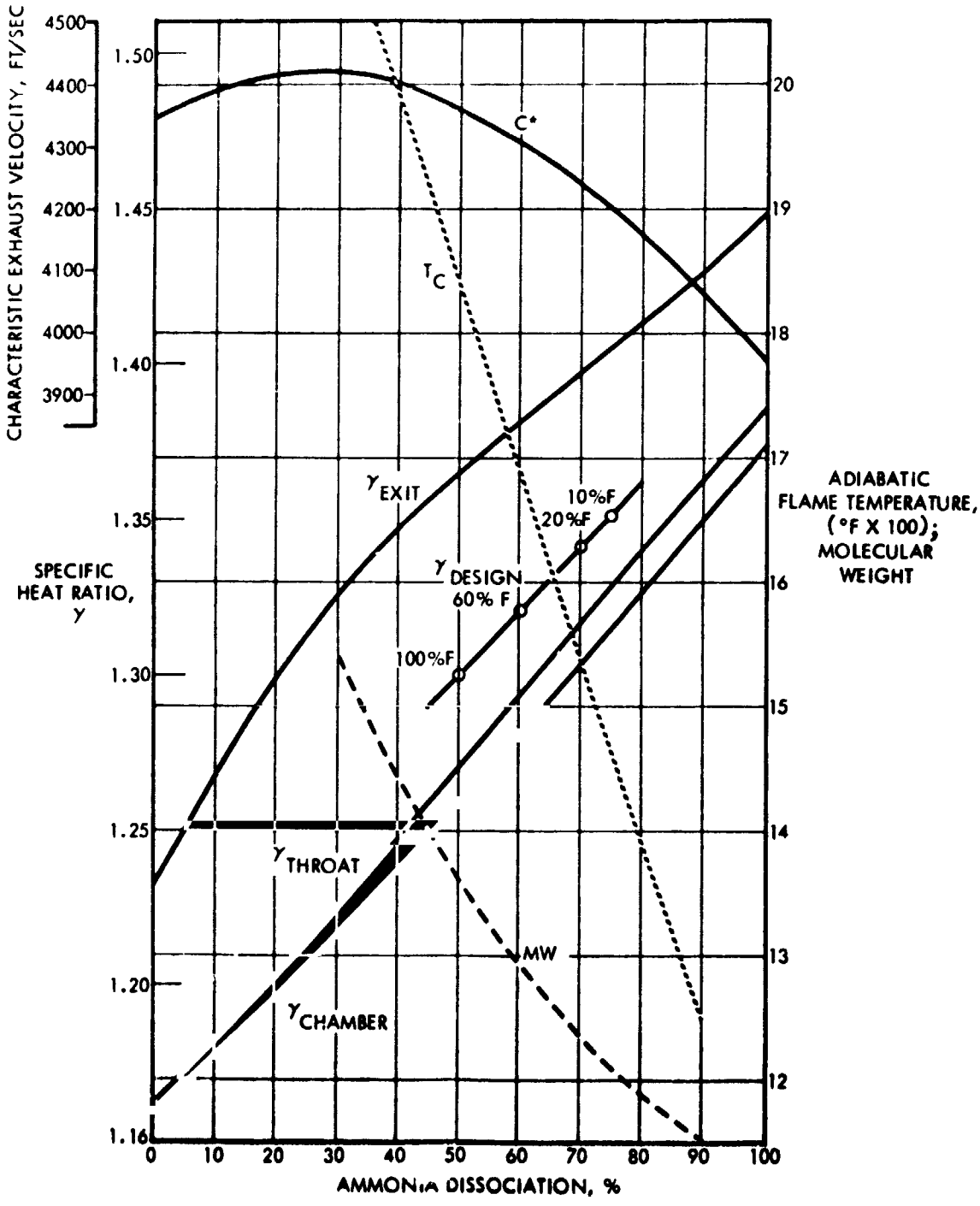

Figure 3-22. Hydrazine (N_2H_4) Decomposition Characteristics

Table 3-16. Turbine Design Criteria – Monopropellant Gas Generator

Working Fluid	Hydrazine (N_2H_4)
% Ammonia Dissociation, X	80%
Adiabatic Flame Temperature, T_c	1392°F
GG Expansion Ratio, ϵ	50
Molecular Weight, MW	11.72
Universal Gas Constant, R	131.83
Theoretical $I_{sp(vac)}$	224.8
Thrust Coefficient, $C_{F(vac)}$	1.744
Ratio of Specific Heats, $\gamma_{exit} = C_P/C_V =$	1.43
Specific Heat at Constant Pressure, $C_{P(exit)} = \frac{\gamma}{\gamma - 1}\frac{R}{J} =$	0.564 Btu/lb-°F
Specific Heat at Constant Volume, $C_{V(exit)} = \frac{R/J}{k - 1} =$	0.394 Btu/lb-°F
Turbine Inlet Temperature, T_{T_1}	1375°F 1835°R
Turbine Inlet Pressure, P_{T_1}	150 psia
Turbine Outlet Pressure, P_{T_2}	15 psia
Turbine Speed, N	84,000 rpm

Table 3-17. Turbine Analysis – Hydrazine Gas Generator (F = 1000 lbf)

Parameter	Thrust Level		
	1000	1000	1000
Chamber Pressure, P_c, psia	150	300	500
Specific Speed, N_s (cfs basis)	5.81	7.34	8.99
Specific Diameter, D_{s_t}	8.0	7.0	6.0
Turbine Efficiency, η_t (Fig. 3-22)	~0.70	~0.72	~0.73
Pitch Diameter, D_t, inches	3.64	4.03	4.23
Peripheral Velocity, U_t, ft/sec	1334	1477	1550
Nozzle Spouting Velocity, $C_{o(15\%)}$, ft/sec	4064	4064	4064
Velocity Ratio $(U_t/C_o)_{(15\%)}$	0.33	0.36	0.38
Turbine Efficiency, η_t (Fig. 3-23)	~0.78	~0.81	~0.85
Turbine Flow Rate, $\dot{m}$, lb/sec	0.0113	0.0181	0.0271
Turbine Output Power, P_t, BHP	4.65	7.45	11.14
Turbine Speed, N, rpm	84,000	84,000	84,000
Turbine Rotor Weight, W_{t_r}, lb / Inconel X-750; ρ = 0.3 lb/in^3	3.12	3.83	4.22
Turbine Weight, W_t, lb	15.6	19.1	21.1

Table 3-18. Turbine Analysis – Hydrazine Gas Generator (F = 2500 lbf)

Parameter	Thrust Level		
	2500	2500	2500
Chamber Pressure, P_c, psia	150	300	500
Specific Speed, N_s (cfs basis)	8.82	11.2	13.69
Specific Diameter, D_{s_t}	7.0	6.0	5.0
Turbine Efficiency, η_t (Fig. 3-22)	~0.72	~0.74	~0.76
Pitch Diameter, D_t, inches	4.85	5.26	5.37
Peripheral Velocity, V_t, ft/sec	1777	1927	1968
Nozzle Spouting Velocity, $C_{o(15\%)}$, ft/sec	4064	4064	4064
Velocity Ratio $(U_t/C_o)_{(15\%)}$	0.437	0.474	0.484
Turbine Efficiency, η_t (Fig. 3-23)	~0.87	~0.88	~0.89
Turbine Flow Rate, $\dot{m}$, lb/sec	0.0261	0.0419	0.0628
Turbine Output Power, P_t, BHP	10.76	17.24	25.83
Turbine Speed, N, rpm	84,000	84,000	84,000
Turbine Rotor Weight, W_{t_r}, lb	5.54	6.52	6.79
Turbine Weight, W_t, lb	27.7	32.6	34.0

Table 3-19. Turbine Analysis – Hydrazine Gas Generator (F = 4000 lbf)

Parameter	Thrust Level		
	4000	4000	4000
Chamber Pressure, P_c, psia	150	300	500
Specific Speed, N_s (cfs basis)	11.0	13.9	17.0
Specific Diameter, D_{s_t}	6.25	5.4	4.6
Turbine Efficiency, η_t (Fig. 3-22)	~0.75	~0.76	~0.77
Pitch Diameter, D_t, inches	5.40	5.85	6.10
Peripheral Velocity, V_t, ft/sec	1979	2144	2235
Nozzle Spouting Velocity, $C_{o(15\%)}$, ft/sec	4064	4064	4064
Velocity Ratio $(U_t/C_o)_{(15\%)}$	0.487	0.527	0.550
Turbine Efficiency, η_t (Fig. 3-23)	~0.86	~0.87	~0.87
Turbine Flow Rate, $\dot{m}$, lb/sec	0.0406	0.0650	0.0973
Turbine Output Power, P_t, BHP	16.7	26.76	40.03
Turbine Speed, N, rpm	84,000	84,000	84,000
Turbine Rotor Weight, W_{t_r}, lb	6.87	8.06	8.76
Turbine Weight, W_t, lb	34.4	40.3	43.8

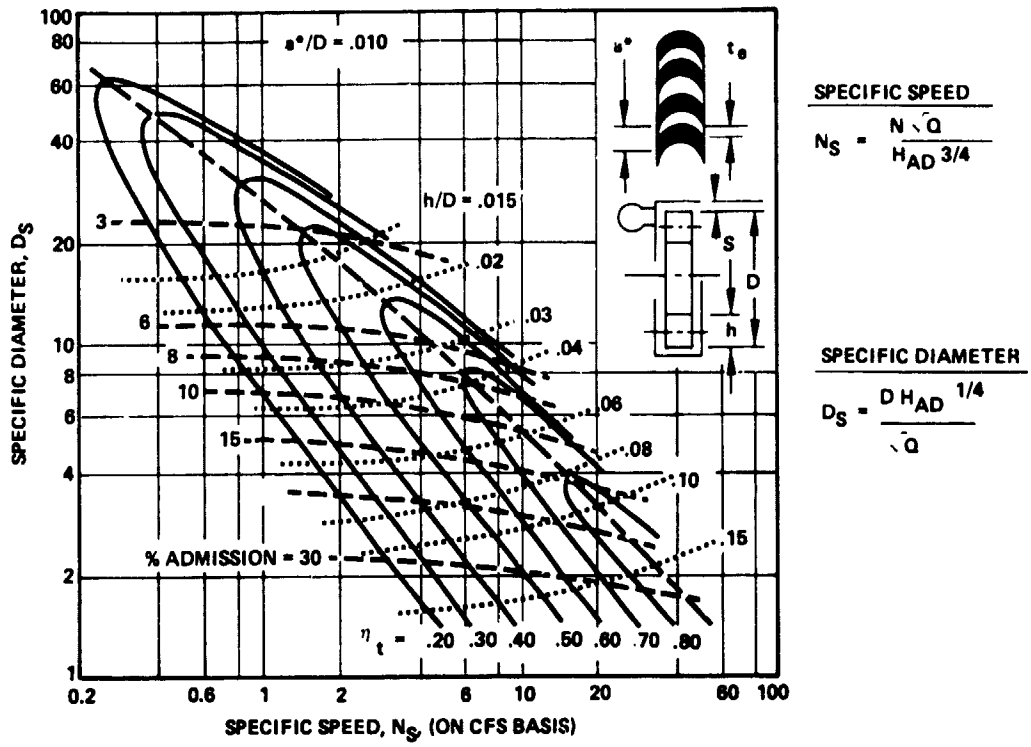

Figure 3-22a. Partial Admission Turbine Performance Chart

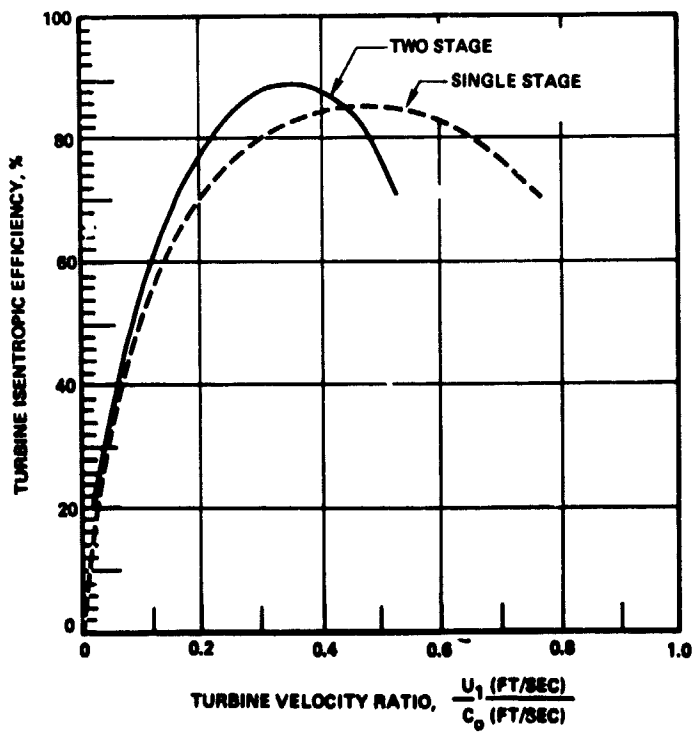

Figure 3-23. Partial Admission Turbine Performance Chart

Table 3-20. Monopropellant (N_2H_4) Gas Generator Design Criteria

Characteristic Velocity, C^*	4160 ft/sec
Characteristic Length, L^*	700
Ratio of Specific Heats, $\gamma_{(throat)}$	1.335
$\gamma_{(exit)}$	1.430
$\gamma_{(comb.chbr.)}$	1.320
Combustion Chamber Pressure, P_G	200 psia

Table 3-21. Gas Generator Analysis (N_2H_4) – (F = 1000 lbf)

Parameter	Thrust Level		
	1000	1000	1000
Chamber Pressure, P_c, psia	150	300	500
Turbine Flow Rate, $\dot{m}$, lb/sec	0.0113	0.0181	0.0271
Characteristic Velocity, C^*, ft/sec	4160	4160	4160
Combustion Chamber Pressure, P_G, psia	200	200	200
Throat Area, A_t, sq in	0.0073	0.0117	0.0175
Throat Diameter, D_t, inch	0.0964	0.122	0.149
Characteristic Length, L* (est), ft/sec-ft^2	700	700	700
Combustion Chamber Volume, V_G, in^3	5.11	8.19	12.25
Combustion Chamber Diameter, D_G, inch	2.0	2.0	2.0
Combustion Chamber Length, L_G, inch	1.63	2.61	3.90
Wall Thickness, t_G, inch	0.0625	0.0625	0.0625
Density of Material, ρ_{GM}, lb/in^3	0.231	0.231	0.231
Combustion Chamber Weight, W_G, lb	0.148	0.2368	0.3538

Table 3-22. Gas Generator Analysis (N_2H_4) – (F = 2500 lbf)

Parameter	Thrust Level		
	2500	2500	2500
Chamber Pressure, P_c, psia	150	300	500
Turbine Flow Rate, $\dot{m}$, lb/sec	0.0261	0.0419	0.0628
Characteristic Velocity, C^*, ft/sec	4160	4160	4160
Combustion Chamber Pressure, P_c, psia	200	200	200
Throat Area, A_t, sq in	0.0169	0.0271	0.0406
Throat Diameter, D_t, inch	0.147	0.1858	0.2274
Characteristic Length, L^* (est), ft/sec-ft^2	700	700	700
Combustion Chamber Volume, V_G, in^3	11.83	18.97	28.42
Combustion Chamber Diameter, D_G, inch	3.0	3.0	3.0
Combustion Chamber Length, L_G, inch	1.67	2.68	4.02
Wall Thickness, t_g, inch	0.0625	0.0625	0.0625
Density of Material, ρ_{GM}, lb/in^3	0.231	0.231	0.231
Combustion Chamber Weight, W_G, lb	0.227	0.365	0.547

Table 3-23. Gas Generator Analysis (N_2H_4) – (F = 4000 lbf)

Parameter	Thrust Level		
	4000	4000	4000
Chamber Pressure, P_c, psia	150	300	500
Turbine Flow Rate, $\dot{m}$, lb/sec	0.0406	0.0650	0.0973
Characteristic Velocity, C^*, ft/sec	4160	4160	4160
Combustion Chamber Pressure, P_c, psia	200	200	200
Throat Area, A_t, in^2	0.0262	0.0420	0.0629
Throat Diameter, D_t, inch	0.1826	0.2312	0.2830
Characteristic Length, L^* (est), ft/sec-ft^2	700	700	700
Combustion Chamber Volume, V_G, in^3	18.34	29.4	44.03
Combustion Chamber Diameter, D_G, inch	3.75	3.75	3.75
Combustion Chamber Length, L_G, inch	1.66	2.66	3.98
Wall Thickness, t_g, inch	0.0625	0.0625	0.0625
Density of Material, ρ_{GM}, lb/in^3	0.231	0.231	0.231
Combustion Chamber Weight, W_G, lb	0.282	0.4524	0.677

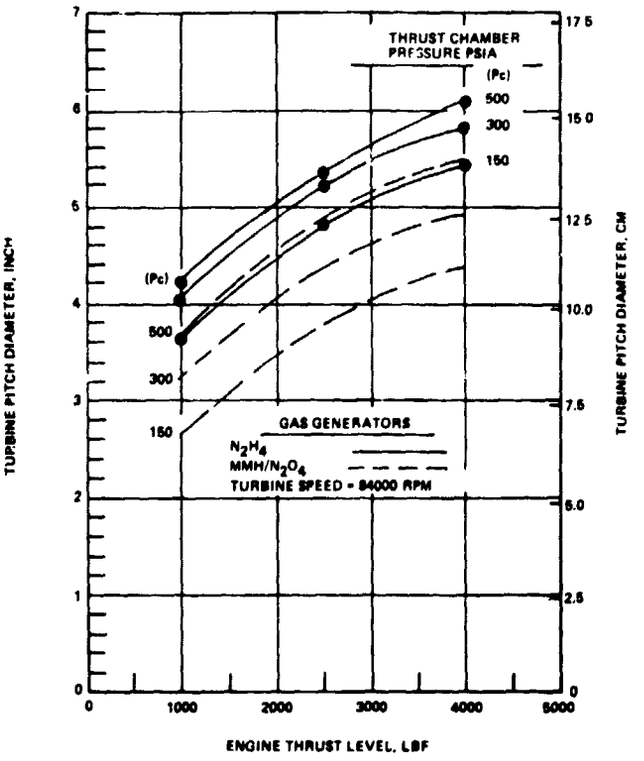

Figure 3-23a. Turbine Pitch Diameter vs. Engine Thrust Level

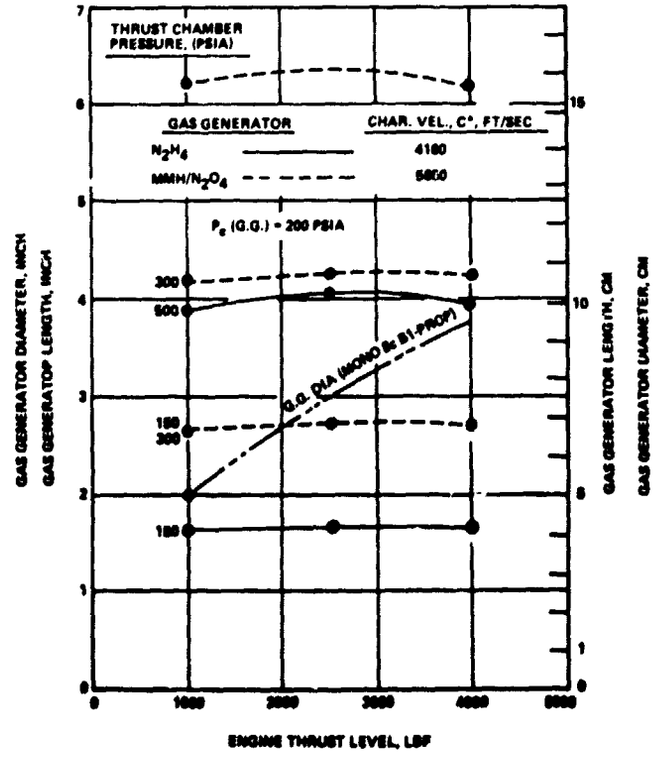

Figure 3-23b. Gas Generator Diameter and Length vs. Engine Thrust Level

ergine propellants and are pressurized to the required gas generator combustion chamber pressure by the propellant feed system pumps.

At a mixture ratio of 1.6 the combustion chamber temperature would be approximately 4600°F (5200°R) (Figure 3-29). This would be much too high for the turbine. Hence, the gas generator is required to operate very fuel rich at a mixture ratio of 0.4. This corresponds to an acceptable combustion gas temperature of 1400°F (1800°R) (Figure 3-24). However, below a mixture ratio of 0.5, there is the possibility of the formation of free carbon. This would have to be investigated for any adverse effects on the turbine. Allowing for a small temperature drop (approximately 25°) from the gas generator exit provides a turbine inlet temperature of 1375°F. For these conditions the turbine design criteria utilized in the study are given in Table 3-24. The results of the turbine analyses for the 2500 lbf thrust level and the various chamber pressures are summarized in Table 3-25. Turbine efficiency estimates were taken from Figures 3-22 and 3-23. The turbine weights at the 1000 lbf and 4000 lbf thrust levels were extrapolated from the data in Table 3-25.

The design criteria for the bipropellant gas generator were given in Table 3-24 and supplemented with the values given in Table 3-26.

The characteristic velocity of Table 3-26 corresponds to a mixture ratio of 0.4 (Figure 3-25) since acceptable gas generator combustion characteristics (i.e., 1400°F) should result under this condition. The results of these analyses are given in Table 3-27 for the 2500 lbf thrust level. Here again, extrapolations were made to the 1000 lbf and 4000 lbf thrust levels in determining bipropellant gas generator weights.

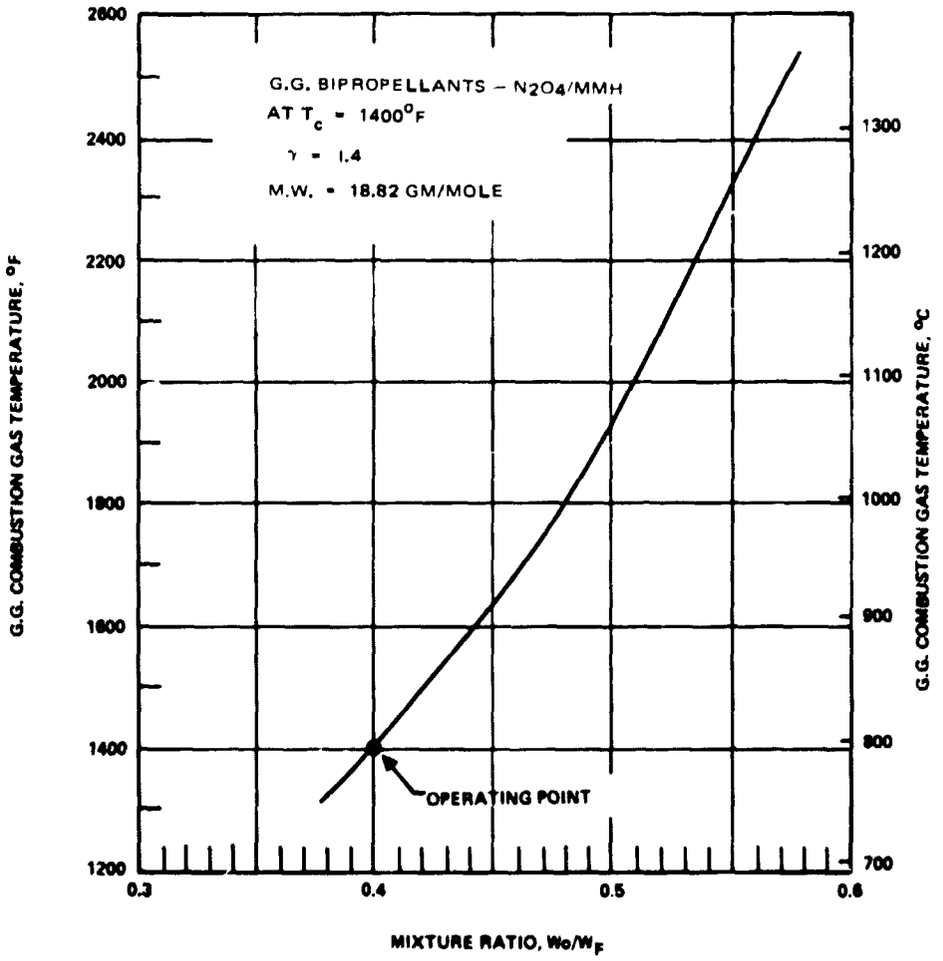

Figure 3-24. Bipropellant Gas Generator Combustion Gas Temperature vs. Mixture Ratio

Table 3-24. Turbine Design Criteria; Bipropellant Gas Generator

Working Fluid	Combustion Products of MMH/N_2O_4
Adiabatic Flame Temperature, T_C	$1400^{\circ}F$ (MR = 0.4)
GG Expansion Ratio, ϵ	50
Molecular Weight, MW	18.82 gm/mole
Universal Gas Constant, R	82.09
Ratio of Specific Heats, $\gamma_{exit} = C_P/C_V =$	1.4
Characteristic Velocity, C*	5000 ft/sec (MR = 0.4)
Specific Heat at Constant Pressure, $C_{P_{(exit)}} = \frac{\gamma}{\gamma - 1} \times \frac{R}{J} =$	0.3693 Btu/lb-$^{\circ}F$
Specific Heat at Constant Volume, $C_{V_{(exit)}} = \frac{1}{\gamma - 1} \times \frac{R}{J} =$	0.2638 Btu/lb-$^{\circ}F$
Turbine Inlet Temperature, T_{T_1}	$1375^{\circ}F$ $1835^{\circ}R$
Turbine Inlet Pressure, P_{T_1}	150 psia
Turbine Outlet Pressure, P_{T_2}	15 psia
Turbine Speed, N	84,000 rpm

Table 3-25. Turbine Analysis – MMH/N_2O_4 Gas Generator (F = 2500 lbf)

Parameter	Thrust Level, lbf		
	2500	2500	2500
Chamber Pressure, P_c, psia	150	300	500
Specific Speed, N_S (cfs basis)	8.63	10.94	13.38
Specific Diameter, D_{St}	6.0	5.5	5.0
Turbine Efficiency, η_t (chart)	~0.72	~0.74	~0.76
Pitch Diameter, D_t, inch	3.76	4.36	4.85
Peripheral Velocity, V_t, ft/sec	1378	1598	1777
Nozzle Spouting Velocity, $C_{o(15\%)}$, ft/sec	3755	3755	3755
Velocity Ratio, $U_t/C_{o(15\%)}$	0.367	0.426	0.473
Turbine Efficiency, η_t (U/C chart)	~0.81	~0.86	~0.88
Turbine Flow Rate, $\dot{m}$, lb/sec	0.0306	0.0491	0.0735
Turbine Output Power, P_t, BHP	10.76	17.24	25.83
Turbine Speed, N, rpm	84,000	84,000	84,000
Turbine Rotor Weight, W_{tr}, lb (ρ = 0.3 lb/in^3), t = 1 inch	3.33	4.48	5.54
Turbine Weight, W_T, lb	16.65	22.4	27.7

Table 3-26. Bipropellant (MMH/N_2O_4) Gas Generator Design Criteria

Characteristic Velocity, C*	5000 ft/sec
Characteristic Length, L*	700 ft/sec-ft^2
Ratio of Specific Heats, $\gamma_{(aver)}$	1.4
Combustion Chamber Pressure, P_G	200 psia

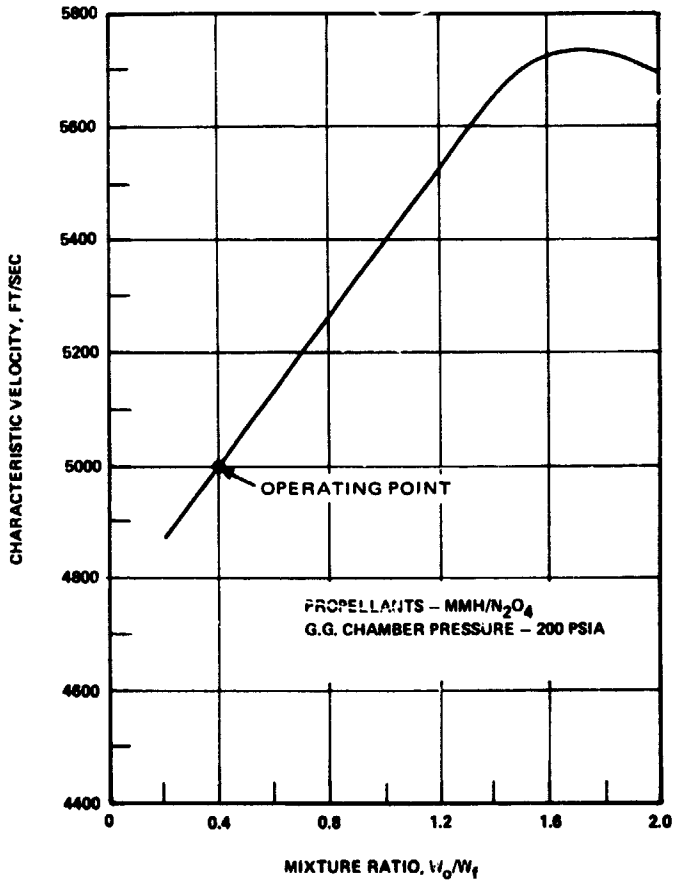

Figure 3-25. Characteristic Velocity vs. Mixture Ratio for Bipropellant Gas Generator

Table 3-27. Bipropellant Gas Generator Analysis – MMH/N_2O_4 (F = 2500 lbf)

Parameter	Thrust Level, lbf		
	2500	2500	2500
Chamber Pressure, P_c, psia	150	300	500
Turbine Flow Rate, $\dot{m}$, lb/sec	0.0306	0.0491	0.0735
Characteristic Velocity, C*, ft/sec	5000	5000	5000
Combustion Chamber Pressure, P_G, psia	200	200	200
Throat Area, A_t, sq in	0.0237	0.0381	0.0571
Throat Diameter, D_t, inch	0.1738	0.2204	0.2696
Characteristic Length, L* (est), ft/sec-ft^2	700	700	700
Combustion Chamber Volume, V_G, in^3	18.76	30.17	45.15
Combustion Chamber Diameter, D_G, inch	3.0	3.0	3.0
Combustion Chamber Length, L_G, inch	2.65	4.27	6.39
Wall Thickness, t_g, inch	0.0625	0.0625	0.0625
Density of Material, ρ_{GB}, lb/m^3	0.231	0.231	0.231
Combustion Chamber Weight, W_G, lb	0.3606	0.581	0.870

3.6 CANDIDATE PROPELLANT FEED SYSTEMS

As a result of the previous analyses, four candidate propellant feed systems were selected for further evaluation. These are listed in Table 3-28.

3.6.1 Battery Powered Electric Motor Driven Pumps

These PFS systems (Numbers 1 and 2) are shown on Figure 3-26. These are essentially the same system except for the type of batteries utilized. By operating at 84,000 rpm, the motor driven pumps can be configured to be lightweight and small in envelope dimensions. The weight of the primary batteries (as discussed in Section 3.5.1) becomes the most significant factor in the overall PFS dry weight. However, for low thrust levels, chamber pressures and short burning times, these type systems are attractive. Power for the controls is in the range of 25 to 56 watts.

Table 3-28. Candidate Propellant Feed Systems

System No.	Description
1	Battery Powered Electric Motor Driven Pumps (Li-Th-Cl Primary Batteries)
2	Battery Powered Electric Motor Driven Pumps (AgZn Primary Batteries)
3	Monopropellant, Gas Generator Powered Turbopumps (N_2H_4)
4	Bipropellant Gas Generator Powered Turbopumps (MMH/N_2O_4)

3.6.2 Monopropellant, Gas Generator Powered Turbopumps

This PFS system (Number 3) is shown in Figure 3-27. A turbine, operating at 84,000 rpm is driven by a monopropellant (N_2H_4) gas generator. Pressurization for the N_2H_4 tank is provided from the main PFS helium storage tank through a pressure regulator. This system decouples the gas generator propellant supply from the main PFS and permits time sequenced starts and stops. Thus, propella.. es in the fuel and oxidizer

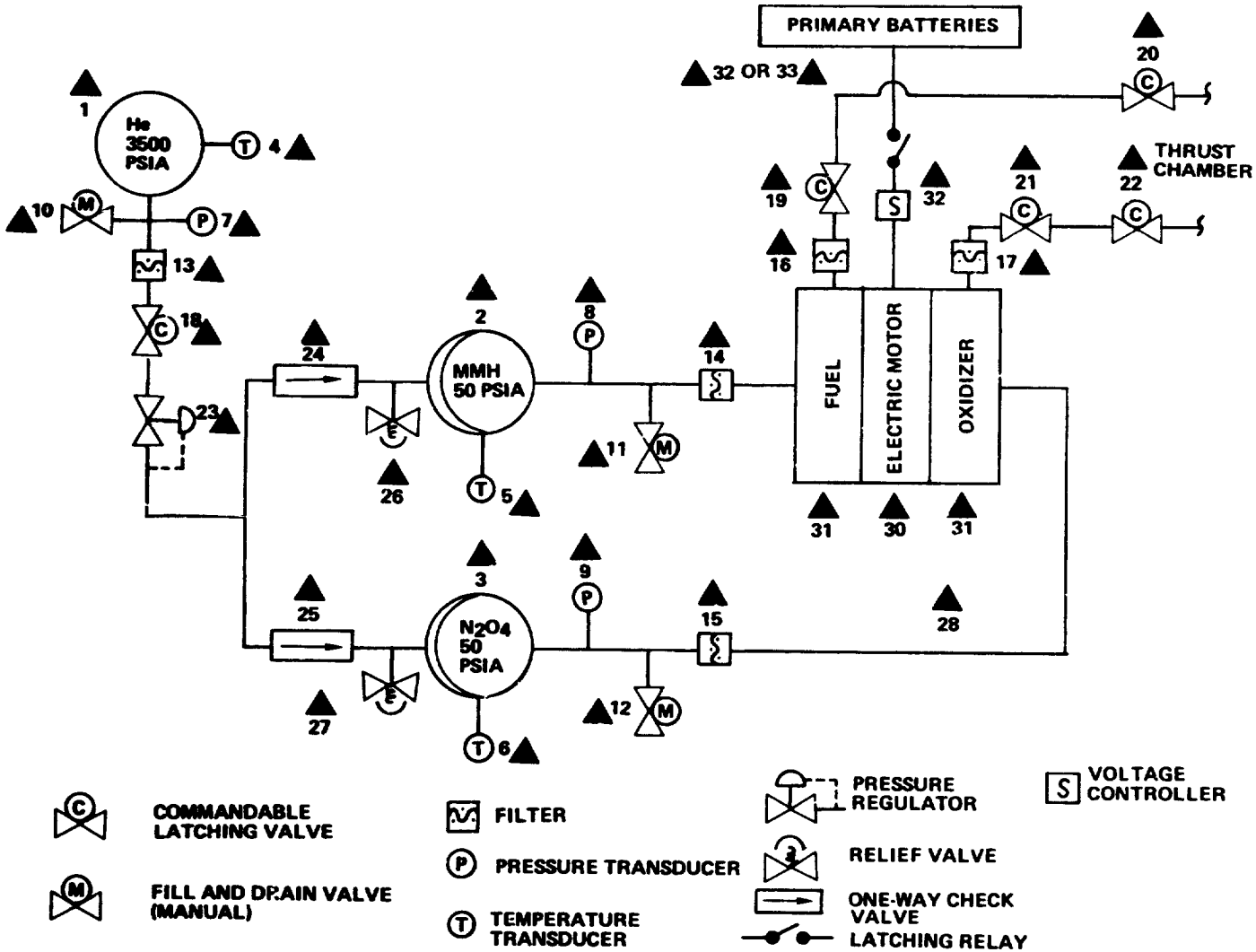

Figure 3-26. Battery Powered, Electric Motor Driven Pumps (Candidate PFS Numbers 1 and 2)

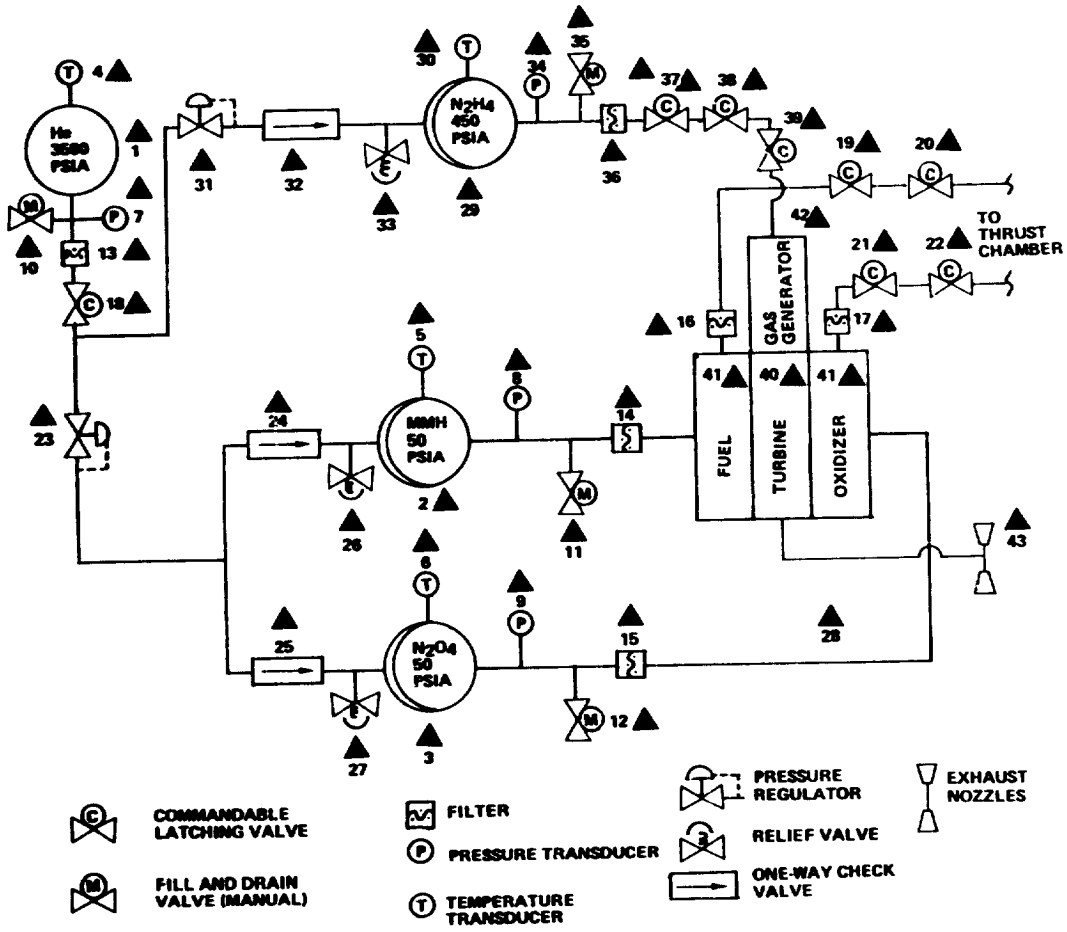

Figure 3-27. Monopropellant, Gas Generator Powered Turbopumps (Candidate PFS Number 3)

pumps can be brought up to fuel pressure before being admitted to the main thrust chamber injector. This flexibility in control of the start-up and shutdown sequencing is somewhat offset by the weight penalty of a separate N_2H_4 tank and the introduction of a third propellant to the PFS. Power for the controls is in the range of 36 to 89 watts.

3.6.3 Bipropellant, Gas Generator Powered Turbopumps

This PFS system (Number 4) is shown in Figure 3-28. In this case the turbine, also operating at 84,000 rpm, is driven by a bipropellant gas generator. These propellants are supplied from the main PFS pumps through pump discharge bypass valves. This eliminates the need for a separate gas generator propellant tank and the use of a third propellant. Start-up and restarts are initiated by an oxidizer and fuel accumulators. When the main propellant pumps have achieved full discharge pressure, the inlet valves to the thrust chamber injector can be opened. Simultaneously, the accumulators can be recharged and in the lockup mode can be available for the next start cycle. While this system can reduce the overall PFS dry weight by eliminating the N_2H_4 propellant tank, the start and stop sequencing is somewhat more complex. This can impact overall PFS reliability. In addition, turbopump speed variations may create combustion stability problems in the gas generator or main thrust chamber. Finally, in order to maintain the gas generator exit gas temperature at 1400°F, it must be operated at either very fuel-rich or oxidizer-rich (not too desirable due to corrosion) mixture ratios (Figure 3-29). Close mixture ratio control will be required if excessive turbine inlet temperatures are to be avoided. Power for the controls is in the range of 36 to 125 watts.

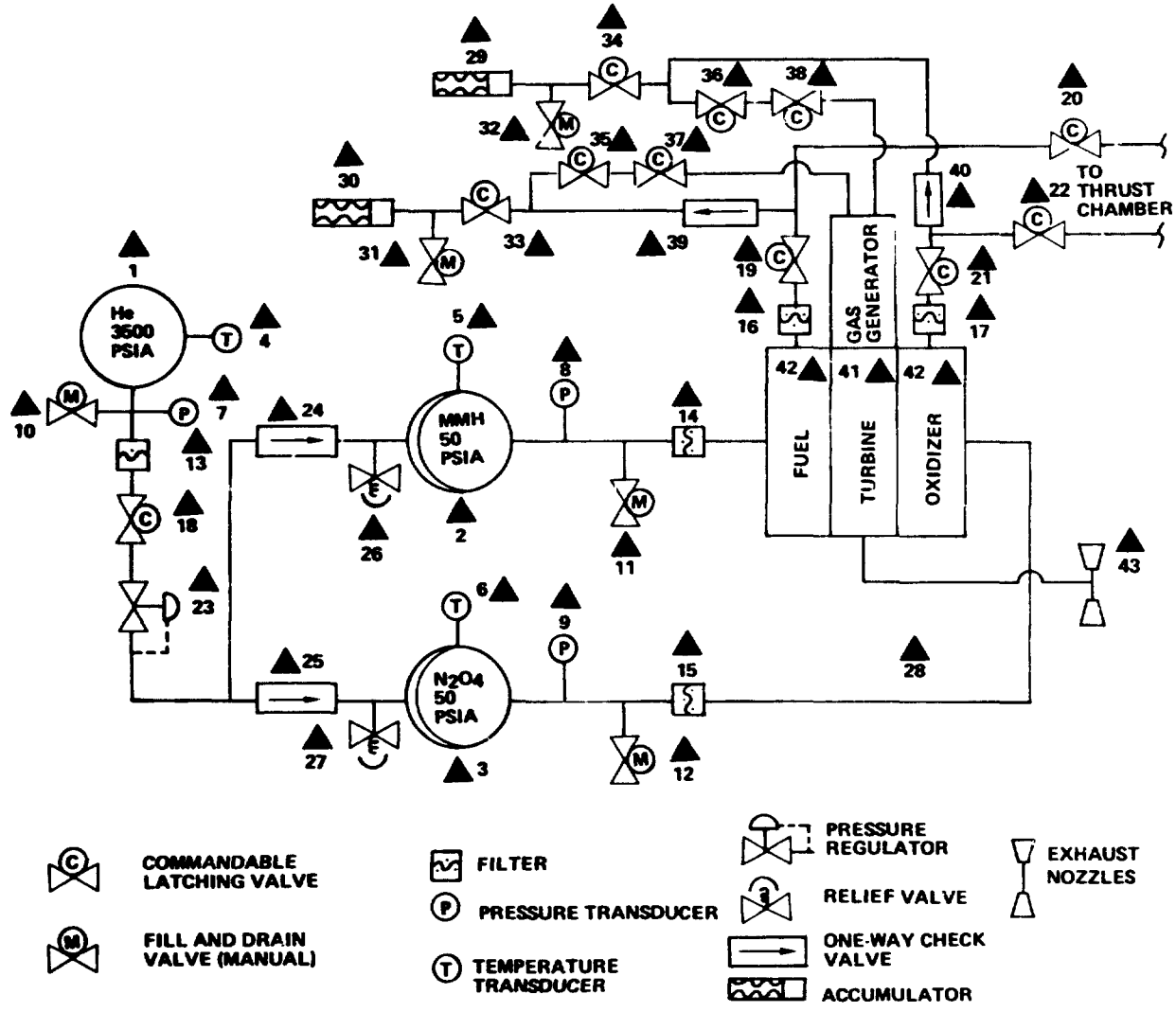

Figure 3-28. Bipropellant, Gas Generator Powered Turbopumps (Candidate PFS Number 4)

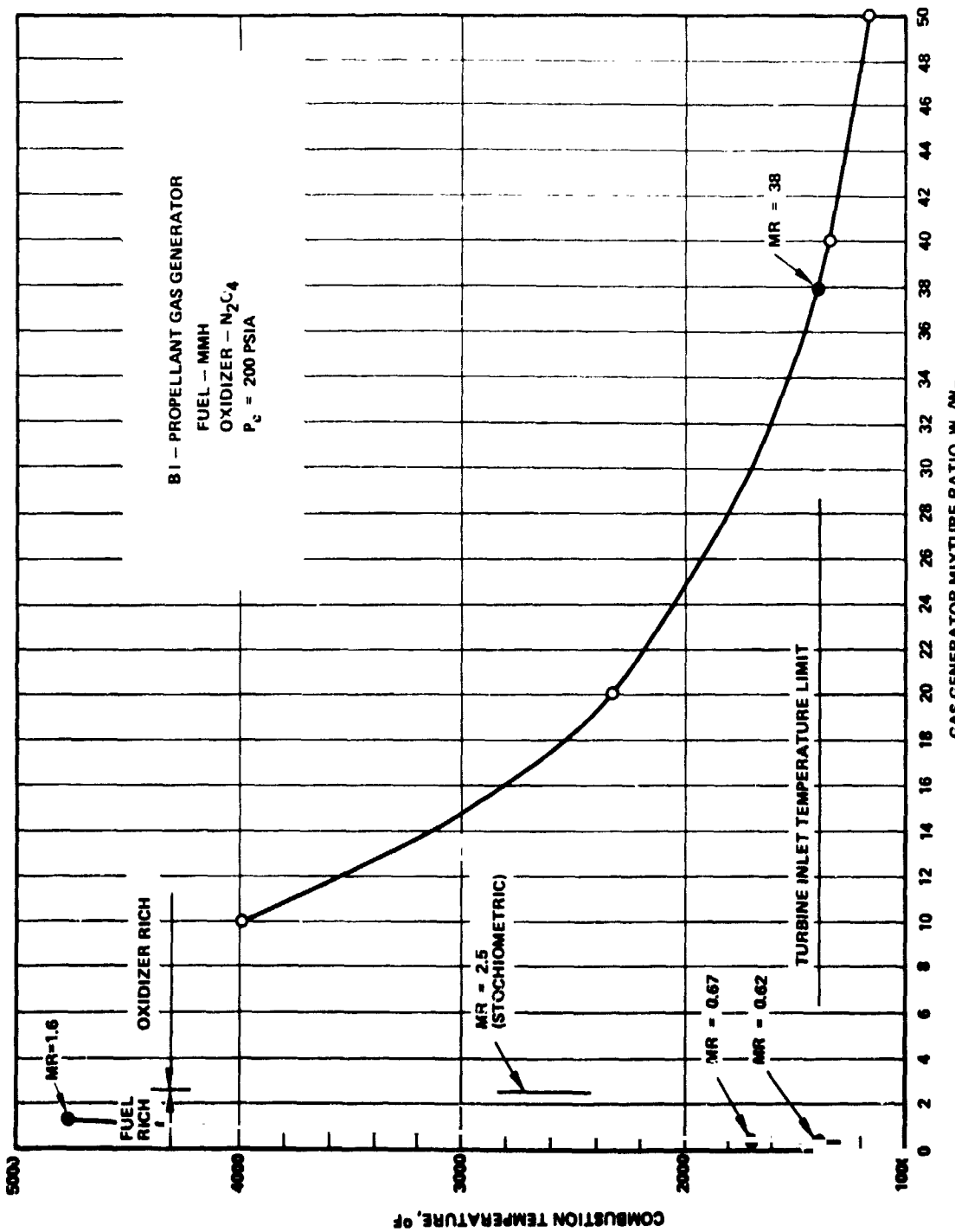

Figure 3-29. Bipropellant Gas Generator Combustion Temperature as a Function of Mixture Ratio

4. SYSTEMS EVALUATION

In evaluating the various candidate PFS's, various qualitative and quantitative factors must be considered that are not directly related to system performance and weight goals. These include system complexity, start system characteristics, combustion stability, and drive system transients. These are discussed below.

4.1 SYSTEM COMPLEXITY

4.1.1 Failure Modes and Effects Analysis

A failure modes and effects analysis (FMEA) was carried out for the four candidate systems. For each system, various failure mode scenarios were postulated. From these, the effect on the system operations were identified. Finally, for each failure mode a system impact category was designated. These were:

Category	Systems Impact
MF	Mission Failure
CF	Catastropic Failure
DMC	Degraded Mission Capability

The results of these analyses are summarized in Table 4-1. The potential failure modes unique to each candidate system are given in Table 4-1. For System Number 1, the lithium-thionyl chloride batteries were assumed to be fully qualified, so that current overpressure explosion problems (by-product sulfur/lithium thermal excursion) have been eliminated. Also, the energy density of 100 watt-hour/lb at high drain rates (1 hour or less) will be achieveable. In System Number 2, it has been assumed that hydrogen gassing problems have been eliminated. Under this assumption, no CF categories were identified for the motor driven pumps. System Number 3 identified two CF categories, both of which were attributable to the monopropellant gas generator portion of the turbine driven pumps. System Number 4 had only one CF category which also was due to a malfunction in the gas generator portion of the system.

Table 4-1. Failure Modes and Effects Analysis for Candidate Propellant Feed Systems

No.	System Description	Failure Mode	Effect on System Operation	System Impact Category
1 & 2	Battery-powered electric motor driven pumps (lithium-thionyl chloride batteries) or (silver-zinc batteries)	1. Solenoid operated relay (Part No. 29) fails to close	1. System will not start up	MF
		2. Battery voltage decreases	2. Motor-pump speed will decrease, reducing pump discharge pressures, flows, and engine thrust level	DMC
		3. Short in motor stator windings	3. System will not start up	MF
		4. Thermal control system fails to maintain required battery temperature causing reduction in voltage and energy density	4. Same as item 2 plus decrease in engine thrusting duration	DMC
3	Monopropellant, gas generator powered turbopump	1. Hydrazine tank pressure regulator (Part No. 31) fails to open	1. System will not start up	MF
		2. Commandable latching valves (Part Nos. 37, 38, 39) fail to open	2. System will not start up	MF
		3. Filter (Part No. 36) becomes partially clogged	3. Filter pressure drop will increase causing a descrease in gas generator mass flow and a drop in turbine output power and speed. Engine thrust level will decrease	DMC
		4. Hydrazine tank pressure regulator (Part No. 31) fails full open and relief valve (Part No. 33) fails to open	4. Hydrazine tank will rupture	CF
		5. Catalyst temperature is not maintained by heater	5. Gas generator explodes due to excess N_2H_4 in combustion chamber at ignition	CF
4	Bipropellant, gas generator powered turbopump	1. Accumulators (Parts 29 and 30) inadequately charged	1. Turbine will not reach full speed and system may fail to start up	MF
		2. Commandable latching valves (Part Nos. 33, 34, 35, 36, 37, and 38) fail to open	2. System will not start up	MF
		3. Filters (Part Nos. 16 and 17) become partially clogged	3. Same as item 3 for System No. 3, and also off-mixture ratio could cause gas generator to burst due to excessive temperature	DMC or CF

Table 4-1. Failure Modes and Effects Analysis for Candidate Propellant Feed Systems (Continued)

No.	System Description	Failure Mode	Effect on System Operation	System Impact Category *
1 to 4	Propellant feed system for all candidate pump drive systems	1. Helium pressure regulator (Part No. 23) fails to open	1. Main pumps will cavitate due to inadequate net positive suction head. Turbine/motor overspeed will result and overspeed signal will shut system down	MF
		2. Helium pressure regulator (Part No. 23) fails full open and relief valves (Part Nos. 26 and 27) fail to open	2. Main propellant tanks will rupture	CF
		3. Filters (Part Nos. 14 and 15) become partially clogged	3. Same as item 1	MF
		4. Pump drive bearings fail	4. Bearing seizure will stop rotation and will stop engine thrusting or cause engine blow-up due to off-mixture ratio operation	MF or CF
		5. Commandable latching valves (Part Nos. 19, 20, 21, 22) fail to open	5. Engine will not start up or may rupture if excessive fuel collects due to partial oxidizer valve opening	MF or CF
		6. Filters (Part Nos. 16 and 17) become partially clogged	6. Filter pressure drop will cause a decrease in mass flow to engine thrust chamber decreasing thrust level or cause off-mixture-ratio operation causing engine thrust chamber to rupture	MF or CF
		7. Start-up and/or shutdown transients excessively long	7. Close control of velocity increments during each thrusting phase will be decreased	

*

Category	System Impact
MF	Mission Failure
CF	Catastrophic Failure
DMC	Degraded Mission Capability

Table 4-1 indicates failure modes common to all four candidate systems. Four CF categories were identified.

In many cases the number of CF categories can be reduced or eliminated by additional component redundancy. This is discussed further in Section 5.5.

4.1.2 Development Risks

There are various levels of development risks associated with each candidate PFS. A qualitative assessment has lead to the summary indicated in Table 4-2.

As can be seen from Table 4-2, the battery-powered electric motor powered pumps constitute the lower development risk approach to pump-feed propellant feed systems. However, for greater growth potential to higher thrust levels and longer burning times, the higher risks associated with the gas-generator, turbine driven pumps must be assumed if a minimum weight system is to be achieved.

Table 4-2. Relative Rating of Development Risks for Candidate Pump-Fed Propellant Feed Systems

System No.	Description	Relative Development Risk Rating	Major Development Risk Factors
2	AgZn Battery-Powered Electric Motor Driven Pumps	1 (Lowest)	• 50 w-hr/lb energy density at high current drain rate must be confirmed by test
1	Li-ThCl Battery-Powered Electric Motor Driven Pumps	2	• 100 w-hr/lb energy density at high current drain rate not yet available
3	Monopropellant GG Turbine Driven Pumps	3	• Gas generator/turbine start/stop transient response must be confirmed
4	Bipropellant GG Turbine Driven Pumps	4 (Highest)	• Same as System 3 plus pump-fed gas generator interactions/stability must be demonstrated

4.1.3 Critical Technologies

There are various critical technologies associated with each candidate PFS. These will require additional development effort in order to arrive at a fully flight-qualified system. These are discussed below for each candidate PFS.

The silver-zinc battery development status is the most critical component of candidate PFS Number 2. These batteries should be able to achieve energy densities of 60 watt-hr/lb and volumetric energy densities of 4.2 watt-hr/cu in. Hence, the values of 50 watt-hr/lb and 2.25 watt-hr/cu in. used in this study are reasonably conservative. The critical technology associated with this component is the hydrogen outgassing that occurs due to the reaction of the electrodes with the electrolyte. To meet Space Shuttle safety requirements, this undesirable characteristic must be minimized electrochemically or by the use of hydrogen getters.

Similarly, for PFS Number 1, the lithium-thionyl chloride batteries involve the most critical technologies. Perhaps the least complex is that long term storage capability has not been fully demonstrated. For the PFS this may be resolvable as a purely logistic problem by avoiding long term storage in operations. The more critical technology is associated with the exothermic reaction of the byproduct formation of sulfur/lithium which can create potential thermal excursion hazards and could lead to an explosion. Lastly, these batteries exhibit a limited current density capability so that rate of discharge must be slow (10-24 hours). At increased discharge rates (i.e., 1 hour), these batteries must be severely downrated so that the achieverable energy density may be as low as 20 watt-hr/lb rather than the 100 watt-hr/lb assumed during this study.

The successful operation of a monopropellant pressure-fed N_2H_4 gas generator has become state of the art. Earlier problems with cold catalyst beds and the hazards of delayed ignition have been resolved. Hence, the only critical technology that can be associated with PFS Number 3 is that associated with the start/stop transients of the gas generator and turbopumps. These can usually be resolved initially by a very detailed transient response analysis. Later this can be confirmed by development testing. The critical factor involved in attaining the required transient response at start-up and shutdown is to avoid combustion

instability in the rocket engine thrust chamber and the minimization of velocity increment dispersions.

The bipropellant PFS Number 4 has the same critical technologies as those outlined for PFS Number 3. In addition, since the gas generator operation is directly linked to the main propellant pumps, the interactions and stability of the system during the start-up and shutdown transient phases, as well as steady-state operation, must be demonstrated by test. Finally, the desired mode of operation to limit the gas generator combustion gas temperature to 1400°F is to use fuel-rich or oxidizer-rich mixture ratios. Because very large temperature excursions will occur with a very small change in mixture ratio (Figure 3-29), this parameter must be very carefully controlled. This will indirectly impose close speed control of the turbopumps in order to minimize pump discharge pressure and flow dispersions.

4.2 FEED SYSTEM TRANSIENT ANALYSES

Each of the three candidate propellant feed systems was analyzed to determine its transient behavior during start-up and shutdown. The systems were modeled with differential equations solved using a fourth order Runge-Kutta integration routine. The controls schematics for each design are shown in Figures 4-1, 4-2, and 4-3.

Since some of the components have not been fully defined, several assumptions were made. These involve:

- Mass properties – The size, weight and mass moment of inertia were not known for each component, therefore, these properties were estimated based on the approximate size of the component.
- Valves – All valves were assumed to be fast-acting, with a time constant of 12 milliseconds.
- Relief valves – To prevent overpressurization of the bipropellant lines downstream of the pumps, it was assumed that a relief valve and bypass were on each line. The cracking pressure for the relief valve was set at 310 psia.
- Pumps – It was assumed that the mass flow from the pumps was a linear function with respect to the pump speed.
- Each line is primed before the pressure increases, i.e., the pipe is filled before the pressure is calculated.

Additional assumptions relating to a specific system are given below.

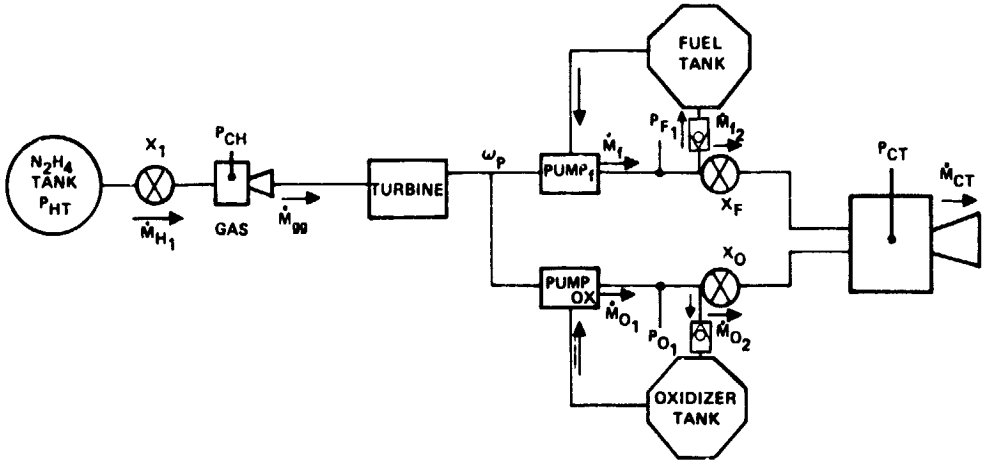

Figure 4-1. Controls Schematic for Monopropellant Gas Generator Powered Turbopump PFS

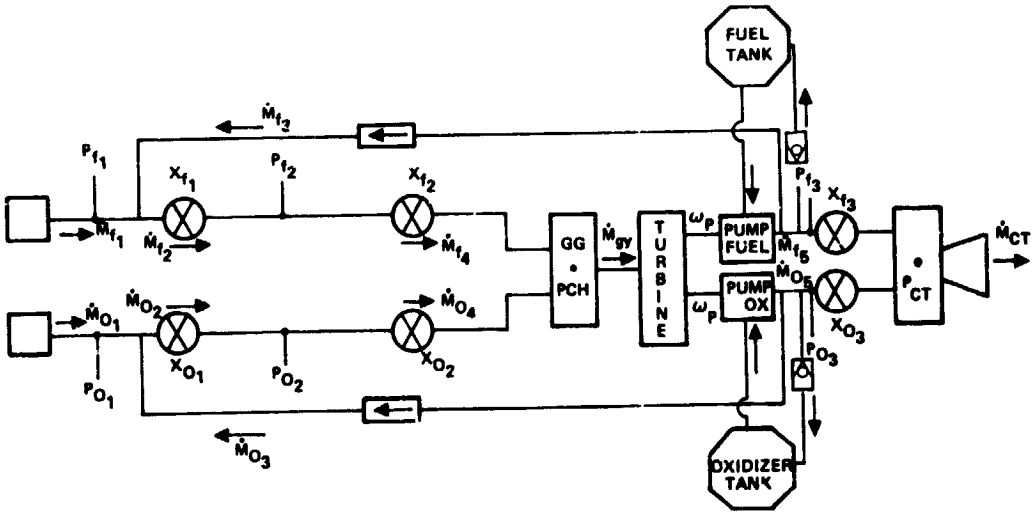

Figure 4-2. Controls Schematic for Bipropellant Gas Generator Powered Turbopump PFS

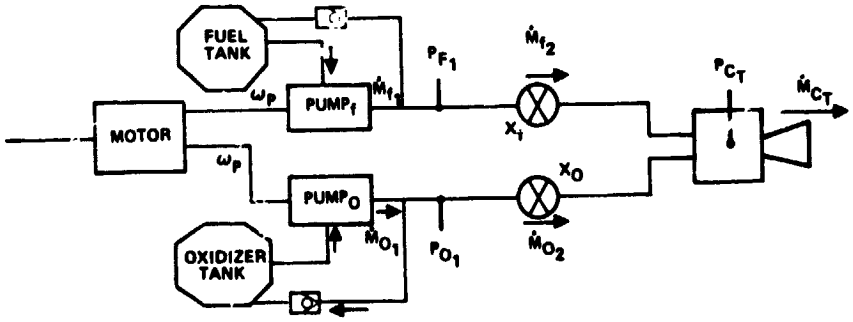

Figure 4-3. Controls Schematic for Battery Powered, Electric Motor Driven Pumps PFS

The pumps for each system had a steady-state speed of 84,000 rpm. The bipropellant engine design mixture ratio was 1.6 with a flame temperature of 5460°R (2760°C). The steady-state flow rates were 1.24 lbm/sec for the fuel and 1.99 lbm/sec for the oxidizer. The chamber pressure was 150 psia.

4.2.1 Monopropellant Gas Generator Powered Turbopumps

This system uses hydrazine to power the turbine. The hydrazine is pressure fed from a constant pressure tank through a gas generator and then into the turbine. The turbine drives the two pumps which feed the engine. The gas generator has a chamber pressure of 200 psia and a mass flow rate of 0.0113 lbm/sec. The steady-state temperature is 2250°R (977°C).

The major assumption for this system involves the temperature in the gas generator. Similar hydrazine thrusters require approximately 4 seconds to get to steady-state temperature from a cold (ambient) start. For this model, a linear temperature rise was assumed with the temperature reaching steady-state 4 seconds after the gas begins flowing into the gas generator.

The pressure ratio across the turbine was assumed to be 20/1. The line diameters downstream of the pumps were 0.480 inch for the fuel and 0.430 inch for the oxidizer. The line length was 5 feet from the pump to the engine.

The valve timing is shown in Figure 4-4. The hydrazine valve was given the signal to open at t = 0 seconds. The valves between the pumps and the engine were opened at t = 2.60 seconds. The opening was delayed to allow the pump speed (Figure 4-5) to increase until it neared the steady-state value. All of the valves were signaled to close at t = 5 seconds.

As can be seen in Figure 4-5, the pump speed rises quickly until the fuel and oxidizer lines are primed. The pressure in both lines (Figure 4-6) rapidly reaches the cracking pressure of the relief valves. The pump speed decreases sharply as the line pressures increase to a minimum value of 63,000 rpm. The pump speed gradually builds up until the fire valves are opened. The pumps reach the steady-state speed of 84,000 rpm

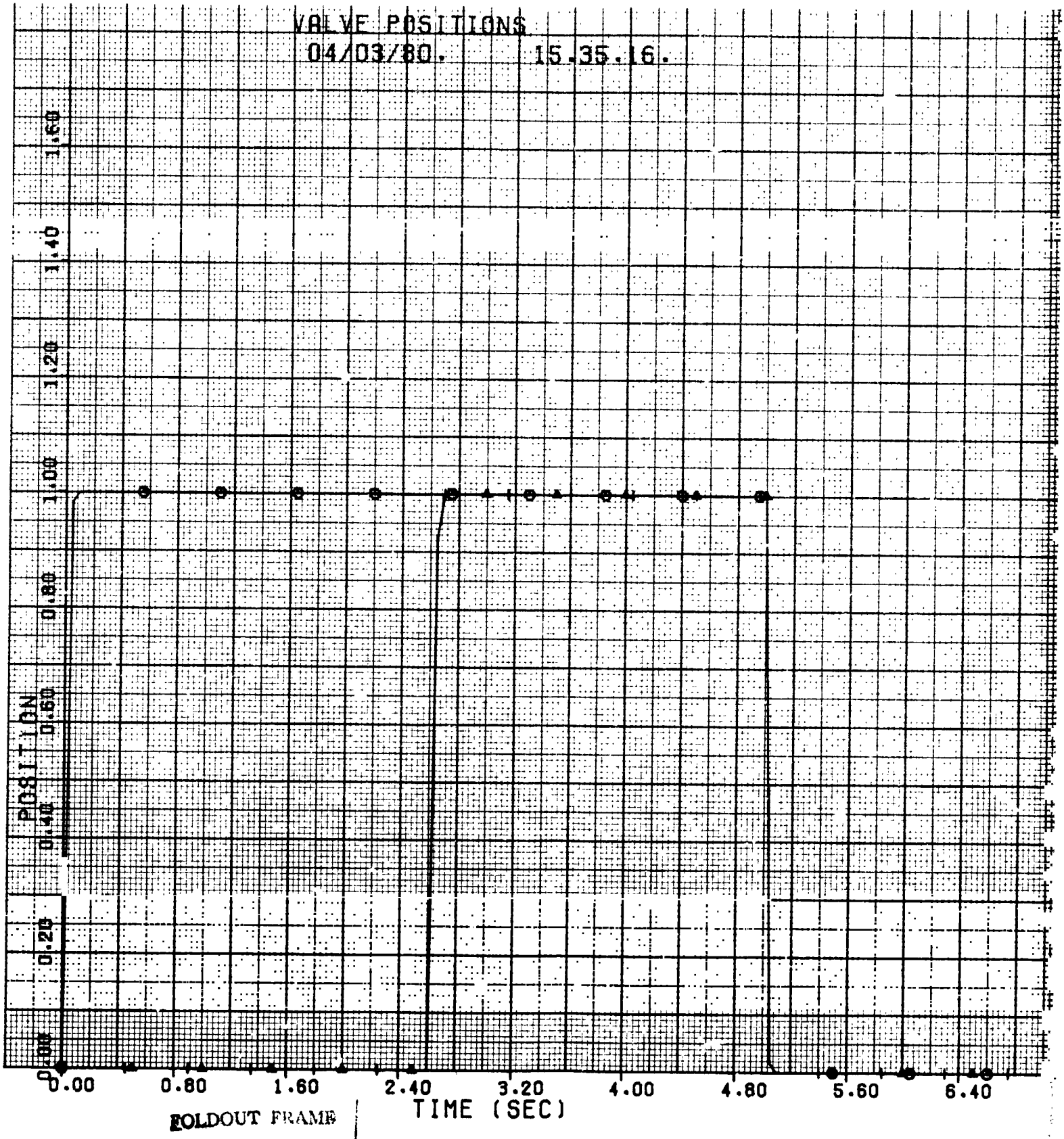

FOLDOUT FRAME

ORIGINAL PAGE IS
OF POOR QUALITY

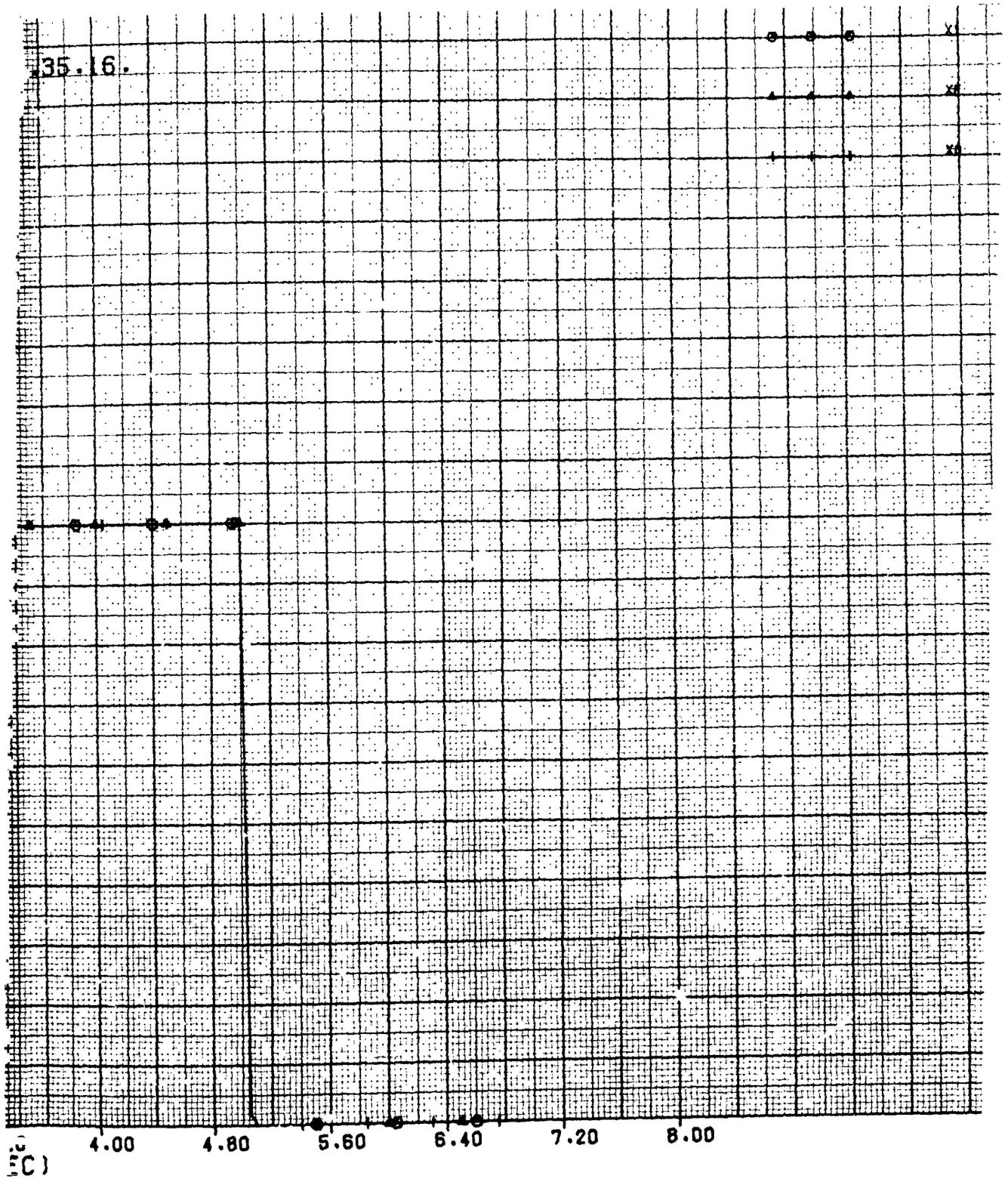

Figure 4-4. Valve Positions

FOLDOUT FRAME 2

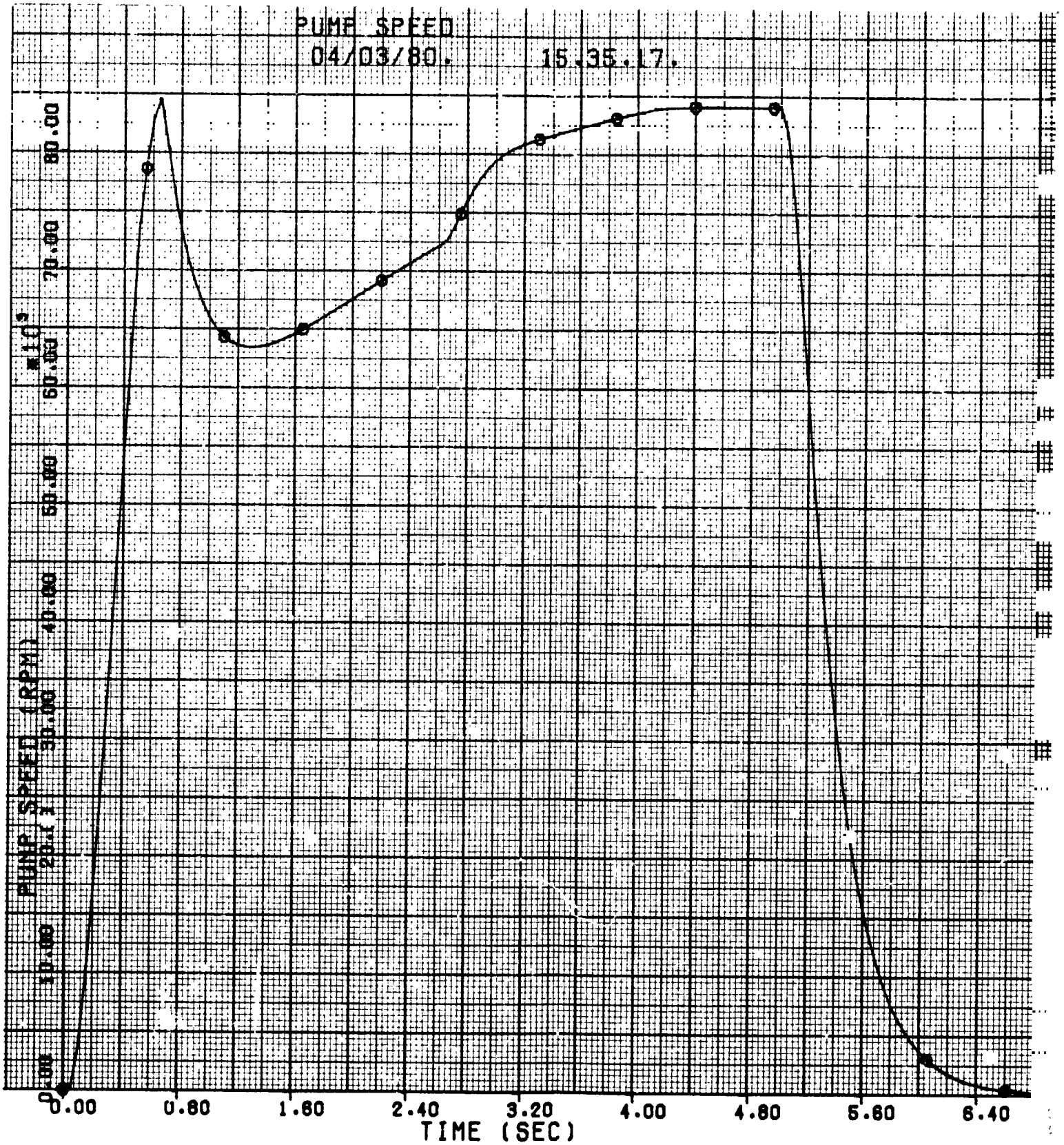

FOLDOUT FRAME

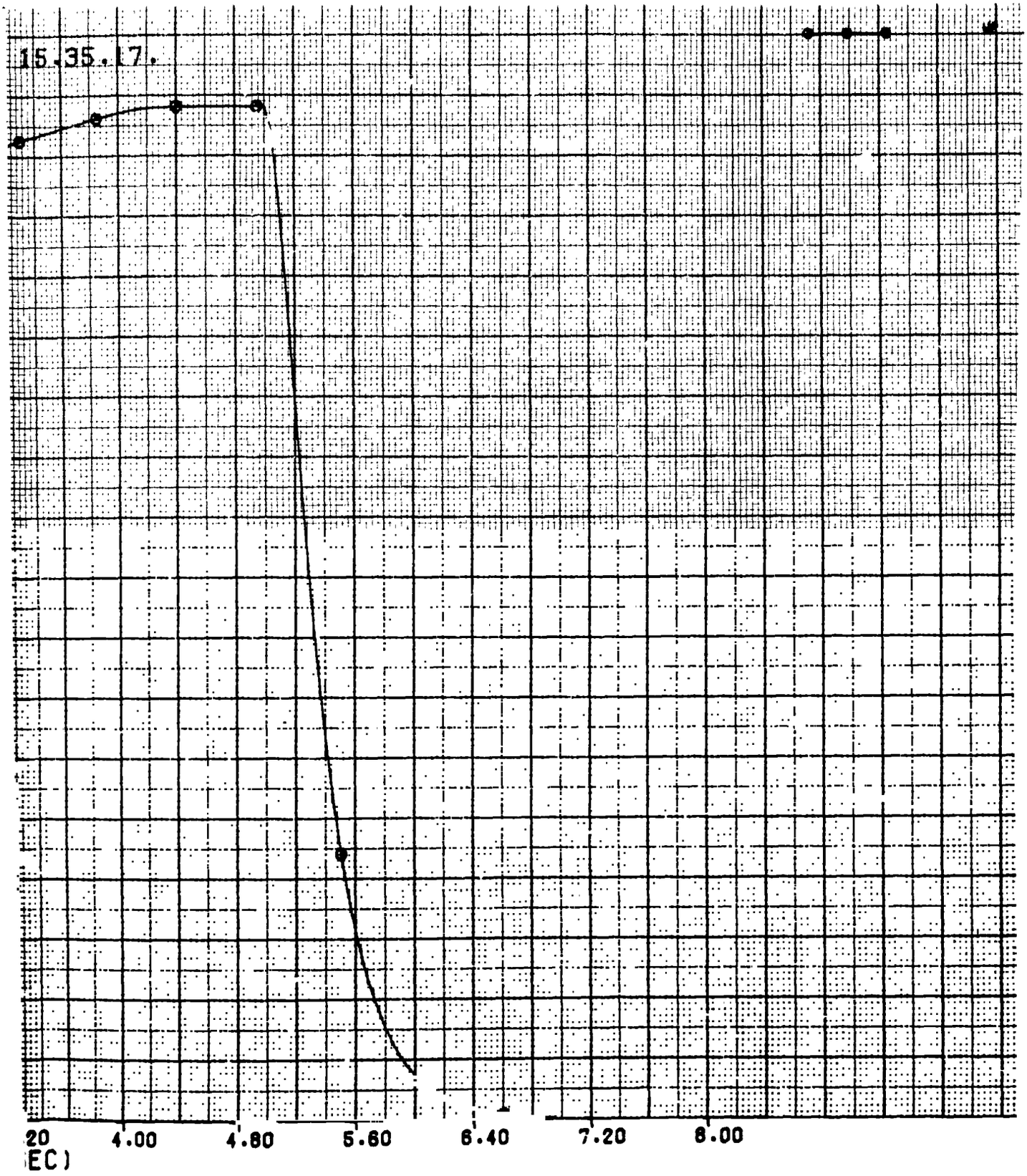

Figure 4-5. Pump Speed

FOLDOUT FRAME 2

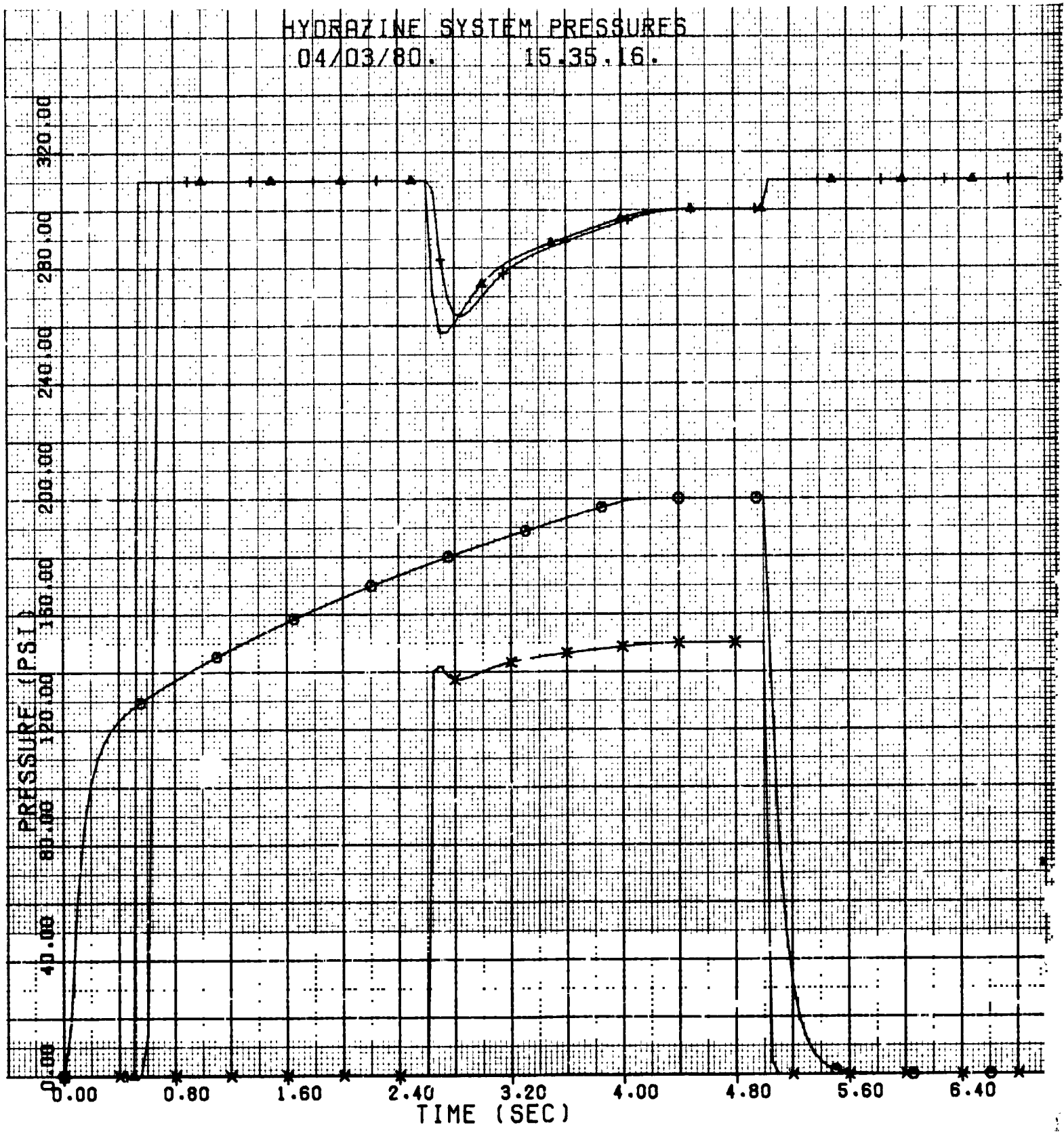

FOLDOUT FRAME

ORIGINAL PAGE IS
OF POOR QUALITY

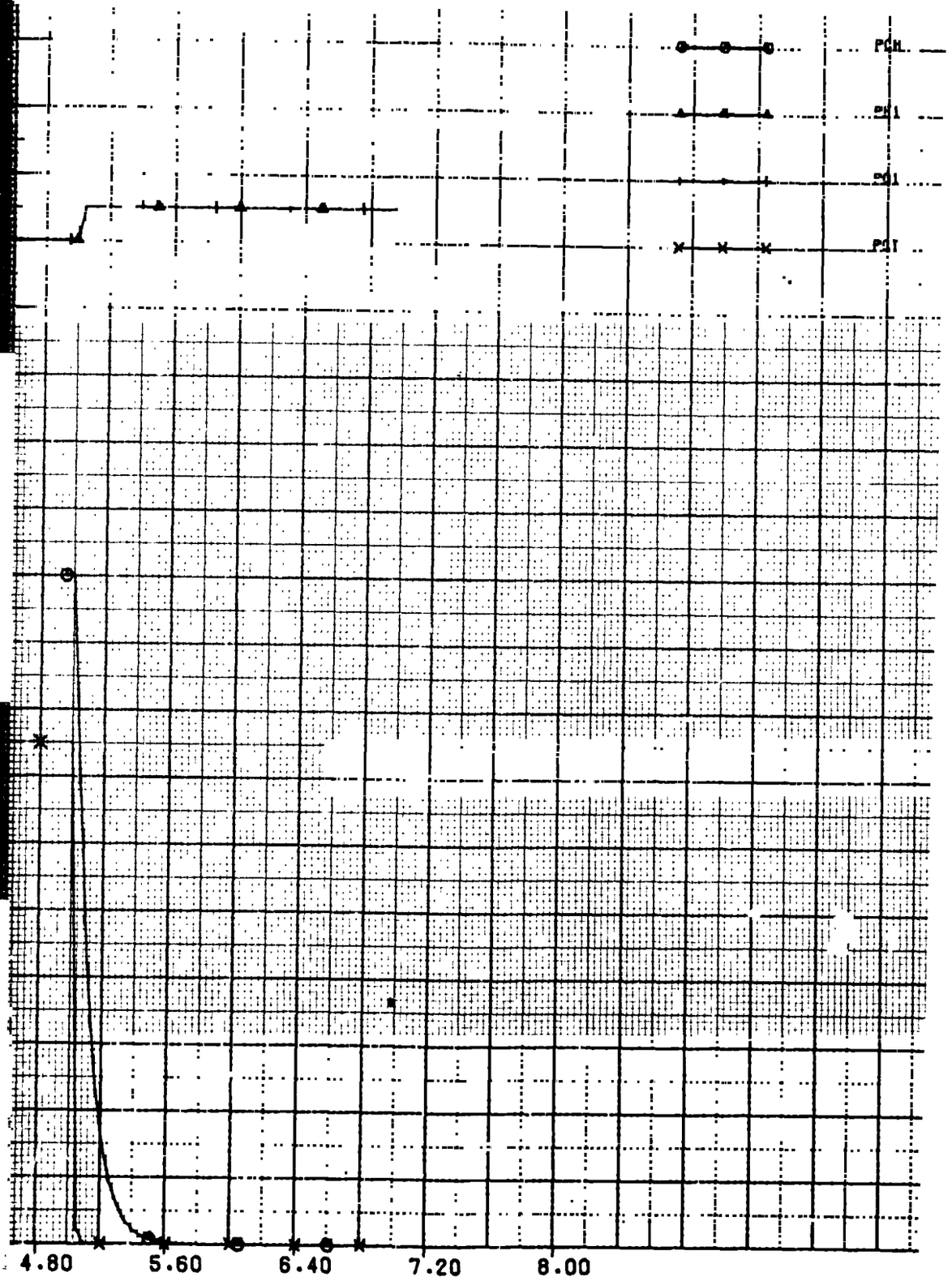

Figure 4-6. Hydrazine System Pressures

FOLDOUT FRAME 2

at t = 4.4 seconds. At t = 5 seconds, the valves are closed and the speed drops to zero within 2 seconds.

The fuel and oxidizer line and gas generator and engine combustor pressures are shown in Figures 4-6 and 4-6a. The pressure in the gas generator reaches its steady-state pressure in 4 seconds as a result of the temperature dependency. The oxidizer and fuel pressures increase to 310 psia very quickly once the lines are primed. At t = 2.6 seconds, when the valves are opened, the pressures drop to approximately 260 psia on the fuel side and 265 psia on the oxidizer side. They both reach 300 psia at t = 4.4 seconds. When the valves are closed, the pressures rise to their maximum values, 310 psia. As shown in the expanded scale of Figure 4-6a, there is no feed system/engine coupling (chugging) caused by the high injector pressure drop-to-combustor pressure ratio. The engine chamber pressure reaches its steady-state value approximately 1.4 seconds after the valves are opened. This is due to the pump transient, indicating that valves should not be opened until full pump speed is reached if there is a problem operating the engine at less than 100% thrust levels.

Figure 4-7 shows the temperatures in the gas generator and in the engine. The gas generator temperature function is shown as described above. The engine temperature increases quickly when the valves are opened. After a slight overshoot, the temperature decreases to its steady-state value.

The mass flow rates are shown in Figure 4-8. The flows into and out of the gas generator are shown multiplied by 100. The fuel and oxidizer flows can be seen to follow the pump speed. The flows into and out of the engine rise sharply at t = 2.6 seconds, which is when the valves open.

The amount of each propellant used is shown in Figure 4-9. The difference between the summation of MF1 and MF2, and the difference between the summation of M01 and M02 is the amount of propellant discharged through the bypass.

The mixture ratio is shown in Figure 4-10. The actual value of the spike is higher but it not shown because of the limitation of the plot routine.

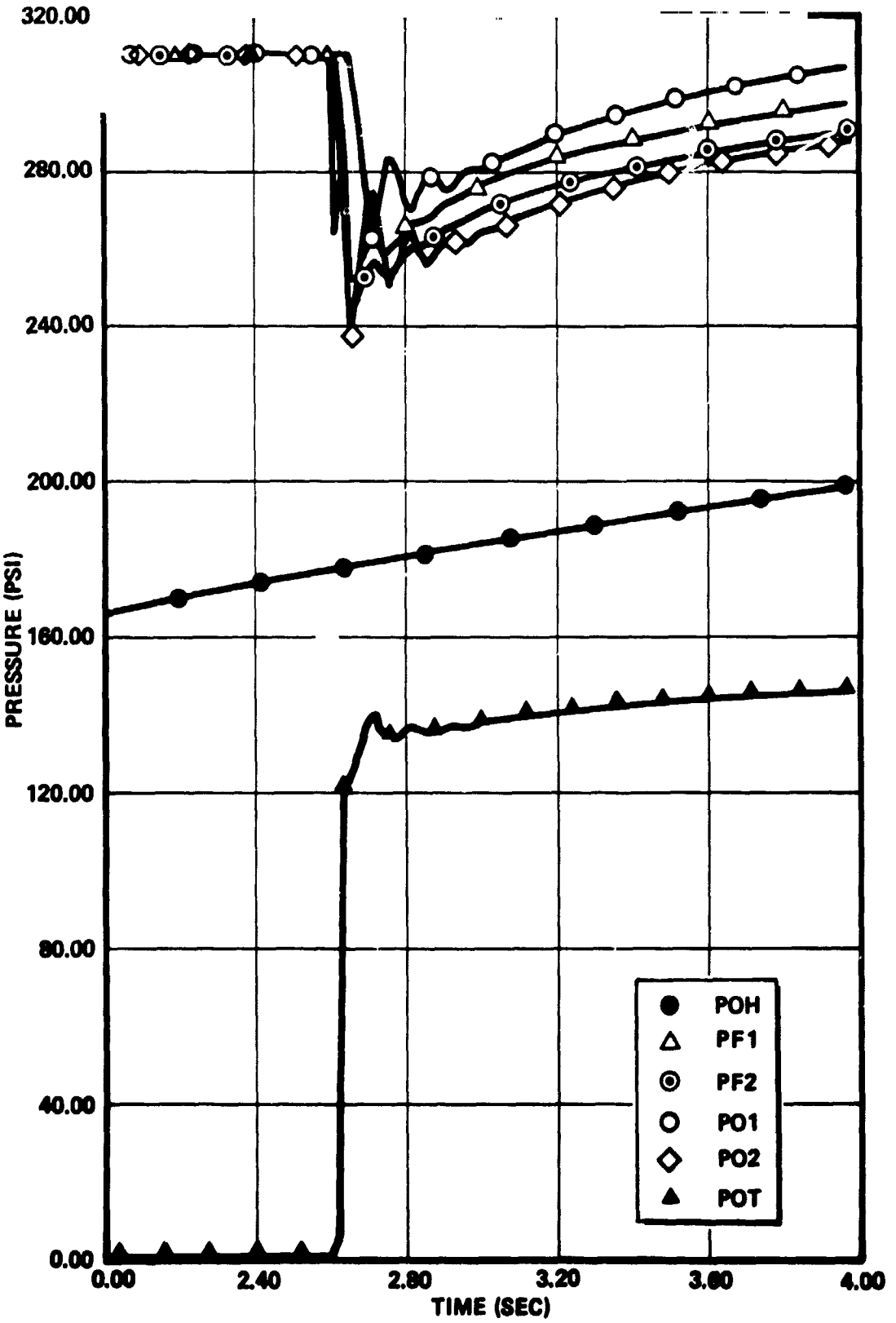

Figure 4-6a. Hydrazine System Pressures

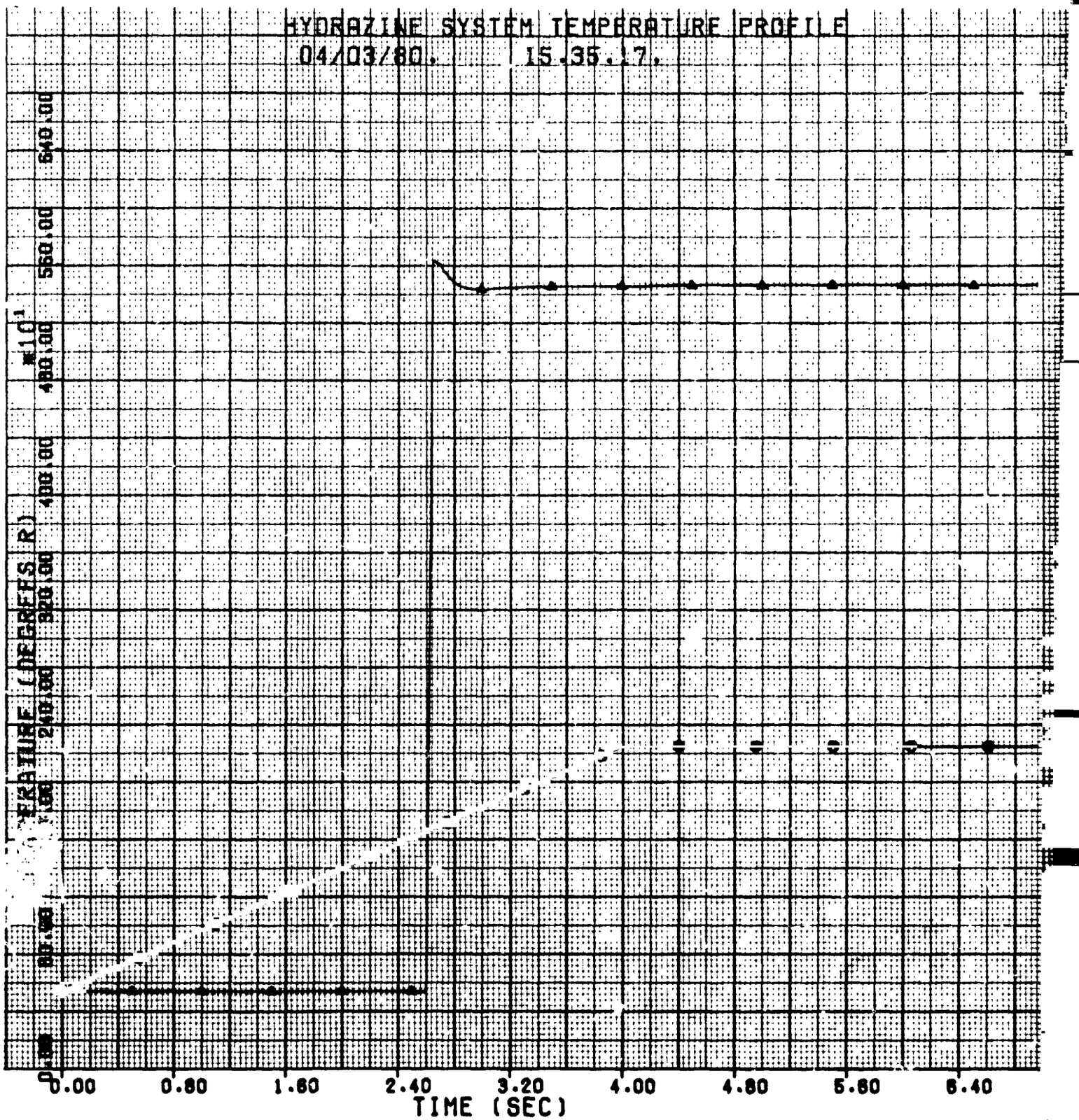

ROLLOUT FRAME

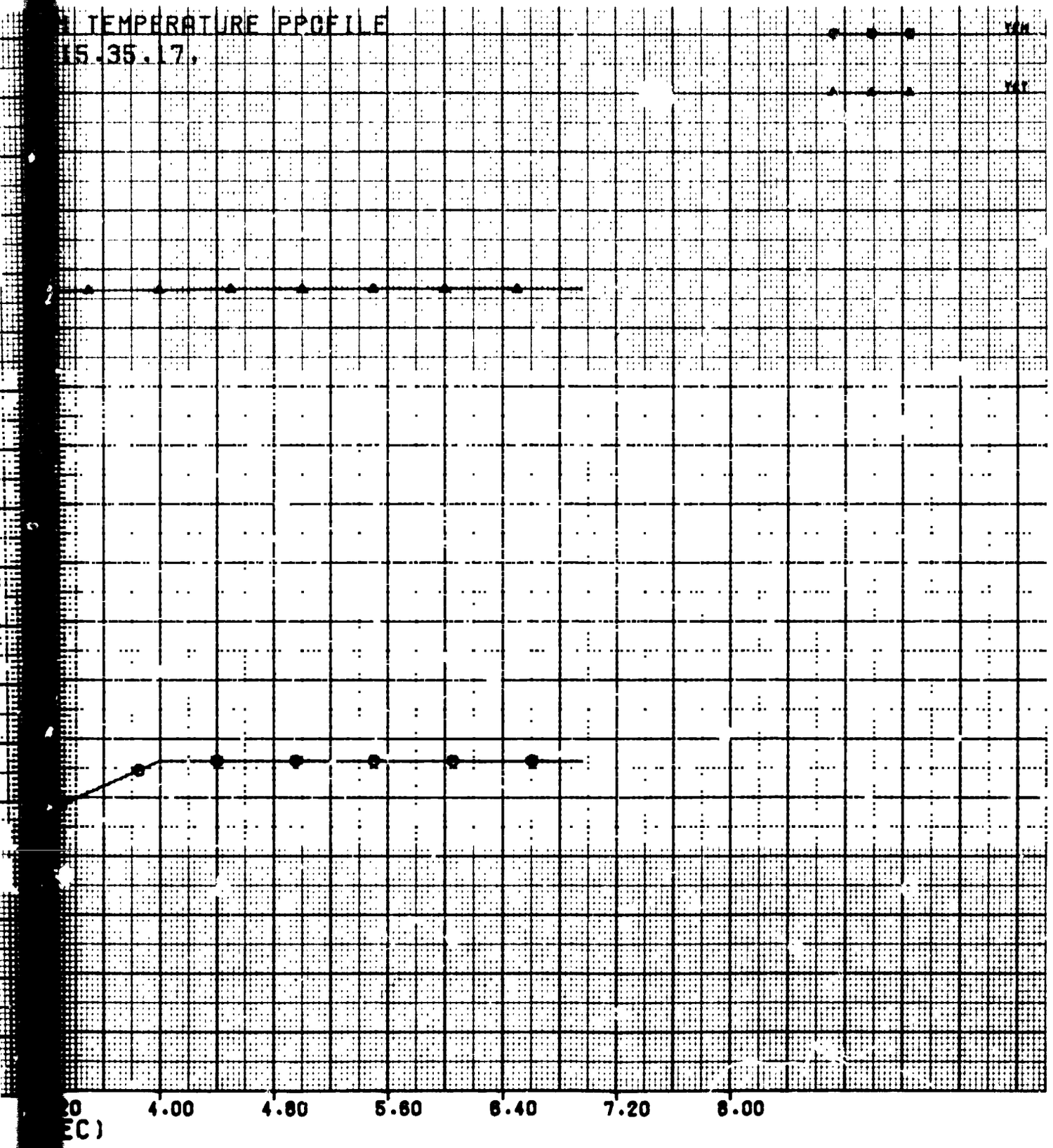

Figure 4-7. Hydrazine System Temperature Profile

FOLDOUT FRAME 2

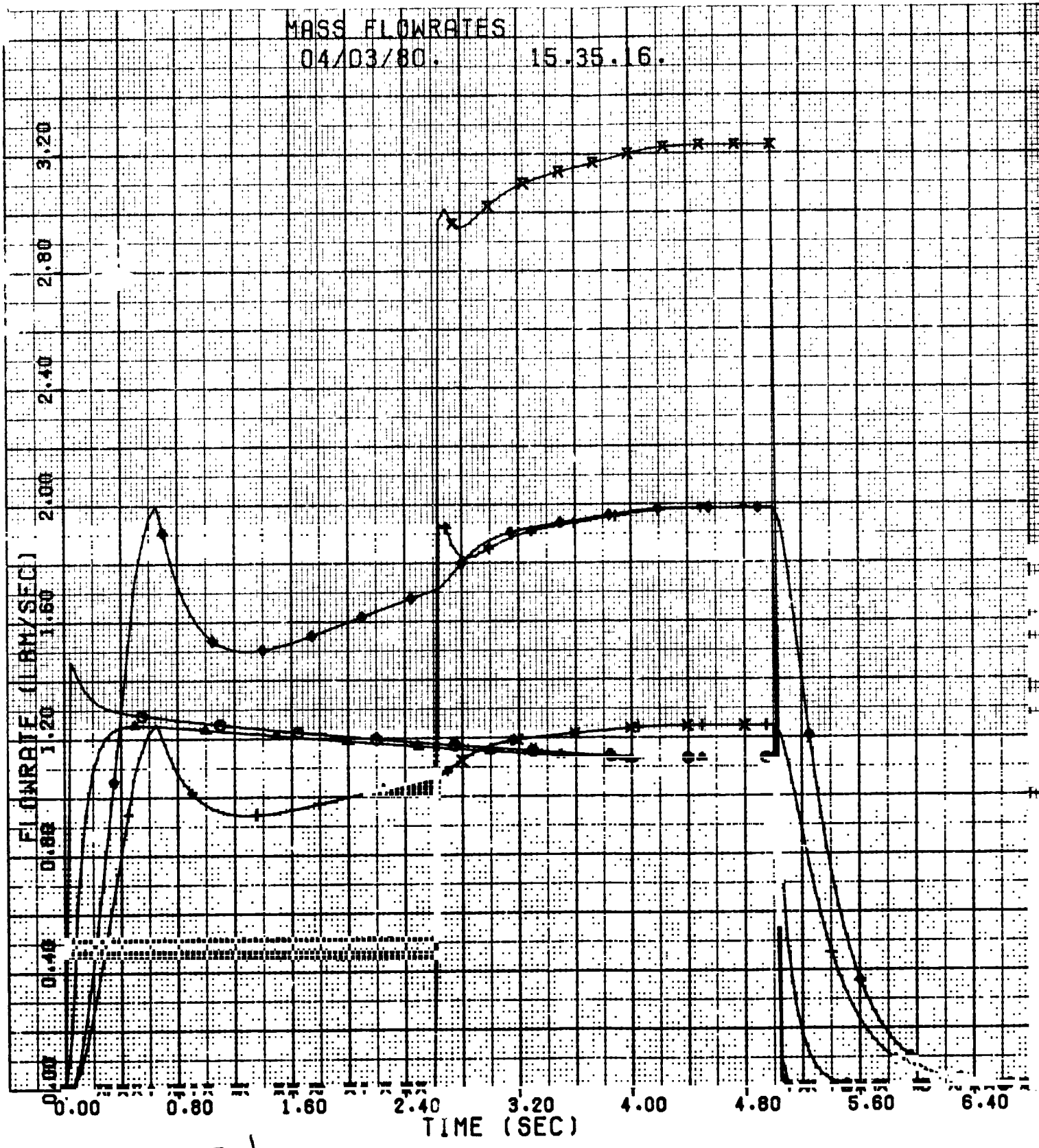

FOLDOUT FRAME 1

C-2

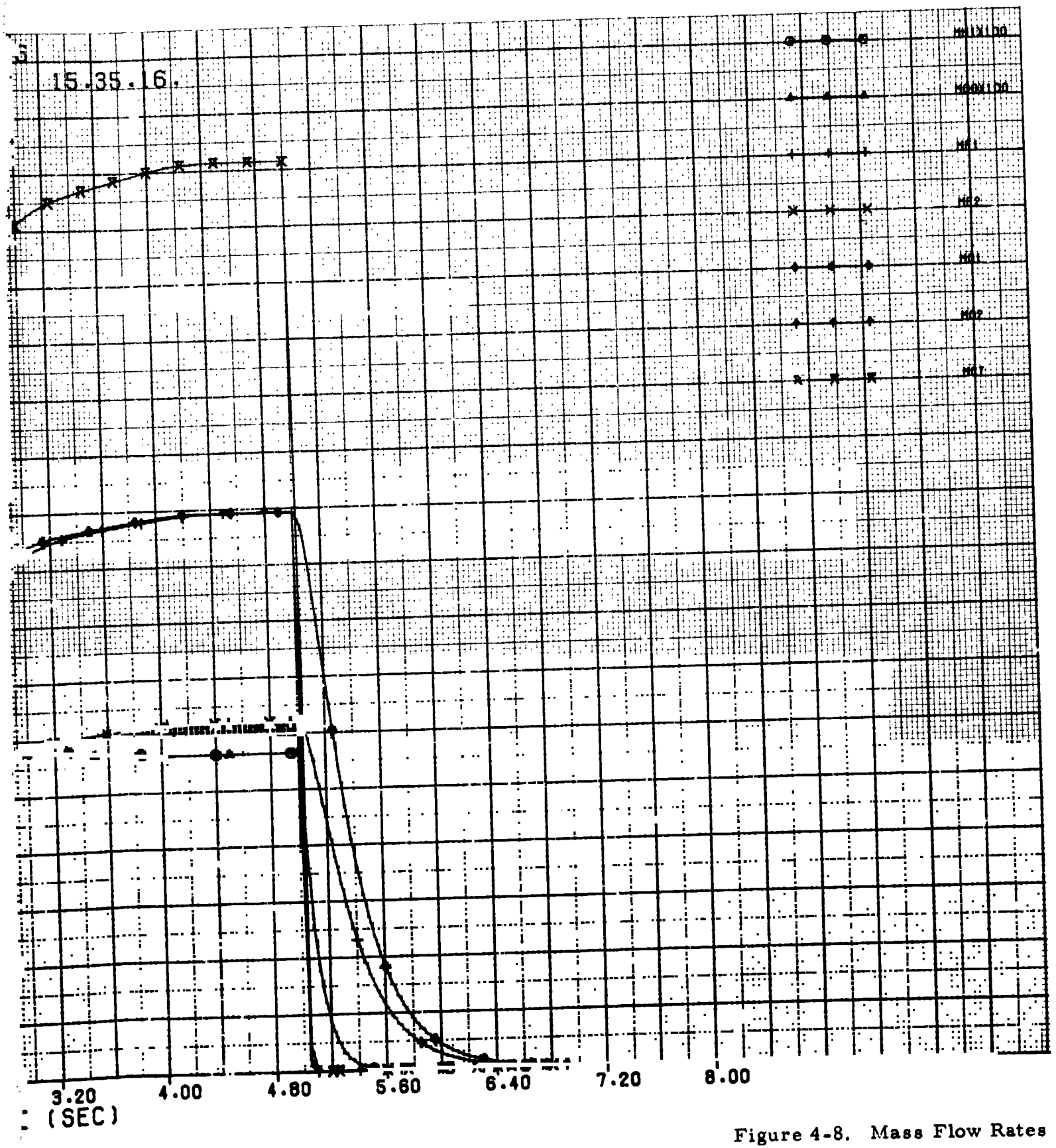

Figure 4-8. Mass Flow Rates

FOLDOUT FRAME 2

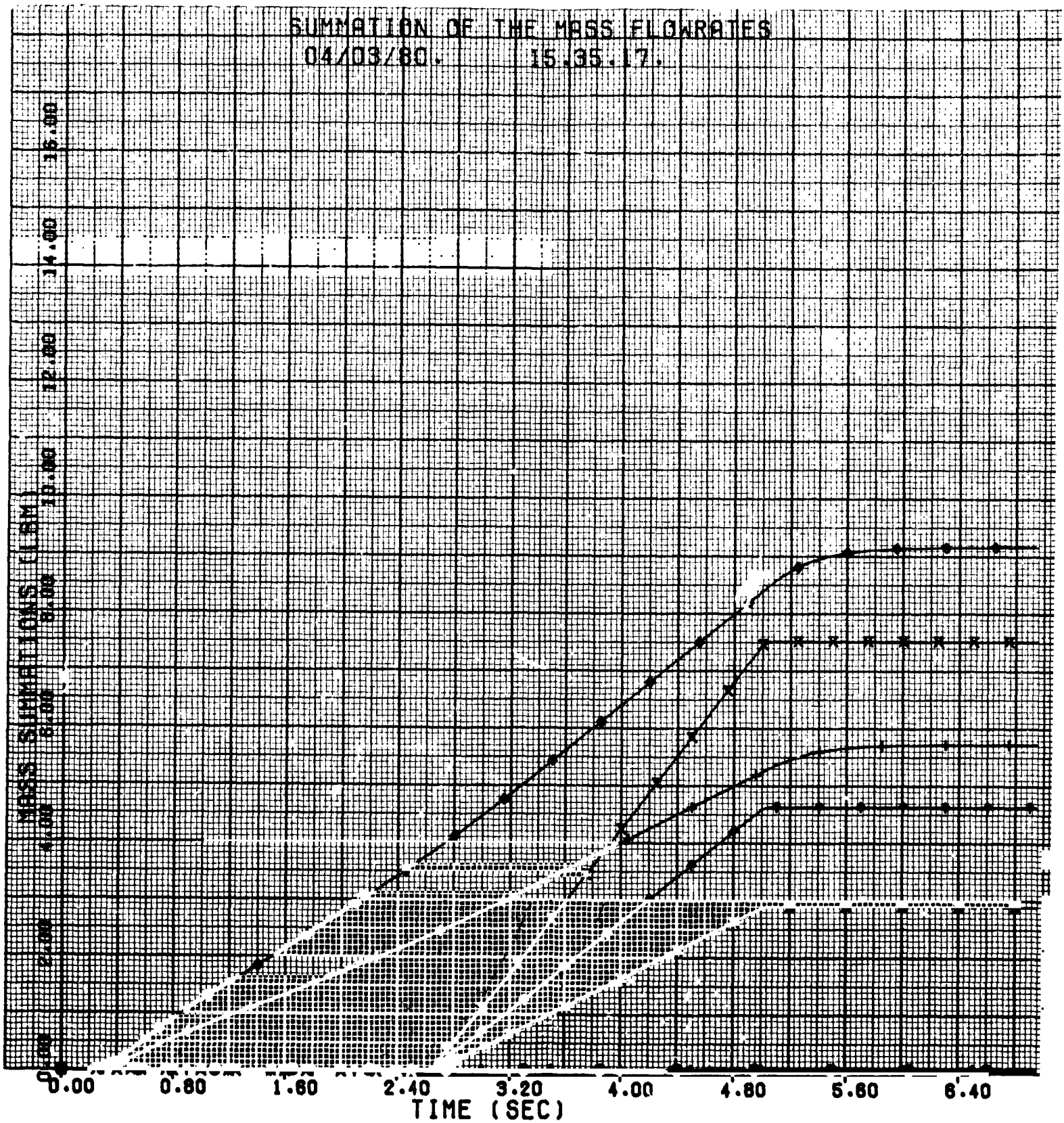

FOLDOUT FRAME

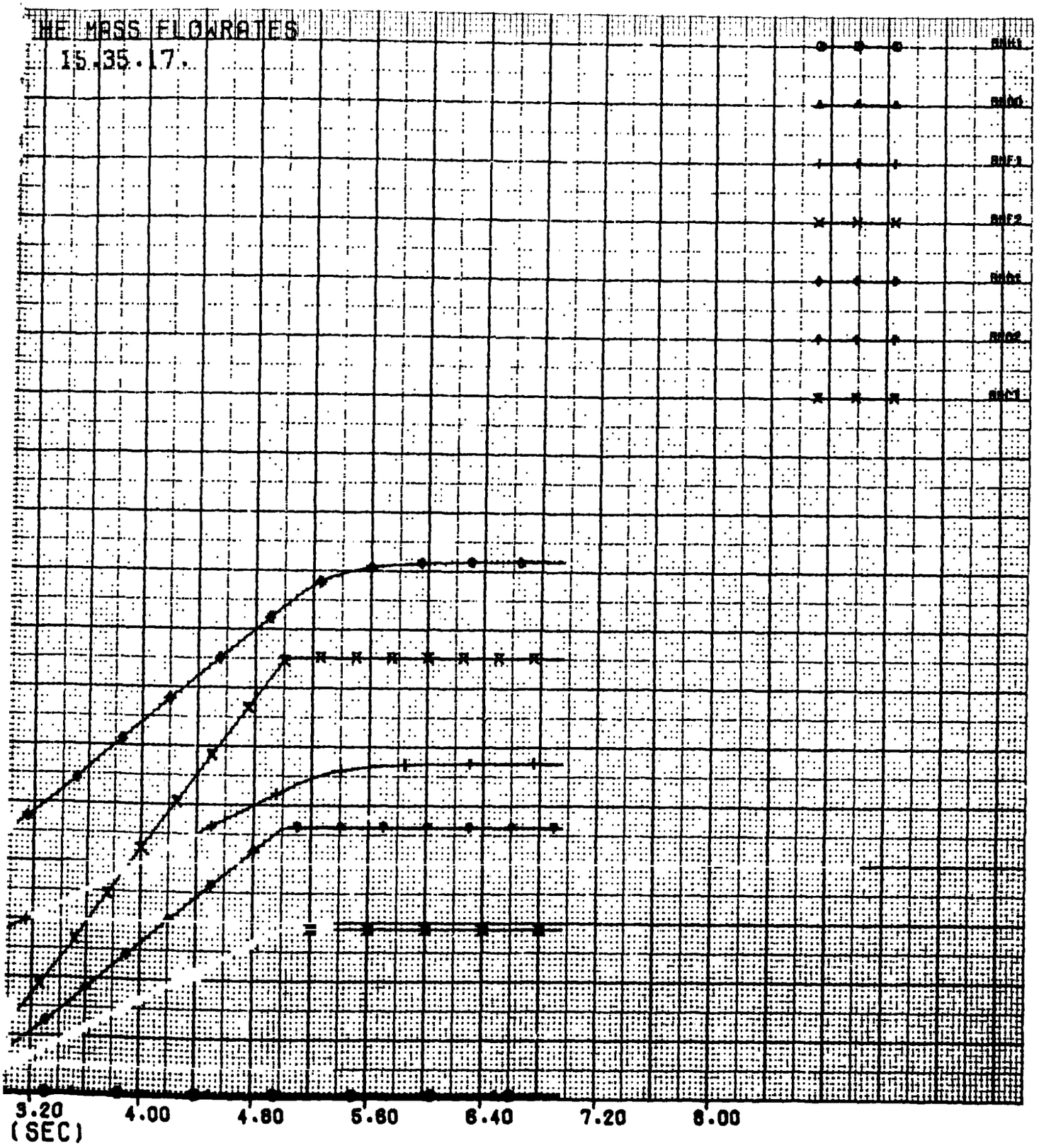

Figure 4-9. Summation of the Mass Flow Rates

2 FOLDOUT FRAME

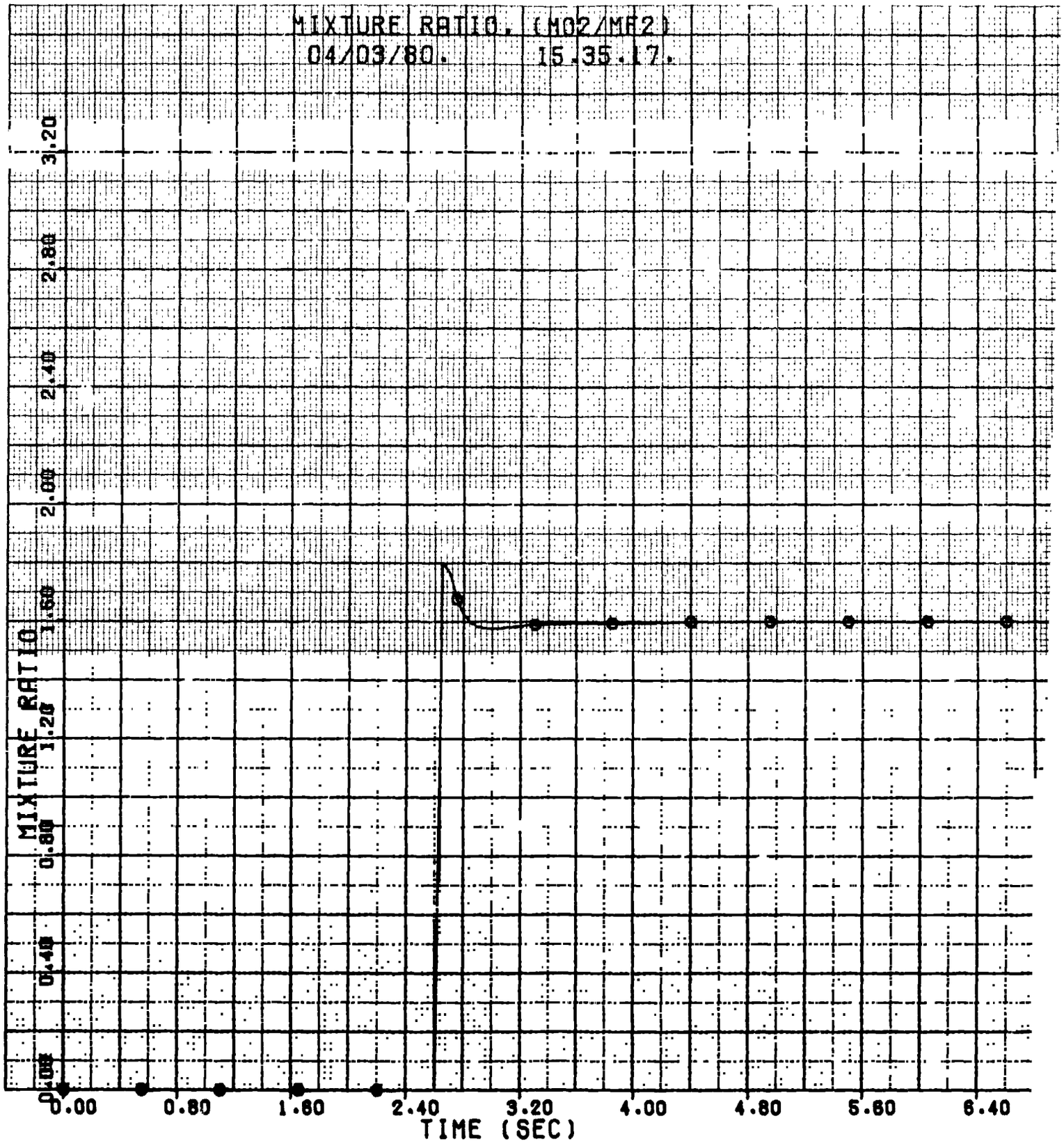

FOLDOUT FRAME

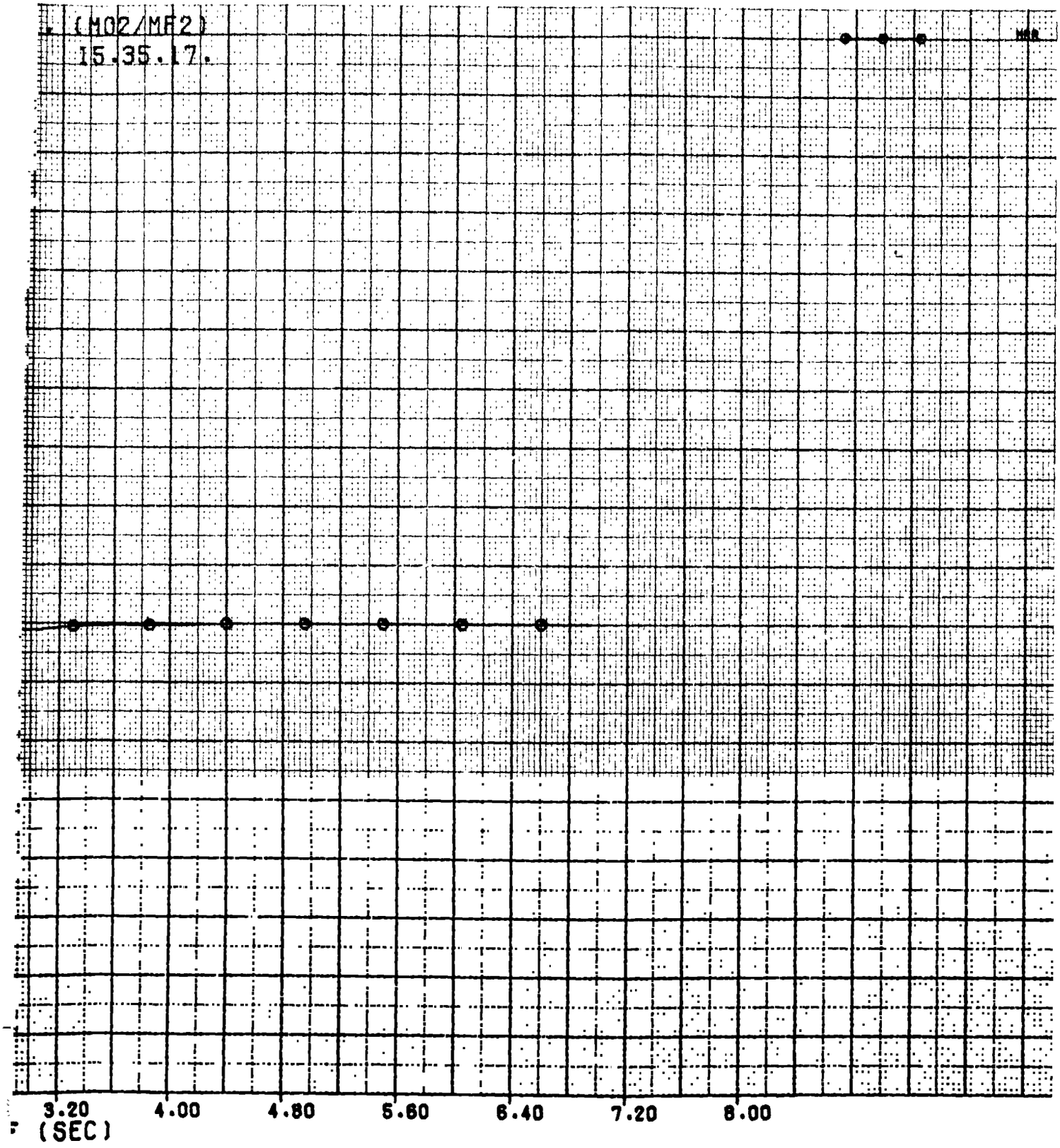

Figure 4-10. Mixture Ratio (MO_2/MF_2)

The primary disadvantage of this system is the time lag required to get the pump to full speed before opening the fire valves. Faster starts can be achieved, if desired, by using higher initial gas generator flows. Once the fire valves are opened, the system reaches steady-state quickly.

4.2.2 Bipropellant Gas Generator Powered Turbopumps

For this system, the MMH and N_2O_4 are used to drive the turbine. Initially, the fuel and oxidizer are fed from accumulators. Once the pumps are working, the accumulators are recharged from the downstream side of the pumps. The mixture ratio (W_O/W_F) for the gas generator used to drive the turbine is 0.4. The steady-state temperature is 1910°R. The mass flow is 0.00588 lbm/sec for the oxidizer and 0.01470 lbm/sec for the fuel. The pressure ratio across the turbine is again 20 to 1.

The accumulators were assumed to be 10 cubic inches in volume and to be charged to an initial pressure of 300 psia. Again, a relief valve and bypass were assumed for the lines.

Figure 4-11 shows the valve opening sequence. For this run, the valves were set to open as soon as the lines were primed. As a result, the oxidizer valve feeding the turbine opens immediately. The fuel valve opens at approximately 0.35 second. This oxidizer lead causes a large spike in the mixture ratio which can be reduced by adjusting the valve sequence logic. The fire valves open much sooner than in the hydrazine system. The pump speed (figure 4-12) does not have the sudden drop that the hydrazine system exhibited, therefore, there is no need to wait for the speed to build back up. All of the valves are closed at t = 5.5 seconds.

Figure 4-13 shows the pressure profiles. The system responds very quickly and reaches steady-state in 1.5 seconds. The oxidizer accumulator pressure drops approximately 10 psi before it is recharged by the pump. The pressure in the fuel accumulator decreases very slightly. When the valves are closed, the accumulator pressures and the pressures downstream of the pump rise to their maximum value. The full propellant line dynamics were not included in this model but the stability results would be the same as shown in the hydrazine case because of the injector resistance.

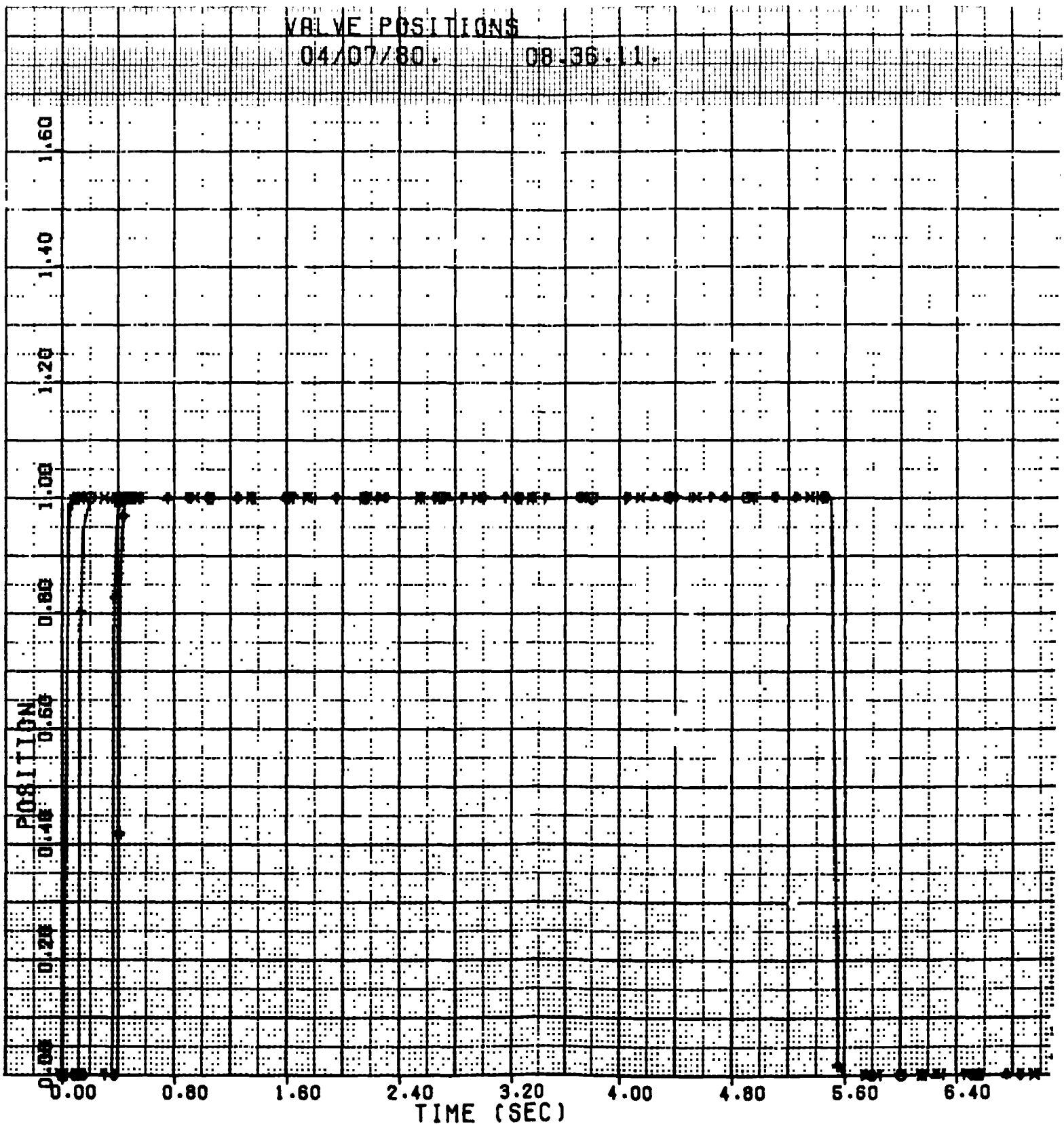

FOLDOUT FRAME

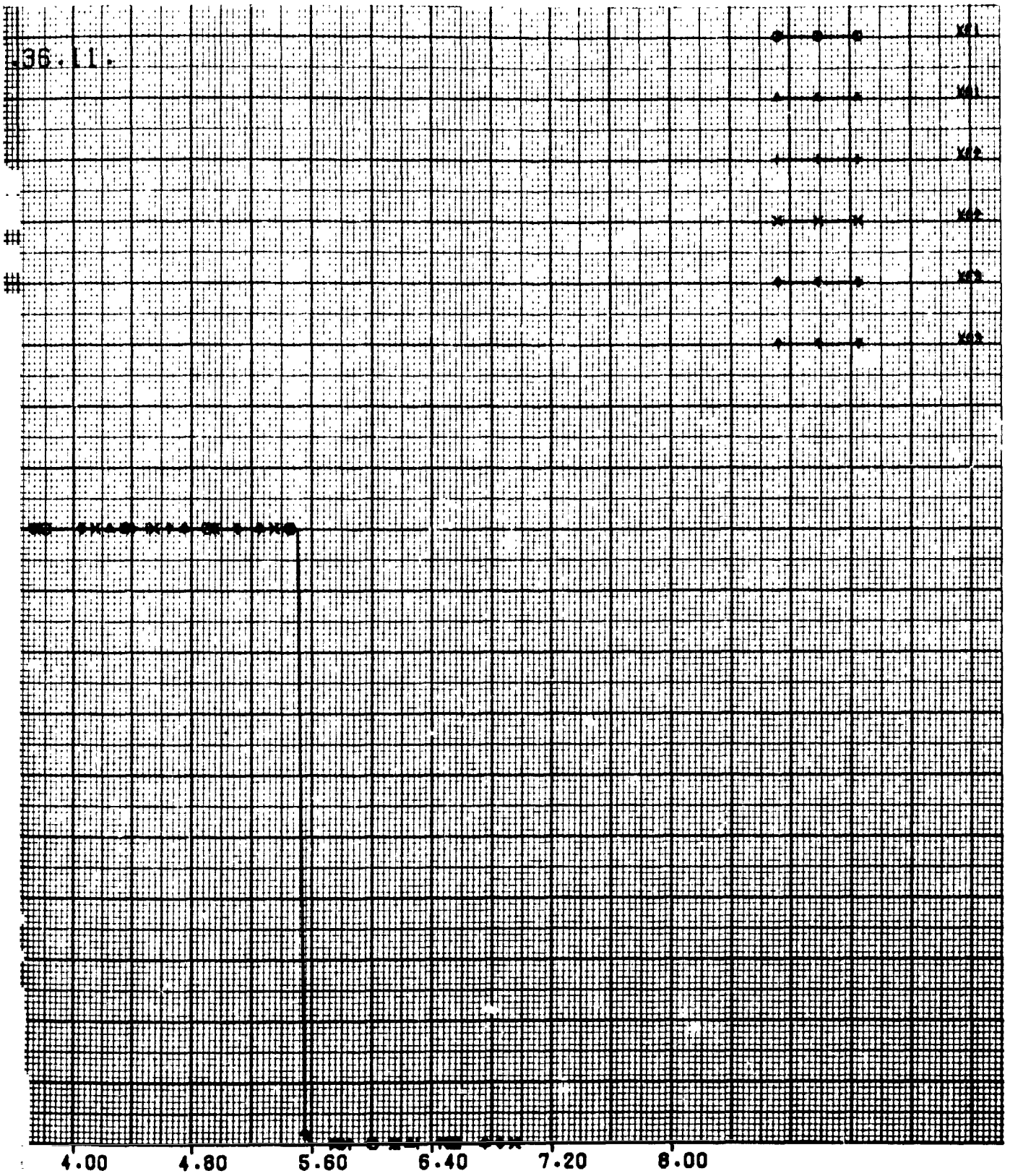

Figure 4-11. Valve Positions

FOLDOUT FRAME 2

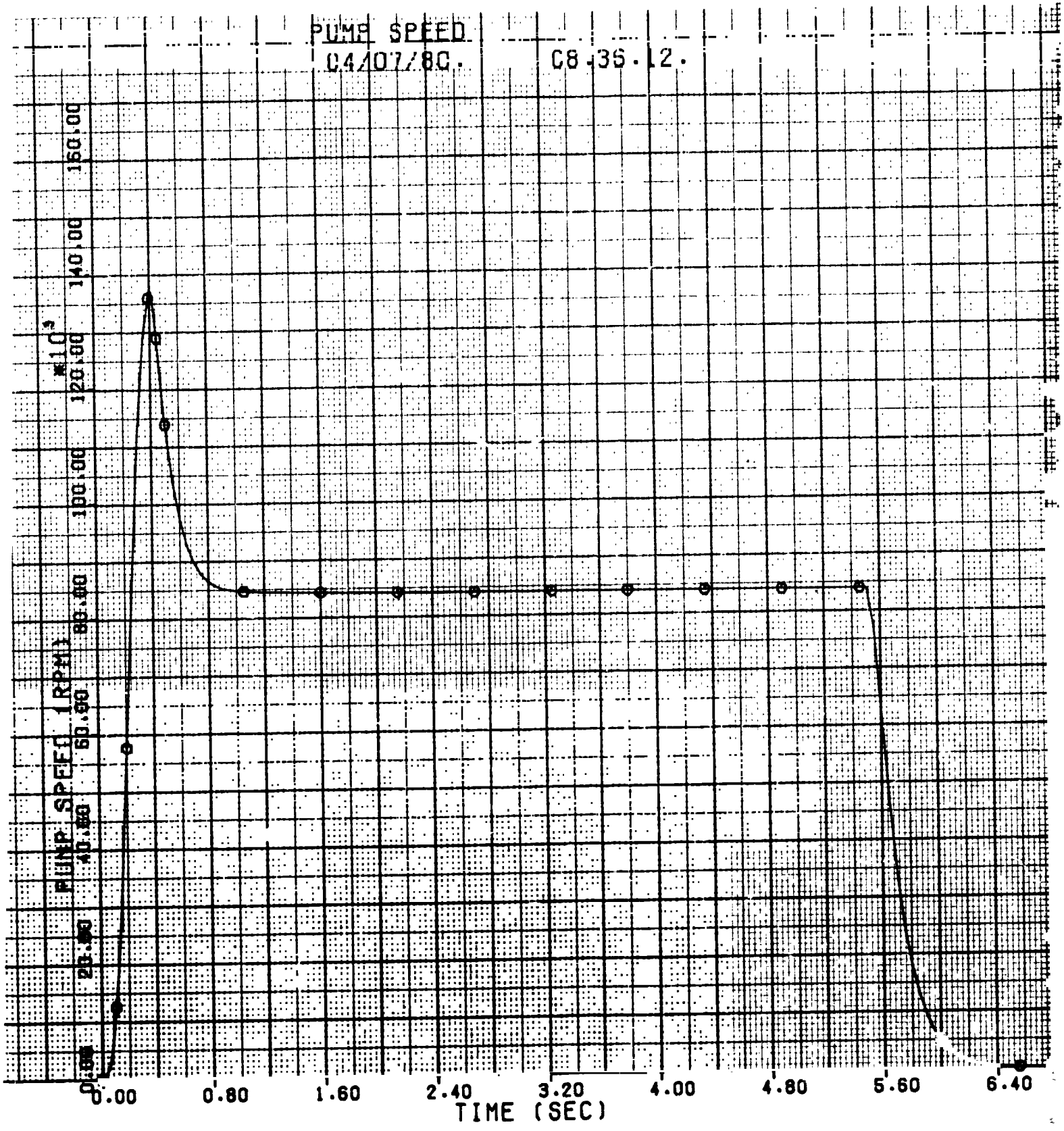

FOLDOUT FRAME

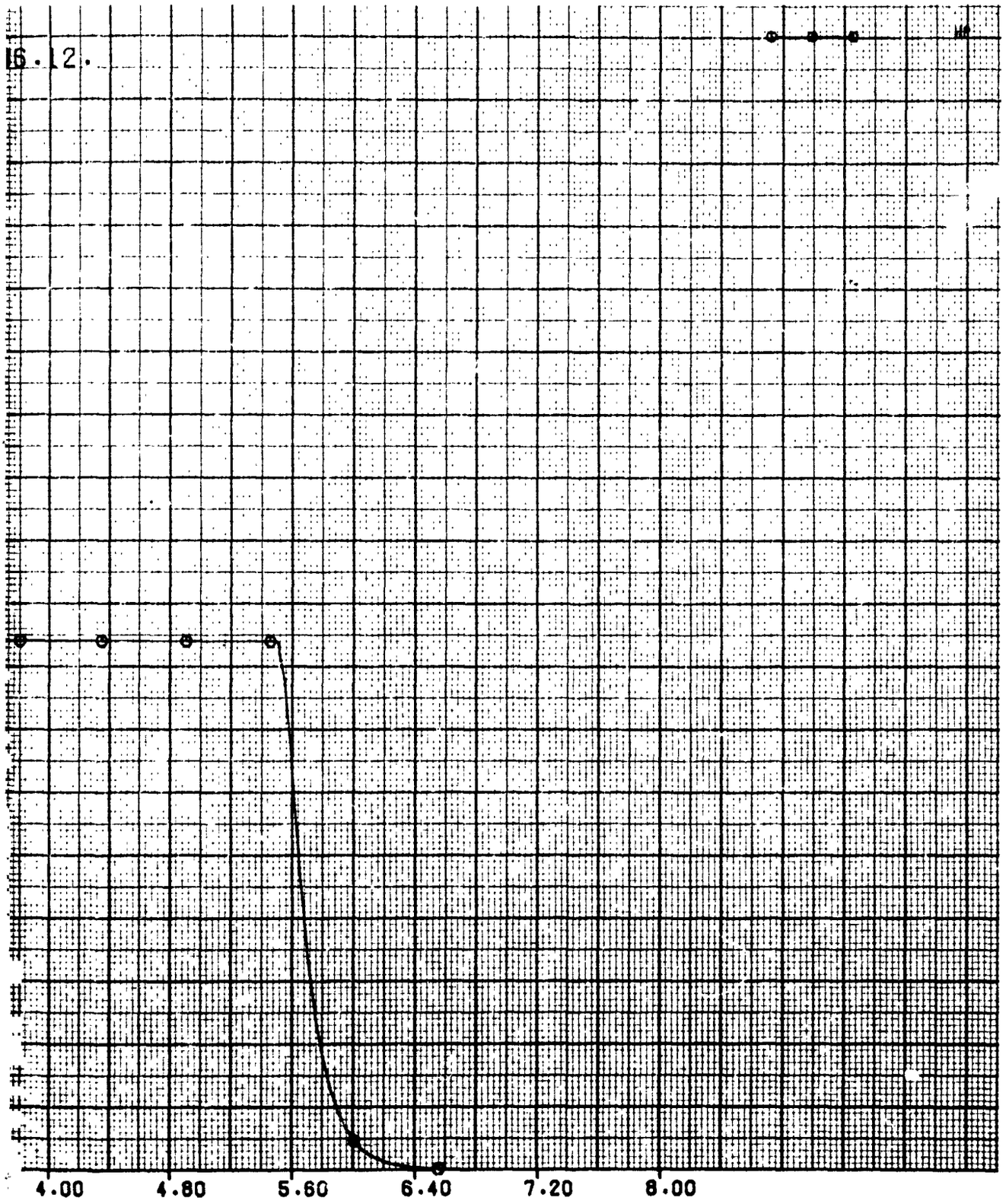

Figure 4-12. Pump Speed

FOLDOUT FRAME 2

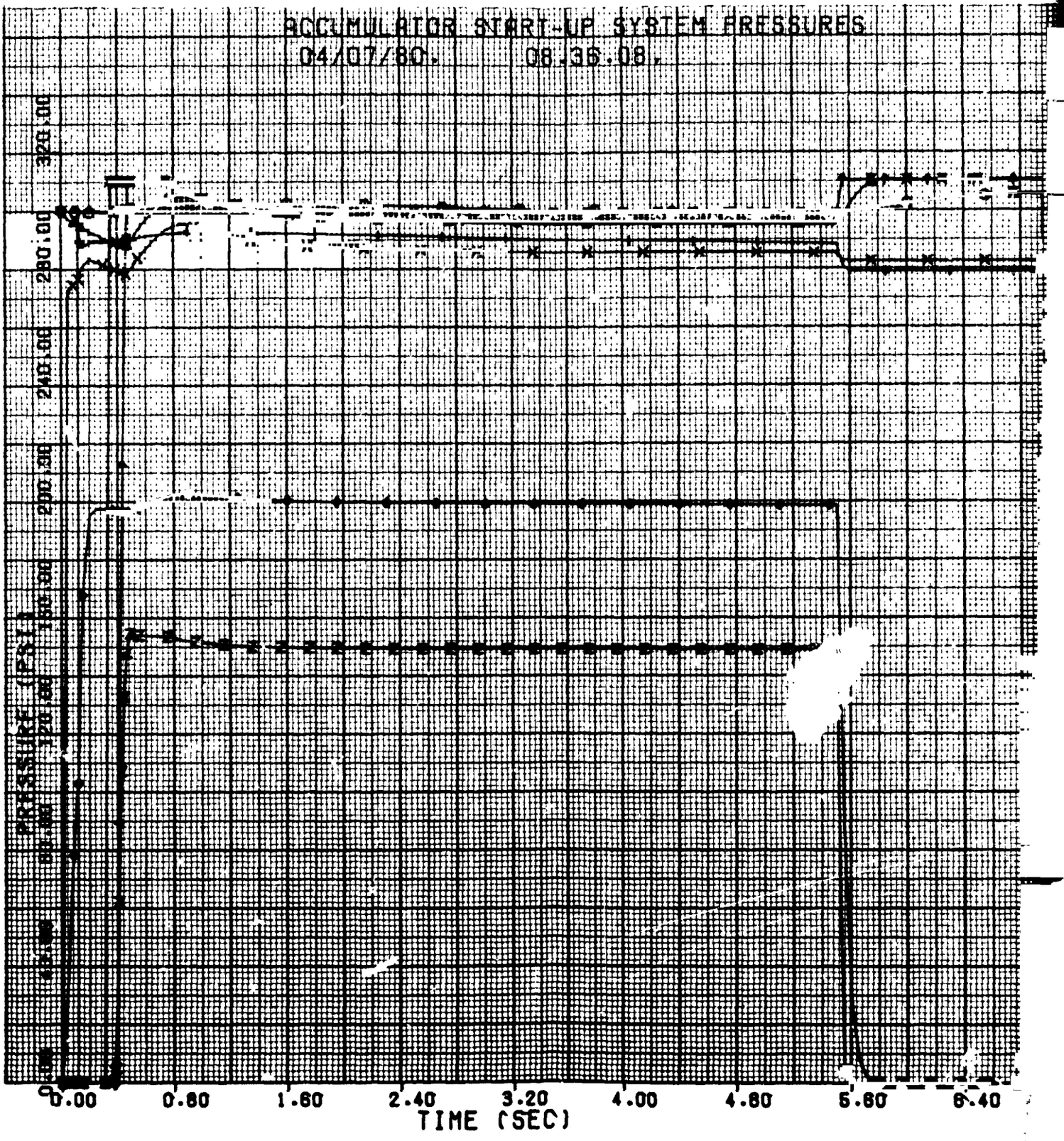

FOLDOUT FRAME

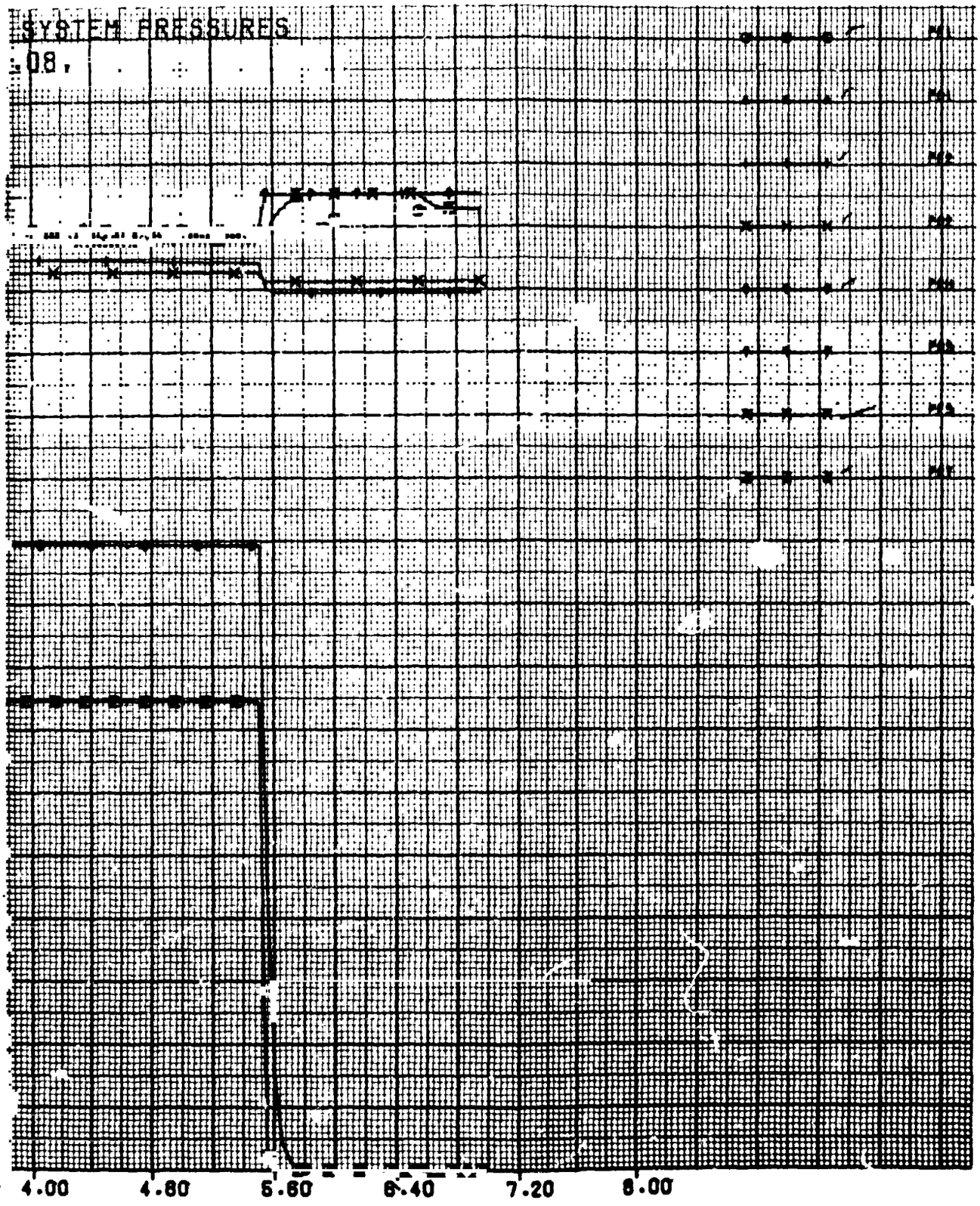

Figure 13. Accumulator Start-Up System Pressure

FOLDOUT FRAME 2

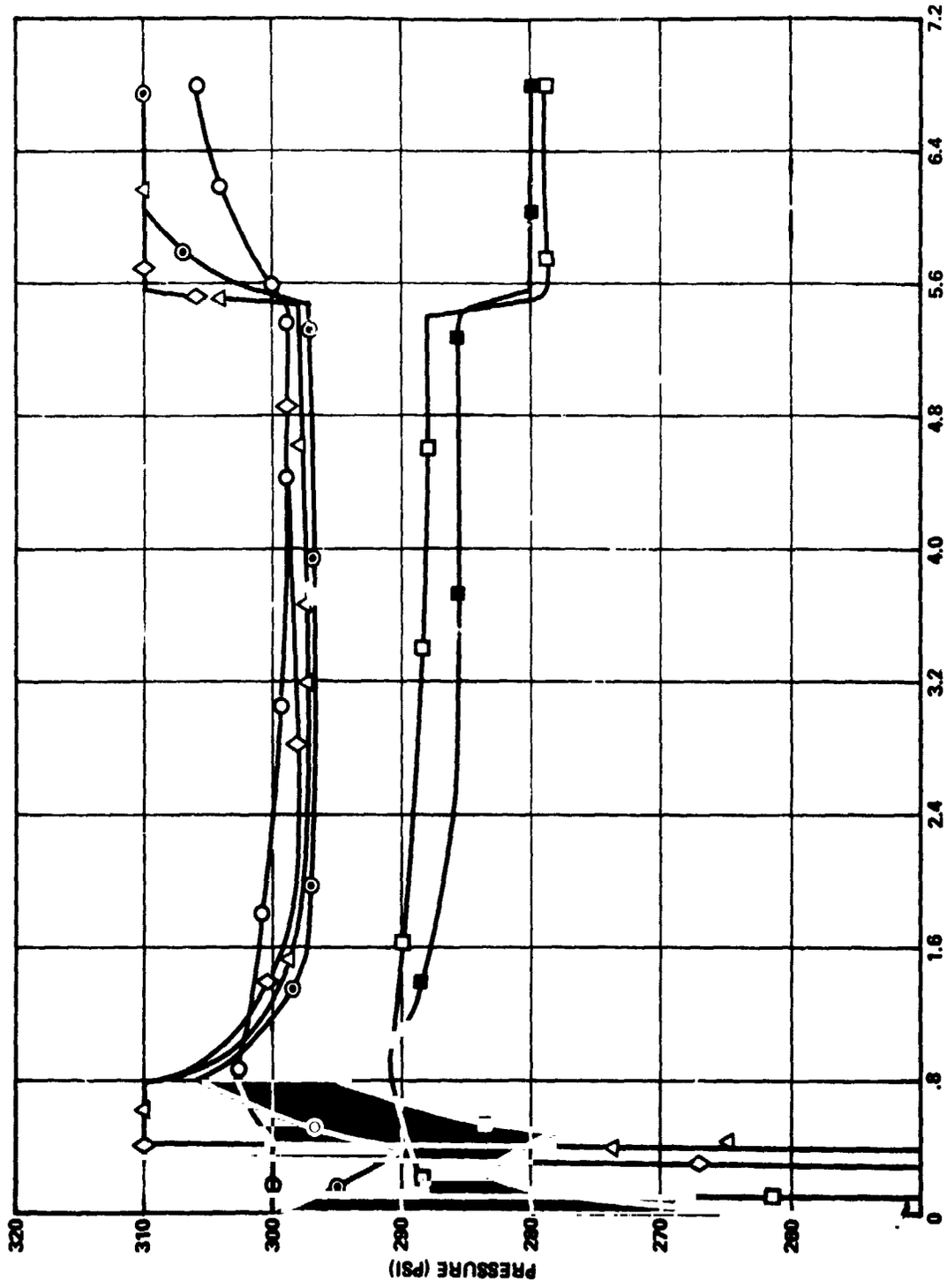

Figure 4-13a. Accumulator Start-Up System Pressures

The pressure in the gas generator rises very quickly, approximately 0.80 second, to reach its maximum value. The engine pressure also responds very fast.

As stated above, the oxidizer mass flow into the gas generator is almost immediate (Figure 4-14). Both the fuel and oxidizer go to this steady-state value in approximately 1.5 seconds.

Figure 4-15 shows the flow rates coming out of the pump. Except for a small surge at the beginning, the mass flow to the oxidizer accumulator is very small. The other flow rates also reach their steady-state values quickly.

Figures 4-16 and 4-17 show the total fuel and oxidizer consumption for the gas generator and engine supply systems, respectively. Figure 4-18 shows the temperature profiles for the two combustors.

The mixture ratios for the two combustors are shown in Figure 4-19. The gas generator has a large spike initially, but it quickly drops to the steady-state value of 36. The engine also has a high mixture ratio for a very short duration.

4.2.3 Battery Powered Motor Pumps

For this system, a 5 kW, 28 volt dc motor is used to drive the pumps that feed the fuel and oxidizer to the engine.

Since the motor has not been designed, the torque speed, resistance, inductance, and back emf characteristics are not known. Therefore, an equation relating pump speed to voltage was assumed. The time constants used were based on similar motors, however, this method will only give an approximation to the actual system. An effective current (that is not the actual value of the current for that motor) is used in the formula.

The valve positions are shown in Figure 4-20. They were opened simultaneously, and are closed at t = 4 seconds.

The pump speed (Figure 4-21) has an overshoot during the start-up which is decreased when the pressures reach their maximum value (Figure 4-22). A mechanical time constant of 20 ms was assumed for the

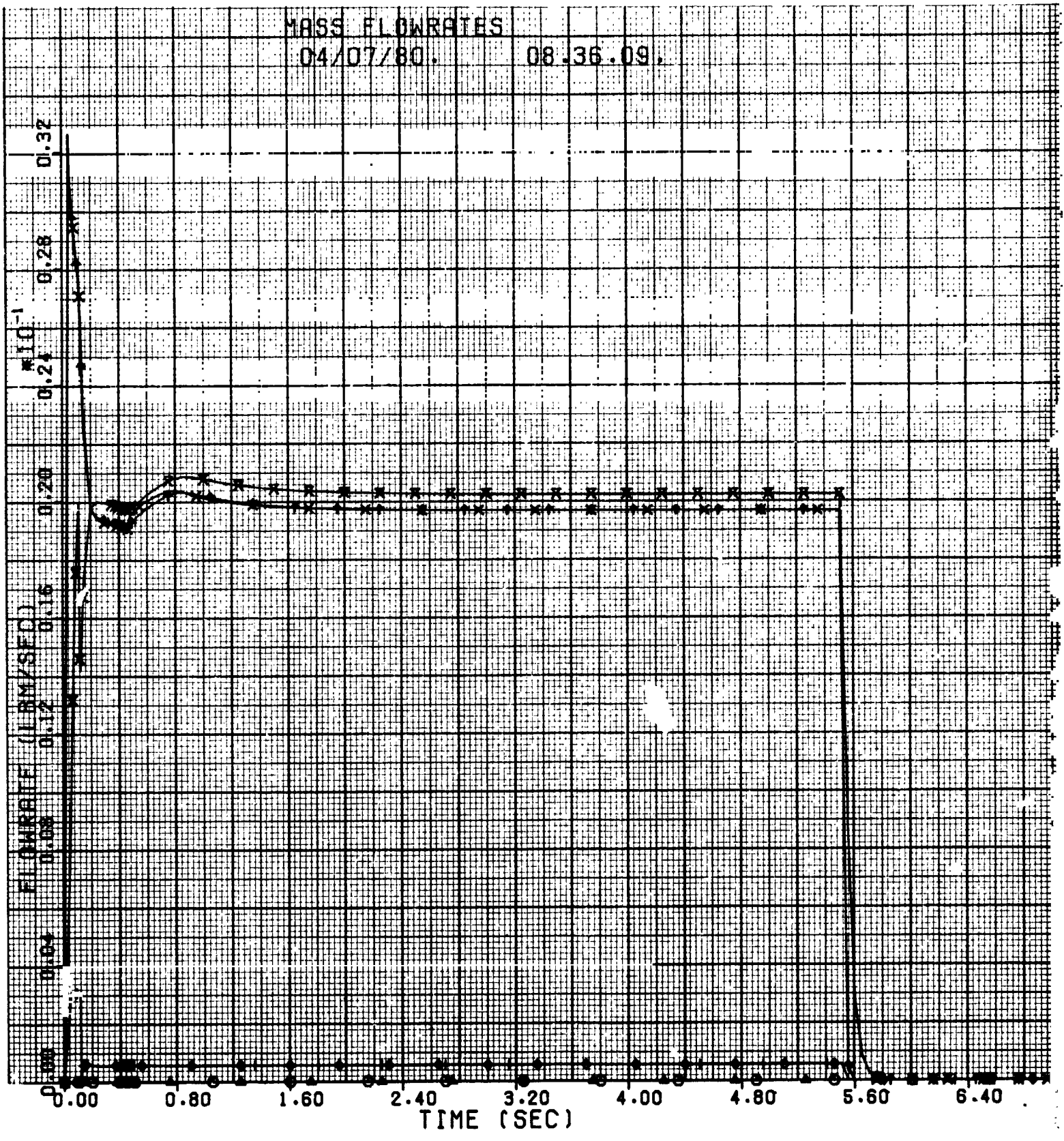

BOLDOUT FRAME

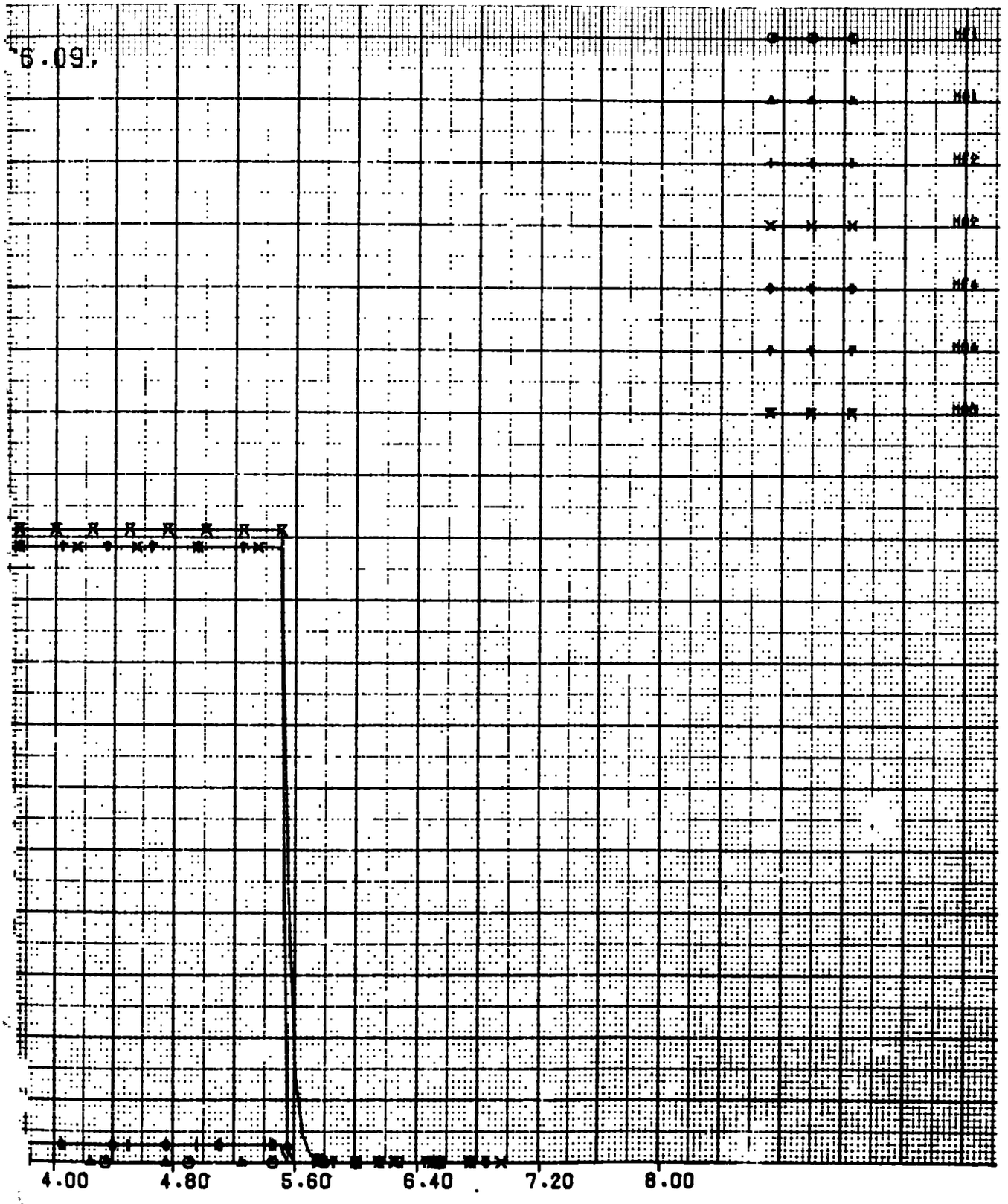

Figure 4-14. Mass Flow Rates

FOLDOUT FRAME 2

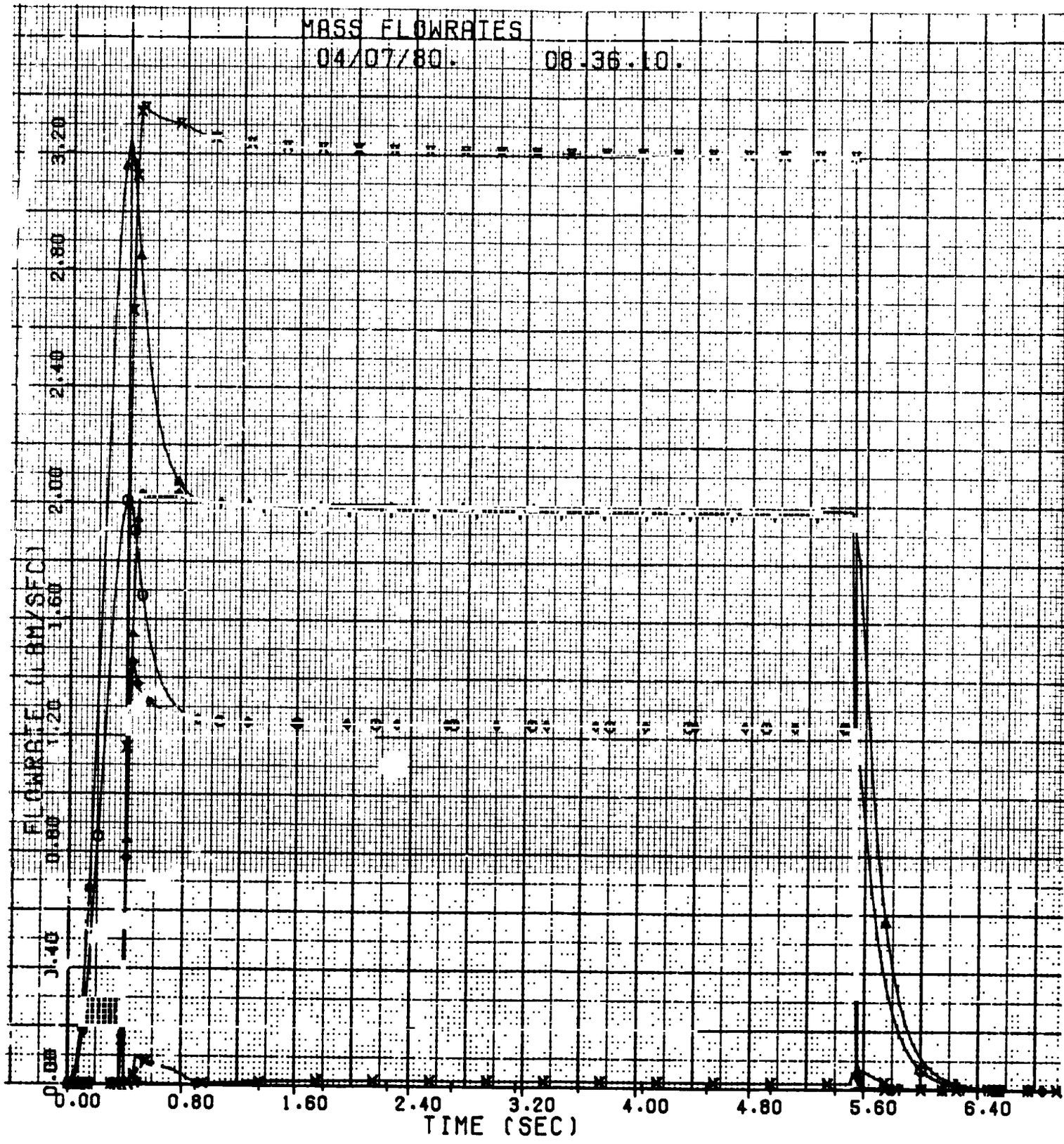

FOLDOUT FRAME

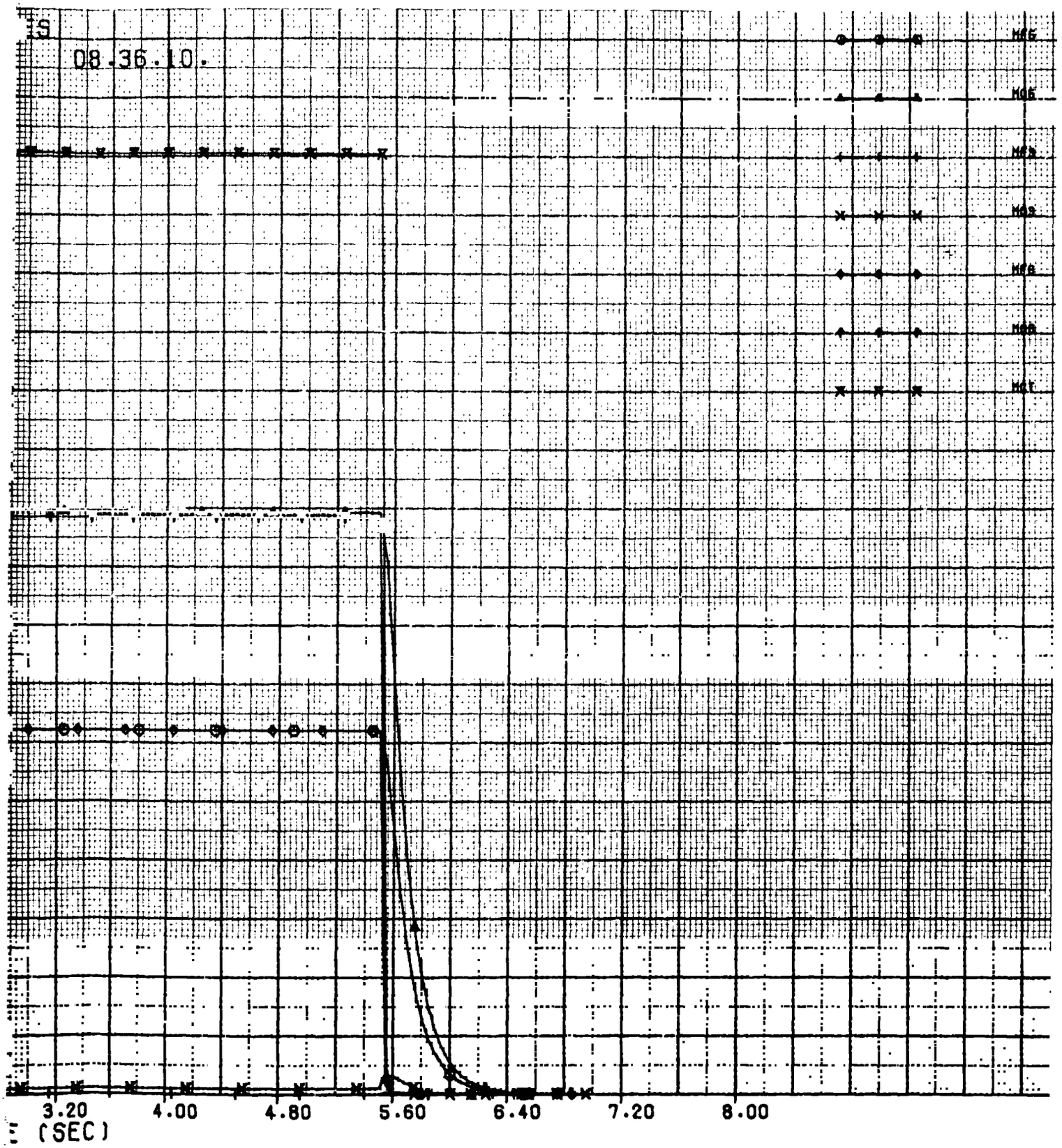

Figure 4-15. Mass Flow Rates

FOLDOUT FRAME 2

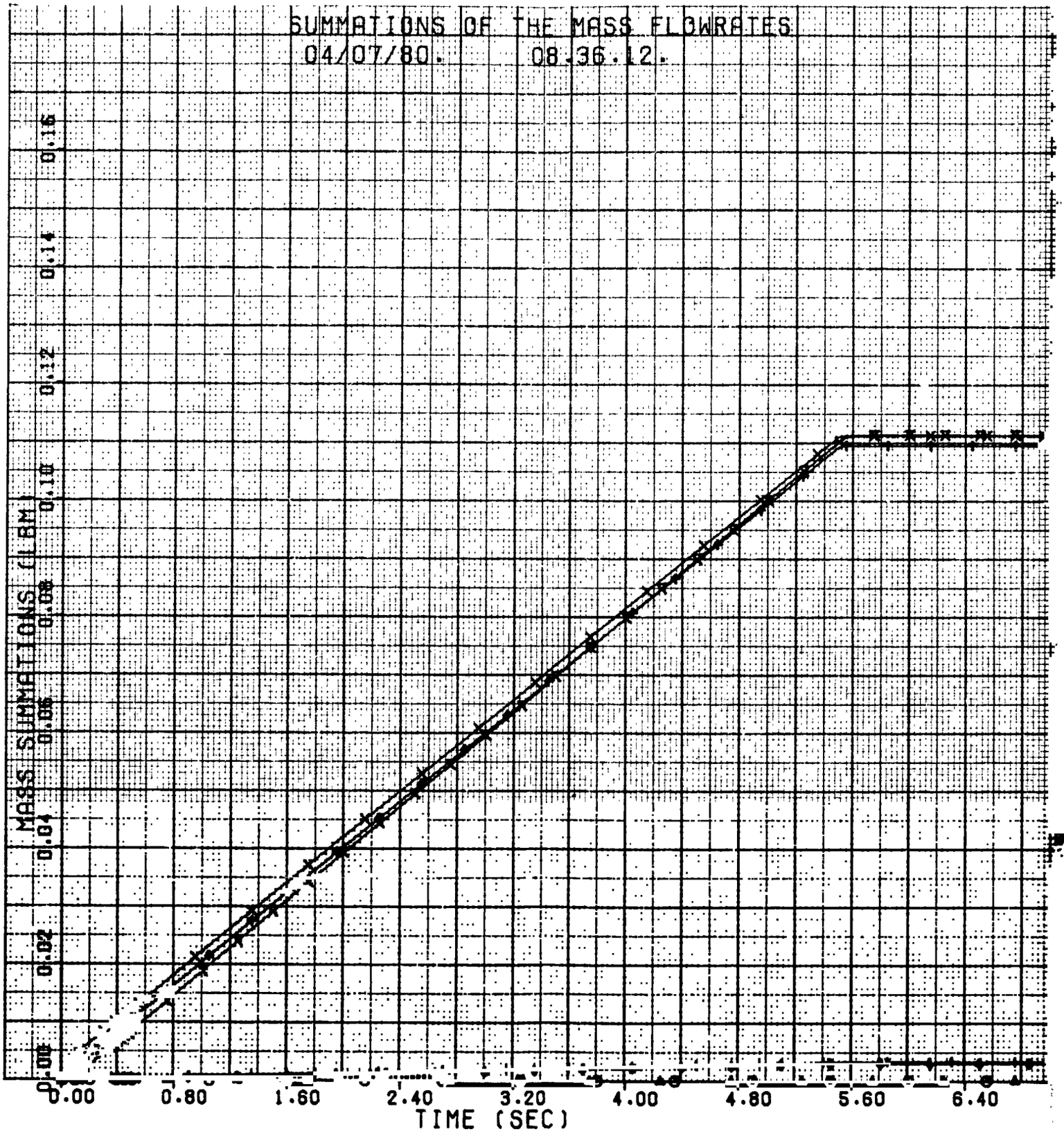

FOLDOUT FRAME

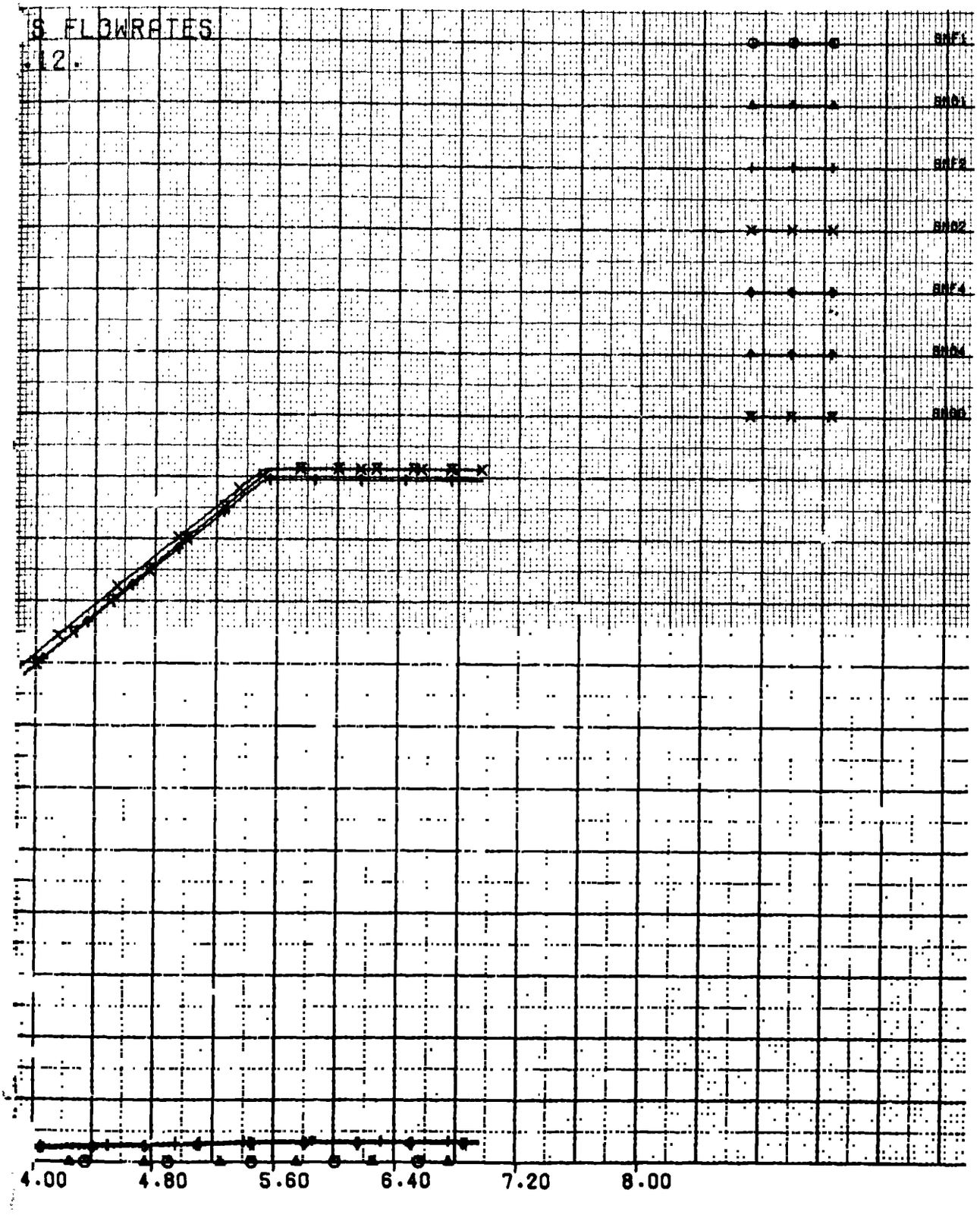

Figure 4-16. Summarization of the Mass Flow Rates

FOLDOUT FRAME 2

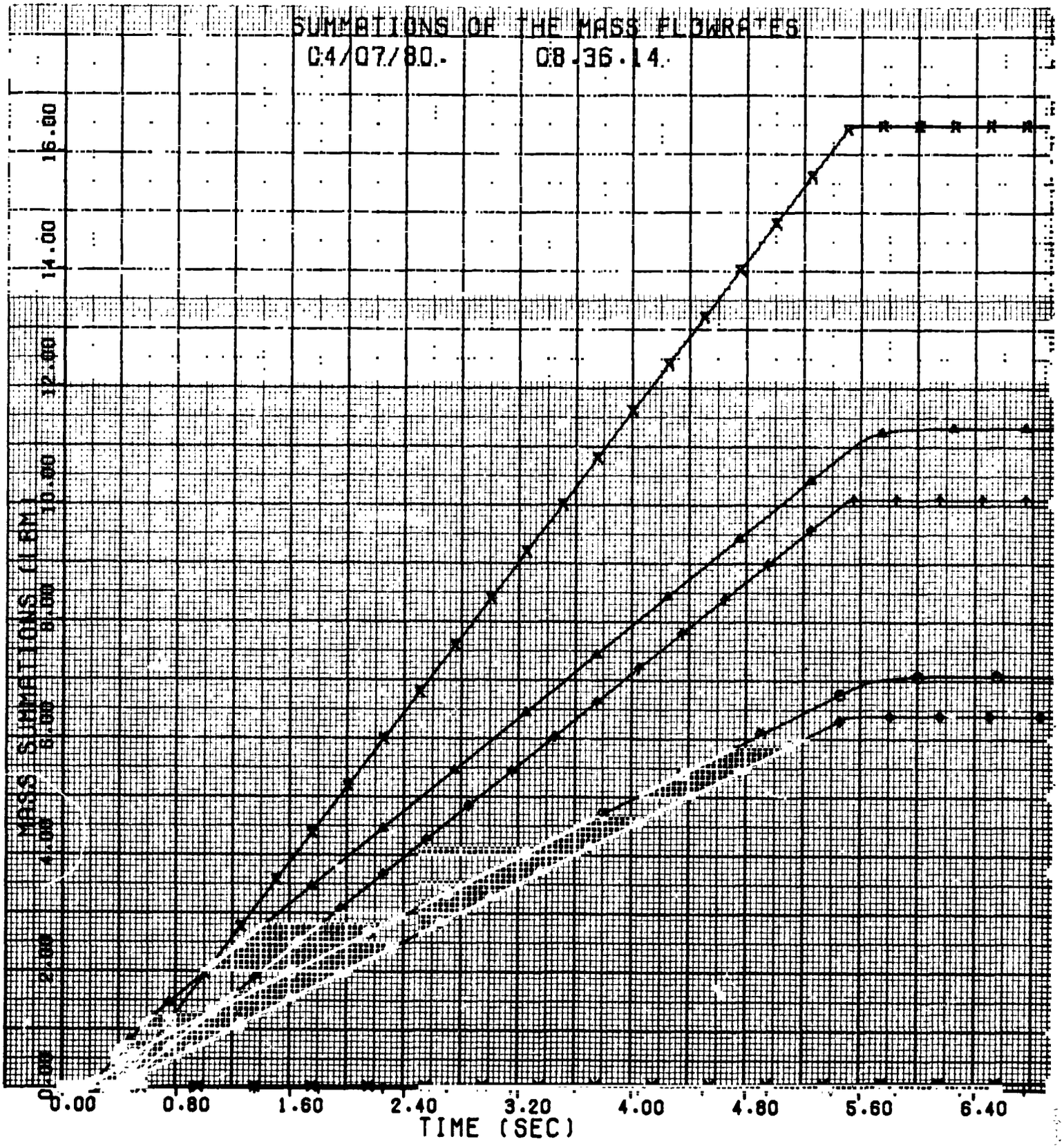

FOLDOUT FRAME

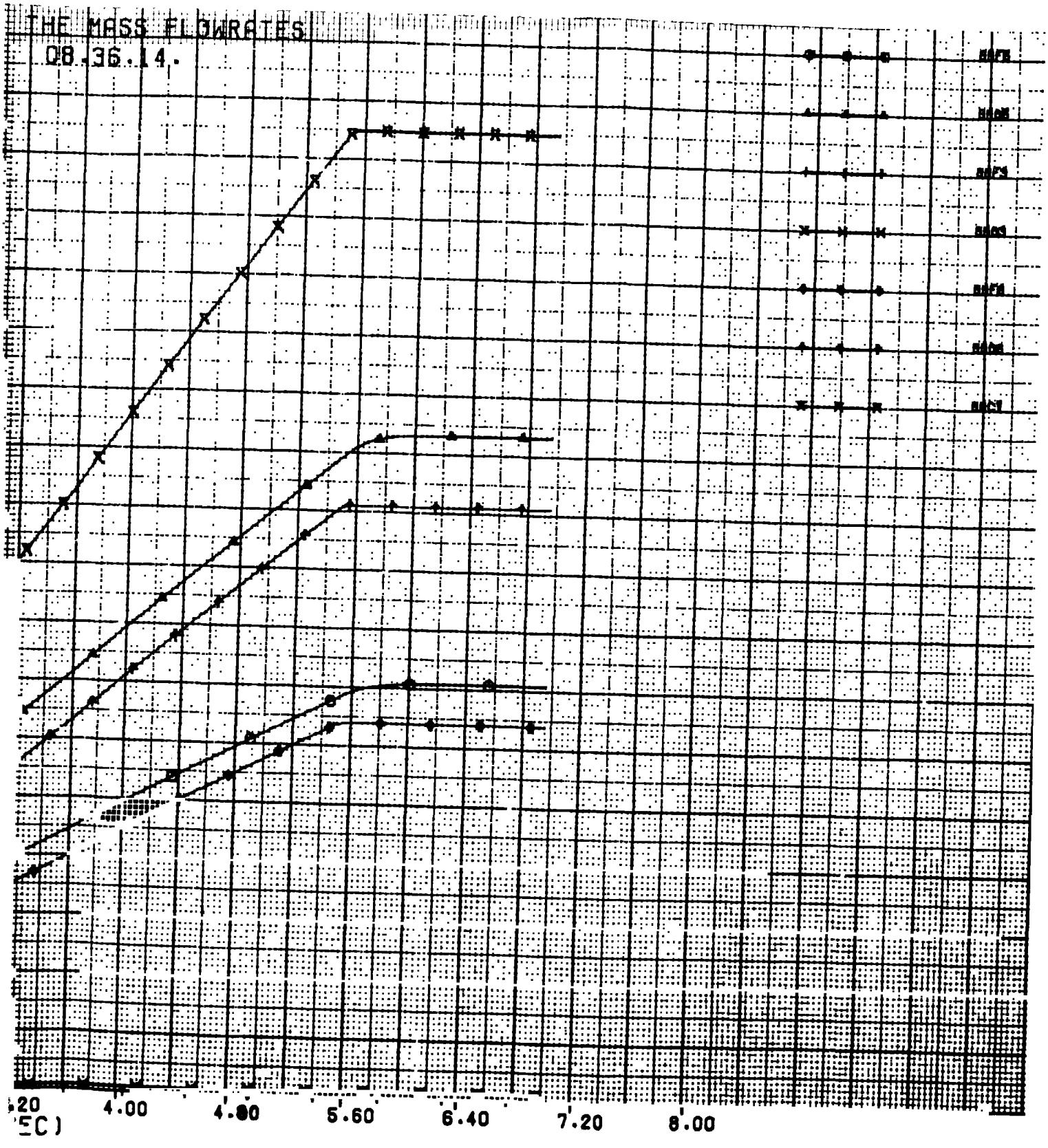

Figure 4-17. Summarization of the Mass Flow Rates

FOLDOUT FRAME

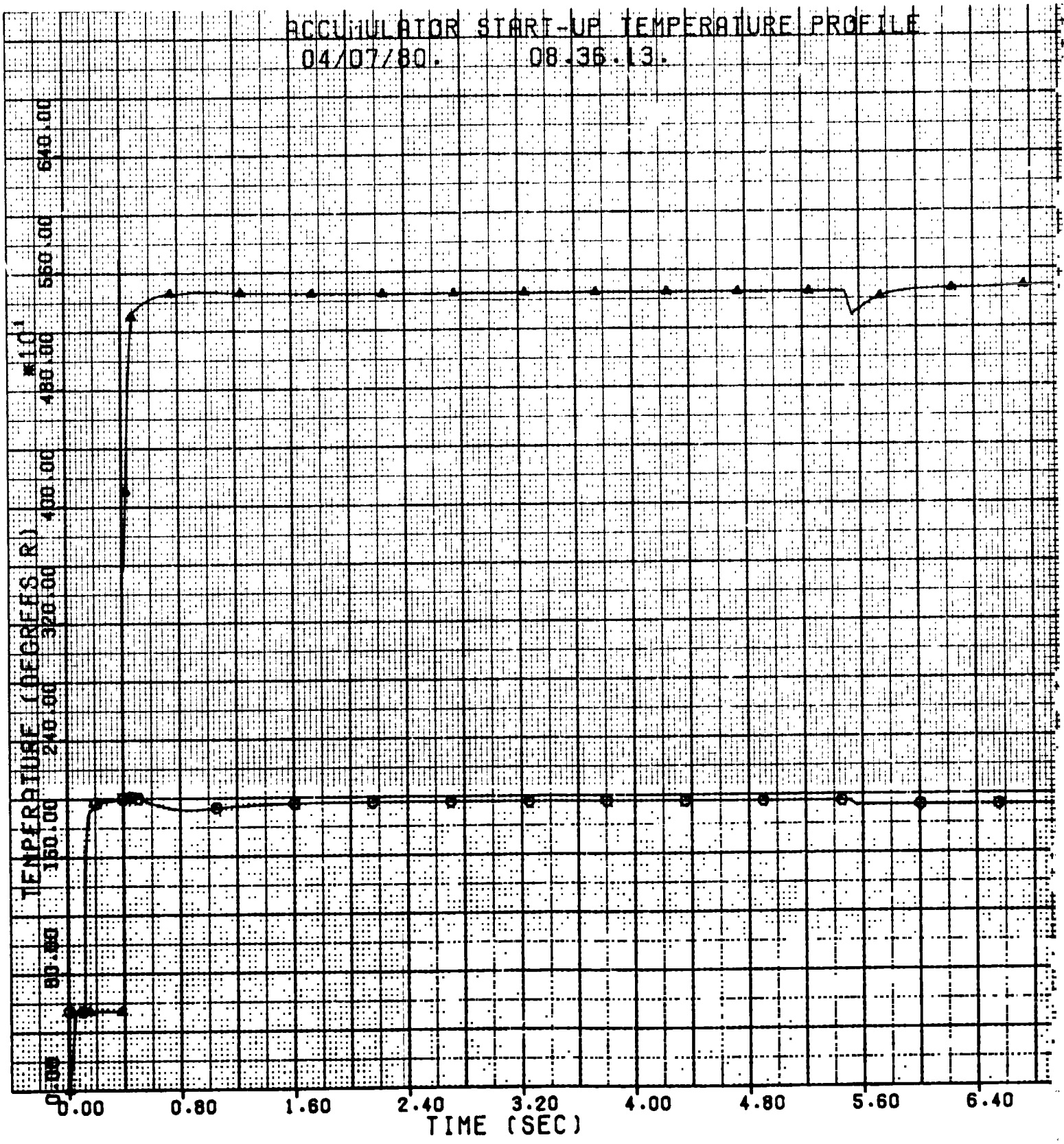

FOLDOUT FRAME

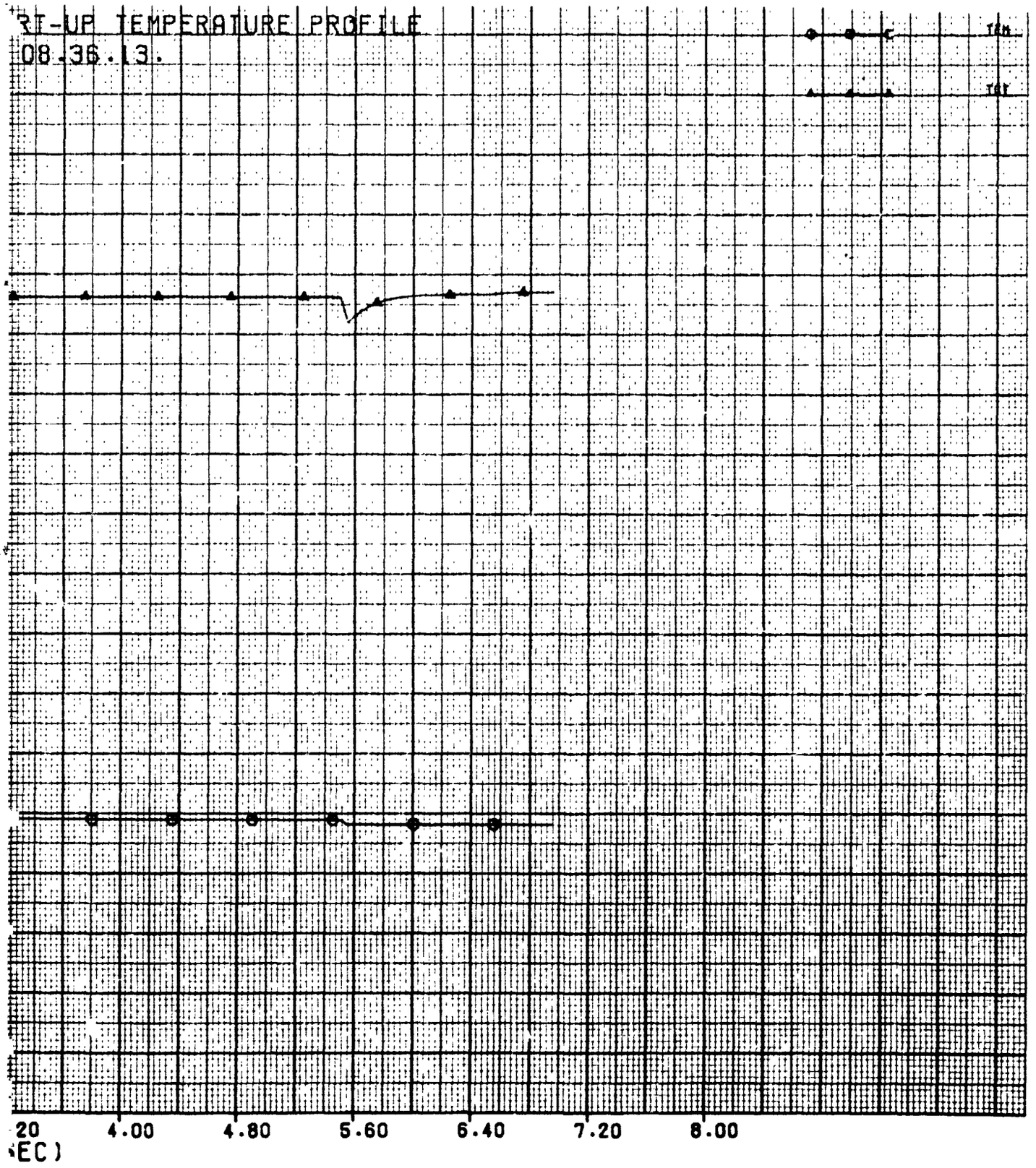

Figure 4-18. Accumulator Start-Up Temperature Profile

FOLDOUT FRAME 2

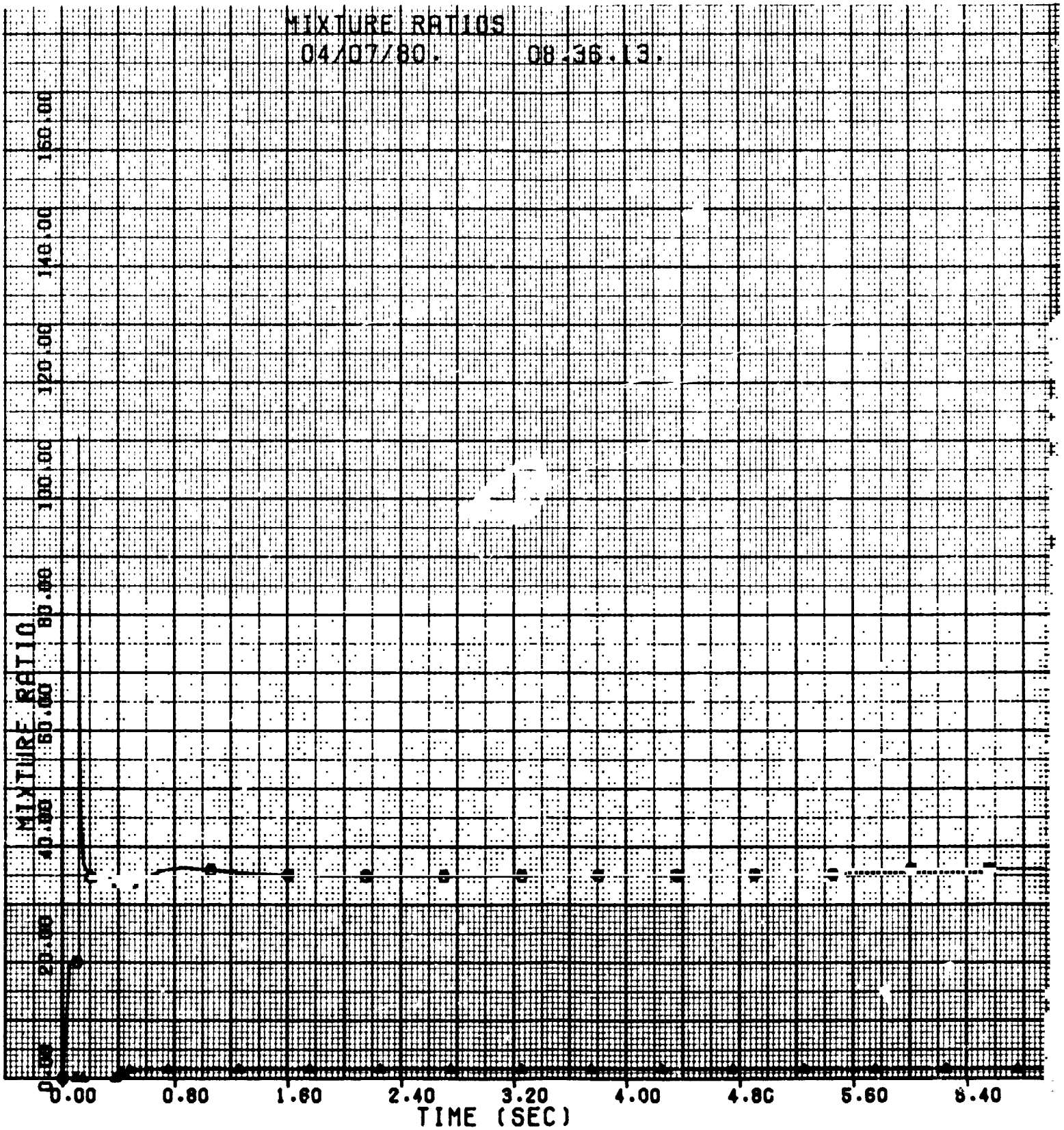

FOLDOUT FRAME

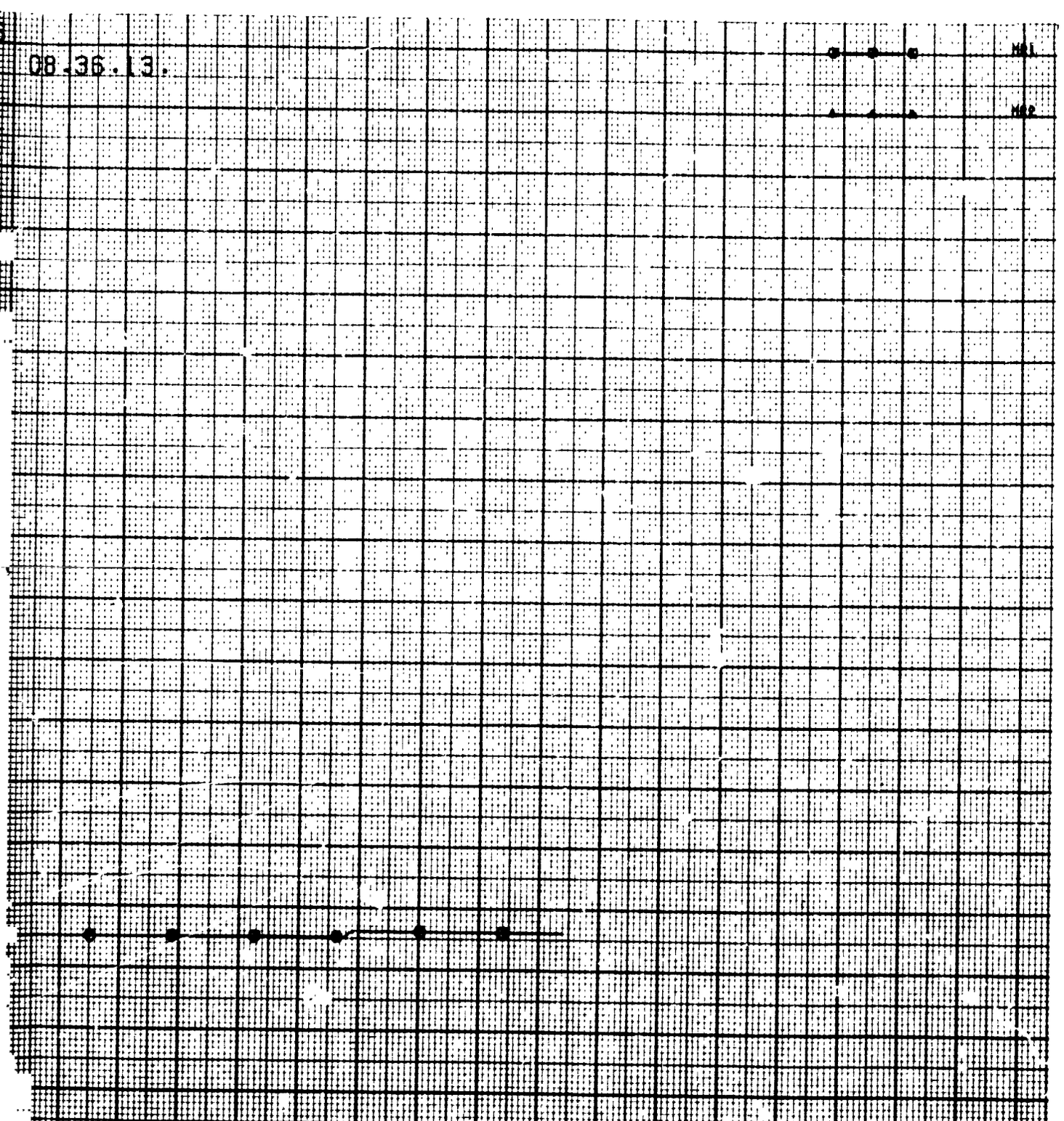

Figure 4-19. Valve Positions

FOLDOUT FRAME 2

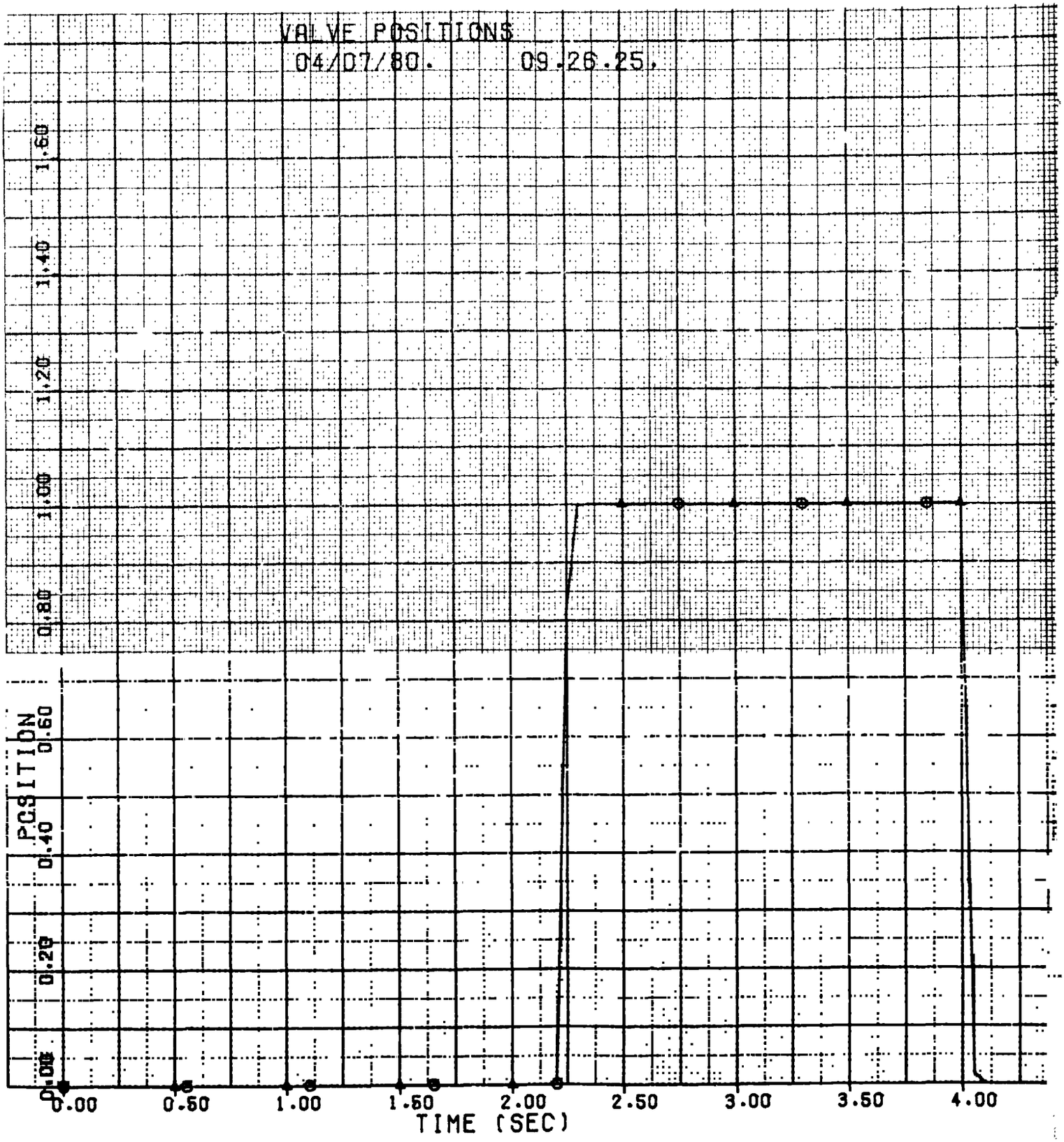

FOLDOUT FRAME

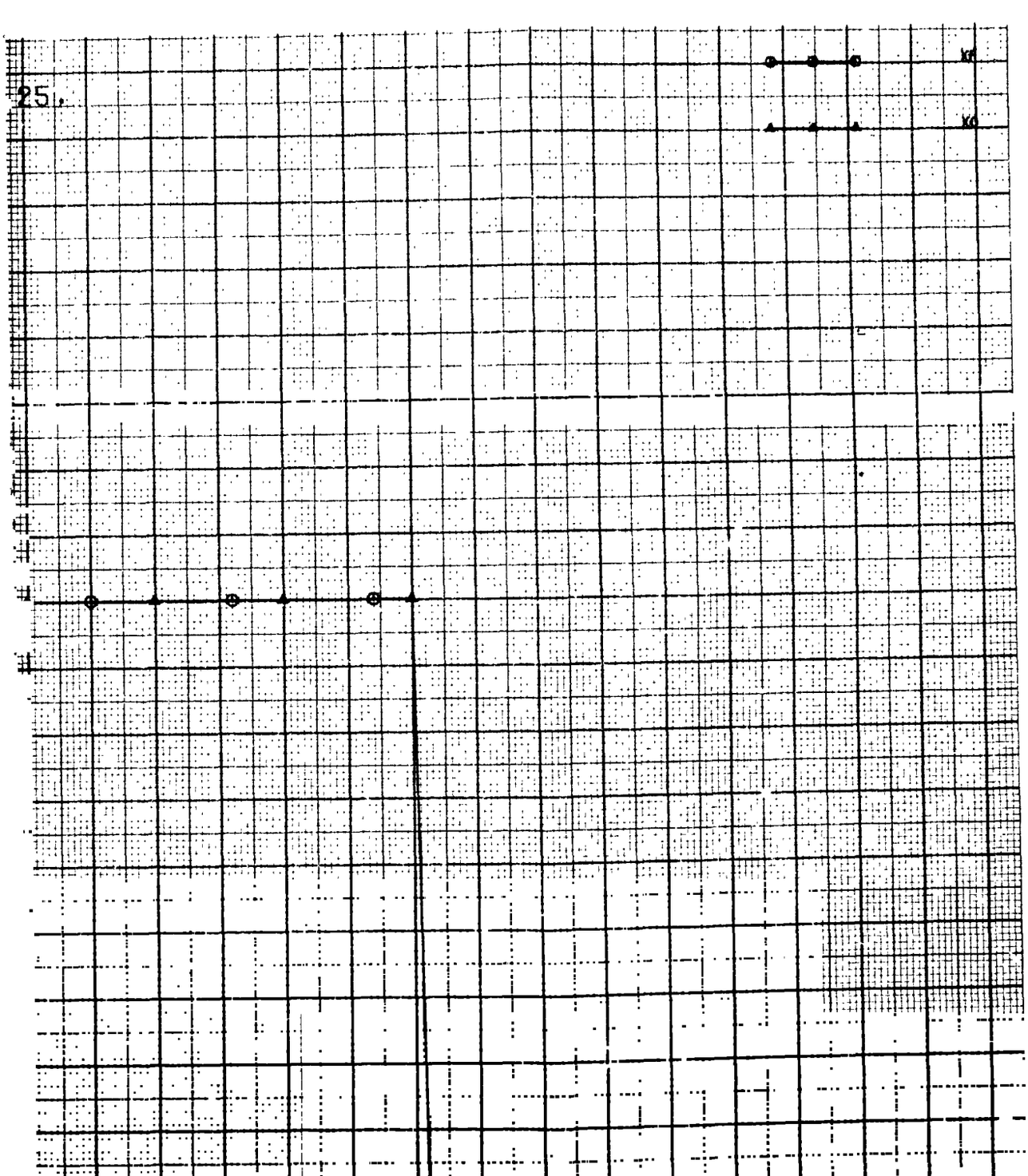

Figure 4-20. Valve Positions

FOLDOUT FRAME 2

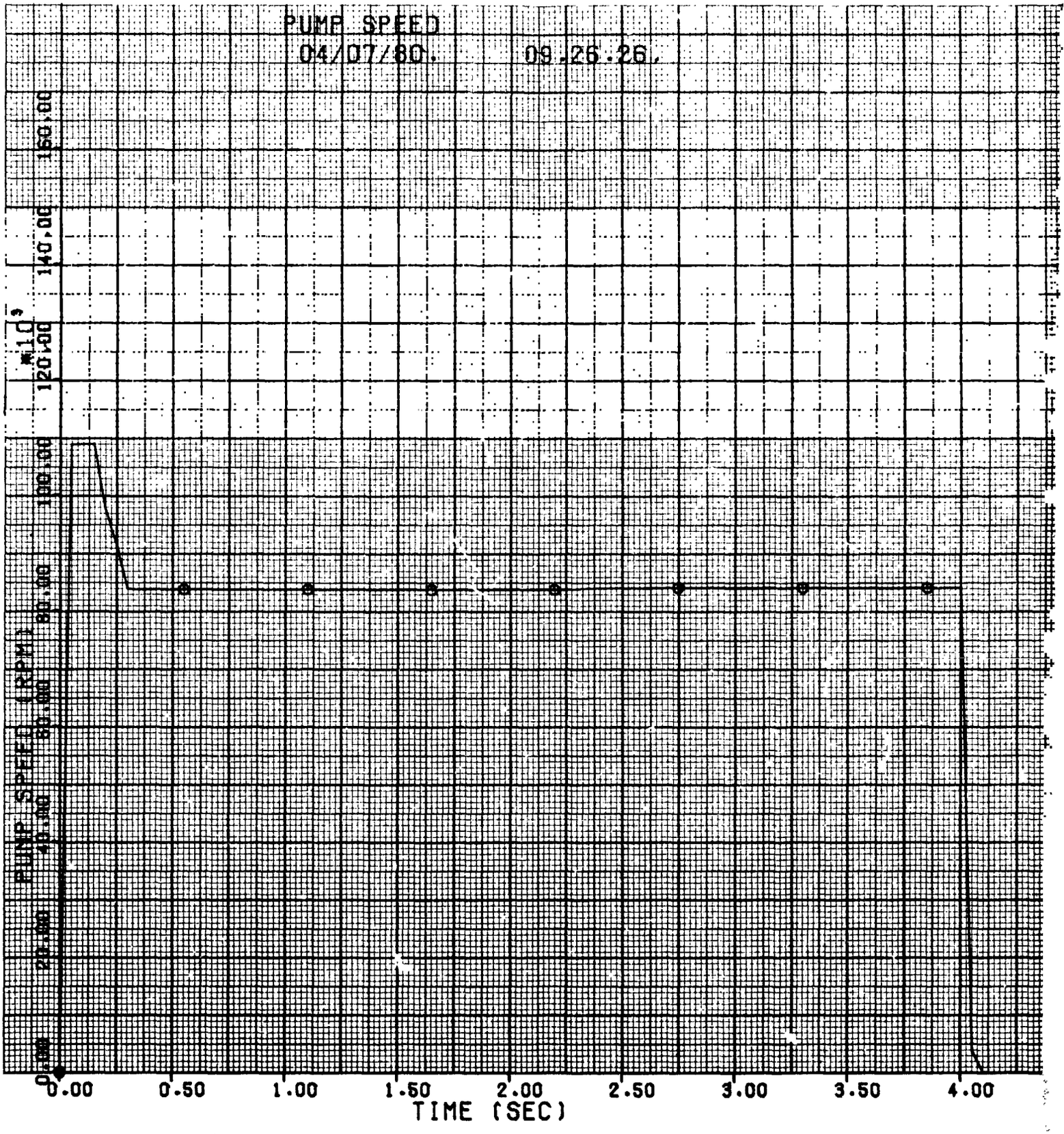

FOLDOUT FRAME

ORIGINAL PAGE IS
OF POOR QUALITY

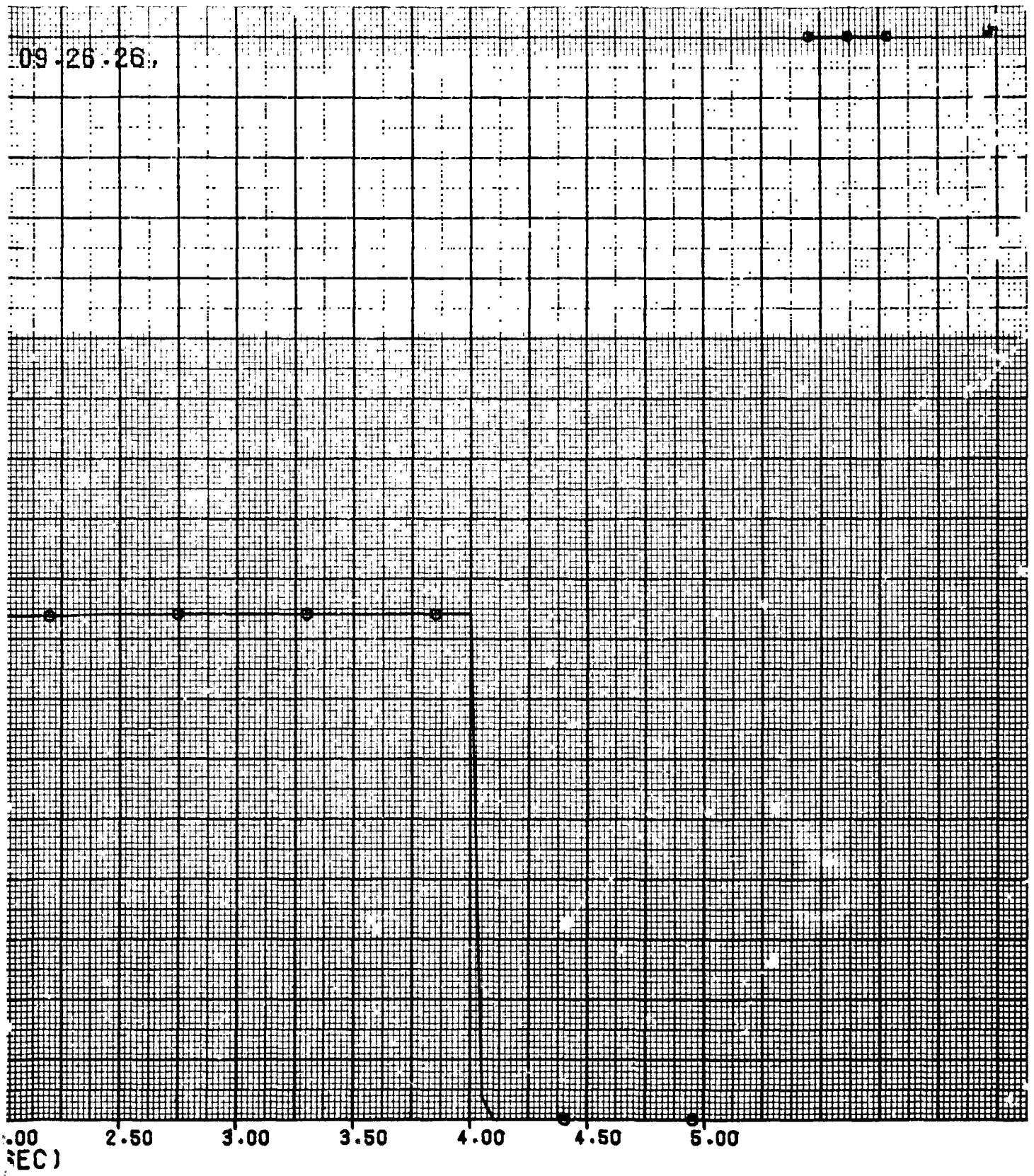

Figure 4-21. Pump Speed

FOLDOUT FRAME 2

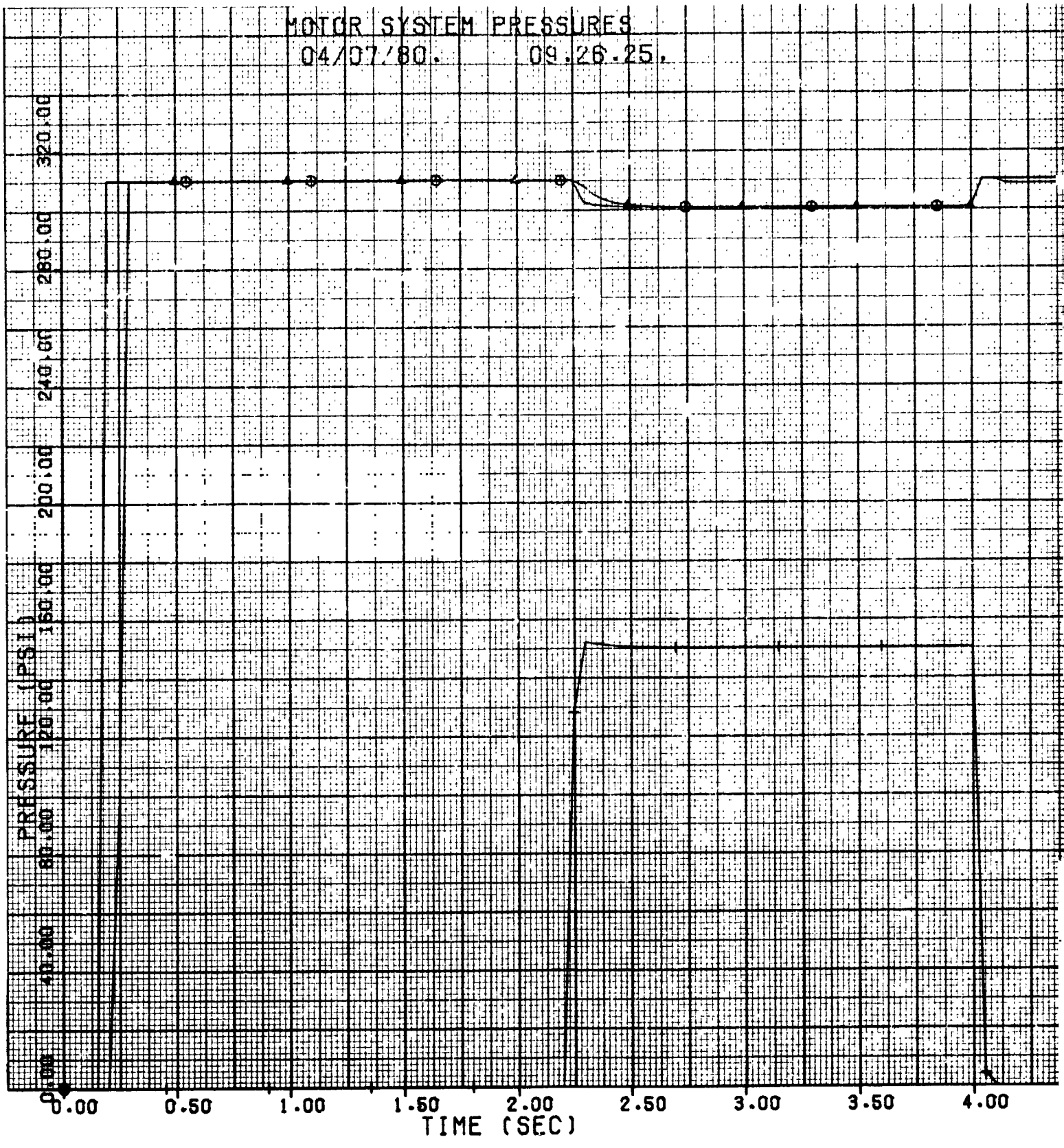

FOLDOUT FRAME

ORIGINAL PAGE IS
OF POOR QUALITY

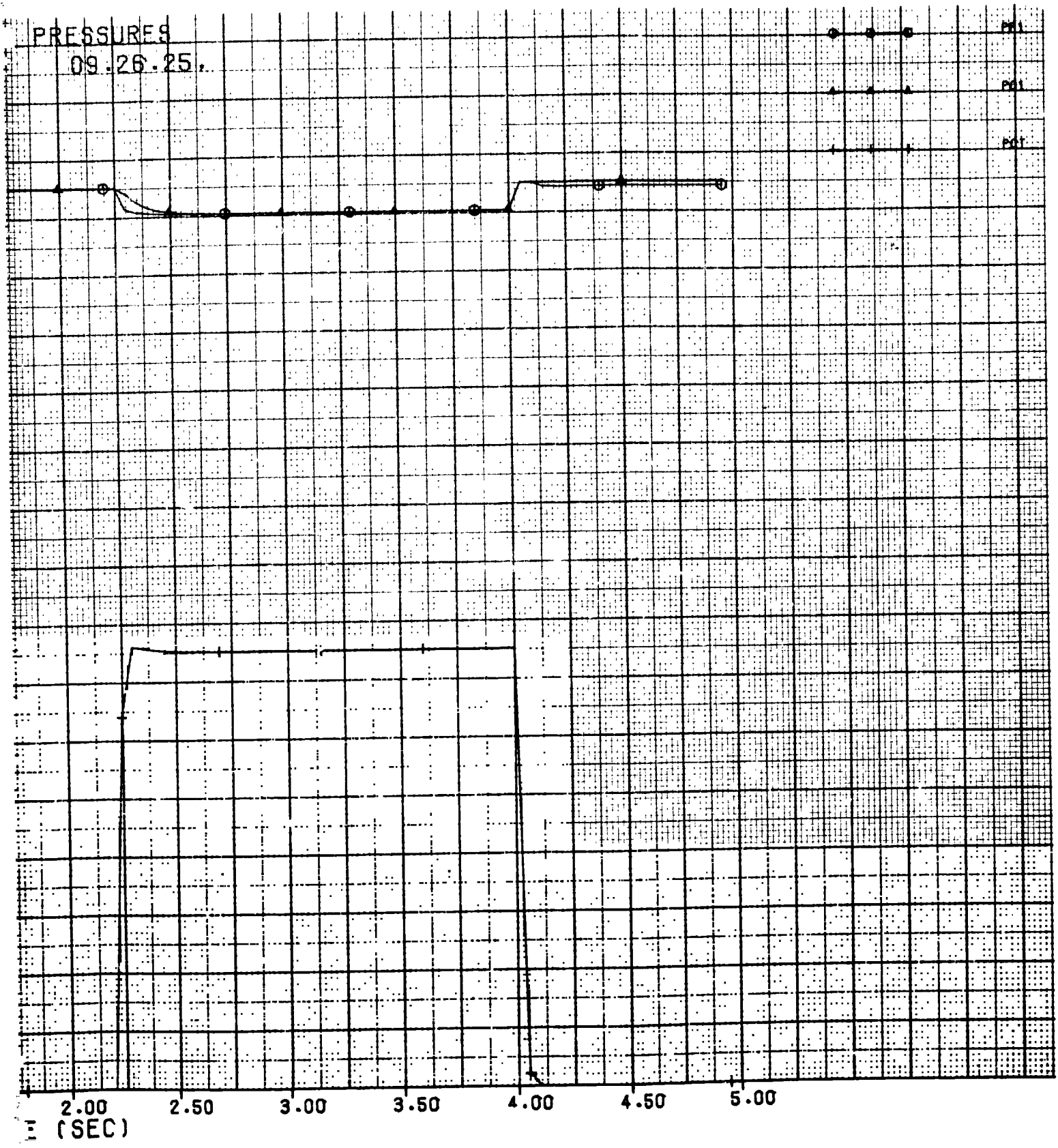

Figure 4-22. Motor System Pressures

FOLDOUT FRAME 2

motor. A much larger value can actually be anticipated which would reduce the magnitude of the overshoot.

The pressures rise to their maximum value very quickly and drop to steady-state levels when the valves are opened at t = 2.25 seconds. At t = 4 seconds the valves are closed and the pressures increase to their limiting values again.

The engine pressure has a very small overshoot before it settles into steady-state. Again the full line dynamics were not included as they were in the hydrazine system case.

The mass flow rates are shown in Figure 4-23. The flows can be seen to follow the pump speed exactly. The summation of the flow rates is shown in Figure 4-24.

The temperature profile is given in Figure 4-25, and the mixture ratio is shown in Figure 4-26.

4.2.4 Combustion Stability

The results of this study, which are based on the use of a first-order model, are valid in terms of overall system response and engine/feed system coupling. The Marquardt engine has a problem with chugging (combustion stability) if the $\Delta P/Pc$ becomes less than 0.45. None of the three systems analyzed showed a problem in that regard. The pressure upstream of the injector was assumed to be 300 psia. Therefore, the $\Delta P/P_c$ will have a nominal value of 1.0 for a P_c of 150 psia. Figures 4-27 through 4-29 show the $\Delta P/P_c$ versus time for the motor driven system, the hydrazine system, and the bipropellant system, respectively. The lowest value of P/P_c is 0.81 for the hydrazine system, which is well above the minimum requirement. A detailed stability evaluation, however, requires additional modeling of the engine and the pump, including the power spectral densities of both components.

From a system response standpoint, the bipropellant (accumulator) gas generator system provides the best performance although better definition of the motor driven system is required.

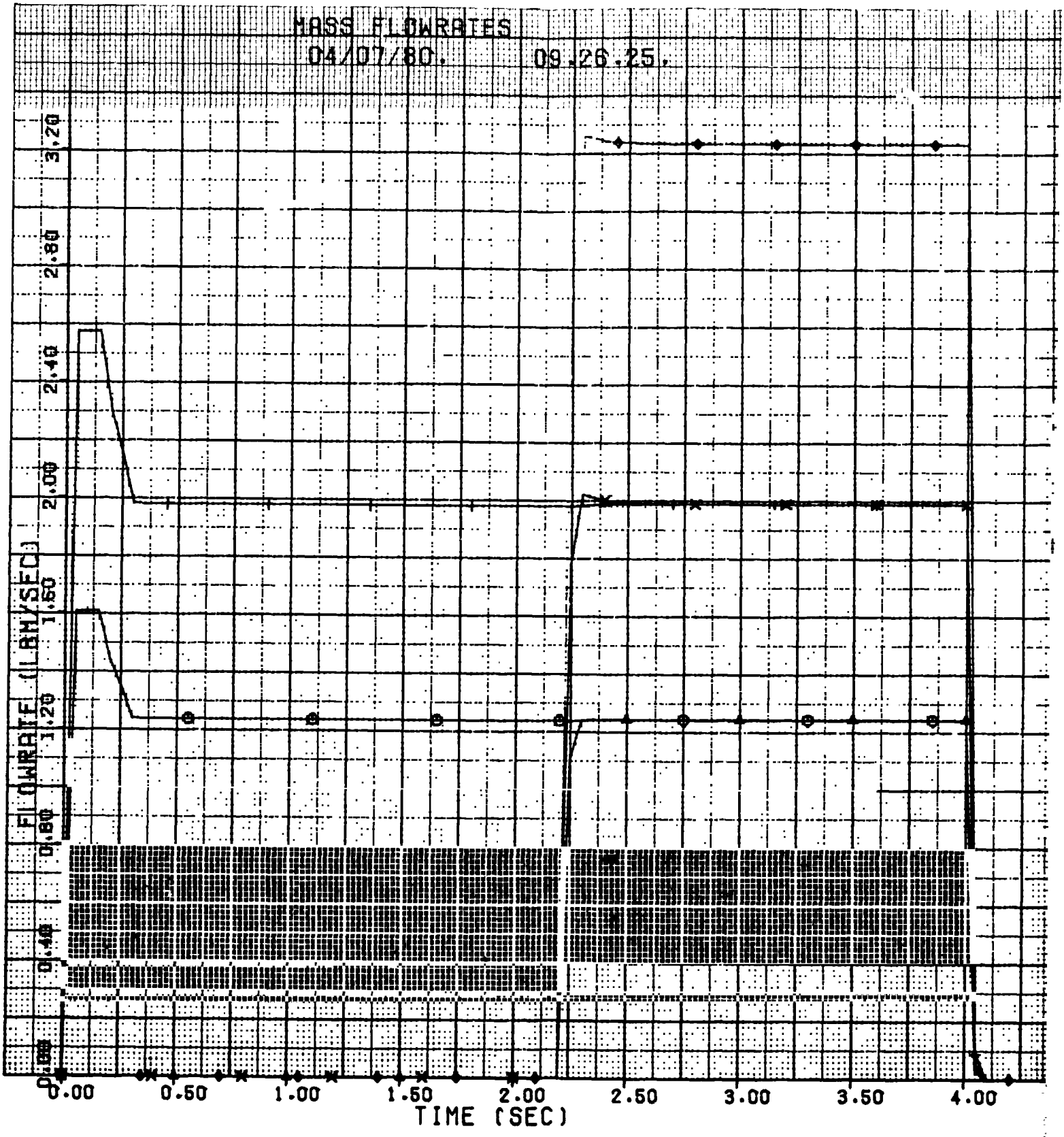

FOLDOUT FRAME

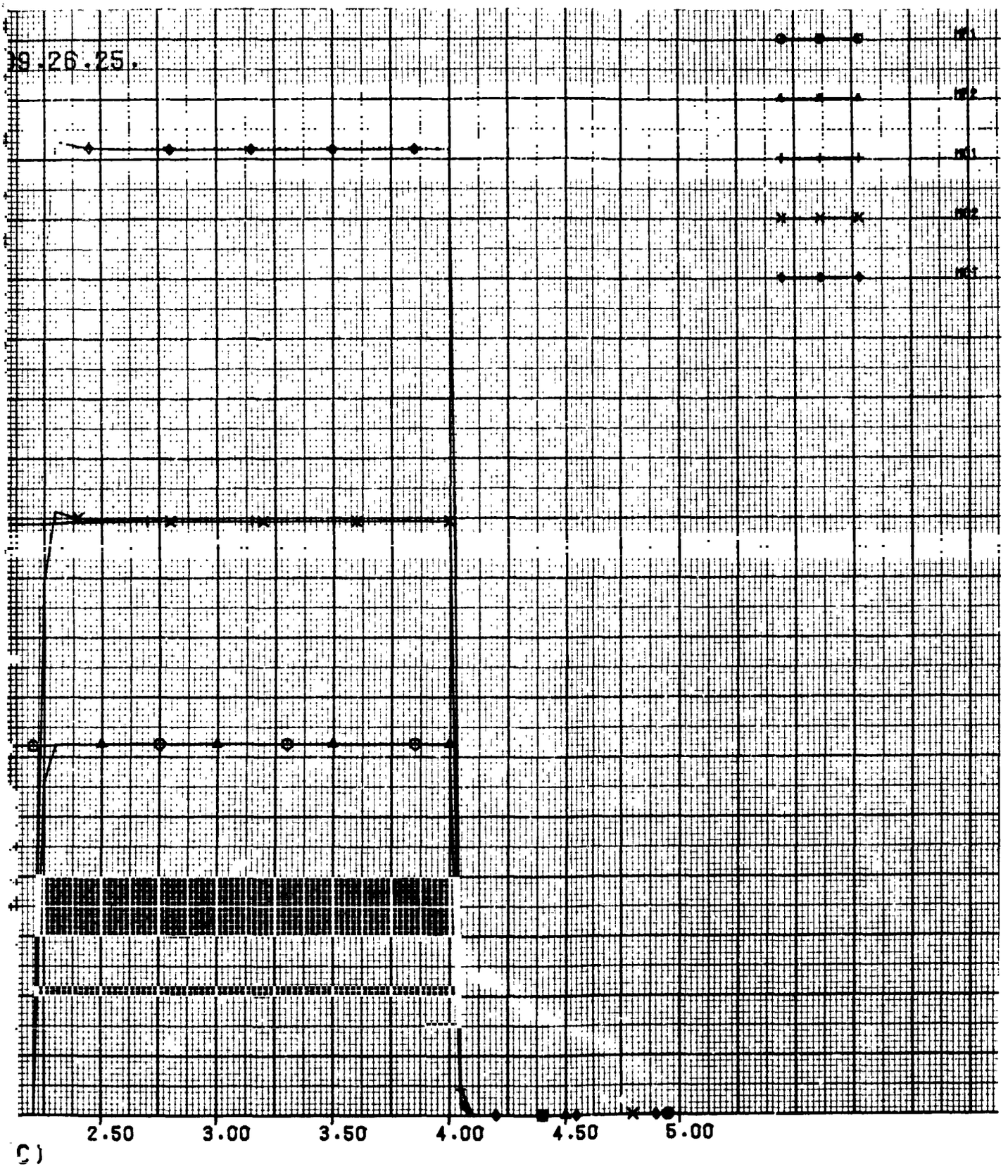

Figure 4-23. Mass Flow Rate

FOLDOUT FRAME 2

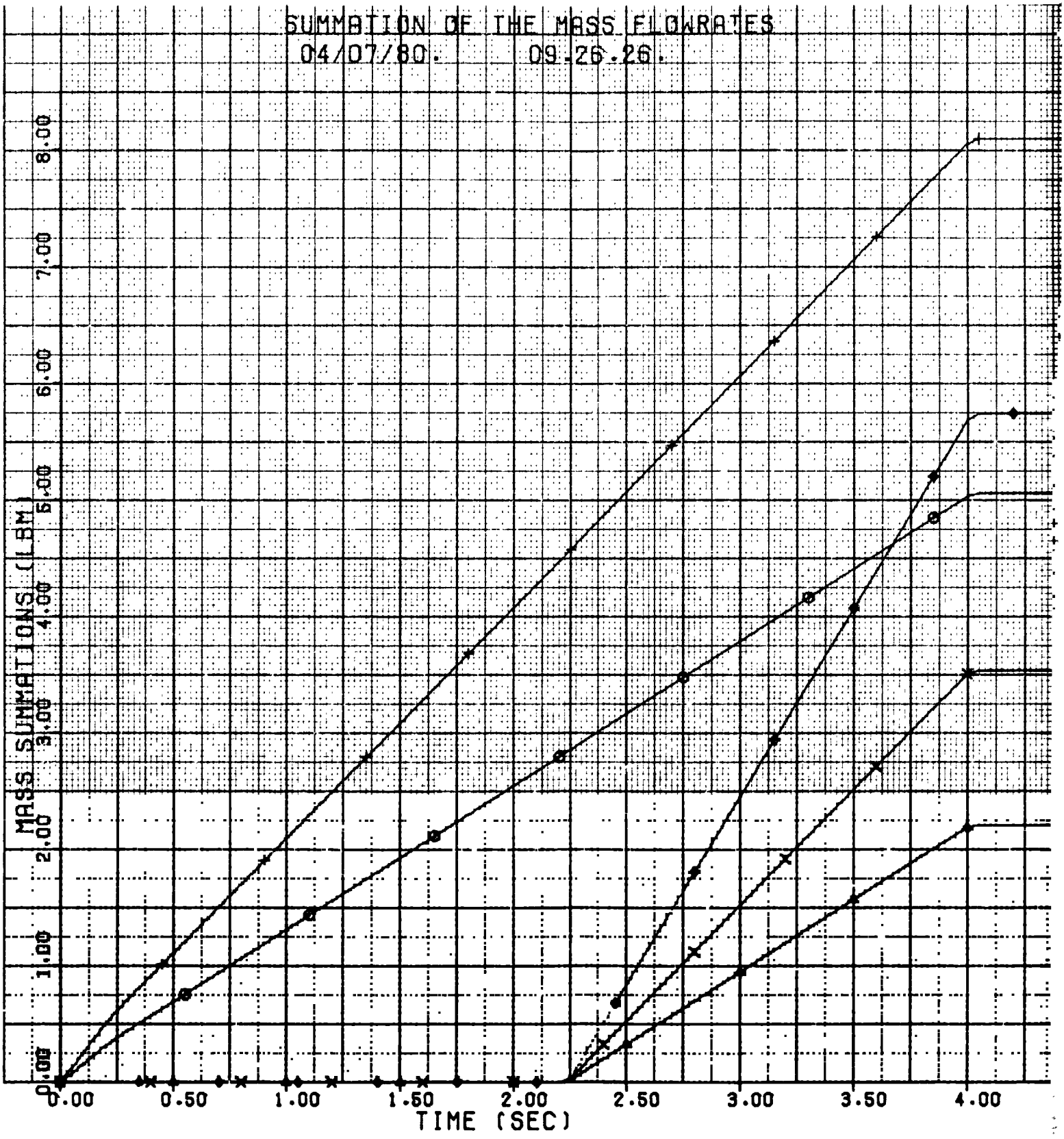

FOLDOUT FRAME

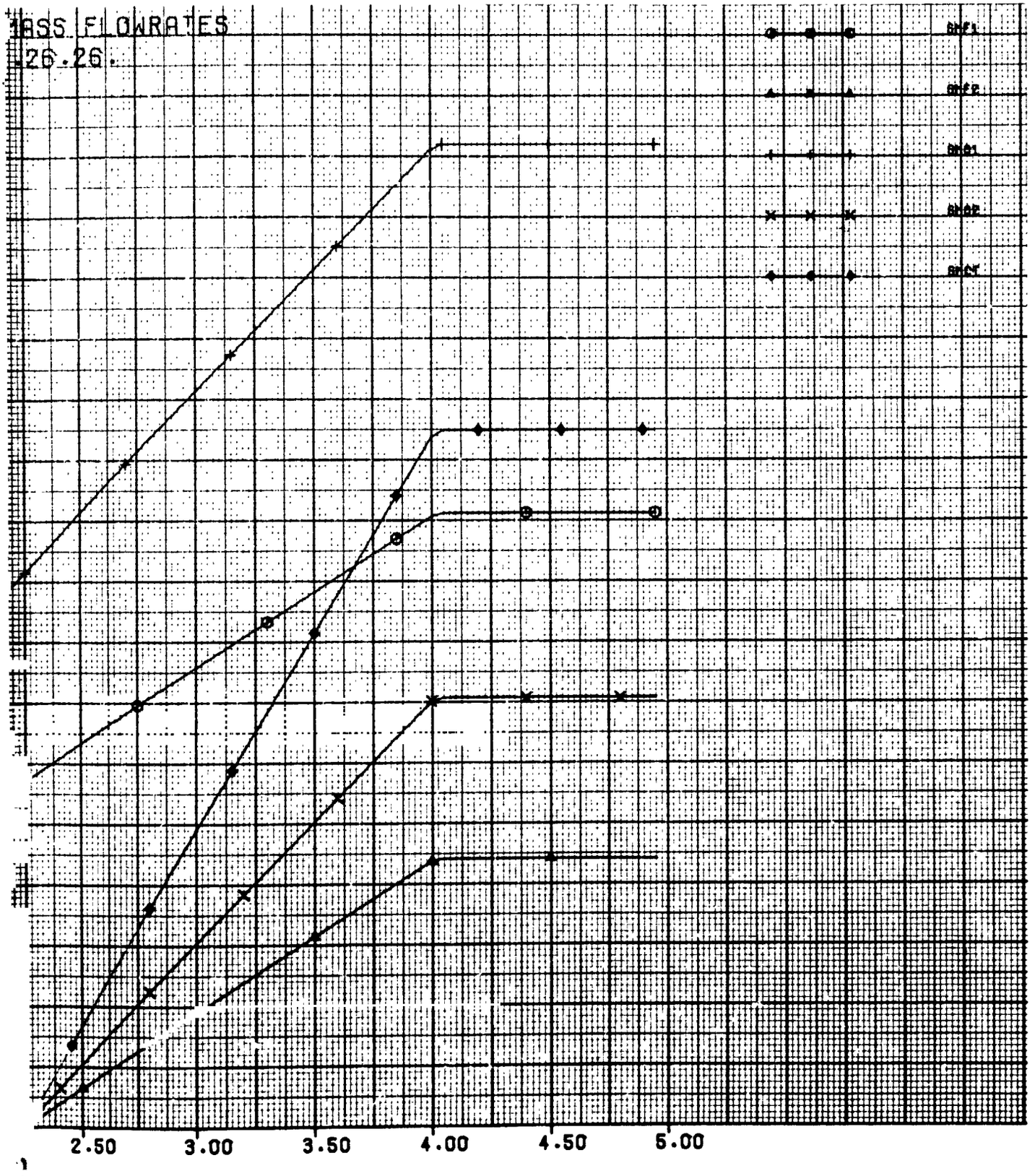

Figure 4-24. Summation of the Mass Flow Rates

FOLDOUT FRAME 2

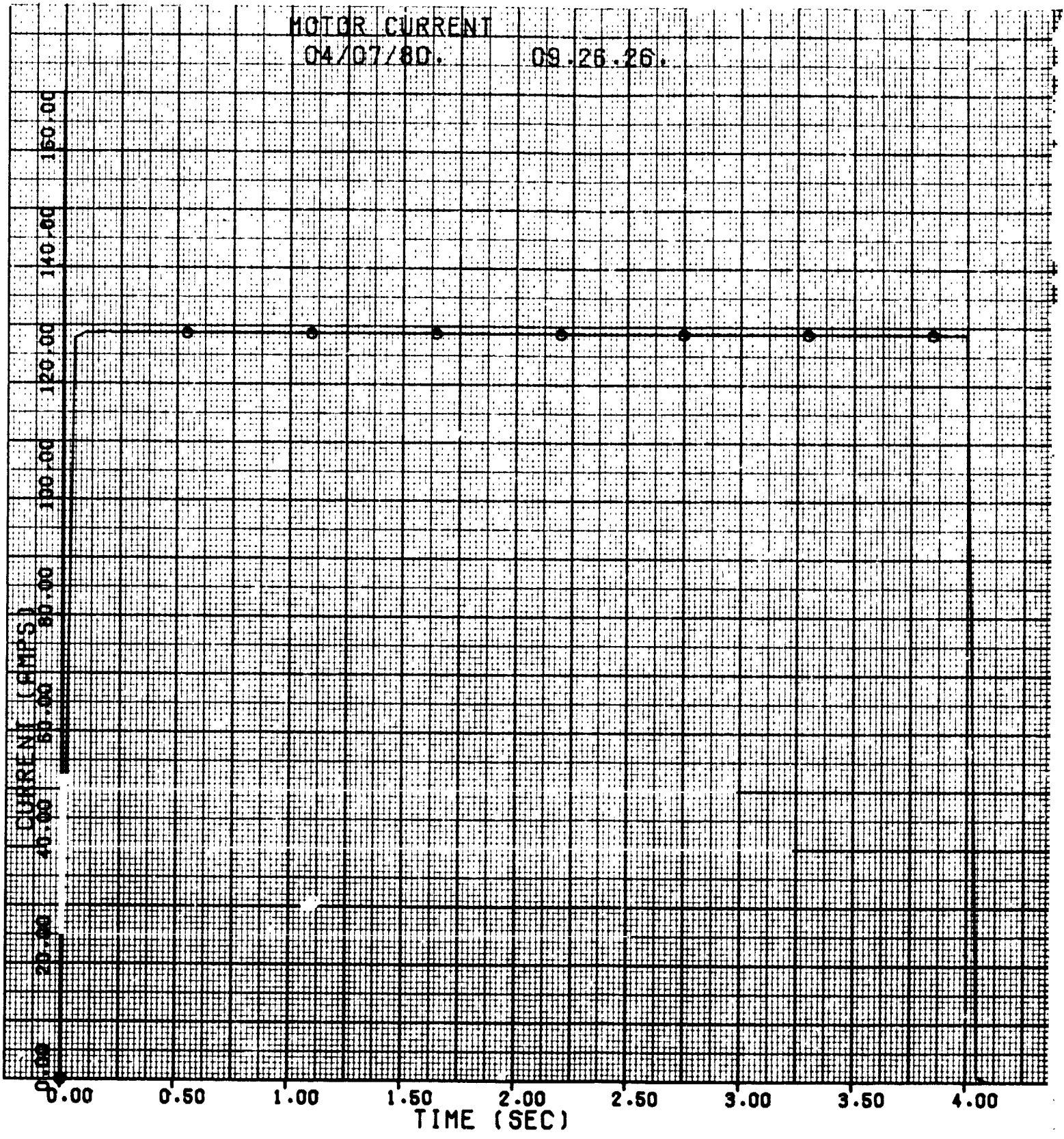

FOLDOUT FRAME

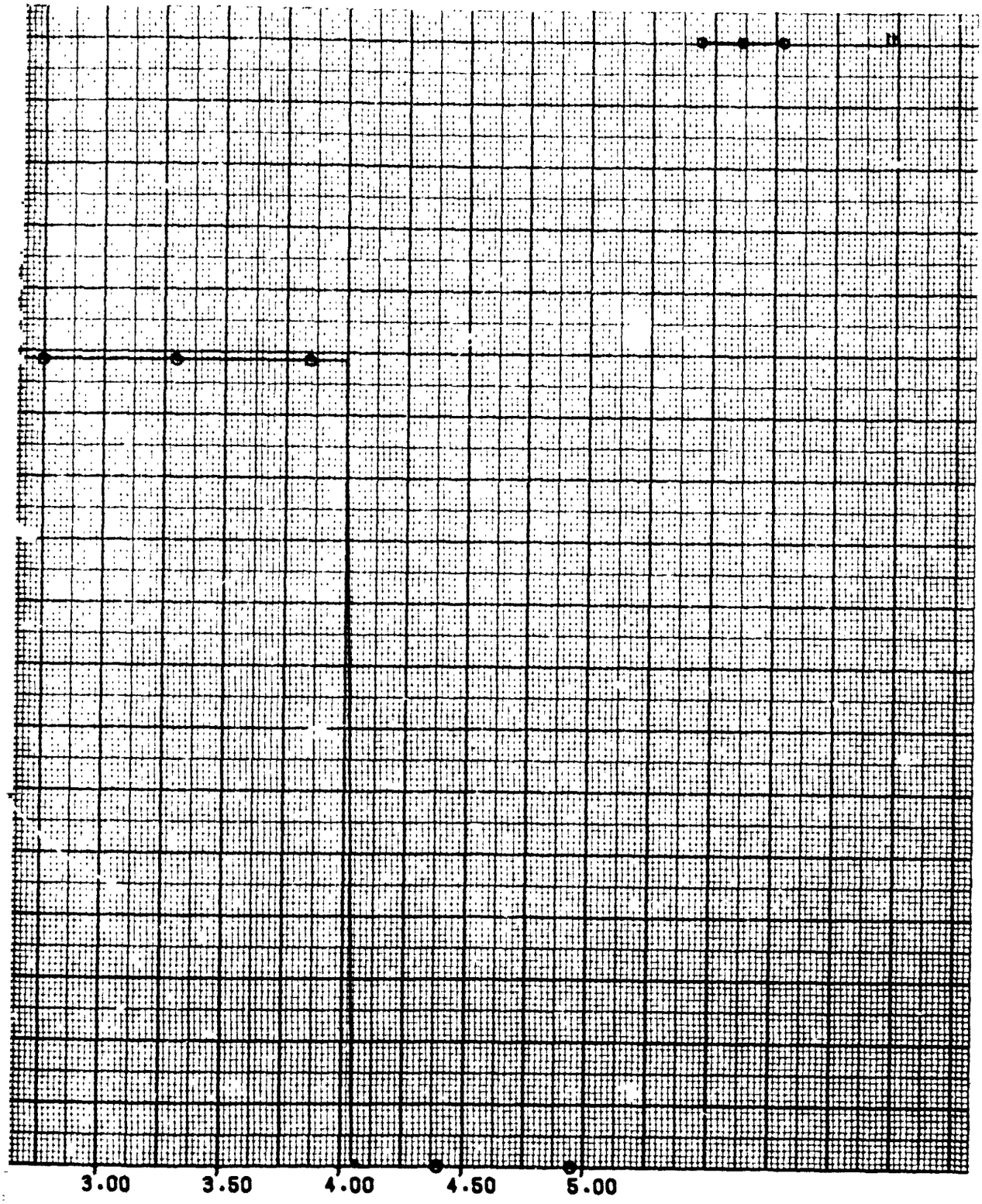

Figure 4-25. Motor System Temperature Profile

FOLDOUT FRAME 2

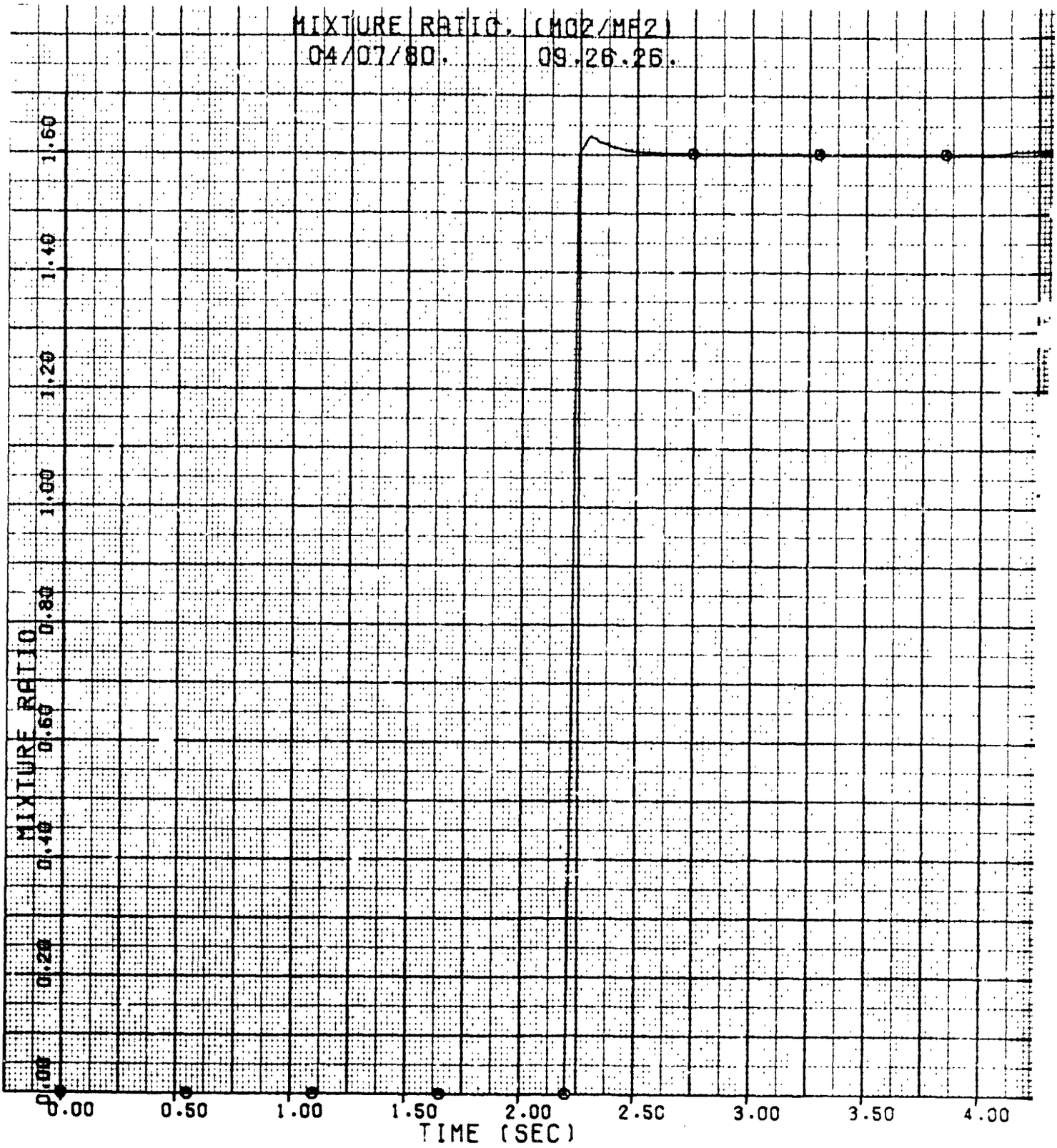

FOLDOUT FRAME

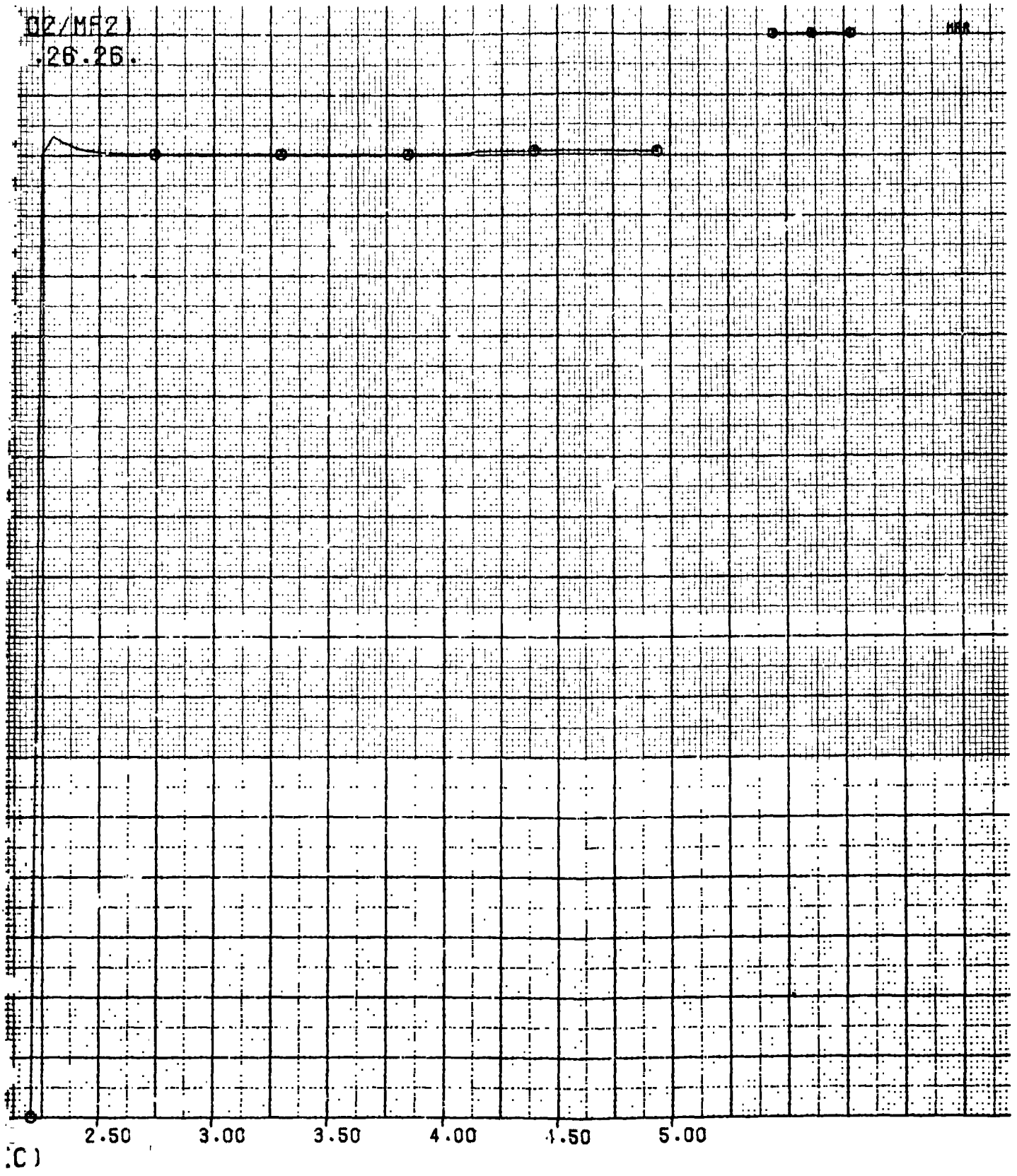

Figure 4-26. Mixture Ratio (MO_2/MF_2)

FOLDOUT FRAME 2

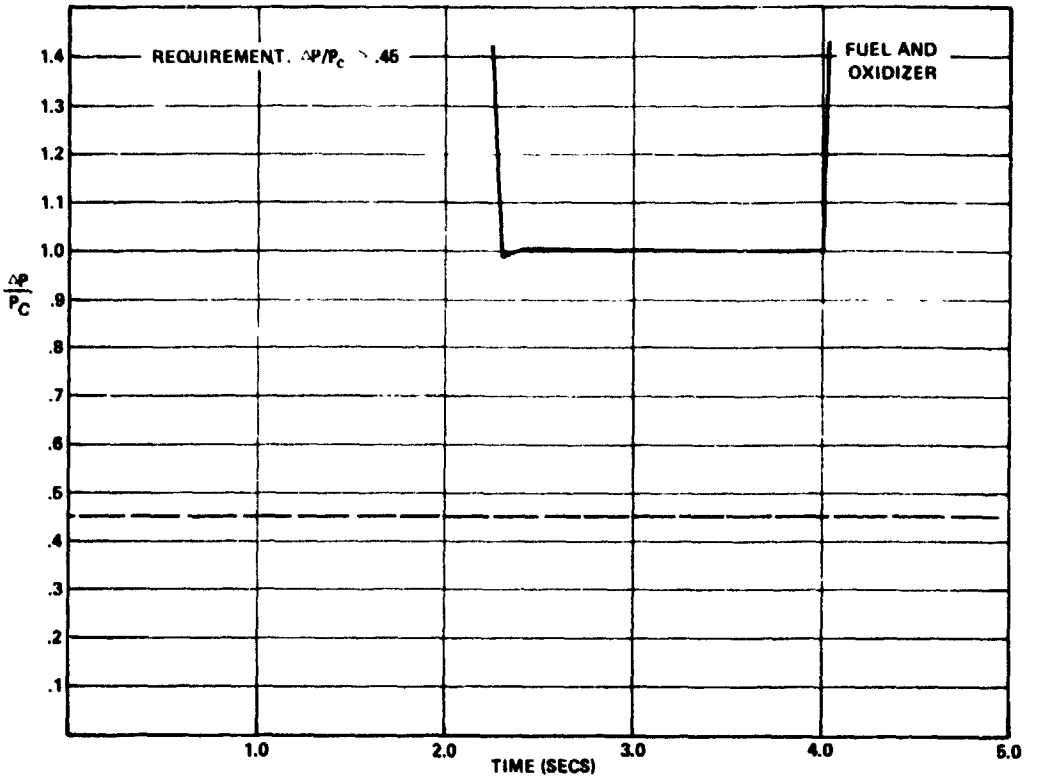

Figure 4-27. Motor Driven System (System No. 1) $\Delta P / P_c$ Versus Time

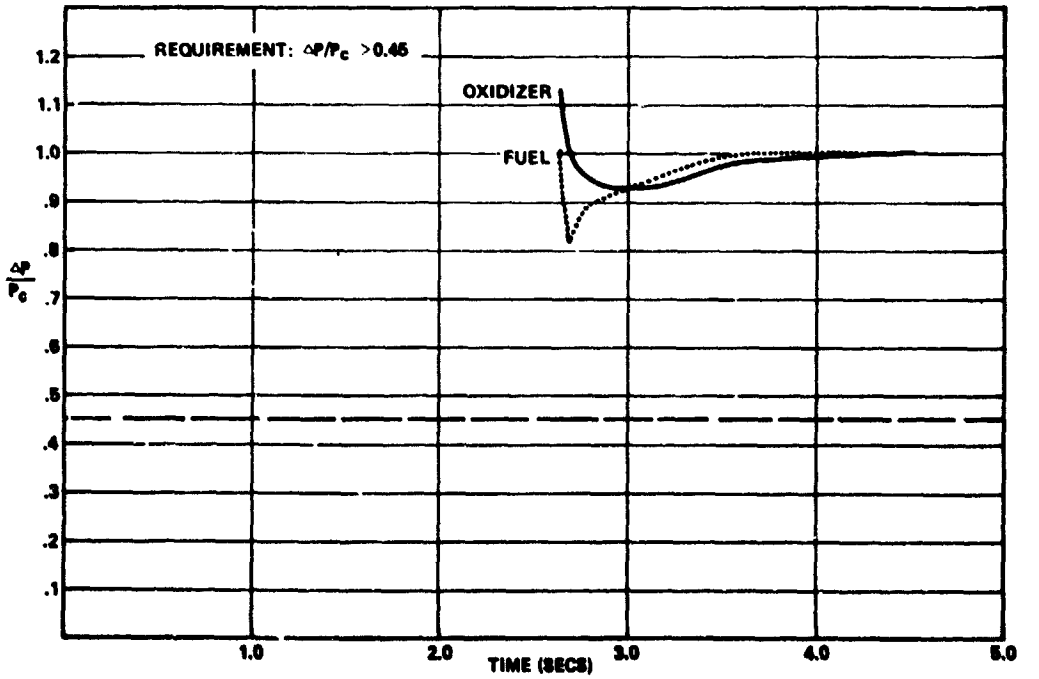

Figure 4-28. Hydrazine System (System No. 3) $\Delta P / P_c$ Versus Time

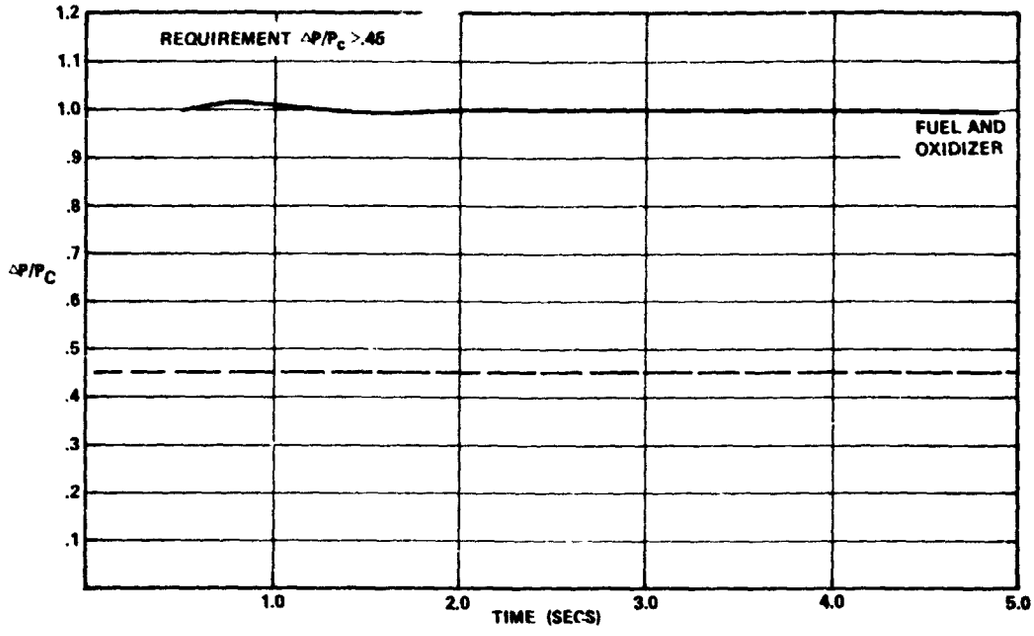

Figure 4-29. Accumulator System (System No. 4) $\Delta P / P_c$ Versus Time

For very short periods of time, approximately 5 milliseconds. the mixture ratio becomes very high. Although not shown in the graphs because of plot routine limitations, these mixture ratios may get as high as 40/1 in the engine for 0.4 millisecond. This usually occurs immediately after the valves are opened. The system settles down quickly to the design mixture ratio but can be further attenuated by adjusting the start sequence.

5. SYSTEM TRADEOFFS

Four viable pump-fed propellant feed systems have been identified. This section discusses a detailed tradeoff of these systems to select the most desirable system with the emphasis on minimum weight, minimum development risk, and highest reliability.

5.1 PUMP BRAKE HORSEPOWER

The total pump brake horsepowers (BHP) as a function of engine thrust level and thrust chamber pressure were provided in Section 3.5 (Figures 3-18 and 3-19). At the 1000 lbf thrust level, these ranged from 4.65 to 11.14 HP (3.47 to 8.31 KW_E). High speed (i.e., 84000 rpm), permanent magnet electric motors are available in this range. Hence, for the 1000 lbf thrust level candidate PFS Numbers 1 and 2 are attractive options. In the 2500 and 4000 lbf thrust levels the pump BHP's are in the 10.76 to 25.83 HP (8.03 to 19.27 KW_E) and 16.7 to 40.03 HP (12.46 to 29.86 KW_E) ranges respectively. At these higher power levels the use of battery powered electric motor drives becomes somewhat marginal. High current drain rates require downrating of the battery specific energy densities. Rotor lengths (for a given motor outside diameter) tend to become excessive and have a direct effect on shaft critical speeds. Also, increased centrifugal stresses required thicker stainless steel retaining cylinders around the samarium cobalt permanent magnet. This results in increased motor weight and reduced motor efficiences due to the greater rotor-to-stator "air" gap. Because of the foregoing, at the higher thrust levels, candidate PFS Number 3 and 4 that employ a turbine drive appear to be the more desirable systems despite their increased complexities.

5.2 WEIGHT COMPARISONS

A detailed weight estimate was prepared for each candidate PFS. The results are summarized in Tables 5-1, 5-2, and 5-3. For the components common to all candidate PFS, as would be anticipated, the heaviest were the helium tank and gas, the MMH fuel tank, and the N_2O_4 oxidizer tank. In general, these components comprised 70 to 87% of the total PFS dry weight. For the battery-powered, electric motor driven pump, the weight of the batteries was the next most significant factor. For the monopropellant, gas generator powered turbopump PFS, the weight of the hydrazine

Table 5-1. Battery-Powered, Electric Motor Driven Pump Propellant Feed System Weight Summary (System Nos. 1 and 2)

(All Values in Pounds)

No.	Component Description	No. Req'd	F = 1000 lbf			F = 2500 lbf			F = 4000 lbf		
			P_c = 150 psia	P_c = 300 psia	P_c = 500 psia	P_c = 150 psia	P_c = 300 psia	P_c = 500 psia	P_c = 150 psia	P_c = 300 psia	P_c = 500 psia
1	Helium Tank and Gas	1	105	105	105	105	105	105	105	105	105
2	MMH Fuel Tank	1	267	267	267	267	267	267	267	267	267
3	N_2H_4 Oxidizer Tank	1	267	267	267	267	267	267	267	267	267
4-6	Temperature Transducers and Cabling	3	1	1	1	1	1	1	1	1	1
7-9	Pressure Transducers and Cabling	3	2	2	2	2	2	2	2	2	2
10-12	Fill and Drain Valve	3	1	1	1	1	1	1	1	1	1
13-17	Filter	5	5	5	5	5	5	5	5	5	5
18-22	Commandable Latching Valve	5	3	3	3	3	3	3	3	3	3
23	Pressure Regulator	1	1	1	1	1	1	1	1	1	1
24-25	One-Way Check Valve	2	2	2	2	2	2	2	2	2	2
26-27	Relief Vavle	2	2	2	2	2	2	2	2	2	2
28	Tubing	100 ft	40	40	40	40	40	40	40	40	40
29	Latching Relay	1	0.2	0.2	0.2	0.2	0.2	0.2	0.2	0.2	0.2
	Subtotal		696.2	696.2	696.2	696.2	696.2	696.2	696.2	696.2	696.2
30	Electric Motor	1	5.0	7.5	12.5	12.0	19.0	30.0	20.0	32.0	47.5
31	Pumps	2	0.7	1.0	1.3	1.1	1.4	1.8	1.4	1.8	2.2
32	Batteries (50 w-hr/lb)	As Req'd	81.6	130.7	195.5	75.6	121.0	181.4	73.2	117.4	165.6
33	Batteries (100 w-hr/lb)	As Req'd	40.8	65.4	97.7	37.8	60.5	90.7	36.6	58.7	87.8
	Total PFS Dry Weight (50)		783	835	905	785	838	909	790	847	911
	Total PFS Dry Weight (100)		743	770	808	747	777	819	754	789	834
	Propellant Weight		11628	11628	11628	11628	11628	11628	11628	11628	11628
	Total Propellant Feed System Weight (lb)										
	(at 50 w-hr/lb) (Sys. No. 2)		12411	12463	12533	12412	12466	12537	12419	12475	12539
	(at 100 w-hr/lb) (Sys. No. 1)		12371	12400	12436	12375	12405	12447	12382	12417	12461

Table 5-2. Monopropellant Gas Generator Powered Turbopump Propellant Feed System Weight Summary (System No. 3)

(All Values in Pounds)

No.	Component Description	No. Req'd	F = 1000 lbf			F = 2500 lbf			F = 4000 lbf		
			P_c = 150 psia	P_c = 300 psia	P_c = 500 psia	P_c = 150 psia	P_c = 300 psia	P_c = 500 psia	P_c = 150 psia	P_c = 300 psia	P_c = 500 psia
1	Helium Tank and Gas	1	105	105	105	105	105	105	105	105	105
2	MMH Fuel Tank	1	267	267	267	267	267	267	267	267	267
3	N_2O_4 Oxidizer Tank	1	267	267	267	267	267	267	267	267	267
4-6	Temperature Transducer and Cabling	3	1	1	1	1	1	1	1	1	1
7-9	Pressure Transducer and Cabling	3	2	2	2	2	2	2	2	2	2
10-12	Fill and Drain Valve	3	1	1	1	1	1	1	1	1	1
13-17	Filter	5	5	5	5	5	5	5	5	5	5
18-22	Commandable Latching Valve	5	3	3	3	3	3	3	3	3	3
23	Pressure Regulator	1	1	1	1	1	1	1	1	1	1
24-25	One-Way Check Valve	2	2	2	2	2	2	2	2	2	2
26-27	Relief Valve	2	2	2	2	2	2	2	2	2	2
28	Tubing	125 ft	50	50	50	50	50	50	50	50	50
29	Hydrazine Tank and Hydrazine	1	44	69	105	41	64	96	38	62	94
30	Temperature Transducer and Cabling	1	0.3	0.3	0.3	0.3	0.3	0.3	0.3	0.3	0.3
31	Pressure Regulator	1	1	1	1	1	1	1	1	1	1
32	One-Way Check Valve	1	1	1	1	1	1	1	1	1	1
33	Relief Valve	1	1	1	1	1	1	1	1	1	1
34	Pressure Transducer and Cabling	1	1	1	1	1	1	1	1	1	1
35	Fill and Drain Valve	1	0.2	0.2	0.2	0.2	0.2	0.2	0.2	0.2	0.2
36	Filter	1	1	1	1	1	1	1	1	1	1
37-39	Commandable Latching Valve	3	2	2	2	2	2	2	2	2	2
	Subtotal		757.5	782.5	818.5	754.5	777.5	809.5	751.5	775.5	807.5
40	Turbine (including Housings, Bearings, and Shaft)	1	15.6	19.1	21.1	27.7	32.6	34.0	34.4	40.3	43.8
41	Pumps (including Housing)	2	0.2	0.3	0.4	0.3	0.4	0.5	0.4	0.5	0.7
42	Gas Generator	1	0.2	0.3	0.4	0.3	0.4	0.6	0.3	0.5	0.1
	Overall PFS Dry Weight		773.5	802.2	840.4	782.8	810.9	844.6	786.6	816.8	852.7
	Propellant Weight		11628	11628	11628	11628	11628	1.628	11628	11628	11628
	Total Propellant Feed System Weight (lb)		12402	12430	12468	12411	12439	12473	12415	12445	12481

Table 5-3. Bipropellant Gas Generator Powered Turbopump Propellant Feed System Weight Summary (System No. 4)

(All Values in Pounds)

No.	Component Description	No. Req'd	F = 1000 lbf			F = 2500 lbf			F = 4000 lbf		
			P_c = 150 psia	P_c = 300 psia	P_c = 500 psia	P_c = 150 psia	P_c = 300 psia	P_c = 500 psia	P_c = 150 psia	P_c = 300 psia	P_c = 500 psia
1	Helium Tank and Gas	1	105	105	105	105	105	105	105	105	105
2	MMH Fuel Tank	1	267	267	267	267	267	267	267	267	267
3	N_2O_4 Oxidizer Tank	1	267	267	267	267	267	267	267	267	267
4-6	Temperature Transducer and Cabling	3	1	1	1	1	1	1	1	1	1
7-9	Pressure Transducer and Cabling	3	2	2	2	2	2	2	2	2	2
10-12	Fill and Drain Valve	3	1	1	1	1	1	1	1	1	1
13-17	Filter	5	5	5	5	5	5	5	5	5	5
18-22	Commandable Latching Valve	5	3	3	3	3	3	3	3	3	3
23	Pressure Regulator	1	1	1	1	1	1	1	1	1	1
24-25	One-Way Check Valve	2	2	2	2	2	2	2	2	2	2
26-27	Relief Valve	2	2	2	2	2	2	2	2	2	2
28	Tubing	150 ft	60	60	60	60	60	60	60	60	60
29-30	Accumulator	2	2	2	2	2	2	2	2	2	2
31-32	Fill and Drain Valve	2	0.5	0.5	0.5	0.5	0.5	0.5	0.5	0.5	0.5
33-38	Commandable Latching Valve	6	4	4	4	4	4	4	4	4	4
39-40	One-Way Check Valve	2	2	2	2	2	2	2	2	2	2
	Subtotal		724.5	724.5	724.5	724.5	724.5	724.5	724.5	724.5	724.5
41	Turbine		9.4	13.2	17.2	16.7	22.4	27.7	20.7	27.7	35.7
42	Pumps		0.2	0.3	0.4	0.3	0.4	0.5	0.4	0.5	0.7
43	Gas Generator		0.2	0.4	0.6	0.4	0.6	0.8	0.5	0.7	0.9
	Overall PFS Dry Weight		734.3	738.4	742.7	741.9	747.9	753.4	746.1	753.4	761.8
	GG Propellant Weight		48	76	114	44	71	106	43	68	103
	Propellant Weight		11628	11628	11628	11628	11628	11628	11628	11628	11628
	Total Propellant Feed System Weight (lb)		12410	12442	12485	12414	12447	12488	12417	12449	12493

tank, hydrazine fuel, and tubing became the next most important weight contributors. Finally, for the bipropellant gas generator powered turbopump PFS, the accumulators, tubing, and the extra propellants required to supply the gas-generator are the next major weight contributors. Since the gas generator propellant weights are significant, a comparison was made for these weights at the 2500 lbf level. This is shown in Figure 5-1. In all cases the N_2H_4 propellant weights were less than the MMH/N_2O_4 propellant weights. This results from the poorer thermodynamic performance caused by having to operate the latter gas generator at very high oxidizer-rich mixture ratios to stay within allowable turbine temperature limits. This offsets some of the weight advantage gained by PFS Number 4 in eliminating the N_2H_4 storage tank.

Using the data in Tables 5-1, 5-2 and 5-3, weight comparisons were then made for total propellant feed system dry weights (Figures 5-2 and 5-3) and total propellant feed system weights including propellants (Figures 5-4, 5-5, and 5-6). Figure 5-2 compares the dry weights of PFS Number 1 (lithium-thionyl chloride batteries) with PFS Number 3 and 4 (turbine driven pumps). In this comparison, the bipropellant gas generator turbopump system was the lightest. The motor driven pumps using 100 watt-hr/lb batteries were the next lightest and the monopropellant gas generator turbopump system was the heaviest. A similar comparison with the 50 watt-hr/lb batteries is shown in Figure 5-3. PFS Number 4 was still the lightest, but now PFS Number 3 was found to be the next lightest and the battery powered PFS Number 2 the heaviest. Thus, from a total dry weight standpoint Figures 5-2 and 5-3 clearly indicated the importance of the achieveable specific energy density of the batteries.

The comparisons for the total PFS weights are shown on Figures 5-4, 5-5, and 5-6. Figure 5-4 was prepared primarily to show the total PFS weight differences between the two battery powered systems (i.e., PFS 1 and 2). The AgZn battery powered systems were approximately 50 to 100 pounds heavier than the lithium-thionyl chloride battery power systems, depending upon thrust chamber pressure level.

A comparison of PFS Number 1 with PFS Numbers 3 and 4 is shown in Figure 5-5. Here, on a total PFS weight basis, the LiTCl battery powered system (PFS Number 1) is the lightest. The monopropellant, gas generator

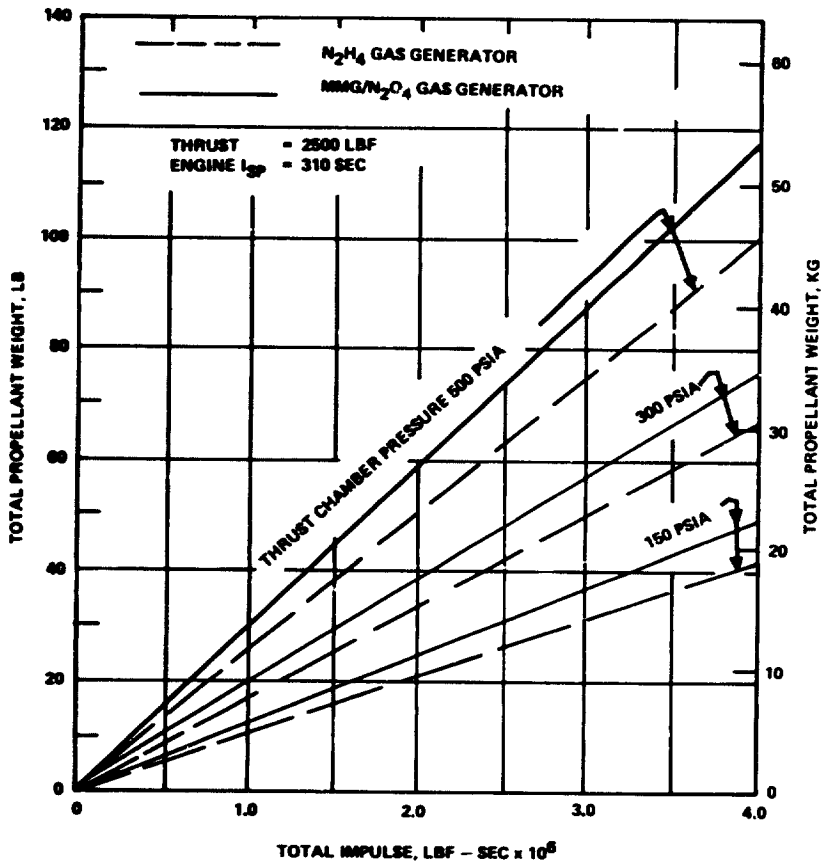

Figure 5-1. Comparison Between Monopropellant and Bipropellant Gas Generator Propellant Weights

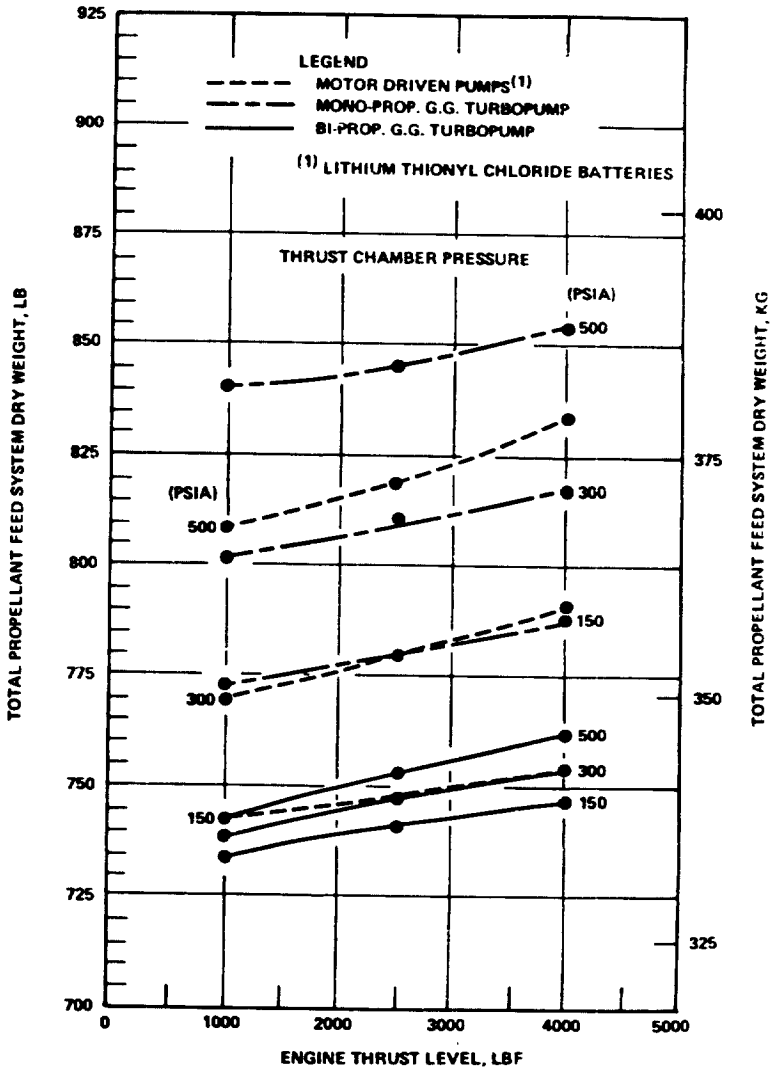

Figure 5-2. Total Propellant Feed System Dry Weight vs. Engine Thrust Level

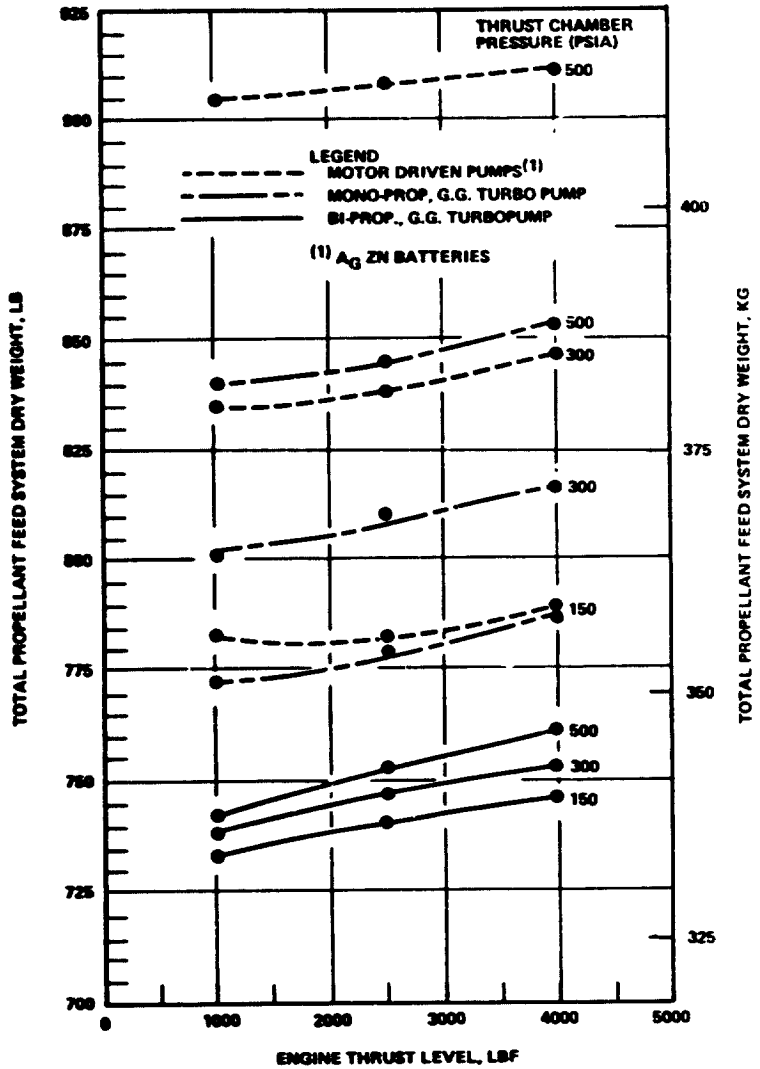

Figure 5-3. Total Propellant Feed System Dry Weight vs. Engine Thrust Level

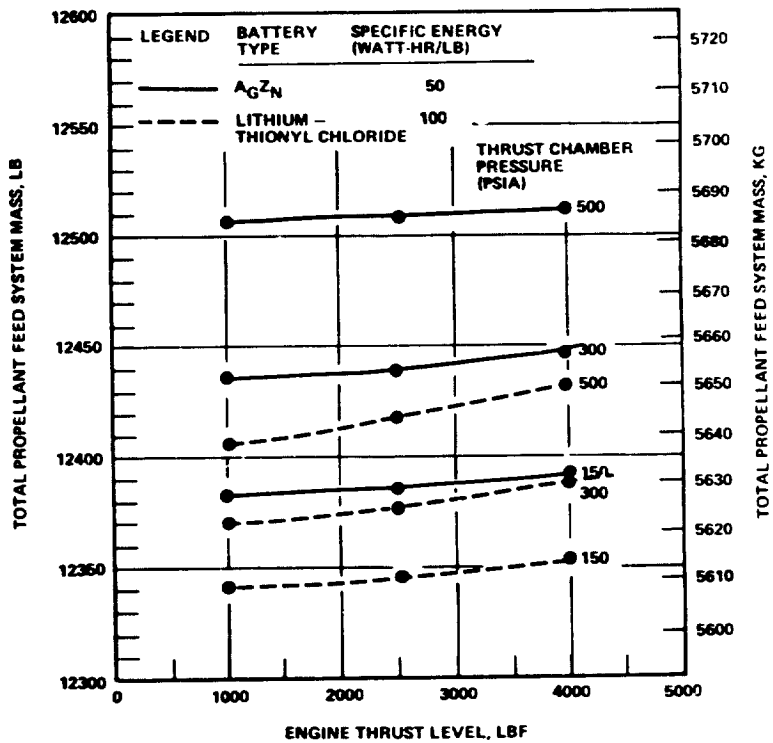

Figure 5-4. Total Propellant Feed System Mass vs. Engine Thrust Level

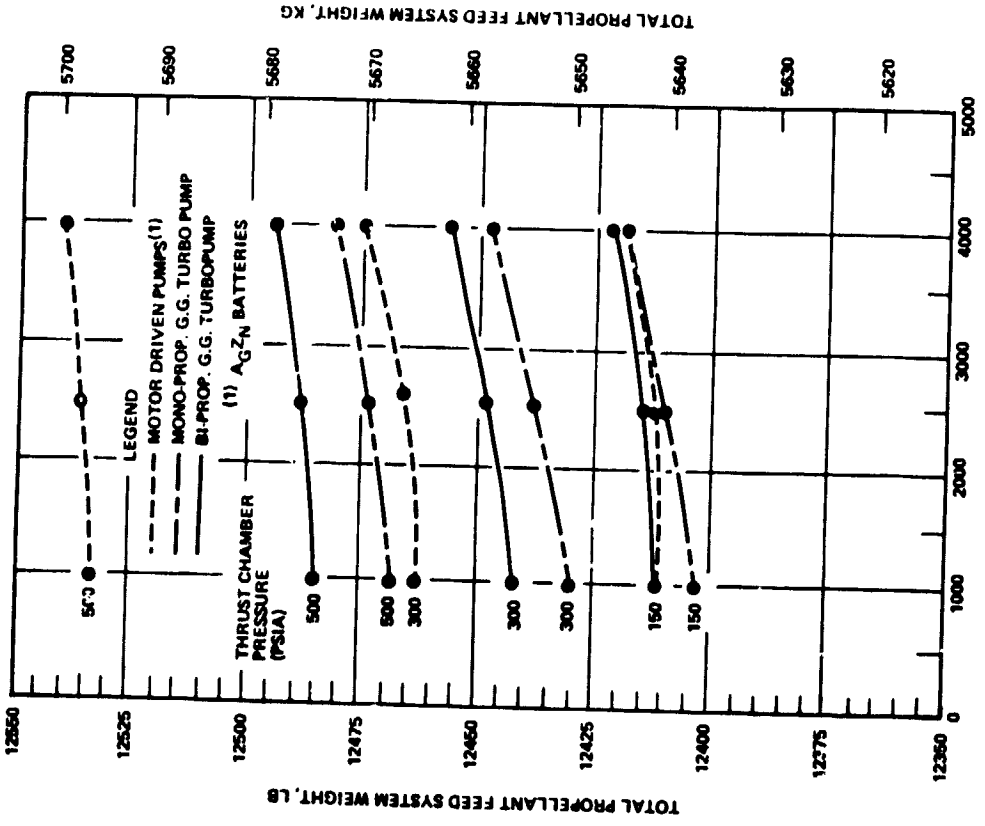

Figure 5-6. Total Propellant Feed System Weight vs. Engine Thrust Level

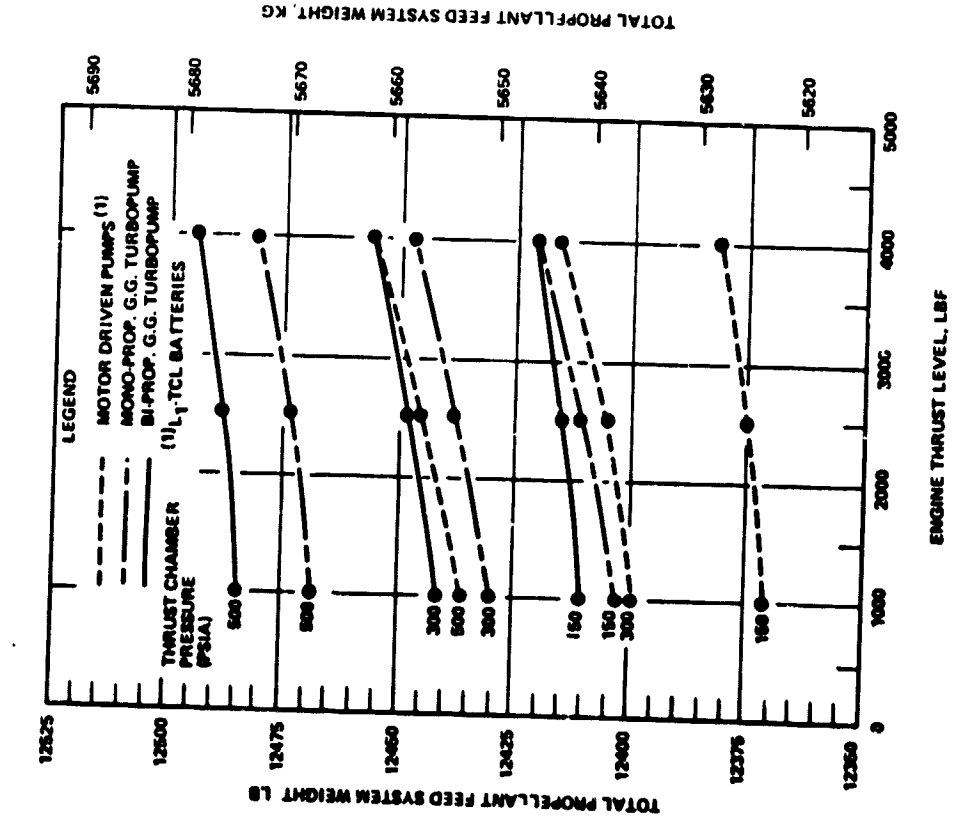

Figure 5-5. Total Propellant Feed System Weight vs. Engine Thrust Level

turbopump system was the next lightest and the bipropellant gas generator turbopump system became the heaviest. This reversal in weights between PFS Number 3 and 4 stems from the increased gas generator propellant weights and tubing weights associated with the latter system. A similar comparison was made for the AgZn battery powered system (PFS Number 2) and is shown on Figure 5-6. Due to the lower specific energy density of the AgZn batteries, it now results in the heaviest total PFS system, except at the lowest thrust chamber pressure (150 psia), where all three systems are very nearly equal.

5.3 PROPELLANT FEED SYSTEM PRELIMINARY RELIABILITY ANALYSIS

The Propellant Feed System (PFS) reliability analysis addresses the four candidate configurations as follows:

System 1 - Battery (lithium thionyl choride) powered electric-motor driven turbopump propellant feed system

System 2 - Battery (silver zinc) powered electric-motor-driven turbopump propellant feed system

System 3 - Monopropellant gas-generator-powered turbopump propellant feed system

System 4 - Bipropellant gas-generator-powered turbopump propellant feed system.

The PFS reliability analysis was based on current design data as described throughout this document. These data were not reproduced here but are referenced for convenience. Among the data utilized were:

- Schematic diagrams (Figure 3-26, 3-27, 3-28)
- System descriptions (Section 3.6)
- Component descriptions (Sections 3.4, 3.5, 3.6)
- Failure mode and effects analysis (Section 4.1.1).

5.3.1 Mission Profile

The PFS pump feeds oxidizer (N_2O_4) and fuel (MMH) to a bipropellant thruster. This rocket engine (PFS plus thruster) will be used as an orbit insertion engine around another planet such as Venus or Mars.

Based on this intended usage, the following nonactive mission phase breakdown is assumed:

- One month prelaunch (from consumable loading to Shuttle launch)
- Five months nonactive flight (from Shuttle launch to unit deployment).

The active mission profile for the PFS is given as one hour of reactive firing including up to 20 starts/stops.

The PFS component failure rates are much higher during the active mission phase than they are during the nonactive phases. Also, the PFS nonactive phases are short relative to typical satellite propulsion system mission nonactive phases which are often measured in years. Therefore, the PSF reliability during the nonactive phaser can be expected to be much higher relative to the active phase and can be ignored without introducing undue error into the total mission reliability estimation. This reliability analysis, therefore, addresses only the active PFS mission phases. It is noted, however, that the system is designed to meet all of the Space Shuttle safety requirements in effect during the nonactive phases.

5.3.2 System Component Lists and Failure Rate Data

Tables 5-4 and 5-5 show the components that are common and those that are unique to each of the four systems under consideration. Components common to all systems are shown with no lower case letter designation following their number (component number from Figures 3-26, 3-27, and 3-28). Components (numbers) unique to system 1 are followed with one lower case letter (a) and components (numbers) unique to systems 2, 3 and 4 are followed with lower case letters (b), (c), and (d), respectively. This convention is carried throughout this analysis.

Table 5-4 is a listing of components that are inactive during the mission and/or that are noncritical to a successful mission. Rationale for the assignment of this status is given on the table. These components (fill and drain valves and pressure/temperature transducers) are not considered further in this analysis in the interest of simplification.

Table 5-4. Inactive and/or Noncritical* Components

Component	Component Designation Number	System 1	System 2	System 3	System 4	Failure Rate ($\times 10^{-6}$)/ Failure Probability	Remarks
Temperature Transducer	4	X	X	X	X	Negligible	These temperature transducers provide system status information only and are not essential to successful system operation. These transducers are mounted on the hardware and do not penetrate the fluid carrying ducting components.
Temperature Transducer	5	X	X	X	X	Negligible	
Temperature Transducer	6	X	X	X	X	Negligible	
Pressure Transducer	7	X	X	X	X	Negligible	These pressure transducers provide system status information only and are not essential to successful system operations. These transducers are welded into the system.
Pressure Transducer	8	X	X	X	X	Negligible	
Pressure Transducer	9	X	X	X	X	Negligible	
Fill and Drain Valve (Manual)	10	X	X	X	X	Negligible	These fill and drain valves are inactive during the mission and must only remain free of external leakage. These valves are a redundant seal design with an additional redundant (third) seal provided in their cap. These valves are welded into the system.
Fill and Drain Valve (Manual)	11	X	X	X	X	Negligible	
Fill and Drain Valve (Manual)	12	X	X	X	X	Negligible	
Temperature Transducer	30c			X		Negligible	
Pressure Transducer	34c			X		Negligible	
Fill and Drain Valve (Manual)	35c			X		Negligible	
Fill and Drain Valve (Manual)	31d				X	Negligible	
Fill and Drain Valve (Manual)	32d				X	Negligible	

*Noncritical to successful system operation.

Table 5-5. Mission Critical* Components

Component	Component Designation Number	System 1	2	3	4	Failure Rate** ($\times 10^{-6}$) / Failure Probability	Remarks
Pressure Vessel (He, 3500 psia)	1	X	X	X	X	0.9999	Conservative success probability estimate. Reliability pressure vessel success estimation using stress/strength techniques (using accepted design margins and material of known characteristics) should indicate R > 0.9999 for structural reliability.
Fuel Storage Vessel (MMH, 50 psia)	2	X	X	X	X	0.9999 + 240	
Oxidizer Storage Vessel (H_2O_4, 50 psia)	3	X	X	X	X	0.9999 + 240	
Pressurant Filter	13	X	X	X	X	14	
Fuel Filter	14	X	X	X	X	56	
Oxidizer Filter	15	X	X	X	X	56	
Fuel Filter	16	X	X	X	X	56	
Oxidizer Filter	17	X	X	X	X	56	
Commandable Latching Valve (Pressurant Line)	18	X	X	X	X	632	
Commandable Latching Valve (Fuel Line)	19	X	X	X	X	632	
Commandable Latching Valve (Fuel Line)	20	X	X	X	X	632	
Commandable Latching Valve (Oxidizer Line)	21	X	X	X	X	632	
Commandable Latching Valve (Oxidizer Line)	22	X	X	X	X	632	
Pressure Regulator (Pressurant 3500-50 psia)	23	X	X	X	X	2105	
Check Valve (Pressurant Line)	24	X	X	X	X	131	
Check Valve (Pressurant Line)	25	X	X	X	X	131	

*Includes components included in the system to preclude a component failure from resulting in a catastrophic failure.

**Failure rates for all components except the gas generators were obtained from FARADA handbooks with necessary application factors used per MIL-STD-756A.

Table 5-5. Mission Critical* Components (Continued)

Component	Component Designation Number	System 1	2	3	4	Failure Rate** ($\times 10^{-6}$)/ Failure Probability	Remarks
Relief Valve (Pressurant Line)	26	X	X	X	X	1427 (0.9999 burst disc)	This relief valve incorporates a burst disc to preclude external leakage at low pressure.
Relief Valve (Pressurant Line)	27	X	X	X	X	1427 (0.9999 burst disc)	This relief valve incorporates a burst disc to preclude external leakage at low pressure.
Pressurant/Fuel/Oxidizer Lines	28	X	X	X	X	Negligible	
Latching Relay (Battery/Motor Circuit)	29a, b	X	X			453	
Electric Motor	30a, b	X	X			529	
Fuel/Oxidizer Pump	31a, b	X	X			2345	These are separate pumps connected by a common shaft and driven by common motor.
Primary Battery	32a	X				1099	
Primary Battery	33b		X			1099	
Propellant Storage Vessel (N_2H_4, 450 psia)	29c			X		0.9999 + 240	
Pressure Regulator (Pressurant 3500-50 psia)	31c			X		2105	
Check Valve (Pressurant Line)	32c			X		131	
Relief Valve (Pressurant Line)	33c			X		1427 (0.9999 burst disc)	This relief valve incorporates a burst disc to preclude external leakage at low pressure.
Propellant Filter	36c			X		56	
Commandable Latching Valve (Propellant Line)	37c			X		632	
Commandable Latching Valve (Propellant Line)	38c			X		632	
Commandable Latching Valve (Propellant Line)	39c			X		632	
Turbine	40c			X		1274	

*Includes components included in the system to preclude a component failure from resulting in a catastrophic failure.

**Failure rates for all components except the gas generators were obtained from FARADA handbooks with necessary application factors used per MIL-STD-756A.

Table 5-5. Mission Critical* Components (Continued)

Component	Component Designation Number	System 1	2	3	4	Failure Rate** ($\times 10^{-6}$)/ Failure Probability	Remarks
Fuel/Oxidizer Pump	41c			X		2345	These are separate pumps connected by a common shaft and driven by a common turbine.
Gas Generator (Monopropellant)	42c			X		3150	This is a monopropellant gas generator.
Accumulator (Oxidizer)	29d				X	0.9999 + 240	
Accumulator (Fuel)	30d				X	0.9999 + 240	
Commandable Latching Valve (Fuel Line)	33d				X	632	
Commandable Latching Valve (Oxidizer Line)	34d				X	632	
Commandable Latching Valve (Fuel Line)	35d				X	632	
Commandable Latching Valve (Oxidizer Line)	36d				X	632	
Commandable Latching Valve (Fuel Line)	37d				X	632	
Commandable Latching Valve	38d				X	632	
Check Valve (Fuel Line)	39d				X	131	
Check Valve (Oxidizer Line)	40d				X	131	
Turbine	41d				X	1274	
Fuel/Oxidizer Pump	42d				X	2345	These are separate pumps connected by a common shaft and driven by a common turbine.
Gas Generator (Bipropellant)	43d				X	6300	This is a bipropellant gas generator

*Includes components included in the system to preclude a component failure from resulting in a catastrophic failure.

**Failure rates for all components except the gas generators were obtained from FARADA handbooks with necessary application factors used per MIL-STD-756A.

Table 5-5 lists components critical to a successful mission and/or those that have been included to preclude a component failure from propagating to a catastrophic failure rather than a mission failure.

The failure rates shown represent "best readily available data" and are believed to be conservative (high). These data should be reviewed for current status and applicability during a more detailed analysis.

5.3.3 Analysis Ground Rules and Assumptions

The ground rules and assumptions affecting this reliability analysis are:

- PFS expected reliability is much higher during non-active mission phases than active mission phases and is therefore ignored in this preliminary reliability analysis (reference paragraph 5.3.1)
- Inactive and/or "noncritical to mission success" components are omitted from this preliminary reliability analysis in the interest of analysis simplification (reference paragraph 5.3.2)
- All components are operated well within their design margins.

5.3.4 Reliability Logic Diagrams

The reliability logic diagrams for each of the four PFS systems are shown in Figure 5-7, 5-8, and 5-9. The logic diagrams are shown in two segments – elements common to all systems and elements unique to a given system. The logic diagrams indicate all areas of redundancy. The logic diagrams represent elements necessary for a successful mission. Corresponding logic diagrams addressing the avoidance of catastrophic failures (but not necessarily a successful mission) would be somewhat different in areas such as the pressure regulator/relief valve relationship.

5.3.5 Reliability Analysis Results

Qualitative Analysis

This qualitative reliability assessment is based on component design status and relative system complexity. All components are considered to represent existing mature design or to be components whose design and manufacture would not represent state-of-the-art advancement. That is, there are no unique, unknown, high risk, potentially high failure probability (development) components included on any of the systems. All

ELEMENTS COMMON TO ALL SYSTEMS:

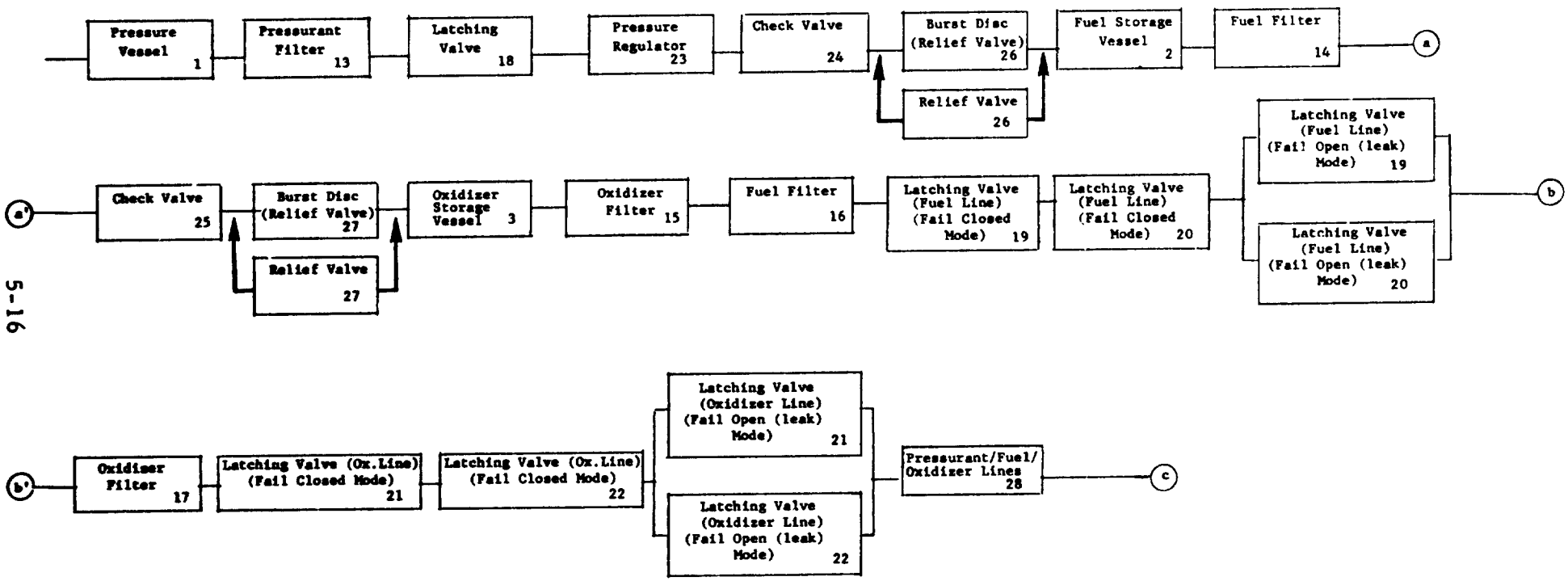

* This reliability logic diagram represents elements necessary for a successful mission. The logic diagram addressing the avoidance of catastrophic failure (but not necessarily a successful mission) would be somewhat different in areas such as the Pressure Regulator/Relief Valve relationship.

Figure 5-7. Reliability Logic Diagrams *

ELEMENTS UNIQUE TO EACH SYSTEM:

SYSTEM 1: BATTERY (LITHIUM THIONYL CHLORIDE) POWERED ELECTRIC-MOTOR-DRIVEN TURBOPUMP PROPELLANT FEED SYSTEM

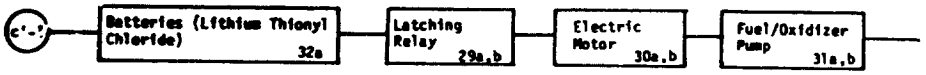

SYSTEM 2: BATTERY (SILVER ZINC) POWERED ELECTRIC-MOTOR-DRIVEN TURBOPUMP PROPELLANT FEED SYSTEM

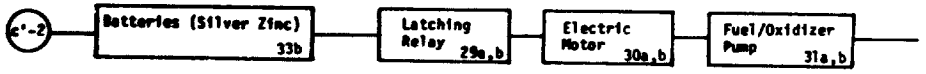

SYSTEM 3: MONOPROPELLANT GAS-GENERATOR POWERED TURBOPUMP PROPELLANT FEED SYSTEM

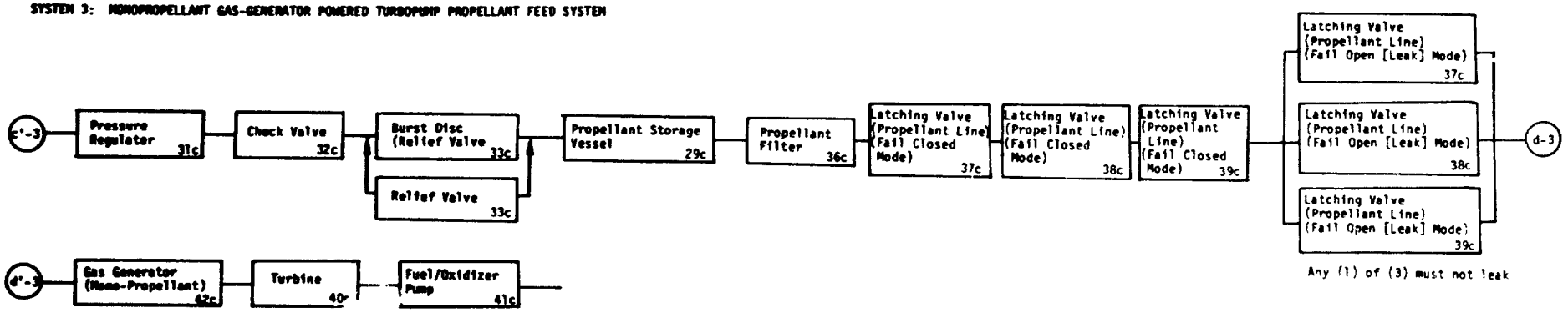

Figure 5-8. Reliability Logic Diagrams

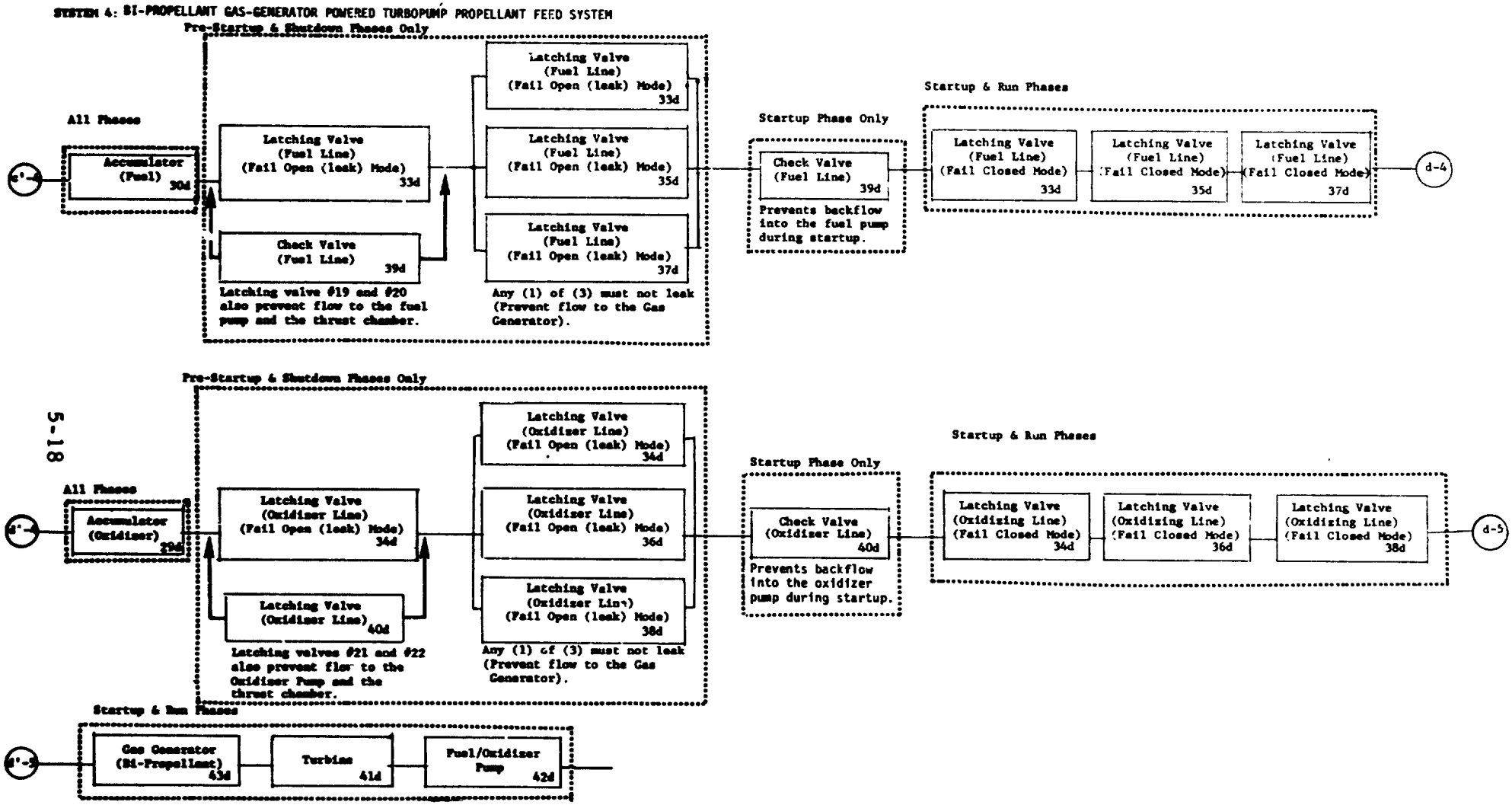

Figure 5-9. Reliability Logic Diagrams

potential component failure probabilities are, therefore, expected to be inherent and random in nature.

Given the reliability assumption that all other things are equal, the simpler, least complex system is inherently the least likely to fail, an evaluation of relative system complexity has been made. Table 5-5 (Mission Critical Components) and Figures 5-7 to 5-9 (Reliability Logic Diagrams) clearly indicate, after accounting for components common to all, the relative complexity of the systems. On this basis the battery powered systems (1 and 2) would be expected to be the most reliable followed by the monopropellant gas-generator powered system (3) and lastly by the relatively complex bipropellant gas-generator powered system (4). Relative relability of the battery powered systems would be based on the relative expected reliability of lithium thionyl chloride (system 1) and silver zinc (system 2) batteries and the number of each necessary to power the system. Silver zinc batteries have extensive satisfactory usage history while lithium thionyl chloride batteries are relatively new. Therefore, confidence exists in the reliability level of the silver zinc batteries. The same confidence cannot exist in the reliability level of lithium thionyl chloride batteries. However, the lithium thionyl chloride batteries may prove to be as reliable as the silver zinc batteries as a usage history is generated. There is no indication that lithium thionyl chloride batteries are inherently unreliable. Also, since battery failure usually occurs on a cell-by-cell basis, cell redundancy could be added to improve the overall reliability of a given battery. Based on data available at this time, the expected reliability of the silver zinc battery powered system (system 2) should be greater than the expected reliability of the lithium thionyl chloride battery powered system (system 1).

Quantitative Analysis

This preliminary quantitative reliability assessment is based on the mission profile (Section 5.3.1), system component lists and failure rate data (Section 5.3.2), analysis ground rules and assumptions (Section 5.3.3), and the reliability logic diagrams (Section 5.3.4) presented previously. The failure rate source for the data shown in Table 5-5 is almost exclusively the Converged Failure Rate Data Handbook (February 1972)

supplied by the *FARADA Program. This source was chosen as the "best readily available" data book containing information on most of the components contained and in the systems. The FARADA data were adjusted by the environmental factors suggested in **MIL-STD-756A in those cases where the data given were not from the appropriate environment. The environmental factor chosen as most appropriate was 80 (missiles/ satellite: launch and boost phase). This is believed to make the results conservative since the PFS firing environment generated will be less than that generated during main booster firing at vehicle launch. The analysis indicates the conservative expected reliability levels given in Table 5-6.

The FARADA battery data bank consists almost exclusively of nickel cadmium battery source inputs. These data are considered to represent the failure rate that could be expected from a proven mature battery design. This quantitative analysis, therefore, can show no difference between PFS systems 1 and 2. Based on the qualitative analysis which indicates a long successful history of silver-zinc battery operation, System 2 (silver zinc battery system) is expected to be slightly more relable than system 1 (lithium thionyl chloride battery system) given that the battery design contains only enough cells to achieve the PFS mission (i.e., assumes no cell redundancy).

Table 5-6. Reliability Estimates for Candidate Propellant Feed Systems

System No.	Common Element Reliability	Unique Element Reliability	Expected System Reliability
1	0.9955	0.9956	0.9911
2	0.9955	0.9956	0.9911
3	0.9955	0.9903	0.9858
4	0.9955	0.9884	0.9839

*Failure Rate Data (FARADA), Fleet Missile Systems Analysis and Evaluation Group Annex, Naval Weapons Stations, Seal Beach, Corona, California.

**MIL-STD-756A, 5-15-63, Military Standard, Reliability Prediction.

5.4 ADVANTAGES AND DISADVANTAGES

A comparison was made of the advantages and disadvantages between the various candidate PFS. The results are summarized in Table 5-7. In general, the LiTCl battery powered electric motor driven pumps (System Number 1) is the lightest total weight system at all engine thrust levels and chamber pressures. However, several critical technology issues (listed under disadvantages) must be resolved in order to achieve the necessary performance and reliability goals. The silver-zinc battery powered pumps (System Number 2) have the potential for the highest reliability. However, except at the low thrust chamber pressure of 150 psia, they become the heaviest of the four candidate PFS. The monopropellant, gas generator powered turbopumps (System Number 3) are the next lightest system but rate third in reliability. However, if total propellant system dry weight is considered, the bipropellant, gas generator powered turbopumps (System Number 4) are the lightest system. However, this system rates lowest in reliability due to the increased complexity of its controls and potential pump/gas generator interactions.

5.5 FAILURE MODES AND EFFECTS ANALYSIS IMPACT

All four candidate PFS have at least one or more modes which could result in a catastrophic failure. However, all these modes can be minimized or eliminated with additional development effort to resolve the outstanding critical technologies. In addition, increased redundancy of the system controls can also aid in eliminating catastrophic failure modes and increase system reliability with only a comparatively small total system dry weight penalty.

5.6 DEVELOPMENT RISK ASSESSMENT

Based upon the system tradeoffs conducted during the study, the candidate PFS that appears to have the least development risk is the AgZn battery powered motor pumps (System Number 2). These batteries are fairly well-developed and the high-speed drive motor is based on state-of-the-art technology. The electrical controls are also fully developed so that start/stop sequences and motor speed control can be made very reliable. In addition, if the low thrust chamber regime is utilized for the rocket engine, the total weight of this system is very competitive with either of the gas generator powered turbopump systems.

Table 5-7. Comparison Between Candidate Propellant Feed Systems

No.	System Description	Advantages	Disadvantages
1	**Battery-powered electric motor driven pumps (lithium-thionyl chloride batteries)**	1. Lightest total system mass at all engine thrust levels and thrust chamber pressures 2. Eliminates need for high temperature gas generator and turbine 3. Motor characteristics will provide close speed regulation for pumps 4. High motor efficiencies (i.e., 0.85-0.90) minimizes input power requirements and heat rejection 5. Operates at room temperature rather than at 600-700°F for high temperature NaS or LiS batteries	1. Battery drain rate must be over 10 to 24 hour period if 100 watt-hour/lb energy density is to be achieved 2. Still in R&D phase. Flight qualified battery not available until 1982 or later 3. Safety hazard exists since over-discharge of battery results in high pressures due to gas evolution 4. Dry weight (i.e., burnout weight) increases appreciably at increased thrust levels and thrust chamber pressures 5. Power conditioning to provide constant voltage output increases complexity of motor controls 6. Thermal control system required to maintain batteries at room temperature to avoid decrease in energy density
2	**Battery-powered electric motor driven pumps (silver-zinc batteries)**	1. Batteries state-of-the-art and flight qualified 2. High drain rate acceptable (1 hr or less) with no degradation in achievable energy densities 3. Same as items 2, 3, 4, and 5 for system No. 1	1. Thermal control system required to maintain batteries at room temperature to avoid decrease in energy density 2. Heaviest total system mass at all engine thrust levels and thrust chamber pressures 3. High dry weight (i.e., burnout weight) has detrimental effect on achievable velocity increments, particularly at increased thrust levels and thrust chamber pressures 4. Power conditioning to provide constant voltage output increases complexity of motor controls
3	**Monopropellant gas generator powered turbopump propellant feed system**	1. Gas generator operates independent of rocket engine pumps and is not affected by turbopump speed variations 2. Eliminates need for GG mixture ratio control and simplifies injector design 3. Can operate from propellant feed system helium storage bottle with minimum weight penalty	1. Thermal control required for decomposition catalyst to avoid hazards of a cold start 2. Introduces a third fluid to the propellant feed system 3. Requires separate hydrazine storage tank which results in dry weight penalty

Table 5-7. Comparison Between Candidate Propellant Feed Systems (Continued)

No.	System Description	Advantages	Disadvantages
3		4. Requires less GG propellant weight due to superior performance over bipropellants which must operate at very fuel-rich mixture ratio to avoid excessive turbine inlet temperature 5. Does not require accumulator for turbopump start-up 6. Has lower total propellant feed system weight than bipropellant GG system	
4	Monopropellant gas generator powered turbopump propellant feed system	1. Eliminates need for third fluid for propellant feed system 2. Eliminates hydrazine storage tank which results in lowest dry weight GG powered turbopump system	1. Requires more complex bipropellant GG injector 2. Must operate GG at very fuel rich mixture ratio to avoid excessive turbine inlet temperature thus increasing propellant consumption 3. Requires accumulators for start-up and dual controls increasing system complexity 4. Has higher total propellant feed system weight than monopropellant GG system

The minimum total weight LiTCl battery powered motor pumps (System Number 1) is attractive, but these batteries have not yet achieved the high current drain rates associated with orbit injection rocket engine mission profiles and duty cycles. In addition, thermal excursions still remain as a critical technology issue still to be resolved.

The bipropellant gas generator powered turbopumps (System Number 4) have the desirable feature of offering the lowest total dry weight system. For missions where minimum burnout weight is critical, this is obviously an attractive feature. However, the complexity of component interaction and controls must relegate this to the highest development risk system.

The monopropellant gas generator powered turbopumps (System Number 3) would result in the lightest total weight system if the LiTCl battery system is omitted. In addition, the use of a separate, pressure-fed gas generator considerably simplifies component interactions and control complexity. The introduction of a third propellant (N_2H_4) is the only negative aspect of this system since this complicates the operational logistics, checkout, and handling of this system. It also makes this the heaviest total dry weight system since the separate N_2H_4 tank is a major weight element.

5.7 FIGURES OF MERIT

In a study of this type, arriving at a definitive, quantitative, figure-of-merit is always a difficult objective. However, it is possible to evaluate the candidate PFS on a qualitative basis using the data created in the study combined with good engineering judgment.

The various parameters that are important at arriving at a figure-of-merit are given in Table 5-8 together with judgmental weighting factors.

Using these weighting factors and the ranking of the four candidate PFS on a basis of 1 to 4, a relative figure-of-merit was determined for each system. The results are summarized in Table 5-9.

Table 5-8. Figure-of-Merit Parameters and Weighting Factors

Parameter	Weighting Factor
Weight (Total System)	0.40
Reliability	0.15
Development Risk	0.15
Weight (Total Dry)	0.10
Complexity	0.10
Growth Potential	0.10
	1.00

The results of Table 5-9 indicate that, based upon a qualitative, relative figure-of-merit, the candidate PFS would be rated:

Rating	System No.	System Description
1	1	Li-Th-Cl Battery Powered Motor Pumps
2	3	Monopropellant, Gas Generator Powered Turbopumps
3	2	AgZn Battery Powered Motor Pumps
4	4	Bipropellant, Gas Generator Powered Turbopumps

However, from an engineering judgement point of view, if only the low thrust chamber (150 psi), 1000 lbf thrust level rocket engine is considered, System Number 2 would have to be selected as the candidate PFS. This is because it constitutes the lowest development risk and hence, indirectly implies the lowest development cost. In addition, for small rocket engines (i.e., 1000 lbf) and short total burn times of 1 hour (i.e., low total impulse), the weight penalties (both total system and total dry weight) are minimal.

Table 5-9. Ranking of Candidate Propellant Feed Systems and Figure-of-Merit

Parameter	Weighting Factor	System Number				System Number			
		1	2	3	4	1	2	3	4
		System Ranking*				Propellant Feed System Figure of Merit = W. F. x R			
Weight (Total System)	0.40	4	1	3	2	1.60	0.50	1.20	0.80
Reliability	0.15	3	4	2	1	0.45	0.60	0.30	0.15
Development Risk	0.15	1	4	3	2	0.15	0.60	0.45	0.30
Weight (Total Dry)	0.10	4	1	2	3	0.40	0.10	0.20	0.30
Complexity	0.10	3	4	2	1	0.30	0.40	0.20	0.10
Growth Potential	0.10	2	1	3	4	0.20	0.10	0.30	0.40
		Relative Figure-of-Merit				2.80	2.20	2.65	2.05
		Relative Systems Ranking				①	③	②	④

*Highest number is best system.

6. CONCLUSIONS AND RECOMMENDATIONS

6.1 CONCLUSIONS

This study has identified three candidate pump feed systems for supplying propellants to an "orbit insertion" rocket engine. These were:

- Battery-powered, motor driven pumps (system Nos. 1 and 2)
- Monopropellant, gas generator powered turbopumps (system No. 3)
- Bipropellant, gas generator powered turbopumps (system No. 4)

The main objective of this study was to determine the lightest weight system capable of supplying propellants for a total impulse of 3.6×10^6 lbf-sec at an engine specific impulse of 310 seconds. Under these conditions, the total propulsive propellant weight is 11613 pounds (5279 kg). Hence, the total dry weight of each propellant feed system becomes a small fraction (less than 10%) of the total weight of the system. However, since for a desired propulsive velocity increment, the smaller the burnout weight, the greater the achievable payload weight, the dry weight becomes an important parameter for maximizing payloads.

During this study, it was established that the heaviest PFS components were the propellant tanks together with the helium tank and gas. Their total weight was 639 pounds (290.5 kg). Since these components comprise approximately 80% of the total PFS dry weight and are common to all three candidate systems, they represent the most significant factor in minimizing PFS dry weight. Minimum propellant tank wall thicknesses are dictated by manufacturing considerations rather than stresses. However, the tank wall thicknesses in this study were based upon state-of-the-art manufacturing techniques. Hence, any significant weight savings for these components can only be accomplished if new manufacturing methods can be developed. If low NPSH, tank-mounted boost pumps can be utilized, the need for the helium pressurization system could be eliminated. This would save 105 pounds (47.7 kg). However, the boost pump weights would have to be added and this would also tend to increase the complexity

of the PFS. An alternate approach would be to tank mount the main propellant pumps to the tanks using a separate motor or turbine drive for each. The MMH propellant has a vapor pressure of 3.5 psia at a temperature of 110°F. At an achievable suction specific speed of 30,000, the required net positive suction head is 19 feet or 7.2 psi. Hence, a residual blowdown pressure of only 10.7 psia would be required in the fuel tank. The vapor pressure of N_2O_4 at 110°F is 38.6 psia. This would require a residual blowdown pressure in the oxidizer tank of 50 psia. Because of this, a very high initial main oxidizer tank pressure would be needed, resulting in high stresses, and offsetting weight penalties. If the oxidizer temperature could be maintained at 70°F (v_p = 14.0 psia), the residual tank pressure could be reduced to 25.4 psia. Here again, the propellant temperature conditioning system would add to both the weight and complexity of the PFS.

From the foregoing it was concluded that the optimum PFS should be selected based on an overall figure-of-merit rather than on a minimum weight basis alone. The results of this assessment are given in Table 5-9 which indicates that the LiTCl battery-powered motor-pump system is the most attractive PFS. This is particularly true for the low thrust (1000 lbf), low chamber pressure (150 psia) application where the pump brake horsepower requirements are the lowest. The monopropellant, gas generator powered turbopump system was the next most attractive PFS. Low development risk and high growth potential were two parameters which contributed significantly to this ranking. The AgZn battery-powered motor-pump system ranked third primarily because of its higher weights and lower growth potential. Also, the bipropellant, gas-generator powered turbopump ranked last because of its increased complexity and resulting lowest reliability.

In addition, since ultimate conversion to LF_2/N_2H_4 propellants will lead to the most significant reduction in total PFS weight (because of the higher achievable specific impulse of 385 seconds), the motor-driven pumps are more easily adaptable to this change. This is primarily due to the avoidance of the use of a high temperature (1400°F) turbine since close proximity to the extremely low temperature (-306°F) LF_2 pump

could produce complex insulation, thermal differential expansion/ contraction, and thermal soakback problems.

6.2 RECOMMENDATIONS

Based upon the results of this study, the following recommendations are offered:

- The battery-powered, electric motor driven pump propellant feed system (Nos. 1 and 2) should be developed for use with an "orbit insertion" rocket engine.

- The decision, whether lithium-thionyl-chloride batteries or silver-zinc batteries should be used to power the motor-driven pumps, should depend upon the development status and reliability levels demonstrated by each type at the time of implementation.

- Because of the considerable propellant weight savings (approximately 20%) achievable with LF_2/N_2H_4, early conversion to these propellants should be considered.

- For larger total impulse rocket engine requirements the monopropellant gas-generator powered turbopump system (No. 3), using the LF_2/N_2H_4 propellants, would be the lightest weight candidate. Propellant for the gas generator would be stored in the main N_2H_4 tank and pressure fed to the gas generator from the main engine fuel pump. This eliminates the need for a separate N_2H_4 tank and pressure regulator but does require the use of an accumulator (similar to system No. 4) for multiple starts.